Heterogeneous Catalysis and Solid Catalysts

Olaf Deutschmann, Institut für Technische Chemie und Polymerchemie, Universität Karlsruhe (TH), Engesserstr. 20, Karlsruhe, Germany

Helmut Knözinger, Department Chemie, Universität München, Butenandtstr. 5 – 13 (Haus E), München, Germany 81377

Karl Kochloefl, Schwarzenbergstr. 15, Rosenheim, Germany 83026

Thomas Turek, Institut für Chemische Verfahrenstechnik, TU Clausthal, Leibnizstr. 17, Clausthal-Zellerfeld, Germany

10.1002/14356007.a05_313.pub2

1. Introduction

Catalysis is a phenomenon by which chemical reactions are accelerated by small quantities of foreign substances, called *catalysts*. A suitable *catalyst* can enhance the rate of a thermodynamically feasible reaction but cannot change the position of the thermodynamic equilibrium. Most catalysts are solids or liquids, but they may also be gases.

The catalytic reaction is a cyclic process. According to a simplified model, the reactant or reactants form a complex with the catalyst, thereby opening a pathway for their transformation into the product or products. Afterwards the catalyst is released and the next cycle can proceed.

However, catalysts do not have infinite life. Products of side reactions or changes in the catalyst structure lead to catalyst deactivation. In practice spent catalysts must be reactivated or replaced (see Chapter Catalyst Deactivation and Regeneration).

1.1. Types of Catalysis

If the catalyst and reactants or their solution form a common physical phase, then the reaction is called *homogeneously catalyzed*. Metal salts of organic acids, organometallic complexes, and carbonyls of Co, Fe, and Rh are typical *homogeneous catalysts*. Examples of *homogeneously catalyzed* reactions are oxidation of toluene to benzoic acid in the presence of Co and Mn benzoates and hydroformylation of olefins to give the corresponding aldehydes. This reaction is catalyzed by carbonyls of Co or Rh.

Heterogeneous catalysis involves systems in which catalyst and reactants form separate physical phases. Typical *heterogeneous catalysts* are inorganic solids such as metals, oxides, sulfides, and metal salts, but they may also be organic materials such as organic hydroperoxides, ion exchangers, and enzymes.

Examples of *heterogeneously catalyzed* reactions are ammonia synthesis from the elements over promoted iron catalysts in the gas phase and hydrogenation of edible oils on Ni – kieselguhr catalysts in the liquid phase, which are examples of *inorganic* and *organic catalysis*, respectively.

Electrocatalysis is a special case of heterogeneous catalysis involving oxidation or reduction by transfer of electrons. Examples are the use of catalytically active electrodes in electrolysis processes such as chlor-alkali electrolysis and in fuel cells.

In *photocatalysis* light is absorbed by the catalyst or a reactant during the reaction. This can take place in a *homogeneous* or *heterogeneous* system. One example is the utilization of semiconductor catalysts (titanium, zinc, and iron oxides) for photochemical degradation of organic substances, e.g., on self-cleaning surfaces.

In *biocatalysis*, enzymes or microorganisms catalyze various biochemical reactions. The catalysts can be immobilized on various carriers such as porous glass, SiO_2, and organic polymers. Prominent examples of biochemical reactions are isomerization of glucose to fructose, important in the production of soft drinks, by using enzymes such as glucoamylase immobilized on SiO_2, and the conversion of acrylonitrile to acrylamide by cells of corynebacteria entrapped in a polyacrylamide gel.

The main aim of *environmental catalysis* is environmental protection. Examples are the reduction of NO_x in stack gases with NH_3 on $V_2O_5 - TiO_2$ catalysts and the removal of NO_x, CO, and hydrocarbons from automobile exhaust gases by using the so-called *three-way catalyst* consisting of $Rh - Pt - CeO_2 - Al_2O_3$ deposited on ceramic honeycombs.

The term *green catalytic processes* has been used frequently in recent years, implying that chemical processes may be made environmentally benign by taking advantage of the possible high yields and selectivities for the target products, with little or no unwanted side products and also often high energy efficiency.

The basic chemical principles of catalysis consist in the coordination of reactant molecules to central atoms, the ligands of which may be molecular species (homogeneous and biocatalysis) or neighboring atoms at the surface of the solid matrix (heterogeneous catalysis). Although there are differences in the details of various types of catalysis (e.g., solvation effects in the liquid phase, which do not occur in solid – gas reactions), a closer and undoubtedly fruitful collaboration between the separate communities representing homogeneous, heterogeneous, and biocatalysis should be strongly supported. A statement by David Parker (ICI) during the 21st Irvine Lectures on 24 April 1998 at the University of St. Andrews should be mentioned in this connection, namely, that, "... at the molecular level, there is little to distinguish between homogeneous and heterogeneous catalysis, but there are clear distinctions at the industrial level" [1].

1.2. Catalysis as a Scientific Discipline

Catalysis is a well-established scientific discipline, dealing not only with fundamental principles or mechanisms of catalytic reactions but also with preparation, properties, and applications of various catalysts. A number of academic and industrial institutes or laboratories focus on the study of catalysis and catalytic processes as well as on the improvement of existing and development of new catalysts.

International journals specializing in catalysis include *Journal of Catalysis*, *Journal of Molecular Catalysis* (Series A: Chemical; Series B: Enzymatic), *Applied Catalysis* (Series A: General; Series B: Environmental), *Reaction Kinetics and Catalysis Letters*, *Catalysis Today*, *Catalysis Letters*, *Topics in Catalysis*, *Advances in Organometallic Catalysis*, etc.

Publications related to catalysis can also be found in *Journal of Physical Chemistry*, *Langmuir*, and *Physical Chemistry Chemical Physics*.

Well-known serials devoted to catalysis are *Handbuch der Katalyse* [edited by G.-M. Schwab, Springer, Wien, Vol. 1 (1941) - Vol. 7.2 (1943)], *Catalysis* [edited by P. H. Emmett, Reinhold Publ. Co., Vol. 1 (1954) - Vol. 7 (1960)], *Catalysis — Science and Technology* [edited by J. R. Anderson and M. Boudart, Springer, Vol. 1 (1981) - Vol. 11 (1996)], *Catalysis Reviews* (edited by A. T. Bell and J. J. Carberry, Marcel Dekker), *Advances in Catalysis* (edited by B. C. Gates and H. Knözinger, Academic Press), *Catalysis* (edited by J. J. Spivey, The Royal Society of Chemistry), *Studies in Surface Science and Catalysis* (edited by B. Delmon and J. T. Yates), etc.

Numerous aspects of catalysis were the subject of various books. Some, published since 1980, are mentioned here:

C. N. Satterfield, *Heterogeneous Catalysis in Practice*, McGraw Hill Book Comp., New York, 1980.

D. L. Trimm, *Design of Industrial Catalysts*, Elsevier, Amsterdam, 1980.

J. M. Thomas, R. M. Lambert (eds.), *Characterization of Heterogeneous Catalysts*, Wiley, Chichester, 1980.

R. Pearce, W. R. Patterson (eds.), *Catalysis and Chemical Processes*, John Wiley, New York, 1981.

B. L. Shapiro (ed.), *Heterogeneous Catalysis*, Texas A & M Press, College Station, 1984.

B. E. Leach (ed.), *Applied Industrial Catalysis*, Vol. 1, 2, 3, Academic Press, New York, 1983 – 1984.

M. Boudart, G. Djega-Mariadassou, *Kinetics of Heterogeneous Reactions*, Princeton University Press, Princeton, 1984.

F. Delannay (ed.), *Characterization of Heterogeneous Catalysts*, Marcel Dekker, New York, 1984.

R. Hughes, *Deactivation of Catalysts*, Academic Press, New York, 1984.

M. Graziani, M. Giongo (eds.), *Fundamental Research in Homogeneous Catalysis*, Wiley, New York, 1984.

H. Heinemann, G. A. Somorjai (eds.), *Catalysis and Surface Science*, Marcel Dekker, New York, 1985.

J. R. Jennings (ed.), *Selective Development in Catalysis*, Blackwell Scientific Publishing, London, 1985.

G. Parshall, *Homogeneous Catalysis*, Wiley, New York, 1985.

J. R. Anderson, K. C. Pratt, *Introduction to Characterization and Testing of Catalysts*, Academic Press, New York, 1985.

Y. Yermakov, V. Likholobov (eds), *Homogeneous and Heterogeneous Catalysis*, VNU Science Press, Utrecht, Netherlands, 1986.

J. F. Le Page, *Applied Heterogeneous Catalysis — Design, Manufacture, Use of Solid Catalysts*, Technip, Paris, 1987.

G. C. Bond, *Heterogeneous Catalysis*, 2nd ed., Clarendon Press, Oxford, 1987.

P. N. Rylander, *Hydrogenation Methods*, Academic Press, New York, 1988.

A. Mortreux, F. Petit (eds.), *Industrial Application of Homogeneous Catalysis*, Reidel, Dordrecht, 1988.

J. F. Liebman, A. Greenberg, *Mechanistic Principles of Enzyme Activity*, VCH, New York, 1988.

J. T. Richardson, *Principles of Catalytic Development*, Plenum Publishing Corp., New York, 1989.

M. V. Twigg (ed.), *Catalyst Handbook*, Wolfe Publishing, London, 1989.

J. L. G. Fierro (ed.), *Spectroscopic Characterization of Heterogeneous Catalysts*, Elsevier, Amsterdam, 1990.

R. Ugo (ed.), *Aspects of Homogeneous Catalysis*, Vols. 1 – 7, Kluwer Academic Publishers, Dordrecht, 1990.

W. Gerhartz (ed.), *Enzymes in Industry*, VCH, Weinheim, 1990.

R. A. van Santen, *Theoretical Heterogeneous Catalysis*, World Scientific, Singapore, 1991.

J. M. Thomas, K. I. Zamarev (eds.), *Perspectives in Catalysis*, Blackwell Scientific Publications, Oxford, 1992.

B. C. Gates, *Catalytic Chemistry*, Wiley, New York, 1992.

G. W. Parshall, S. D. Ittel, *Homogeneous Catalysis*, 2nd ed., Wiley, New York, 1992.

J. J. Ketta (ed.), *Chemical Processing Handbook*, Marcel Dekker, New York, 1993.

J. A. Moulijn, P. W. N. M. van Leeuwen, R. A. van Santen (eds.), Catalysis — An Integrated Approach to Homogeneous, Heterogeneous and Industrial Catalysis, Elsevier, Amsterdam, 1993.

J. W. Niemantsverdriet, *Spectroscopy in Catalysis*, VCH, Weinheim, 1993.

J. Reedijk (ed.), *Bioinorganic Catalysis*, M. Dekker, New York, 1993.

G. A. Somorjai, *Introduction to Surface Chemistry and Catalysis*, Wiley, New York, 1994.

J. M. Thomas, W. J. Thomas, *Principles and Practice of Heterogeneous Catalysis*, VCH, Weinheim, 1996.

R. J. Wijngarden, A. Kronberg, K. R. Westerterp, *Industrial Catalysis — Optimizing Catalysts and Processes*, Wiley-VCH, Weinheim, 1998.

G. Ertl, H. Knözinger, J. Weitkamp (eds.), *Environmental Catalysis*, Wiley-VCH, Weinheim, 1999.

G. Ertl, H. Knözinger, J. Weitkamp (eds.), *Preparation of Solid Catalysts*, Wiley-VCH, Weinheim, 1999.

B. Cornils, W. A. Herrmann, R. Schlögl, C.-H. Wong, *Catalysis from A – Z*, Wiley-VCH, Weinheim, 2000.

B. C. Gates, H. Knözinger (eds.), *Impact of Surface Science on Catalysis*, Academic, San Diego, 2000.

A comprehensive survey of the principles and applications: G. Ertl, H. Knözinger, F. Schüth, J. Weitkamp (eds.): *Handbook of Heterogeneous Catalysis*, 2nd ed. with 8 volumes and 3966 pages, Wiley-VCH, Weinheim 2008.

The first *International Congress on Catalysis* (ICC) took place in 1956 in Philadelphia and has since been held every four years in Paris (1960), Amsterdam (1964), Moscow (1968), Palm Beach (1972), London (1976), Tokyo (1980), Berlin (1984), Calgary (1988), Budapest (1992), Baltimore (1996), Granada (2000)), Paris (2004) and Seoul (2008). The 15th Congress will be held in Munich in 2012. Presented papers and posters have been published in the *Proceedings* of the corresponding congresses. *The International Congress on Catalysis Council (ICC)* was renamed at the Council meeting in Baltimore 1996. The international organization is now called *International Association of Catalysis Societies (IACS)*.

In 1965 the *Catalysis Society of North America* was established and holds meetings in the USA every other year.

The European Federation of Catalysis Societies (EFCATS) was established in 1990. The *EUROPACAT* Conferences are organized under the auspices of *EFCATS*. The first conference took place in Montpellier (1993) followed by Maastricht (1995), Cracow (1997), Rimini (1999), and Limerick (2001).

Furthermore, every four years (in the even year between two International Congresses on Catalysis) an *International Symposium* focusing on *Scientific Basis for the Preparation of Heterogeneous Catalysts* is held in Louvain-La Neuve (Belgium).

Other international symposia or congresses devoted to catalysis are: *International Zeolite Conferences*, *International Symposium of Catalyst Deactivation*, *Natural Gas Conversion Symposium*, *Gordon Conference on Catalysis*, TOCAT (*Tokyo Conference on Advanced Catalytic Science and Technology*), *International Symposium of Acid-Base Catalysis*, the European conference series, namely the *Roermond, Sabatier- and Schwab-conference*, and the *Taylor Conference*.

1.3. Industrial Importance of Catalysis

Because most industrial chemical processes are catalytic, the importance and economical significance of catalysis is enormous. More than 80 % of the present industrial processes established since 1980 in the chemical, petrochemical, and biochemical industries, as well as in the production of polymers and in environmental protection, use catalysts.

More than 15 international companies have specialized in the production of numerous catalysts applied in several industrial branches. In 2008 the turnover in the catalysts world market was estimated to be about US-$ 13×10^9 (see Chapter Production of Heterogeneous Catalysts).

1.4. History of Catalysis

The phenomenon of catalysis was first recognized by Berzelius [2,3] in 1835. However, some catalytic reactions such as the production of alcoholic beverages by fermentation or the manufacture of vinegar by ethanol oxidation were practiced long before. Production of soap by fat hydrolysis and diethyl ether by dehydration of ethanol belong to the catalytic reactions that were performed in the 16th and 17th centuries.

Besides Berzelius, Mitscherlich [3] was also involved at the same time in the study of catalytic reactions accelerated by solids. He introduced the term *contact catalysis*. This term for heterogeneous catalysis lasted for more than 100 years.

In 1895 Ostwald [3,4] defined catalysis as the acceleration of chemical reactions by the presence of foreign substances which are not consumed. His fundamental work was recognized with the Nobel prize for chemistry in 1909.

Between 1830 and 1900 several practical processes were discovered, such as flameless combustion of CO on a hot platinum wire, and the oxidation of SO_2 to SO_3 and of NH_3 to NO, both over Pt catalysts.

In 1912 Sabatier [3,5] received the Nobel prize for his work devoted mainly to the hydrogenation of ethylene and CO over Ni and Co catalysts.

The first major breakthrough in industrial catalysis was the synthesis of ammonia from the elements, discovered by HABER [3,6,7] in 1908, using osmium as catalyst. Laboratory recycle reactors for the testing of various ammonia catalysts which could be operated at high pressure and temperature were designed by BOSCH [3]. The ammonia synthesis was commercialized at BASF (1913) as the *Haber – Bosch* [8] process. MITTASCH [9] at BASF developed and produced iron catalysts for ammonia production.

In 1938 BERGIUS [3,10] converted coal to liquid fuel by high-pressure hydrogenation in the presence of an Fe catalyst.

Other highlights of industrial catalysis were the synthesis of methanol from CO and H_2 over $ZnO - Cr_2O_3$ and the cracking of heavier petroleum fractions to gasoline using acid-activated clays, as demonstrated by HOUDRY [3,6] in 1928.

The addition of isobutane to $C_3 - C_4$ olefins in the presence of $AlCl_3$, leading to branched $C_7 - C_8$ hydrocarbons, components of high-quality aviation gasoline, was first reported by IPATIEFF et al. [3,7] in 1932. This invention led to a commercial process of UOP (USA).

Of eminent importance for Germany, which possesses no natural petroleum resources, was the discovery by FISCHER and TROPSCH [11] of the synthesis of hydrocarbons and oxygenated compounds from CO and H_2 over an alkalized iron catalyst. The first plants for the production of hydrocarbons suitable as motor fuel started up in Germany 1938. After World War II, Fischer-Tropsch synthesis saw its resurrection in South Africa. Since 1955 Sasol Co. has operated two plants with a capacity close to 3×10^6 t/a.

One of the highlights of German industrial catalysis before World War II was the synthesis of aliphatic aldehydes by ROELEN [12] by the addition of CO and H_2 to olefins in the presence of Co carbonyls. This homogeneously catalyzed reaction was commercialized in 1942 by Ruhr-Chemie and is known as Oxo Synthesis.

During and after World War II (till 1970) numerous catalytic reactions were realized on an industrial scale (see also Chapter Application of Catalysis in Industrial Chemistry). Some important processes are compiled in Table 1.

Table 2 summarizes examples of catalytic processes representing the current status of the chemical, petrochemical and biochemical industry as well as the environmental protection (see also Chapter Application of Catalysis in Industrial Chemistry).

Table 1. Important catalytic processes commercialized during and after World War II (until 1970) [13,14]

Year of commercialization	Process	Catalyst	Products
1939 – 1945	dehydrogenation	$Pt - Al_2O_3$	toluene from methylcyclohexane
	dehydrogenation	$Cr_2O_3 - Al_2O_3$	butadiene from *n*-butane
	alkane isomerization	$AlCl_3$	*i*-$C_7 - C_8$ from *n*-alkanes
1946 – 1960	oxidation of aromatics	V_2O_5	phthalic anhydride from naphthalene and *o*-xylene
	hydrocracking	Ni – aluminosilicate	fuels from high-boiling petroleum fractions
	polymerization (Ziegler – Natta)	$TiCl_4 - Al(C_2H_5)_3$	polyethylene from ethylene
	dehydrogenation	$Fe_2O_3 - Cr_2O_3 - KOH$	styrene from ethylbenzene
	oxidation (Wacker process)	$PdCl_2 - CuCl_2$	acetaldehyde from ethylene
1961 – 1970	steam reforming	$Ni - \alpha\text{-}Al_2O_3$	Co, (CO_2), and H_2 from methane
	ammoxidation	Bi phosphomolybdate	acrylonitrile from propene
	fluid catalytic cracking	H zeolites + aluminosilicates	fuels from high boiling fractions
	reforming	bimetallic catalysts (Pt, Sn, Re, Ir)	gasoline
	low-pressure methanol synthesis	$Cu - ZnO - Al_2O_3$	methanol from CO, H_2, CO_2
	isomerization	enzymes immobilized on SiO_2	fructose from glucose (production of soft drinks)
	distillate dewaxing	ZSM-5, mordenites	removal of *n*-alkanes from gasoline
	hydrorefining	Ni – , CO – MoS_x	hydrodesulfurization, hydrodenitrification

Table 2. Important catalytic processes commercialized after 1970 [15–18]

Year of commercialization	Process	Catalyst	Product
1971 – 1980	automobile emission control	Pt – Rh – CeO_2 – Al_2O_3 (three-way catalyst)	removal of NO_x, CO, CH_x
	carbonylation (Monsanto process)	organic Rh complex	acetic acid from methanol
	MTG (Mobil process)	zeolite (ZSM-5)	gasoline from methanol
1981 – 1985	alkylation (Mobil – Badger)	modified zeolite (ZSM-5)	ethylbenzene from ethylene
	selective catalytic reduction (SCR; stationary sources)	V Ti (Mo, W) oxides (monoliths)	reduction of NO_x with NH_3 to N_2
	esterification (MTBE synthesis)	ion-exchange resin	methyl-*tert*-butyl ether from isobutene + methanol
	oxidation (Sumitomo Chem., 2-step process)	1. Mo, Bi oxides 2. Mo, V, PO (heteropolyacids)	acrylic acid from propene
	oxidation (Monsanto)	vanadylphosphate	maleic anhydride from *n*-butane
	fluid-bed polymerization (Unipol)	Ziegler – Natta type	polyethylene and polypropylene
	hydrocarbon synthesis (Shell)	1. Co – (Zr,Ti) – SiO_2 2. Pt – SiO_2	middle distillate from CO + H_2
	environmental control (combustion process)	Pt – Al_2O_3 (monoliths)	deodoration
1986 – 2000	oxidation with H_2O_2 (Enichem)	Ti silicalite	hydroquinone and catechol from phenol
	hydration	enzymes	acrylamide from acrylonitrile
	ammoxidation (Montedipe)	Ti silicalite	cyclohexanone oxime from cyclohexanone, NH_3, and H_2O_2
	dehydrogenation of C_3, C_4 alkanes (Star and Oleflex processes)	Pt(Sn) – zinc aluminate, Pt – Al_2O_3	C_3, C_4 olefins
2000 –	catalytic destruction of N_2O from nitric acid tail gases (EnviNOx process, Uhde)	Fe zeolite	removal of nitrous oxide
	HPPO (BASF-Dow, Degussa-Uhde)	Ti silicalite	propylene from propene

2. Theoretical Aspects

The classical definition of a catalyst states that "a catalyst is a substance that changes the rate but not the thermodynamics of a chemical reaction" and was originally formulated by Ostwald [4]. Hence, catalysis is a dynamic phenomenon.

As emphasized by Boudart [19], the conditions under which catalytic processes occur on solid materials vary drastically. The reaction temperature can be as low as 78 K and as high as 1500 K, and pressures can vary between 10^{-9} and 100 MPa. The reactants can be in the gas phase or in polar or nonpolar solvents. The reactions can occur thermally or with the assistance of photons, radiation, or electron transfer at electrodes. Pure metals and multicomponent and multiphase inorganic compounds can act as catalysts. Site-time yields (number of product molecules formed per site and unit time) as low as 10^{-5} s^{-1} (corresponding to one turnover per day) and as high as 10^{9} s^{-1} (gas kinetic collision rate at 1 MPa) are observed.

It is plausible that it is extremely difficult, if not impossible, to describe the catalytic phenomenon by a general theory which covers the entire range of reaction conditions and observed site-time yields (reaction rates). However, there are several general *principles* which are considered to be laws or rules of thumb that are useful in many situations. According to Boudart [19], the value of a principle is directly related to its generality. In contrast, *concepts* are more specialized and permit an interpretation of phenomena observed for special classes of catalysts or reactions under given reaction conditions.

In this chapter, important principles and concepts of heterogeneous catalysis are discussed, followed by a section on kinetics of heterogeneously catalyzed reactions. The chapter is concluded by a section on the determination of reaction mechanisms in heterogeneous catalysis.

2.1. Principles and Concepts

2.1.1. Sabatier's Principle

The Sabatier principle proposes the existence of an unstable intermediate compound formed between the catalyst surface and at least one of the reactants [5]. This intermediate must be stable enough to be formed in sufficient quantities and labile enough to decompose to yield the final product or products. The Sabatier principle is related to linear free energy relationships such as a Brønsted relation [19]. These relations deal with the heat of reaction q (thermodynamic quantity) and the activation barrier E (kinetic quantity) of an elementary step in the exothermic direction ($q > 0$). With an empirical parameter a ($0 < a < 1$) and neglecting entropy effects, a Brønsted relation can be written as

$$\Delta E = a\,\Delta q,$$

where ΔE is the decrease in activation energy corresponding to an increase Δq in the heat of reaction. Hence, an elementary step will have a high rate constant in the exothermic direction when its heat of reaction q increases. Since the activation barrier in the endothermic direction is equal to the sum of the activation energy E and the heat of reaction, the rate constant will decrease with increasing q.

The Brønsted relationship represents a bridge between thermodynamics and kinetics and, together with the Sabatier principle, permits an interpretation of the so-called *volcano plots* first reported by Balandin [20]. These volcano curves result when a quantity correlated with the rate of reaction under consideration is plotted against a measure of the stability of the intermediate compound. The latter quantity can be the heat of adsorption of one of the reactants or the heat of formation of a bulk compound relative to the surface compound, or even the heat of formation of any bulk compound that can be correlated with the heat of adsorption, or simply the position of the catalytic material (metal) along a horizontal series in the Periodic Table [263].

As an example, Figure 1 shows the volcano plot for the decomposition of formic acid on transition metals [21]. The intermediate in this reaction was shown to be a surface formate. Therefore, the heats of formation ΔH_f of the bulk metal formates were chosen as the measure of the stability of the intermediate. At low values of ΔH_f, the reaction rate is low and corresponds to the rate of adsorption, which increases with increasing heat of formation of the bulk formates (representing the stability of the surface compound). At high values of ΔH_f the reaction rate is also low and corresponds to the desorption rate, which increases with decreasing ΔH_f. As a consequence, a maximum in the rate of reaction (decomposition of formic acid) is observed at intermediate ΔH_f values which is neither a pure rate of adsorption nor a pure rate of desorption but which depends on both.

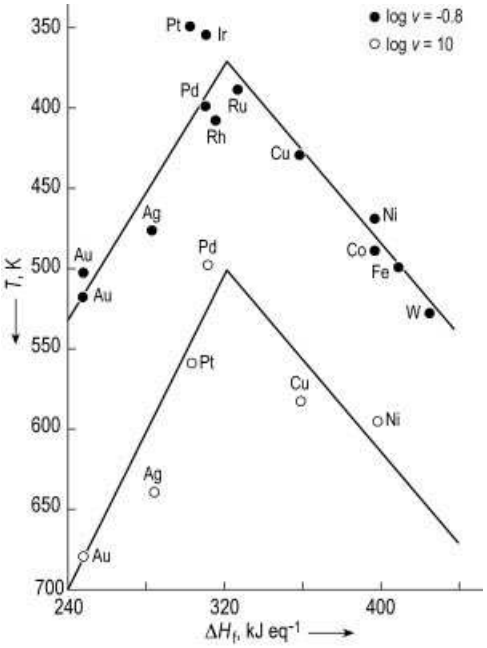

Figure 1. Volcano plot for the decomposition of formic acid. The temperature T at which the rate of decomposition ν has a fixed value is plotted against the heat of formation ΔH_f of the metal formate (adopted from [31]).

2.1.2. The Principle of Active Sites

The Sabatier principle of an unstable surface intermediate requires chemical bonding of reactants to the catalyst surface, most likely between atoms or functional groups of reactant and surface atoms. This leads to the *principle of active sites*. When Langmuir formulated his model of chemisorption on metal surfaces [22],

he assumed an array of sites which were energetically identical and noninteracting, and which would adsorb just one molecule from the gas phase in a localized mode. The Langmuir adsorption isotherm results from this model. The sites involved can be considered to be active sites.

LANGMUIR was already aware that the assumption of identical and noninteracting sites was an approximation which would not hold for real surfaces, when he wrote [23]: "Most finely divided catalysts must have structures of great complexity. In order to simplify our theoretical consideration of reactions at surfaces, let us confine our attention to reactions on plane surfaces. If the principles in this case are well understood, it should then be possible to extend the theory to the case of porous bodies. In general, we should look upon the surface as consisting of a checkerboard." LANGMUIR thus formulated the surface science approach to heterogeneous catalysis for the first time.

The heterogeneity of active sites on solid catalyst surfaces and its consequences were emphasized by TAYLOR [24], who recognized that "There will be all extremes between the case in which all atoms in the surface are active and that in which relatively few are so active." In other words, exposed faces of a solid catalyst will contain terraces, ledges, kinks, and vacancies with sites having different coordination numbers. Nanoscopic particles have edges and corners which expose atoms with different coordination numbers [25]. The variation of coordination numbers of surface atoms will lead to different reactivities and activities of the corresponding sites. In this context, Schwab's adlineation theory may be mentioned [26], which speculated that one-dimensional defects consisting of atomic steps are of essential importance. This view was later confirmed by surface science studies on stepped single-crystal metal surfaces [27].

In addition to variable coordination numbers of surface atoms in one-component solids, the surface composition may be different from that of the bulk and different for each crystallographic plane in multicomponent materials (*surface segregation* [28]). This would lead to a heterogeneity of the local environment of a surface atom and thus create nonequivalent sites.

Based on accurate kinetic measurements and on the Taylor principle of the existence of inequivalent active sites, BOUDART et al. [29] coined the terms *structure-sensitive* and *structure-insensitive reactions*. A truly structure-insensitive reaction is one in which all sites seem to exhibit equal activity on several planes of a single crystal. Surprisingly, many heterogeneously catalyzed reactions turned out to be structure-insensitive. Long before experimental evidence for this phenomenon was available and before a reliable interpretation was known, TAYLOR predicted it by writing [24]: "The amount of surface which is catalytically active is determined by the reaction catalyzed." In other words, the surface of a catalyst adapts itself to the reaction conditions for a particular reaction. The driving force for this reorganization of a catalyst surface is the minimization of the surface free energy, which may be achieved by *surface-reconstruction* [30,31]. As a consequence, a meaningful characterization of active sites requires experiments under working (in situ) conditions of the catalytic system.

The principle of active sites is not limited to metals. Active sites include metal cations, anions, Lewis and Brønsted acids, acid – base pairs (acid and base acting simultaneously in chemisorption), organometallic compounds, and immobilized enzymes. Active sites may include more than one species (or atom) to form multiplets [20] or ensembles [32]. A mandatory requirement for these sites to be active is that they are accessible for chemisorption from the fluid phase. Hence, they must provide free coordination sites. Therefore, BURWELL et al. [33,34] coined the term *coordinatively unsaturated sites* in analogy with homogeneous organometallic catalysts. Thus, active sites are to be considered as atoms or groups of atoms which are embedded in the surface of a matrix in which the neighboring atoms (or groups) act as ligands. *Ensemble* and *ligand effects* are discussed in detail by SACHTLER [35] and quantum chemical treatments of geometric ensemble and electronic ligand effects on metal alloy surfaces are discussed by HAMMER and NØRSKOV [36].

2.1.3. Surface Coordination Chemistry

The surface complexes formed by atoms or molecules are now known to usually

resemble a local structure similar to molecular coordination complexes. The bonding in these surface complexes can well be described in a localized picture [37,38]. Thus, important phenomena occuring at the surface of solid catalysts may be described in the framework of *surface coordination chemistry* or *surface organometallic chemistry* [39,40].

This is at variance with the so-called *band theory* of catalysis, which attempted to correlate catalytic performance with bulk electronic properties [41–43]. The shortcomings of this theory in oxide catalysis are discussed by STONE [44].

2.1.4. Modifiers and Promoters

The performance of real industrial catalysts is often adjusted by *modifiers* (additives) [45,46]. A modifier is called a *promoter* when it increases the catalyst activity in terms of reaction rate per site. Modifiers may also affect a catalyst's performance in an undesired manner. In this case the modifier acts as a catalyst *poison*. However, this simple distinction between promoters and poisons is less straightforward for reactions yielding more than one product in parallel or consecutive steps, of which only one is the desired product. In this case not only high activity but also high selectivity is desired. The selectivity can be improved by adding substances that poison undesirable reactions. In exothermic reactions excessively high reaction rates may lead to a significant temperature increase (sometimes only locally: hot spots) which can yield undesirable products (e.g., CO and CO_2 in selective catalytic oxidation). A deterioration of the catalyst due to limited catalyst stability may also occur. Consequently, a modifier is required which decreases the reaction rate so that a steady-state temperature and reaction rate can be maintained. Although the modifier acts as a poison in these cases, it is in fact a promoter as far as selectivity and catalyst stability are concerned.

Modifiers can change the binding energy of an active site or its structure, or disrupt an ensemble of atoms, e.g., by alloying an active with an inactive metal. A molecular approach toward an understanding of promotion in heterogeneous catalysis was presented by HUTCHINGS [47].

As an example, the iron-based ammonia synthesis catalyst is promoted by Al_2O_3 and K_2O [48]. Alumina acts as a *textural* promoter, as it prevents the rapid sintering of pure iron metal. It may also stabilize more active sites on the iron surface (*structural promoter*). Potassium oxide appears to affect the adsorption kinetics and dissociation of dinitrogen and the binding energy of nitrogen on adjacent iron sites (*electronic promoter*).

The addition of Co to MoS_2-based catalysts supported on transitional aluminas has a positive effect on the rate of hydrodesulfurization of sulfur-containing compounds at Co/(Co + Mo) ratios below ca. 0.3 [49] (see Section Supported Metal Catalysts). The active phase is proposed to be the so-called CoMoS phase which consists of MoS_2 platelets, the edges of which are decorated by Co atoms. The latter may act as structural and electronic promoters simultaneously.

Another example concerns bifunctional catalysts for catalytic reforming [50], which consist of Pt supported on strongly acidic aluminas, the acid strength of which is enhanced by modification with chloride. Since these materials lose chlorine during the catalytic process, the feed contains CCl_4 as a precursor of the surface chloride promoter.

2.1.5. Active Phase – Support Interactions

Several concepts have proved valuable in interpreting phenomena which are pertinent to certain classes of catalysts. In supported catalysts, the active phase (metal, oxide, sulfide) undergoes active phase-support interactions [51–53]. These are largely determined by the surface free energies of the support and active phase materials and by the interfacial free energy between the two components [51–53]. Active transition metal oxides (e.g., V_2O_5, MoO_3, WO_3) have relatively low surface free energies as compared to typical oxidic support materials such as γ-Al_2O_3, TiO_2 (anatase), and SiO_2. Although the interfacial free energies between active phase and support are not known, the interaction between the two components appears to be favorable, with the exception of SiO_2-supported transition metal oxides. As a

consequence spreading and wetting phenomena occur if the thermal treatment of the oxide mixtures is carried out at temperatures sufficiently high to induce mobility of the active oxide. As a rule of thumb, mobility of a solid typically occurs above the Tammann temperature, which is equal to half the melting point of the bulk solid. As a result, the active transition metal oxide tends to wet the support surface and forms a monolayer (monolayer-type catalysts).

Transition and noble metals typically have high surface free energies [52], and therefore, small particles or crystallites tend to agglomerate to reduce their surface area. Stabilization of nanosize metal particles therefore requires deposition on the surface of supports providing favorable *metal-support interactions* (MSI). The smaller the particle the more its physical properties and morphology can be affected by these interactions. Therefore, the nature of the support material for a given metal also critically influences the catalytic properties of the metal particle.

Supported metals are in a nonequilibrium state and therefore still tend to agglomerate at sufficiently high temperatures in reducing atmospheres. Hence, deactivation occurs because of the reduced metal surface area. Regeneration can typically be achieved by thermal treatment in an atmosphere in which the active metal is oxidized. The surface free energies of transition and noble metal oxides are significantly lower than those of the parent metals, so that their spreading on the support surface becomes more favorable. Subsequent reduction under sufficiently mild conditions can restore the high degree of metal dispersion [dispersion D is defined as the ratio of the number of metal atoms exposed at the particle surface (N_S) to the total number of metal atoms N_T in the particle ($D = N_S/N_T$)].

So-called *strong metal-support interactions* (SMSI) may occur, e.g., for Pt – TiO_2 and Rh – TiO_2 [51,53,54]. As shown experimentally, the adsorption capacity for H_2 and CO is drastically decreased when the precursor for the catalytically active metal on the support is reduced in H_2 at temperatures above ca. 770 K [51,54]. Simultaneously, the oxide support is slightly reduced. Although several explanations have been proposed for the SMSI effect, the most probable explanation is encapsulation of the metal particle by support oxide material. Encapsulation may occur when the support material becomes mobile. Although the electronic properties of the metal particle may be affected by the support oxide in the SMSI state, the decrease of the adsorption capacity appears to be largely due to a geometric effect, namely, the resulting inaccessibility of the metal surface.

The various possible morphologies and dispersions of supported metals are schematically shown in Figure 2. The metal precursor typically is well dispersed after impregnation of the support. Low-temperature calcination may lead to well-dispersed oxide overlayers, while direct low-temperature reduction leads to highly dispersed metal particles. This state can also be reached by low-temperature reduction of the dispersed oxide precursor, this step being

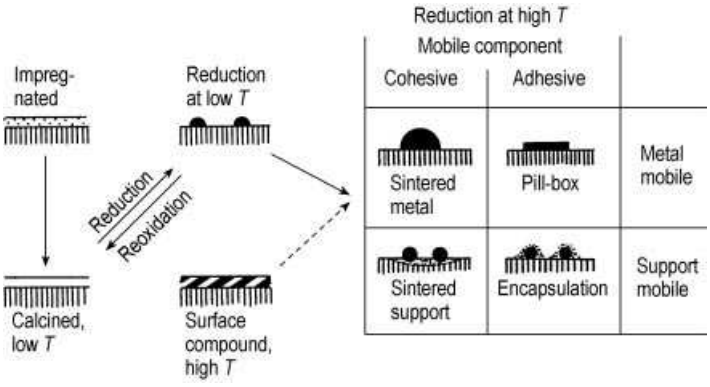

Figure 2. Schematic representation of metal-support interactions (adopted from [50])

reversible by low-temperature reoxidation. For the preparation of highly dispersed Ni catalysts, it is important to remove the water that is formed by hydrogen reduction of NiO. H_2 diluted with N_2 is used for this purpose. Surface compound formation may also occur by a solid-state reaction between the active metal precursor and the support at high calcination temperatures. Reduction at high temperatures may lead to particle agglomeration when cohesive forces are dominant, and to so-called pillbox morphologies when adhesive forces are dominant. In both cases, the metal must be mobile. In contrast, when the support is mobile, sintering of the support can occur, and the small metal particles are stabilized on the reduced surface area (cohesive forces). Alternatively, if adhesive forces are dominant encapsulation (SMSI effect) may occur.

2.1.6. Spillover Phenomena

In multiphase solid catalysts *spillover* may occur of an active species (spillover species) adsorbed or formed on one phase (donor phase) onto a second phase (acceptor) which does not form the active species under the same conditions [55–57]. A well-known example is hydrogen spillover from Pt, on which dihydrogen chemisorbs dissociatively, onto WO_3 with formation of a tungsten bronze [58]. According to SOMORJAI [59] the spillover phenomenon must be regarded as one of the "modern concepts in surface science and heterogeneous catalysis". Nevertheless, the exact physical nature of spillover processes has only rarely been verified experimentally. The term is typically used to explain nonlinear effects (synergistic effects) of the combination of chemically different components of a catalytic material on its performance.

Besides hydrogen spillover, oxygen spillover has been postulated to play an important role in oxidation reactions catalyzed by mixed oxides. For example, the addition of antimony oxide to selective oxidation catalysts enhances the catalytic activity at high levels of selectivity by a factor of up to five relative to the Sb-free system, although antimony oxide itself is completely inactive.

Observations of this kind motivated DELMON et al. [60,61] to formulate the *remote-control concept* to explain the fact that all industrial catalysts used for the partial oxidation of hydrocarbons or in hydrotreatment are multiphasic and that particular phase compositions develop synergy effects. The remote-control concept is, however, not undisputed.

2.1.7. Phase-Cooperation and Site-Isolation Concepts

GRASSELLI [62] proposed the *phase-cooperation concept* for partial oxidation and ammoxidation reactions. It is suggested that two phases (e.g., α-$Bi_2Mo_3O_{12}$ and γ-Bi_2MoO_6) cooperate in the sense that one phase performs the actual catalytic function (α-phase) and the other (γ-phase) the reoxidation function. The concept could be verified for many other multiphase, multicomponent mixed metal oxide catalysts, such as multicomponent molybdates and multicomponent antimonates [62,63].

Another concept most relevant for selective oxidation and ammoxidation is the *site-isolation concept* first formulated by CALLAHAN and GRASSELLI [64]. Site isolation refers to the separation of active sites from each other on the surface of a heterogeneous catalyst and is considered to be the prerequisite for obtaining the desired selective partial oxidation products. The concept states that reactive surface lattice oxygen atoms must be structurally isolated from each other in defined groupings on a catalyst surface to achieve selectivity. The number of oxygen atoms in a given isolated grouping determines the reaction channel through the stoichiometry requirements imposed on the reaction by the availability of oxygen at the reaction site. It was postulated that two and up to five adjacent surface oxygen atoms would be required for the selective oxidation of propene to the desired product acrolein. Lattice groupings with more than five oxygen atoms would only produce total oxidation products (CO and CO_2), while completely isolated single oxygen atoms would be either inactive or could produce allyl radicals. The latter would couple in the vapor phase to give hexadiene and ultimately benzene. These scenarios are schematically shown in Figure 3.

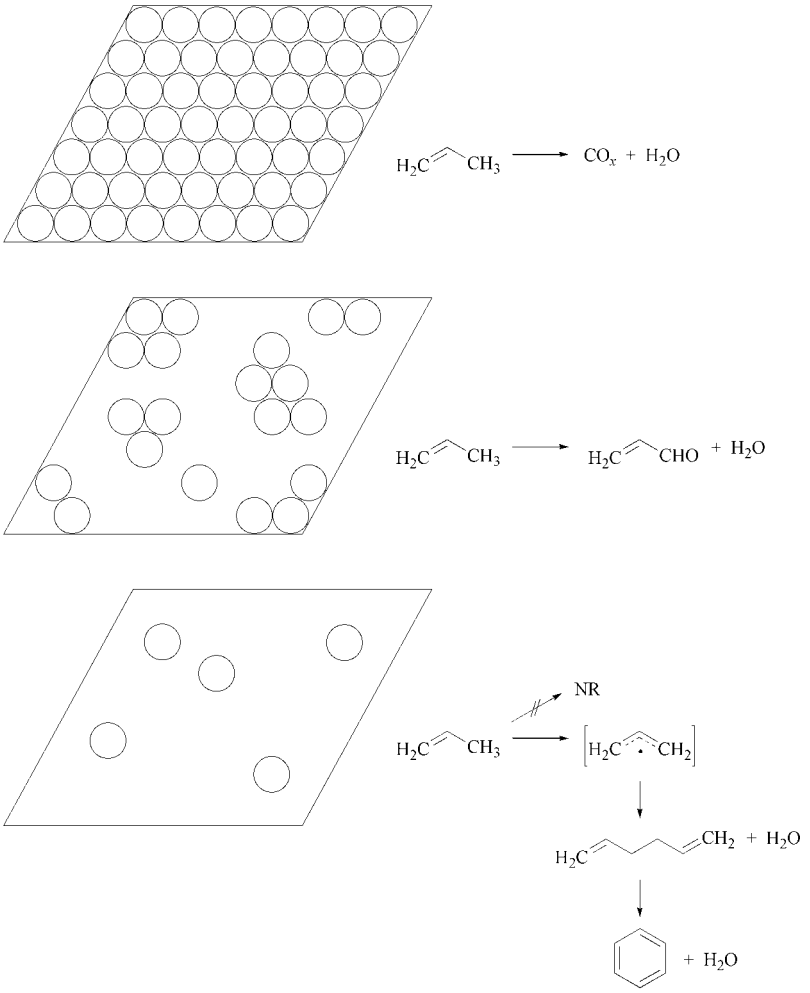

Figure 3. Site-isolation principle. Schematic of lattice oxygen arrangements on hypothetical surfaces. Anticipated reaction paths of propene upon contact with these surfaces (NR = no reaction; adopted from [62])

2.1.8. Shape-Selectivity Concept

Zeolites and related materials have crystalline structure and contain regular micropores, the diameters of which are determined by the structure of the materials. The pore sizes are well defined and have dimensions similar to those of small organic molecules. This permits *shape-selective catalysis* to occur. The geometric constraints may act on the sorption of reactants, on the transition state of the catalyzed reaction, or on the desorption of products. Correspondingly, shape-selective effects have been classified as providing reactant shape selectivity, restricted transition state shape selectivity, and product shape selectivity [65,66]. These scenarios are schematically illustrated in Figure 4 for the cracking of *n*-heptane and 1-methylhexane (reactant shape selectivity), for the transalkylation of *m*-xylene (transition state shape selectivity), and for the alkylation of toluene by methanol (product shape selectivity). In the first example, the kinetic diameter of *n*-heptane is smaller than that of 1-methylhexane. The latter is not able to enter micropores, so that shape-selective cracking of *n*-heptane takes place when both hydrocarbons are present in the feed. An example for shape-selective control of the transition

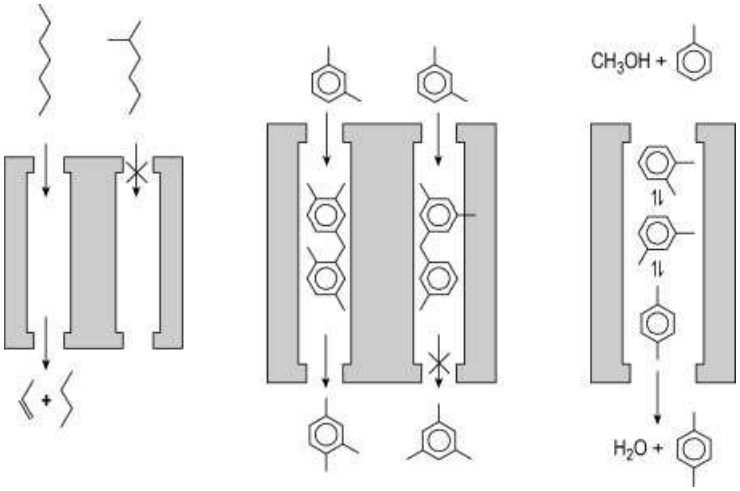

Figure 4. Classification of shape-selective effects

state is the transalkylation of *m*-xylene. The reaction is bimolecular and the formation of 1,2,4-trimethylbenzene has a less bulky transition state than the formation of 1,3,5-trimethylbenzene. The latter product can thus not be formed if the pore size and geometry is carefully adapted to the transition state requirements. Finally, p-xylene can be selectively formed by methylation of toluene with methanol and zeolites whose pore openings only allow *p*-xylene to be released. The *o* and *m* isomers either accumulate in zeolite cages or are isomerized to *p*-xylene.

2.1.9. Principles of the Catalytic Cycle

The most fundamental principle in catalysis is that of the *catalytic cycle*, which may be based on a redefinition of a catalyst by BOUDART [67]: "A catalyst is a substance that transforms reactants into products, through an *uninterrupted* and *repeated* cycle of elementary steps in which the catalyst is changed through a sequence of *reactive intermediates*, until the last step in the cycle regenerates the catalyst in its original form".

The catalytic substance or active sites may not be present originally, but may be formed by activation during the start-up phase of the catalytic reaction. The cycle must be uninterrupted and repeated since otherwise the reaction is stoichiometric rather than catalytic. The *number of turnovers*, a measure of catalyst life, must be greater than unity, since the catalyst would otherwise be a reagent. The total amount of catalyst (active sites) is typically small relative to the amounts of reactants and products involved (catalytic amounts). As a consequence, the reactive intermediates can be treated by the kinetic quasi-steady-state approximation of BODENSTEIN.

The *activity* of the catalyst is defined by the number of cycles per unit time or turnovers or turnover frequency (TOF; unit: s^{-1}). The *life* of the catalyst is defined by the number of cycles before it dies.

2.2. Kinetics of Heterogeneous Catalytic Reactions [67–76]

The catalytic cycle is the principle of catalytic action. The mechanism of a catalyzed reaction can be described by the sequence of elementary reaction steps of the cycle, including adsorption, surface diffusion, chemical transformations of adsorbed species, and desorption, and it is the basis for deriving the kinetics of the reaction. It is assumed that for each individual elementary step the transition-state theory is valid. An early treatise of the kinetics of heterogeneously catalyzed reactions was published by SCHWAB [77].

The various aspects of the dynamics of surface reactions and catalysis have been classified

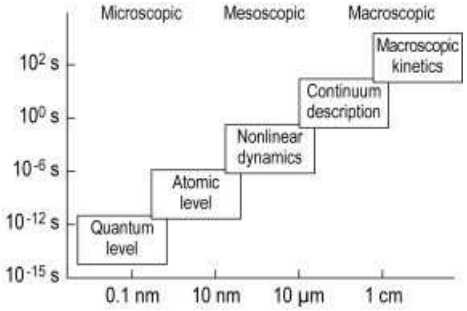

Figure 5. Schematic classification of the various aspects of the dynamics of surface reactions (adopted from [31])

by ERTL [31] into five categories in terms of time and length scales, as shown schematically in Figure 5. In the *macroscopic regime*, the rate of a catalytic reaction is modeled by fitting empirical equations, such as power laws, to experimental data, so as to describe its concentration and pressure dependence and to determine rate constants that depend exponentially on temperature. This approach was very useful in chemical engineering for reactor and process design. Assumptions about reaction schemes (kinetic models) provide correlations between the surface coverages of intermediates and the external variables, an approach that led to the Temkin equation [78] modeling the kinetics of ammonia synthesis.

Improved kinetic models could be developed when atomic processes on surfaces and the identification and characterization of surface species became available. The progress of a catalytic reaction is then described by a *microkinetics* approach by modeling the macroscopic kinetics through correlating atomic processes with macroscopic parameters within the framework of a suitable continuum model. Continuum variables for the partial surface coverages are, to a first approximation, correlated to external parameters (partial pressures and temperature) by the Langmuir lattice model of a surface consisting of identical noninteracting adsorption sites.

The formulation of rate laws for the full sequence of elementary reactions will usually lead to a set of nonlinear coupled (ordinary) differential equations for the concentrations (coverages) of the various surface species involved. The temporal behavior of the reaction system under constant continuous-flow conditions may be nonstationary transient. In certain parameter ranges it may be oscillatory or even chaotic. Also, there may be local variations in surface coverages which lead to coupling of the reaction with transport processes (e.g., particle diffusion, heat transfer). The formation of spatiotemporal concentration profiles on a *mesoscopic scale* is the consequence of these nonlinear dynamic phenomena.

Since the Langmuir lattice model is not valid in reality, the continuum model can describe the reaction kinetics only to a first approximation. Interactions between adsorbed species occur, and adsorbed particles occupy nonidentical sites, so that complications arise in the description of the reaction kinetics. Apart from the heterogeneity of adsorption sites, surfaces may undergo structural transformations. Surface science investigations provide information on these effects on an *atomic scale*.

As mentioned above, it is assumed that the transition-state theory is valid for description of the rates of individual elementary steps. This theory is based on the assumption that at all stages along the reaction coordinate thermal equilibrium is established. Temperature then is the only essential external macroscopic parameter. This assumption can only be valid if energy exchange between all degrees of motional freedom of the particles interacting with the solid acting as a heat bath is faster than the elementary step which induces nuclear motions. Energy transfer processes at the *quantum level* are the basic requirements for chemical transformations.

Nonlinear dynamics and the phenomena occuring at the atomic and quantum levels were reviewed by ERTL [31].

2.2.1. Concepts of Reaction Kinetics (Microkinetics)

The important concepts of (catalytic) reaction kinetics were reviewed by BOUDART [67,68, 79,80], and by CORTRIGHT and DUMESIC [74].

The term *microkinetics* was defined to denote reaction kinetics analyses that attempt to incorporate into the kinetic model the basic surface chemistry involved in the catalytic reaction at a molecular level [73,74]. An important prerequisite for this approach is that reaction rates are measured in the absence of heat- and mass-transfer limitations. The kinetic model is based on a description of the catalytic process in terms of information and/or assumptions about active sites and the nature of elementary steps that make up the catalytic cycle. The ultimate goal of a kinetic analysis is the determination of preexponential factors and activation energies (cf. Arrhenius equation) for all elementary steps in forward and reverse direction. Usually there is not sufficient information available to extract the values of all kinetic parameters. However, it has been established that in many cases the observed kinetics are controlled by a limited number of kinetic parameters [73,74]. Questions to be answered in this situation are: (1) how many kinetic parameters are required to calculate the overall rate from a reaction scheme? (2) What species are the *most abundant intermediates* on the catalyst surface under reaction conditions? (3) Does the reaction scheme include a *rate-determining step* for the kinetic parameters of interest under the reaction conditions? Generally, only a few parameters are kinetically significant, although it is difficult to predict which parameters control the overall rate of the catalytic process. Therefore, initial estimates require a larger set of parameters than are ultimately necessary for the kinetic description of the catalytic process of interest. Besides experimental values of kinetic parameters for individual elementary reactions (often resulting from surface science studies on single-crystal surfaces), quantum chemical calculations permit mechanistic investigations and predictions of kinetic parameters [36–38].

Assume that a kinetic model has been established which consists of n elementary steps, each proceeding at a net rate

$$r_i = r_{\mathrm{f}i} - r_{\mathrm{r}i} \; (\mathrm{i} = 1, 2, ..., n) \tag{1}$$

The subscripts f and r stand for "forward" and "reverse", respectively. As mentioned above, the validity of the Bodenstein steady-state concept can be assumed. The kinetic steady state is then defined by:

$$\sigma_i r = r_i \tag{2}$$

where r is the net rate $r_{\mathrm{f}} - r_{\mathrm{r}}$ of the overall catalytic reaction defined by a stoichiometric equation. σ_{i} is the stoichiometric number of the ith step, i.e., the number of times that this step must occur for the catalytic cycle to turnover once. If the transition-state theory is valid for each individual elementary step, the ratio of the forward rate $r_{\mathrm{f}i}$ to the reverse rate $r_{\mathrm{r}i}$ of step i is given by the De Donder relation [81,82]:

$$r_{\mathrm{f}i}/r_{\mathrm{r}i} = \exp(A_i/RT) \tag{3}$$

where A_i is the affinity of step i:

$$A_i = [\partial G_i/\partial \xi_i]_{T,P} \tag{4}$$

where ξ_i is the extent of reaction of step i.

At steady state, the affinity for each step but one may be very small as compared to the affinity A of the overall reaction. Each step but one is then in quasi-equilibrium. The step that is not in quasi-equilibrium (subscript d) is called the *rate-determining step* (rds) as defined by HORIUTI [83]. As a consequence of this definition, the following inequalities are valid:

$$r_{\mathrm{f}i} \gg r_{\mathrm{fd}}, \text{ and } r_{\mathrm{r}i} \gg r_{\mathrm{rd}} \; (i \neq \mathrm{d})$$

If there is an rds, then the affinity $A_i = 0$ for all values of i except for the rds ($i \neq \mathrm{d}$), i.e., all (or almost all) of the affinity for the catalytic cycle is dissipated in the rds, hence

$$A = \sigma_{\mathrm{d}} A_{\mathrm{d}} \tag{5}$$

It follows that

$$r_{\mathrm{f}}/r_{\mathrm{r}} = r_{\mathrm{fd}}/r_{\mathrm{rd}} \tag{6}$$

At steady state $\sigma_d(r_f - r_r) = r_{fd} - r_{rd}$. Hence

$$\sigma_d r_f = r_{fd} \text{ and } \sigma_d r_r = r_{rd}. \quad (7)$$

The stoichiometric equation for the overall reaction can always be written such that σ_d is equal to unity. It is then clear that the rds is appropriately and uniquely named as the step for which the forward and reverse rates are equal to the forward and reverse rates, respectively, of the overall reaction [67].

Clearly the rds (if there is one) is the only *kinetically significant step*. A kinetically significant step is one whose rate constants or equilibrium constant appear in the rate equation for the overall reaction. In some cases there is no rds in the Horiuti sense, but frequently only a few of the elementary steps in a catalytic cycle are kinetically significant. It is sometimes said that a rate-limiting step is the one having the smallest rate constant. However, rate constants can often not be compared because they have different dimensions.

The relative importance of rate constants of elementary steps in a catalytic cycle provides useful guidelines for the development of activity and selectivity. This can be achieved by *parametric sensitivity analysis* [84], which was first proposed by Campbell [85] for analysis of kinetic parameters of catalytic reactions (see also ref. [74]). Campbell [85] defined a *degree of rate control* for any rate constant k_i in a catalytic cycle turning over at a rate r

$$X_i = k_i/r \cdot \partial r/\partial k_i \quad (8)$$

where the equilibrium constant for step i and all other rate constants are held constant. The main advantage of this mathematical operation is its simplicity. It turns out that Horiuti's rds, as the only kinetically significant step in a catalytic cycle, has a degree of rate control $X_i = 1$, whereas the X values for all other steps are equal to zero. Clearly, all intermediate values of X_i are possible, and probable in most cases.

As a catalytic cycle turns over at the quasi-steady state, the steady-state concentrations (coverages) of the reactive intermediates may be significantly different from the values that they would attain if they were at equilibrium with fluid reactants or products. The steady-state concentrations (coverages) of reactive intermediates may be lower or higher than the equilibrium values. The reason for this phenomenon is *kinetic coupling* between elementary steps at the steady state, where the net rate of each step is equal to the net rate of the overall reaction multiplied by the stoichiometric number of the step. With kinetic coupling, a reactive intermediate can accumulate as a reactant or be depleted as a product [68,79,81].

The principle of *microscopic reversibility* is strictly valid only for reactions at equilibrium. Away from equilibrium, it remains valid provided that transition-state theory is still applicable, which appears to be the case in heterogeneous catalysis [19]. Hence, the principle remains valid for any elementary step in a heterogeneous catalytic reaction. However, the principle must be applied with caution to a catalytic cycle, as opposed to a single elementary reaction. If valid, the principle of microscopic reversibility allows the calculation of a rate constant if the second rate constant and the equilibrium constant K_i of an elementary reaction i are known: $k_{fi}/k_{ri} = K_i$.

2.2.2. Application of Microkinetic Analysis

Two of the most intensively studied systems in heterogeneous catalysis are CO oxidation over noble metals and ammonia synthesis. In both cases, pioneering work using microkinetic analysis led to a better understanding of the catalytic cycle and new fundamental insights, which supported design and optimization of the catalytic applications. In industry, CO oxidation over Pt and Pd was one of the first systems used for automobile emission control and is a key intermediate step in many technical systems for hydrocarbon transformations. Ammonia synthesis — once the driving force for a new chemical industry — still is one of the most important technical applications of heterogeneous catalysis. These technical aspects of CO oxidation and ammonia synthesis are discussed in Chapter Industrial Application and Mechanisms of Selected Technically Relevant Reactions. Since CO oxidation on noble metals has been the major working system in surface science and has led to elucidation of many fundamental issues of reactions on catalytic surfaces, such as oscillatory kinetics and

spatio-temporal pattern formation [86], this system will be exemplarily used for the illustration of microkinetic analysis.

CO oxidation on noble metals (Pt, Pd, etc.)

$$CO + 1/2O_2 \rightarrow CO_2 \quad (9)$$

is relatively well understood, based on surface science studies. Molecular oxygen is chemisorbed dissociatively, while CO binds associatively [87,88]. Molecular CO then reacts with atomic oxygen in the adsorbed state:

$$O_2 + 2^* \rightarrow O_{2,ads} \rightarrow 2O_{ads} \quad (10)$$

$$CO + * \rightarrow CO_{ads} \quad (11)$$

$$CO_{ads} + O_{ads} \rightarrow CO_2 + 2^* \quad (12)$$

Here * denotes a free surface site and the subscript "ads" an adsorbed species. The reaction steps (10)–(12) suggest that CO oxidation is a Langmuir – Hinshelwood process in which both reacting species are adsorbed on the catalyst surface. The reverse of reaction (10), i.e., the recombination of two oxygen atoms is kinetically insignificant at temperatures below ca. 600 K. Possible Eley – Rideal steps such as (13), in which a gas-phase molecule reacts with an adsorbed species

$$CO + O_{ads} \rightarrow CO_2 + * \quad (13)$$

were found to be unlikely.

Quantitative experiments led to a schematic one-dimensional potential-energy diagram characterizing the elementary steps on the Pd(111) surface (Fig. 6). Most of the energy is liberated upon adsorption of the reactants, and the activation barrier for the combination of the adsorbed intermediates is relatively small; this step is only weakly exothermic, and the heat of adsorption (activation energy for desorption) of CO_2 is very low.

The sequence of elementary steps (10) – (12) is quite simple. The overall kinetics, however, is not. This is due to the nonuniformity of the surface and segregation of the reactants into surface domains at higher coverages. As a consequence, the reaction between the surface species CO_{ads} and O_{ads} can only occur at the boundaries between these domains. A simple Langmuir – Hinshelwood treatment of the kinetics is therefore ruled out, except for the special case of low surface coverages by CO_{ads} and O_{ads}, when these are randomly distributed and can be considered to a first approximation as being part of an ideal surface.

2.2.3. Langmuir – Hinshelwood – Hougen – Watson Kinetics [89,70,72,90]

The Langmuir – Hinshelwood – Hougen – Watson (LHHW) approach is based on the Langmuir model describing the surface of a catalyst as an array of equivalent sites which do not interact either before or after chemisorption. Further, for derivation of rate equations, it is assumed that both reactants and products are equilibrated with surface species that react on

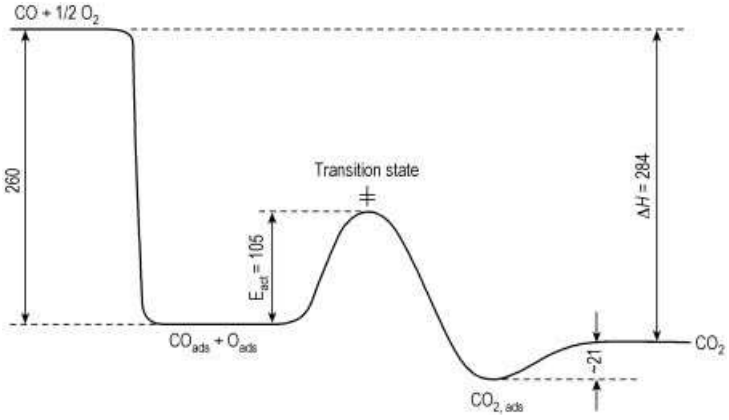

Figure 6. Schematic one-dimensional potential-energy diagram characterizing the CO + O_2 reaction on Pd(111) [88]

the surface in a rate-determining step. Surface coverages are correlated with partial pressures or concentrations in the fluid phase by means of Langmuir adsorption isotherms. It was mentioned above that the Langmuir model is unrealistic. Moreover, it was demonstrated in Section Concepts of Reaction Kinetics (Microkinetics) that the surface coverages of adsorbed species are by no means identical to the equilibrium values predicted by the Langmuir adsorption isotherm for reaction systems in which kinetic coupling occurs, and rate-determining steps do not generally exist.

Despite these weaknesses, the LHHW kinetics approach has proved valuable for modeling heterogeneous catalytic reactions for reactor and process design. The kinetic parameters which are determined by fitting the rate equations to experimental data, however, do not have a straightforward physical meaning. As an alternative, simple power-law kinetics for straightforward reactions (e.g., A $\rightarrow$ B) can be used for technical application.

Often it is difficult to discriminate between two or more kinetic models within the accuracy limits of the experimental data. Sophisticated mathematical procedures have therefore been developed for the discrimination of rival models [91].

As an example for a typical LHHW rate equation consider the reaction

$$A+B \rightleftharpoons C.$$

The form of rate equation is as follows [91]:

$$r = \frac{k_{rds} N_T K_i \,(P_A P_B - P_C/K_{eq})}{(1+K_A P_A + K_B P_B + K_C P_C + \sum_j K_j P_j)^n} = \frac{\text{rate factor} \times \text{driving force}}{\text{inhibition term}} \tag{14}$$

The numerator is a product of the rate constant of the rds k_{rds}, the concentration of active sites N_T, adsorption equilibrium constants K_i, and the driving force for the reaction. The latter is a measure of how far the overall reaction is from thermodynamic equilibrium. The overall equilibrium constant K_{eq}, can be calculated from thermodynamics. The denominator is an inhibition term which takes into account the competitive adsorption of reactants and products.

A few examples of LHHW rate equations are summarized in Table 3. A collection of useful LHHW rate equations and kinetic data for almost 100 industrially important catalytic reactions is available in [92].

Table 3. General structure of Langmuir type rate equations 90

Reaction	Controlling step	Net rate	Kinetic constant	Driving force	Adsorption term
1. $A \rightleftharpoons P$	a. adsorption of A	$k_A p_A(1-\Sigma\Theta) - k_A'\Theta_A$	k_A	$p_A - \frac{p_P}{K}$	$1 + K_A p_A + K_P p_P$
	b. surface reaction single-site mechanism	$k_S\Theta_P - k_S'\Theta_P$	$k_S K_A$	$p_A - \frac{p_P}{K}$	$1 + K_A p_A + K_P p_P$
	c. desorption of P	$k_P'\Theta_P - k_P p_P(1-\Sigma\Theta)$	$k_P' k_S K_A$	$p_A - \frac{p_P}{K}$	$1 + K_A p_A + K_P p_P$
2. $A \rightleftharpoons P+Q$	surface reaction, A (ads) reacts with vacant site	$k_S\Theta_A(1-\Sigma\Theta) - k_S\Theta_P$	$k_S K_A$	$p_A - \frac{p_P p_Q}{K}$	$(1 + K_A p_A + K_P p_P + K_Q p_Q)^2$
3. $A_2 \rightleftharpoons 2P$	a. dissociative adsorption of A_2	$k_A p_{A2}(1-\Sigma\Theta)^2 - k_A'\Theta_A$	k_A	$p_{A_2} - \frac{p_P^2}{K}$	$(1 + K_A p_{A2} + K_P p_P)^2$
	b. surface reaction following dissociative adsorption of A_2	$k_S\Theta_A - k_S'\Theta_P$	$k_S K_A$	$p_{A_2} - \frac{p_P}{K}$	$1 + K_A p_{A2} + K_P p_P$
4. $A+B \rightleftharpoons P$	a. adsorption of A	$k_A p_A(1-\Sigma\Theta) - k_A'\Theta_A$	k_A	$p_A - \frac{p_P}{K_{P_B}}$	$1 + K_A p_A + K_B p_B + K_P p_P$
	b. surface reaction	$k_S\Theta_A\Theta_B - k_S'\Theta_P(1-\Sigma\Theta)$	$k_S K_A K_B$	$p_A p_B - \frac{p_P}{K}$	$(1 + K_A p_A + K_B p_B + K_P p_P)^2$
	c. desorption of p	$k_P'\Theta_P - k_P p_P(1-\Sigma\Theta)$	$k_P' K_S K_A K_B$	$p_A p_B - \frac{p_P}{K}$	$1 + K_A p_A + K_B p_B + K_P p_P$
5. $\frac{1}{2}A+B \rightleftharpoons P$	dissociative adsorption of A_2, only half of which react	$k_A p_{A2}(1-\Sigma\Theta) - k_A'\Theta_A$	k_A	$p_{A_2} - \frac{p_P}{K_{P_B}}$	$1 + K_A p_{A2} + K_B p_B + K_P p_P$
6. $A+\frac{1}{2}B \rightleftharpoons P$	adsorption of A, which reacts with half of B produced from the dissociative adsorption of B_2	$k_A p_A(1-\Sigma\Theta) - k_A'\Theta_A$	k_A	$P_A - \frac{p_P}{K_{P_{B_2}}}$	$1 + K_A p_A + K_B p_{B2} + K_P p_P$
7. $A_2+2B \rightleftharpoons 2P$	a. dissociative adsorption of A_2	$k_A p_{A2}(1-\Sigma\Theta)^2 - k_A'\Theta_A{}^2$	k_A	$P_{A_2} - \frac{p_P^2}{K_{P_{B_2}}}$	$1 + K_A p_A + K_B p_B + K_P p_P$
	b. surface reaction following the dissociative of adsorption A	$k_S\Theta_A\Theta_B - k_S' p(1-\Sigma\Theta)$	$k_S K_A K_B$	$P_{A_2} p_B - \frac{p_P}{K}$	$1 + K_A p_{A2} + K_B p_B + K_P p_P$

2.2.4. Activity and Selectivity

Catalytic activity is expressed in terms of reaction rates, preferably normalized to the surface area of the active phase (e.g., metal surface area for supported metal catalysts). These surface areas can be obtained by suitable chemisorption techniques (see Section Physical Properties). As an alternative to these *areal rates*, *specific rates* are also used which are normalized to catalyst weight. The best possible measure of catalytic activity, however, is the *turnover rate* or *turnover frequency*, since it is normalized to the number of active sites and represents the rate at which the catalytic cycle turns over. For comparison of rates reported by different research groups, the methodology for the determination of the number of active sites must be carefully reported. The hitherto unresolved problem is that the site densities measured prior to the catalytic reaction are not necessarily identical to those available under reaction conditions.

A readily available measure of catalytic activity is *space – time yield*, expressed in units of amount of product made in the reactor per unit time and unit reactor volume.

A considerable obstacle for the comparison of catalytic activities for a given reaction that were obtained in different laboratories for the same catalyst is the use of different reactors. For a series of catalysts, reasonable comparisons of activities or rates are possible when relative values are used.

Conversion data alone, or conversion versus time plots are not sufficient as a measure of catalytic activity.

Selectivity can be defined as the amount of desired product obtained per amount of consumed reactant. Selectivity values are only useful if the conversion is also reported. A simple measure of selectivity is the *yield* (yield = selectivity × conversion). Selectivities can also be used to indicate the relative rates of two or more competing reactions; competition may occur when several reactants form products in parallel (type I):

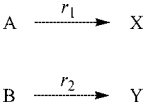

when one reactant transforms into several products in parallel (type II):

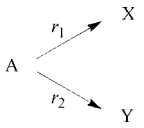

or in consecutive reactions (type III):

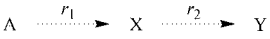

The selectivity is defined as the ratio of the rate of formation of the desired product to the rate of consumption of the starting material [93]. Thus, the selectivities for product X for the first-order reactions I and II is $r_1/(r_1 + r_2)$, whereas it is $(r_1 - r_2)/r_1$ for type III.

In the case of type I or II reactions, selectivity for X or Y is independent of the conversion of the starting material. In type III reactions, the selectivity for X is 100 % initially, decreases gradually with increasing conversion, and drops to zero at 100 % conversion. At an intermediate conversion, there is a maximum yield of X which depends on the ratio of the rate constants k_1 and k_2 of the rates r_1 and r_2. The integrated rate equations are:

$$[\mathrm{A}] = \exp(-k_1 t) \tag{15}$$

$$[\mathrm{X}] = k_1/(k_2 - k_1)\,[\exp(-k_1 t) - \exp(-k_2 t)] \tag{16}$$

where [A] is the concentration of unconverted A, [X] the concentration of A converted to product X, and t time. The maximum yield is reached at

$$t = (k_1 - k_2)^{-1} \ln(k_1/k_2) \tag{17}$$

2.3. Molecular Modeling in Heterogeneous Catalysis

Modeling of catalytic reactions is applied at many levels of complexity covering several orders of length and time scales. It ranges from complete description of the dynamics of a reaction through adsorbate – adsorbate interactions to the simple mean-field approximations

Table 4. Hierarchy of methods of modeling catalytic reactions

Method of modeling	Simplification	Application
Ab initio calculation	Most fundamental approach	Not yet significant in heterogeneous catalysis
Density functional theory (DFT)	Replacement of the *N*-electron wave function by the electron density	Dynamics of reactions, activation barriers, adsorbed structures, frequencies
Kinetic Monte Carlo (kMC)	Details of dynamics neglected	Adsorbate – adsorbate interactions on catalytic surfaces and nanoparticles
Langmuir – Hinshelwood (mean-field approximation, MF)	Detailed configuration of the adsorbate structure neglected	Microkinetic modeling of catalytic reactions in technical systems
Power-law kinetics	All mechanistic aspects neglected	Scaleup and reactor design for "black-box" systems

and macrokinetic models discussed in Section Langmuir – Hinshelwood – Hougen – Watson Kinetics. The different approaches can be represented in a hierarchy of models (Table 4).

In this section, frequently used models are presented that either describe the molecular behavior of the catalytic cycle directly or are based on the molecular picture. Often, the output of a computation using a more sophisticated method serves as input for a computation using a less detailed model; for instance activation energies computed by DFT are often used as parameters in kinetic Monte Carlo and simulations.

2.3.1. Density Functional Theory

In real ab initio calculations, in which the time-dependent Schrödinger equation is solved to obtain the complex *N*-electron wavefunction Ψ, the number of atoms of the system studied is very limited, and therefore quantum mechanical calculations in heterogeneous catalysis are almost exclusively based on the DFT approach. Based on the Hohenberg – Kohn theorem, the ground-state energy of an atom or molecule is completely determined by the electron density. Even though the exact functional dependence of the energy on the electron density is not known, approximate functionals can be developed (Kohn – Sham formalism) that lead to the much simpler computed electron density.

There are two major methods for DFT simulations of catalytic systems: In the first, the cluster algorithm, the molecules studied are metal clusters including the adsorbed particles. The advantage of this approach is that the special shape of catalytic clusters can be taken into account, and methods developed for gas-phase chemistry can be used, so that computational costs are relatively low. Disadvantages are the limited number of atoms in the cluster, currently (ca. 2008) a few hundred, and the fact that metal clusters in general have different properties to three-dimensional metals. Some prominent software tools using the cluster algorithm are GAUSSIAN [94] and TURBOMOLE [95].

The second approach, usually denoted by the terms "planar waves" or "periodic boundaries", is much more popular in heterogeneous catalysis. The algorithm is based on a supercell approach, i.e., structures to be calculated must be periodic in three dimensions. This approach is especially advantageous when considering surface structures, because a real solid surface is built on expansion from a small metal cluster or metal slab into three dimensions. In particular, the metallic properties are better described. The "third dimension" is a disadvantage, because the solid cell must be periodic in this direction as well. Aside from the problem of choosing appropriate functionals, the size of the cell and the convergence criteria are significant for DFT computations to provide reliable information. Some prominent software tools using the planar waves approach are CASTEP [96], DACAPO [97], and VASP [98].

Even though still very computer time consuming, DFT can be used to calculate the stability and frequencies for all reactants, intermediates, and products, as well as activation barriers of the elementary reactions [99–105]. Recently, complete reaction mechanisms including properties of intermediates have been developed based on DFT computations alone, for instance, for CO oxidation over RuO_2(110) [105], epoxidation of ethylene over Ag [106], methanol decomposition over Cu [107], ammonia synthesis over Ru [108], and decomposition of N_2O on Fe-ZSM-5 [109]. DFT simulation not only helps

to understand the fine details of catalytic reactions, for instance, the effect of surface steps on stability of intermediates [108] and the impact of coverage on activation energies [110], but also to elucidate the broader picture, for example, by finding a relationship between activation energy and chemisorption energy [111].

2.3.2. Kinetic Monte Carlo Simulation

Diffusion of adsorbates on catalytic surfaces is crucial for catalytic reactions. Furthermore, interactions between adsorbates can be substantial and lead to ordered structures such as islands and influence the energetic state of the surface, which also implies dependence of the activation barriers for adsorption, diffusion, reaction, and desorption on the surface coverage and the actual configuration of the adsorbates. The adsorbed species can be associated with a surface site, and thus a lattice representation of a two-dimensional surface can be constructed. In the case of catalytic particles, a three-dimensional structure can be used with individual two-dimensional facets that can differ in their catalytic activity. In the three-dimensional case, special care is needed for appropriate treatment of edges and corners. Even reconstruction of surfaces can be taken into account. At each surface site the local environment (presence of adsorbates, catalyst morphology/crystal phase) will determine the activation energies. If the interactions between the adsorbates, the surface, and the gas phase are known, such parameters could theoretically be derived from DFT simulations, and the kinetics can be computed by the kinetic Monte Carlo method (kMC) [105,112–118]. Each molecular event, i.e., adsorption, desorption, reaction, diffusion, is computed and leads to a new configuration of adsorbed species on the surface lattice. Aside from this very detailed description of the process, time averaging of the time-dependent computed reaction rates and surface coverage can then lead to overall rate expressions. However, the computational effort needed is immense, not only due to the kMC simulation but also because of the huge number of fundamental DFT computations needed to provide reliable activation barriers for all possible individual steps. Experimental derivation of this information is even more exhausting. Most of the adsorbate – adsorbate interactions, such as the formation of ordered structures, may appear at low temperature and pressure, where diffusion is slow and the rate of impingement of gas-phase molecules is small, respectively. Under these conditions kMC may be the only description that is accurate, while at high temperature and pressure, the adsorbates are rather randomly dispersed on the surface, and the assumptions of the mean-field approximation may be valid.

2.3.3. Mean-Field Approximation [119–122]

In the mean-field approximation, a continuous description is considered instead of the detailed configurations of the system discussed above. Hence, the local state of the catalytic surface on the macroscopic or mesoscopic scale can be represented by mean values by assuming randomly distributed adsorbates on the surface, which is viewed as being uniform. The state of the catalytic surface is described by the temperature T and a set of surface coverages θ_i, that is, the fraction of the surface covered with adsorbate i. The surface temperature and the coverages depend on time and spatial position in the macroscopic system (reactor), but are averaged over microscopic local fluctuations. Under those assumptions a chemical reaction can be defined as

$$\sum_{i=1}^{N_g+N_s+N_b} \nu'_{ik} A_i \rightarrow \sum_{i=1}^{N_g+N_s+N_b} \nu''_{ik} A_i$$

where A_i denote gas-phase species, surface species, and bulk species. The N_s surface species are those that are adsorbed on the top monoatomic layer of the catalytic particle, while the N_b bulk species are those found in the inner solid catalyst.

Steric effects of adsorbed species and various configurations, e.g., type of chemical bond between adsorbate and solid, can be taken into account by using the following concept: The surface structure is associated with a surface site density Γ that describes the maximum number of species that can be adsorbed on unit surface area. Each surface species is associated with a

coordination number σ_i describing the number of surface sites which are covered by this species. Under the assumptions made, a multistep (quasi-elementary) reaction mechanism can be set up. The molar net production rate is then given as

$$\overline{s}_i = \sum_{k=1}^{K_s} \nu_{ik} k_{f_k} \prod_{j=1}^{N_g+N_s+N_b} c_j^{\nu'_{jk}}.$$

where K_s is the number of surface reactions, c_i are the species concentrations, which are given, e.g., in mol m^{-2} for the N_s adsorbed species and in, e.g., mol m^{-3} for the N_g and N_b gaseous and bulk species. With $\Theta_i = c_i \sigma_i \Gamma^{-1}$, the variations of surface coverages follow:

$$\frac{\partial \Theta_i}{\partial t} = \frac{\overline{s}_i \sigma_i}{\Gamma}.$$

Since the temperature and concentrations of gaseous species depend on the local position in the reactor, the set of surface coverages also varies with position. However, no lateral interaction of the surface species between different locations on the catalytic surface is modeled in this approach. This assumption is justified by the fact that the computational cells in reactor simulations are usually much larger than the range of lateral interactions of the surface processes. In each of these cells, the state of the surface is characterized by mean values (mean-field approximation).

The binding states of adsorption of all species vary with the surface coverage, as discussed in Section Kinetic Monte Carlo Simulation. This additional coverage dependence can be modeled in the expression for the rate coefficient by an additional function leading to:

$$k_{f_k} = A_k T^{\beta_k} \exp\left[\frac{-E_{a_k}}{RT}\right] \prod_{i=1}^{N_s} \Theta_i^{\mu_{i_k}} \exp\left[\frac{\varepsilon_{i_k} \Theta_i}{RT}\right].$$

For adsorption reactions sticking coefficients are commonly used, which can be converted to conventional rate coefficients.

2.3.4. Development of Multistep Surface Reaction Mechanisms [122]

The development of a reliable surface reaction mechanism is a complex process. A tentative reaction mechanism can be proposed based on experimental surface-science studies, on analogy to gas-phase kinetics and organometallic compounds, and on theoretical studies, including DFT and kMC calculations as well as semi-empirical calculations [123,124]. This mechanism should include all possible paths for formation of the chemical species under consideration in order to be "elementary-like" and thus applicable over a wide range of conditions. The mechanistic idea then needs to be evaluated against numerous experimentally derived data, which are compared with theoretical predictions based on the mechanism. Here, simulations of the laboratory reactors require appropriate models for all significant processes in order to evaluate the intrinsic kinetics. Sensitivity analysis leads to the crucial steps in the mechanism, for which refined kinetic experiments and data may be needed.

Since the early 1990s, many groups have developed surface reaction mechanisms following these concepts. In particular, oxidation reactions over noble metals have been modeled extensively, such as those of hydrogen [125–129], CO [130–132], methane [133–137], and ethane [138–140] over Pt and formation of synthesis gas over Rh [141–142]. More recently, mechanisms have been established for more complex systems such as three-way catalysts [143] and chemical vapor deposition (CVD) of diamond [144,145], silica [146], and nanotubes [147]. A more detailed survey on existing microkinetic models can be found in [121].

3. Development of Solid Catalysts

The development of a catalytic process involves the search for the catalyst and the appropriate reactor, and typically occurs in a sequence of steps at different levels. Figure 7 shows a scheme summarizing this evolutionary process.

Small-scale reactors are used for screening to determine the optimal catalyst formulation. Since catalyst development and sequential screening are slow and cost-intensive processes, *high-throughput experimentation (HTE)* techniques [149–155] which permit parallel testing of small amounts of catalyst in automated systems have attracted great interest (see also →

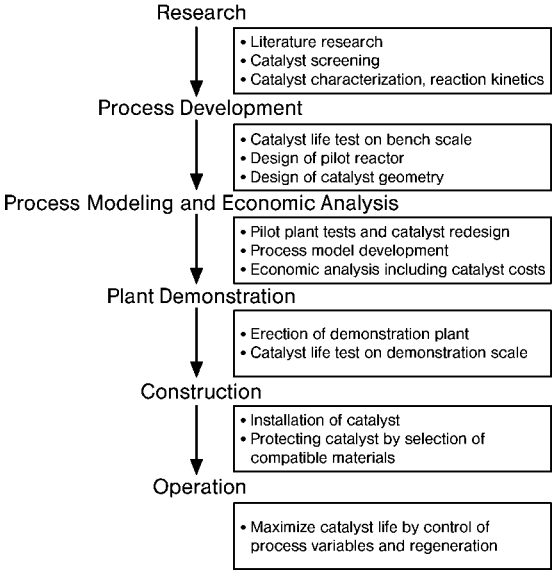

Figure 7. Scheme for catalyst development and design (from [148], modified)

Combinatorial Methods in Catalysis and Materials Science). Companies such as Symyx Technologies, Santa Clara (www.symyx.com), hte, Heidelberg (www.hte-company.de), and Avantium Technologies, Amsterdam (www.avantium.nl) already offer HTE-based development of catalysts or other materials. The HTE-based search for catalysts usually starts with a first phase (stage I or discovery) in which large catalyst libraries, often with several hundred materials, are categorized into promising and less promising candidates by use of relatively simple and fast analysis techniques. One example is infrared thermography for detection of exothermic reactions with spatial resolution. To decrease the number of experiments, optimization methods based on genetic algorithms may be used to derive subsequent catalyst generations from the performance of the members of the preceding generation [156]. In stage II, the more interesting materials, typically less than 50 candidates, are subjected to tests under much more realistic process conditions with more detailed characterization. For this purpose, a variety of parallel-reactor systems has been developed. A crucial point in high-throughput experimentation is the precise and fast analytical quantification of reaction starting materials and products. Especially promising for obtaining fast and detailed on-line information during catalyst testing is high-throughput multiplexing gas chromatography [155]. Instead of performing time-consuming chromatographic analyses during parallelized catalyst testing one after the other, samples are rapidly injected into the separation by means of a special multiplexing injector. The obtained chromatogram is a convolution of overlapping time-shifted single chromatograms and must therefore be mathematically deconvoluted. This new technique was successfully used for the study of palladium-catalyzed hydrogenation reactions [157].

High-throughput experimentation is a modern and accelerated version of classical catalyst development by trial and error. A famous early example of this approach is the discovery of the iron-based ammonia synthesis catalyst, during which 2500 catalysts were tested in 6500 experiments [9]. In recent years is has become evident that the empirical search for new or improved catalyst formulations can be successfully aided by knowledge-based (expert) systems or molecular design [158–160]. State-of-the-art computational tools for the effective molecular-scale design of catalytic materials are summarized in [161]. A striking example is the theoretical prediction of bimetallic ammonia synthesis catalysts [162]. As the rate-limiting step in heterogeneously catalyzed ammonia synthesis is the dissociative adsorption of

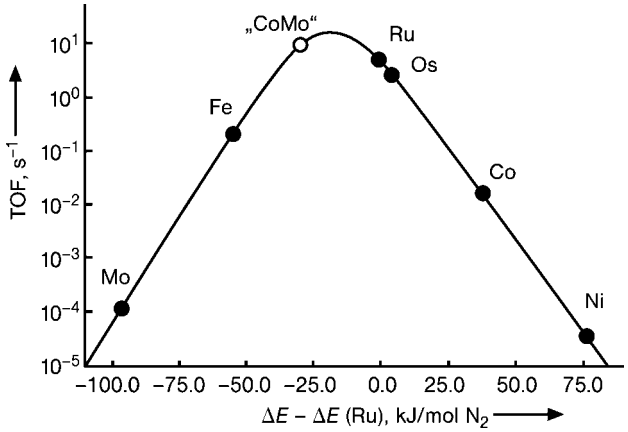

Figure 8. Calculated turnover frequencies (TOF) for ammonia synthesis as a function of the adsorption energy of nitrogen for various transition metals and alloys (reprinted with permission from [162]).

N_2, an optimum strength of the metal – nitrogen interaction is required for high ammonia synthesis activity. The resulting volcano-shaped relationship shows, in agreement with experimental evidence, that Ru and Os, followed by Fe, are the best pure metal catalysts (Figure 8).

First-principles DFT calculations were used to predict that alloys of metals with high and low adsorption energy should give rise to binding energies close to the optimum. Based on these calculations, a Co – Mo catalyst was developed that has much higher ammonium synthesis activity than the individual metals and is even better than Ru and Fe at low ammonia concentrations.

4. Classification of Solid Catalysts

Solid catalysts are extremely important in large-scale processes [163–167] for the conversion of chemicals, fuels, and pollutants. Many solid materials (elements and compounds) including metals, metal oxides, and metal sulfides, are catalysts. Only a few catalytic materials used in industry are simple in composition, e.g., pure metals (e.g., Ni) or binary oxides (such as γ-Al_2O_3, TiO_2). Typical industrial catalysts, however, consist of several components and phases. This complexity often makes it difficult to assess the catalytic material's structure.

In the following a variety of families of existing catalysts are described, and selected examples are given. These families include (1) unsupported (bulk) catalysts; (2) supported catalysts; (3) confined catalysts (ship-in-a-bottle catalysts); (4) hybrid catalysts; (5) polymerization catalysts, and several others. The selected examples not only include materials which are in use in industry, but also materials which are not yet mature for technological application but which have promising potential.

4.1. Unsupported (Bulk) Catalysts

4.1.1. Metal Oxides

Oxides are compounds of oxygen in which the O atom is the more strongly electronegative component. Oxides of metals are usually solids. Their bulk properties largely depend on the bonding character between metal and oxygen. Metal oxides have widely varying electronic properties and include insulators (e.g., Al_2O_3, SiO_2), semiconductors (e.g., TiO_2, NiO, ZnO), metallic conductors (typically reduced transition metal oxides such as TiO, NbO, and tungsten bronzes), superconductors (e.g., $BaPb_{1-x}Bi_xO_3$), and high-T_c superconductors (e.g., $YBa_2Cu_3O_{7-x}$).

Metal oxides make up a large and important class of catalytically active materials, their surface properties and chemistry being determined by their composition and structure, the bonding character, and the coordination of surface atoms and hydroxyl groups in exposed terminating crystallographic faces. They can develop acid-base and redox properties. Metal oxides can

have simple composition, like binary oxides, but many technologically important oxide catalysts are complex multicomponent materials.

4.1.1.1. Simple Binary Oxides

Simple binary oxides of base metals may behave as solid acids or bases or amphoteric materials [168]. These properties are closely related to their dissolution behavior in contact with aqueous solutions. Amphoteric oxides (e.g., Al_2O_3, ZnO) form cations in acidic and anions in basic milieu. Acidic oxides (e.g., SiO_2) dissolve with formation of acids or anions. Transition metal oxides in their highest oxidation state (e.g., V_2O_5, CrO_3) behave analogously. Basic oxides (e.g., MgO, lanthanide oxides) form hydroxides or dissolve by forming bases or cations. These dissolution properties must be considered when such oxides are used as supports and impregnated from aqueous solutions of the active phase precursor [169,170]. The dissolution properties also are closely related to the surface properties of the oxides in contact with a gas phase, where the degree of hydration/hydroxylation of the surface is a critical parameter. Silica, alumina and magnesia are commonly used catalysts and catalyst supports representative for a wide range of surface acid – base properties.

Aluminas are amphoteric oxides, which form a variety of different phases depending on the nature of the hydroxide or oxide hydroxide precursor and the conditions of their thermal decomposition. Bayerite, nordstrandite, boehmite, and gibbsite can be used as starting materials. The thermal evolution of the various poorly crystalline transitional phases (namely η-, Θ-, γ-, χ-, and κ-Al_2O_3) and of the final crystalline, thermodynamically stable α-Al_2O_3 phase (corundum) is shown in Figure 9. The structures of these oxides can be described as close-packed layers of oxo anions with Al^{3+} cations distributed between tetrahedral and octahedral vacancy positions. Stacking variations of the oxo anions result in the different crystallographic forms of alumina. The most commonly used transitional phases are η- and γ-Al_2O_3, which are often described as defect spinel structures [171] that incorporate Al^{3+} cations in both tetrahedral and octahedral sites. The Al sublattice is highly disordered, and irregular occupation of the tetrahedral interstices results in a tetragonal distortion of the spinel structure. There is a higher occupancy of tetrahedral cation positions in γ-Al_2O_3, and a higher density of stacking faults in the oxygen sublattice of η-Al_2O_3. Crystallites are preferentially terminated by anion layers, and these layers are occupied by hydroxyl groups for energetic reasons [172].

Acidic and basic sites and acid-base pair sites have been identified on the surfaces of aluminas [174]. Thermal treatment of hydroxylated oxides leads to partial dehydroxylation with formation of coordinatively unsaturated O^{2-} ions (basic sites) and an adjacent anion vacancy which exposes 3- or 5-coordinate Al^{3+} cations (Lewis acid sites). The remaining hydroxyl groups can be terminal or doubly or triply bridging with the participation of Al^{3+} in tetrahedral and/or octahedral positions. The properties of the resulting OH species range from very weakly Brønsted acidic to rather strongly basic and nucleophilic [172,174]. As a result of this complexity, alumina surfaces develop a rich surface chemistry and specific catalytic properties [175].

Besides their intrinsic catalytic properties and their use as catalysts in their own right (e.g., for elimination reactions, alkene isomerization [175], and the Claus process [176]),

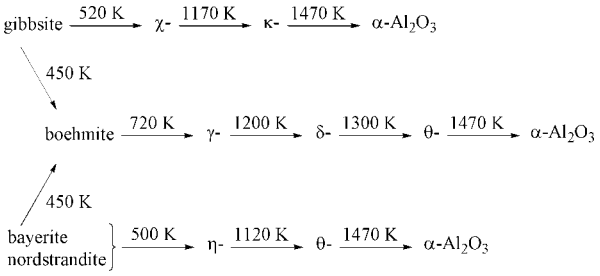

Figure 9. The dehydration sequences of the aluminum trihydroxides in air (adopted from [173])

aluminas are frequently used as catalyst supports for oxides and metals. The surface area and particle size of aluminas can be controlled by the preparation conditions, and their redox and thermal stability give the supported active phases high stability and ensure a long catalyst lifetime.

Silicas are weakly Brønsted acidic oxides which occur in a variety of structures such as quartz, tridymite and cristobalite (→ Silica) [177,178]. The most commonly used silica in catalysis is amorphous silica. The building blocks of silica are linked SiO_4 tetrahedra, with each O atom bridging two Si atoms. Bonding within the solid is covalent. At the fully hydrated surface, the bulk structure is terminated by hydroxyl (silanol) groups, SiOH [174,177,178]. Two types of these groups are usually distinguished: isolated groups and hydrogen-bonded vicinal groups. Fully hydrated samples, calcined at temperatures below 473 K, may contain geminal groups $Si(OH)_2$ [174,177,178]. Heating in vacuum removes the vicinal groups by dehydroxylation, i.e., condensation to form H_2O and Si – O – Si linkages (siloxane bridges). Complete removal of the hydroxyl groups occurs at temperatures well above 973 K in vacuo and is believed to result in significant changes in surface morphology.

The surface hydroxyl groups are only weakly Brønsted acidic and therefore hardly develop any catalytic activity. They are, however, amenable to hydrogen-bonding [179] and they are usually regarded as the most reactive native surface species, which are available for functionalization of silicas. The siloxane bridges are (at least after heating at elevated temperatures) essentially unreactive. For this reason and because of the low acidity of silanol groups, silicas are not used as active catalysts, but they play an important role as oxide supports and for the synthesis of functionalized oxide supports (see Section Supported Sulfide Catalysts).

Tailored silicas can be synthesized by controlling the preparation conditions [177,178]. Thus, surface area, particle size and morphology, porosity and mechanical stability can be varied by modification of the synthesis parameters.

In addition to amorphous silicas, the crystalline microporous silica silicalite I can be obtained by hydrothermal synthesis [180]. This material has MFI structure and can be considered as the parent siliceous extreme of zeolite ZSM-5.

Large-pore mesoporous structures, the so-called porosils, have also been reported [180–182]. The dimensions of their linear and parallel pores can be varied from 2 to 10 nm in a regular fashion. These pores can therefore accommodate bulky molecules and functional groups.

The incorporation of foreign elements such as Al^{3+} substituting for Si^{4+} induces Brønsted acidity and creates activity for acid catalysis.

Magnesium oxide is a basic solid. It has the simple rock salt structure, with octahedral coordination of magnesium and oxygen. Ab initio molecular orbital calculations indicated that the electronic structure is highly ionic, with the $Mg^{2+}O^{2-}$ formalism being an accurate representation of both bulk and surface structures [183]. The lattice is commonly envisaged to terminate in (100) planes incorporating five-coordinate (5c) Mg^{2+} and O^{2-} ions [184] (see Figure 10). This model appears to be physically accurate for MgO smoke, which may be regarded as a model crystalline metal oxide support [185]. Although the (100) plane is electrically neutral, hydroxyl groups are present on the surfaces of polycrystalline MgO. These groups and the O^{2-} anions are responsible for the basic properties, coordinatively unsaturated Mg^{2+} ions being only weak Lewis acid sites. The hydroxyl groups are also highly nucleophilic.

These properties dominate the surface chemistry of MgO. Organic Brønsted acids have been shown to be chemisorbed dissociatively to form surface-bound carbanions and surface hydroxyl groups [186]. Even the heterolytic dissociative adsorption of dihydrogen on polycrystalline MgO has been reported. $Mg^{2+}O^{2-}$ pairs with Mg^{2+} and O^{2-} in 4- or 3-coordination seem to play a crucial role.

The presence of low-coordinate Mg^{2+} and O^{2-} ions (see Figure 10) on the MgO surface after activation at high temperatures has been demonstrated [184,187,188], and the unique reactivity of 3c centers has been discussed [189].

MgO has also been used as a host matrix for transition metal ions (**solid solutions**) [190].

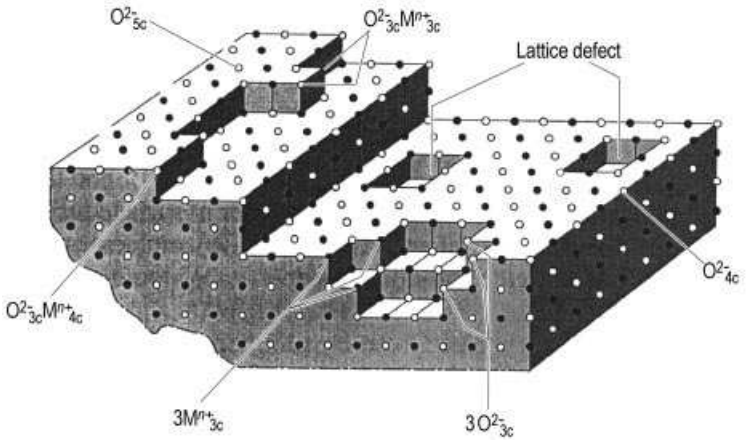

Figure 10. Representation of a surface plane (100) of MgO showing surface imperfections such as steps, kinks, and corners wich provide sites for ions of low coordination (adopted from [184]).

These materials permit the properties of isolated transition metal ions to be studied.

Transition metal oxides [191–193] can be structurally described as more or less dense packings of oxide anions, the interstices of which are occupied by cations. The bonding, however, is never purely ionic, but rather mixed ionic-covalent, sometimes also developing metallic character (e.g., bronzes). The surface of these oxides is often partially occupied by hydroxyl groups, so they possess some acidic character. However, it is the variability in oxidation states and the possibility of forming mixed-valence and nonstoichiometric compounds that are responsible for their important redox catalytic properties. The most frequently used transition metal oxides are those of the early transition metals (mostly suboxides). Fields of application are particularly selective oxidation and dehydrogenation reactions.

Titania TiO_2 exists in two major crystallographic forms: anatase and rutile. Anatase is the more frequently used modification since it develops a larger surface area, although it is a metastable phase and may undergo slow transformation into the thermodynamically stable rutile phase above ca. 900 K. Vanadium impurities seem to accelerate the rutilization above 820 K. Other impurities such as surface sulfate and phosphate seem to stabilize the anatase phase. The anatase → rutile phase transition must be sensitively controlled for supported VO_x/TiO_2, which plays a significant role in selective oxidation and NO_x reduction catalysis.

Titania is a semiconductor with a wide band gap and as such is an important material for photocatalysis [194,195].

Zirconia has attracted significant interest in the recent past as a catalyst support and as a base material for the preparation of strong solid acids by surface modification with sulfate or tungstate groups [196]. The most important crystallographic phases of ZrO_2 for catalytic applications are tetragonal and monoclinic. The latter is the thermodynamically stable phase. Higher surface areas, however, are developed by the metastable tetragonal phase, which is stabilized at low temperatures by sulfate impurities or intentional addition of sulfate or tungstate.

ZrO_2 is the base material for the solid-state electrolyte sensor for the measurement of oxygen partial pressure in, e.g., car exhaust gases [197]. The solid electrolyte shows high bulk conductivity for O^{2-} ions.

Other transition metal oxides are used as supported catalysts or as constituents of complex multicomponent catalysts.

Only a few examples are reported on the application of the unsupported binary oxides as catalysts. Iron oxide Fe_2O_3 and chromium oxide Cr_2O_3 catalyze the oxidative dehydrogenation of butenes to butadiene. Fe_2O_3-based catalysts are used in the high-temperature water gas shift reaction [198] and in the dehydrogenation of ethylbenzene [199]. Vanadium

pentoxide V_2O_5 is active for the selective oxidation of alkenes to saturated aldehydes [200]. Acidic transition metal oxides such as vanadium pentoxide and molybdenum trioxide MoO_3 can be used for the synthesis of formaldehyde by oxidative dehydrogenation of methanol, while the more basic iron oxide Fe_2O_3 leads to total oxidation [201]. Zinc oxide ZnO is used as a catalyst for the oxidation of cyclohexanol to cyclohexanone.

4.1.1.2. Complex Multicomponent Oxides

Complex multicomponent oxides play a major role as catalytic materials.

Aluminum silicates are among the most important ternary oxides. Four-valent Si atoms are isomorphously substituted by trivalent Al atoms in these materials. This substitution creates a negatively charged framework of interconnected tetrahedra. Exchangeable cations are required for charge compensation when protons are incorporated as charge-compensating cations, OH groups bridging Si and Al atoms are created which act as Brønsted acidic sites.

Amorphous silica – alumina can be prepared by precipitation from solution. This mixed oxide is a constituent of hydrocarbon cracking catalysts.

Zeolites Hydrothermal synthesis can be used for preparation of a large family of crystalline aluminosilicates, known as *zeolites* (→ Zeolites), which are microporous solids with pore sizes ranging from ca. 3 to 7 Å [180,202,203]. Characteristic properties of these structurally well-defined solids are selective sorption of small molecules (molecular sieves), ion exchange, and large surface areas. Zeolites possess a framework structure of corner-linked SiO_4^{4-} and AlO_4^{5-} tetrahedra with two-coordinate oxygen atoms that bridge two tetrahedral centers (so-called T atoms). Zeolite frameworks are open and contain channels (straight or sinusoidal) or cages of spherical or other shapes. These cages are typically interconnected by channels. The evolution of several zeolite structures from the primary tetrahedra via secondary building blocks is demonstrated in Figure 11 [204]. The diameter of the channels is determined by the number n of T atoms surrounding the opening of the channels as n-membered rings. Small-pore zeolites contain 6- or 8-membered rings (diameter d: $2.8 < d < 4$ Å), medium-pore zeolites contain 10-membered rings ($5 < d < 6$ Å) and the openings of large-pore zeolites are constructed of 12-membered rings ($d > 7$ Å). Examples of small-pore zeolites are sodalite and zeolite A, of medium-pore zeolites ZSM-type zeolites (see Figure 11), while large-pore zeolites include faujasites and zeolites X and Y (see Figure 11).

The H forms of zeolites develop strong Brønsted acidity and play a major role in large-scale industrial processes such as catalytic cracking, the Mobil MTG (methanol-to-gasoline) process and several others.

Besides Si and Al as T atoms P atoms can also be incorporated in zeolite structures. In addition, transition metal atoms such as Ti, V, and Cr can substitute for Si, which leads to oxidation catalysts of which titanium-silicalite-1 (TS1) is the most outstanding catalyst for oxidation, hydroxylation, and ammoxidation with aqueous H_2O_2 [205].

Basic properties can be created in zeolites by ion-exchange with large alkali metal ions such as Cs^+ and additional loading with CsO [206].

Aluminum phosphates (AlPO) [207,208] are another family of materials whose structures are similar to those of zeolites. They can be regarded as zeolites in which the T atoms are Si and Al. More recently they have been named zeotypes, the T atoms of which are Al and P. In contrast to aluminosilicate zeolites, AlPOs typically have a Al/P atomic ratio of 1/1, so that the framework composition $[AlPO_4]$ is neutral. Therefore, these solids are nonacidic and have hardly any application as catalysts. However, acidity can be introduced by substituting Al^{3+} by divalent atoms, which yields *metal aluminophosphates* (MAPOs), e.g., MnAPO or CoAPO, or by partial substitution of formally pentavalent P by Si^{4+} to give *silicoaluminophosphates* (SAPO). The AlPO family contains members with many different topologies which span a wider range of pore diameters than aluminosilicate zeolites.

Mesoporous solid acids with well-defined pore structures can be obtained by replacing a certain amount of Si atoms in MCM-type oxides by Al atoms.

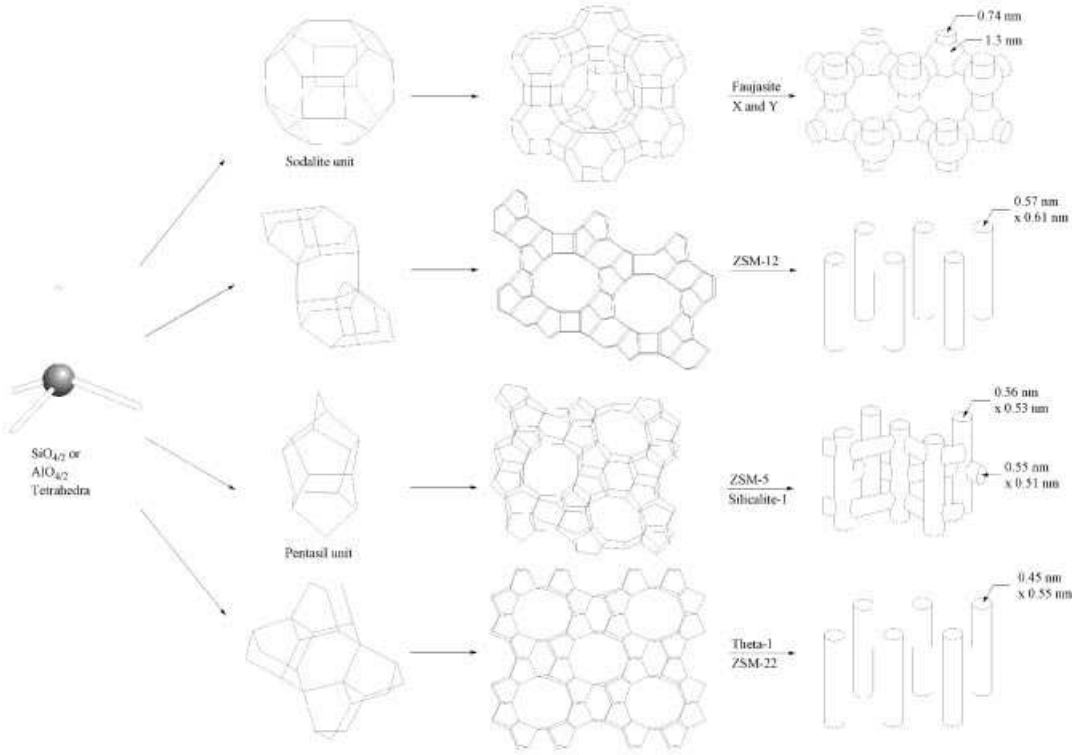

Figure 11. Structures of four representative zeolites and their micropore systems and dimensions [204]

Clays (→ Clays) are aluminosilicate minerals (montmorillonite, phyllosilicates (smectites), bentonites, and others). Montmorillonite is an aluminohydroxysilicate and is the main constituent of most clay minerals. It is a 2 : 1 clay, i.e., one octahedral AlO_6 layer is sandwiched between two tetrahedral SiO_4 layers. Montmorillonites are reversibly swellable and possess ion-exchange capacity. They can be used as catalyst supports. The structural layers can be linked together by introducing inorganic pillars which prevent the layers from collapsing at higher temperatures when the swelling agent is evaporated (pillared clays) [209]. A bimodal micro-/mesoporous pore size distribution can thus be obtained. Pillaring can be achieved with a wide variety of reagents including hydroxy aluminum polymers, zirconia hydroxy polymers, silica, and silicate pillars. Catalytically active components may be built in by the pillaring material, e.g., transition metal oxide pillars.

Mixed metal oxides are multimetal multiphase oxides which typically contain one or more transition metal oxide and exhibit significant chemical and structural complexity [210,211]. Their detailed characterization is therefore extremely difficult, and structure-property relationships can only be established in exceptional cases. Bulk mixed metal oxide catalysts are widely applied in selective oxidation, oxydehydrogenation, ammoxidation and other redox reactions. Several examples of mixed metal oxides and their application in industrial processes are summarized in Table 5.

Vanadium phosphates (e.g., $VOHPO_4 \cdot 0.5\ H_2O$) are precursors for the so-called *VPO catalysts*, which catalyze ammoxidation reactions and the selective oxidation of *n*-butane to maleic anhydride. It is proposed that the crystalline vanadyl pyrophosphate phase $(VO)_2P_2O_7$ is responsible for the catalytic properties of the VPO system. The vanadium phosphate precur-

Table 5. Examples of mixed metal oxide catalysts and their applications*

Catalyst	Active phases	Industrial processes
Copper chromite	$CuCr_2O_4$, CuO	low-temperature CO conversion, oxidations, hydrogenation
Zinc chromite	$ZnCr_2O_4$, ZnO	methanol synthesis (high pressure)
Copper/zinc chromite	$Cu_xZn_{1-x}Cr_2O_4$, CuO	methanol synthesis (low pressure)
Iron molybdate	$Fe(MoO_4)_3$, MoO_3	methanol to formaldehyde
Zinc ferrite	$ZnFe_2O_4$	oxidative dehydrogenation
Chromia – alumina	$Cr_xAl_{2-x}O_3$	dehydrogenation of light alkanes

*Adapted from [210]

sor undergoes transformations in reducing and oxidizing atmospheres, as shown in the following scheme [212]:

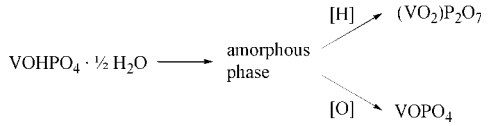

As discussed by GRASSELLI [63] effective ammoxidation (and oxidation) catalysts are multifunctional and need several key properties, including active sites which are composed of at least two vicinal oxide species of optimal metal – oxygen bond strengths. Both species must be readily reducible and reoxidizable.

The individual active sites must be spatially isolated from each other (site-isolation concept) to achieve the desired product selectivities. They should either be able to dissociate dioxygen and to incorporate the oxygen atoms into the lattice, or they must be located close to auxiliary reoxidation sites which contain metals having a facile redox couple. These sites are generally distinct from each other. They must, however, be able to communicate with each other electronically and spatially so that electrons, lattice oxygen, and anion vacancies can readily move between them. The lattice must be able to tolerate a certain density of anion vacancies without structural collapse [63]. It is clear that these complex requirements can only be achieved by multicomponent materials.

GRASSELLI [63,213] has listed three key catalytic functionalities required for effective ammoxidation/oxidation catalysts:

1. An α-H-abstracting component, which may be Bi^{3+}, Sb^{3+}, Te^{4+}, or Se^{4+}.
2. A component that chemisorbs alkene/ammonia and inserts oxygen/nitrogen (Mo^{6+}, Sb^{5+}).
3. A redox couple such as Fe^{2+}/Fe^{3+}, Ce^{3+}/Ce^{4+}, or U^{5+}/U^{6+} to facilitate lattice oxygen transfer between bulk and surface of the solid catalyst.

An empirical correlation was found between the electron configurations of the various metal cations and their respective functionalities [63,213] as shown in Table 6. This correlation can be used to design efficient catalysts.

Bismuth molybdates are among the most important catalysts for selective oxidation and ammoxidation of hydrocarbons [212,63]. The phase diagram shown in Figure 12 demonstrates the structural complexity of this class of ternary oxides [214]. The catalytically most important phases lie in the compositional range Bi/Mo atomic ratio between 2/3 and 2/1 and are

Table 6. Electronic structure of some catalytically active elements and their functionalities [213]

α-H abstraction	Alkene chemisorption/O insertion	Redox couple	Example
Bi^{3+} $5d^{10}6s^26p^0$	Mo^{6+} $4d^05s^0$	Ce^{3+}/Ce^{4+}	$Bi_2O_3 \cdot nMoO_3$
		Fe^{2+}/Fe^{3+}	$M_a^{2+}M_b^{3+}Bi_xMo_yO_z$
Te^{4+} $4d^{10}5s^25p^0$	Mo^{6+} $4d^05s^0$	Ce^{3+}/Ce^{4+}	Te_2MoO_7
			$(Te_aCe_bMo_v)O_z$
Sb^{3+} $4d^{10}5s^25p^0$	Sb^{5+} $5d^05s^0$	Fe^{2+}/Fe^{3+}	$Fe_xSb_yO_z$
U^{5+} $5f^16d^07s^0$	Sb^{5+} $5s^05p^0$	U^{5+}/U^{6+}	USb_3O_{10}
Se^{4+} $3d^{10}4s^24p^0$	Te^{6+} $5s^05p^0$	Fe^{2+}/Fe^{3+}	$Fe_aSe_b^{4+}Te_c^{6+}O_x$

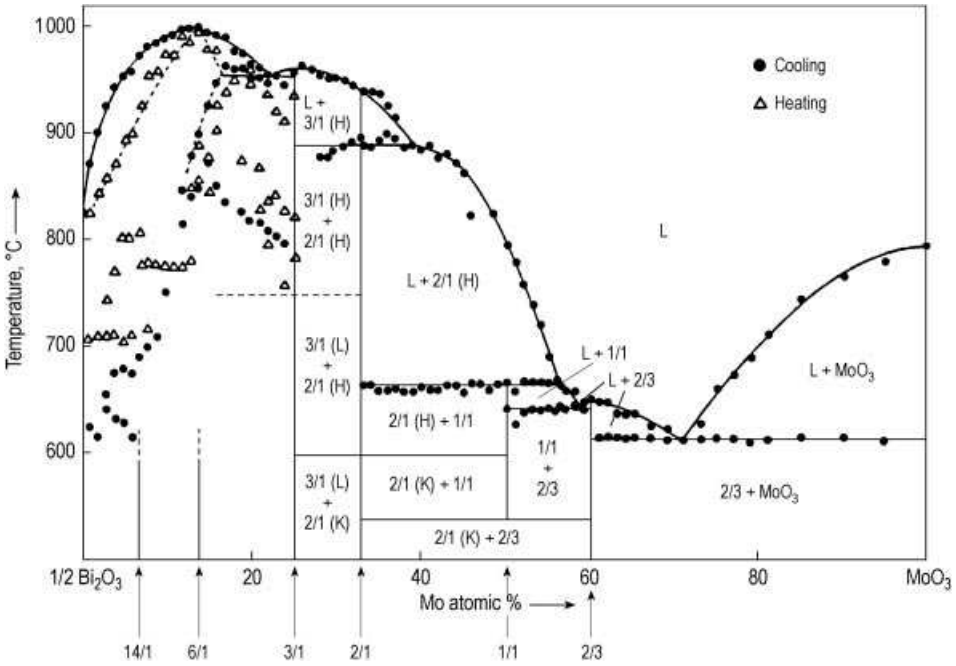

Figure 12. Phase compositions
2/3: $Bi_2O_3 \cdot 3\ MoO_3$; 1/1: $Bi_2O_3 \cdot 2\ MoO_3$; 2/1 (K): $Bi_2O_3 \cdot MoO_3$ (koechlinite); 2/1 (H): $Bi_2O_3 \cdot MoO_3$ (high-temperature form); 3/1 (L): $3\ Bi_2O_3 \cdot 2\ MoO_3$ (low-temperature form); 3/1 (H): $3\ Bi_2O_3 \cdot 2\ MoO_3$ (high-temperature form) [64]

α-$Bi_2Mo_3O_{12}$, β-$Bi_2Mo_2O_9$, and γ-Bi_2MoO_6. An industrially used Bi molybdate catalyst was optimized in several steps and has the empirical formula $(K,Cs)_a(Ni,Co,Mn)_{9.5}(Fe,Cr)_{2.5}BiMo_{12}O_x$ [63]. This material is supported on 50 % SiO_2 and was subsequently optimized further to give a catalyst with the empirical formula $(K,Cs)_a(Ni,Mg,Mn)_{7.5}(Fe,Cr)_{2.3}Bi_{0.5}Mo_{12}O_x$.

Antimonites are a second important class of ammoxidation catalysts [63], the most important of which are those containing at least one of the elements U, Fe, Sn, Mn, or Ce, which all have multiple oxidation states. Many formulations of catalysts have been proposed over the years. Those of current commercial interest have extremely complex compositions, e.g., $Na_{0-3}(Cu,Mg,Zn,Ni)_{0-4}(V,W)_{0.05-1}Mo_{0.1-2.5}Te_{0.2-5}Fe_{10}Sb_{13-20}O_x$ [63,215].

Scheelites Numerous multicomponent oxides adopting the scheelite ($CaWO_4$) structure with the general formula ABO_4 are known [216]. This structure tolerates cation replacements irrespective of valency provided that A is a larger cation than B and that there is charge balance. An additional property of the scheelite structure is that it is often stable with 30 % or more vacancies in the A cation sublattice. As an example, $Pb^{2+}_{1-3x}Bi^{3+}_{2x}\square_x Mo^{6+}O^{2-}_4$, where f indicates a vacancy in the Bi^{3+} (A cation) sublattice, possesses scheelite structure. The materials are active for selective oxidation of C_3 and C_4 alkenes, which involves formation of allyl species followed by extraction of O^{2-} from the lattice. Replenishment of the created vacancies occurs by oxygen chemisorption at other sites and diffusion of O^{2-} ions within the solid. The introduction of A cation vacancies has a significant effect on allyl formation, and the more open structure which prevails when cation vacancies are present facilitates O^{2-} transport.

Perovskite is a mineral ($CaTiO_3$) which is the parent solid for a whole family of multicomponent oxides with the general formula ABO_3 [191,217]. The common feature, which also resembles that of the scheelite-type oxides, is the simultaneous presence of a small, often highly charged, B cation and a large cation A, often having a low charge. The structure also tolerates a wide variety of compositions. As an example,

$La^{3+}_{1-x}Sr^{2+}_{x}Y^{3+}O^{2-}_{3-1/2x}$ is active for methane coupling. Other applications of perovskite-type oxides in catalysis are in fuel cells, as catalysts for combustion and for $DeNO_x$ reactions.

Hydrotalcites are another family of solids which tolerate rather flexible compositions [210,218,219]. Hydrotalcite is a clay mineral. It is a hydroxycarbonate of Mg and Al of general formula $[Mg_6Al_2(OH)_{16}]CO_3 \cdot 4H_2O$. The compositional flexibility of the hydrotalcite lattice permits the incorporation of many different metal cations and anions to yield solids with the general formula $[M^{2+}_{1-x}M^{3+}_{x}(OH)]^{x+}(A^{n-})_{x/n} \cdot nH_2O$ ($M^{2+} = Mg^{2+}$, Ni^{2+}, Zn^{2+} ect.; $M^{3+} = Al^{3+}$, Fe^{3+}, Cr^{3+}, etc.; $A^{n-} = CO_3^{2-}$, SO_4^{2-}, NO_3^-, etc.). Hydrotalcites develop large surface areas and basic properties. They have consequently been applied as solid catalysts for base-catalyzed reactions for fine-chemicals synthesis, polymerization of alkene oxides, aldol condensation, etc. Hydrotalcite-type phases (and also malachite (rosasite)- and copper zinc hydroxycarbonate (aurichalcite)-type phases) can also be used as precursors for the synthesis of mixed oxides by thermal decomposition, for example, Cu – Zn and Cu – Zn – Cr catalysts [210].

Heteropolyanions are polymeric oxo anions (*polyoxometalates*) formed by condensation of more than two kinds of oxo anions [220,221]. The amphoteric metals of Groups 5 (V, Nb, Ta) and 6 (Cr, Mo, W) in the +5 and +6 oxidation states, respectively, form weak acids which readily condense to form anions containing several molecules of the acid anhydride. Isopolyacids and their salts contain only one type of acid anhydride. Condensation can also occur with other acids (e.g., phosphoric or silicic) to form heteropolyacids and salts. About 70 elements can act as central heteroatoms in heteropolyanions. The structures of heteropolyanions are classified into several families according to similarities of composition and structure, such as Keggin type $XM_{12}O_{40}{}^{n-}$, Dawson type $X_2M_{18}O_{62}{}^{n-}$, and Anderson type $XM_6O_{24}{}^{n-}$, where X stands for the heteroatom. The most common structural feature is the Keggin anion, for which the catalytic properties have been studied extensively. Typically the M atoms in catalytic applications are either Mo or W. Heteropoly compounds can be applied as heterogeneous catalysts in their solid state. Their catalytic performance is determined by the primary structure (polyanion), the secondary structure (three-dimensional arrangement of polyanions, counter cations, and water of crystallization, etc.), and the tertiary structure (particle size, pore structure, etc.) [222,223]. In contrast to conventional heterogeneous catalysts, on which reactions occur at the surface, the reactants are accommodated in the bulk of the secondary structure of heteropoly compounds. Certain heteropolyacids are flexible, and polar molecules are easily absorbed in interstitial positions of the bulk solid, where they form a pseudoliquid phase [222,223].

Heteropoly compounds develop acidic and oxidizing functions, so that they can be used for acid and redox catalysis. In addition, polyanions are well-defined oxide clusters. Catalyst design is therefore possible at the molecular level. The pseudoliquid provides a unique reaction environment.

Some solid heteropolyacids have high thermal stability and are therefore suitable for vapor-phase reactions at elevated temperatures. The thermal stability of several heteropolyacids decreases in the sequence $H_3PW_{12}O_{40} > H_4SiW_{12}O_{40} > H_3PMo_{12}O_{40} > H_4SiMo_{12}O_{40}$ [222,223]. It can be enhanced by formation of the appropriate salts [224,225].

Because of their multifunctionality, heteropolyacids catalyze a wide variety of reactions including hydration and dehydration, condensation, reduction, oxidation, and carbonylation chemistry with Keggin-type anions of V, Mo [223,224,226–228]. A commercially important process, the oxidation of methacrolein, is catalyzed by a Cs salt of $H_4PVMo_{11}O_{40}$. Heteropoly salts with extremely complex compositions have been proposed, e.g., for the oxydehydrogenation of ethane. A Keggin-type molybdophosphoric salt with formula $K_2P_{1.2}MO_{10}W_1Sb_1Fe_1Cr_{0.5}Ce_{0.75}O_n$ was found to be the most efficient among the tested solids in terms of activity, selectivity, and stability [229].

4.1.2. Metals and Metal Alloys

Metals and metal alloys are used as bulk, unsupported catalysts in only a few cases. *Metal*

gauzes or *grids* are used as bulk catalysts in strongly exothermic reactions which require catalyst beds of small height. Typical examples are platinum – rhodium grids used for ammonia oxidation in the nitric acid process [230] and silver grids for the dehydrogenation of methane to formaldehyde.

Skeletal (*Raney-type*) *catalysts*, particularly skeletal nickel catalysts, are technologically important materials [231] which are specifically applied in hydrogenation reactions. However, their application is limited to liquid-phase reactions. They are used in particular for the production of fine chemicals and pharmaceuticals. Skeletal catalysts are prepared by the selective removal of aluminum from Ni – Al alloy particles by leaching with aqueous sodium hydroxide [231]. Besides skeletal Ni, cobalt, copper, platinum, ruthenium, and palladium catalysts have been prepared, with surface areas between 30 and 100 $m^2\ g^{-1}$. One of the advantages of skeletal metal catalysts is that they can be stored in the form of the active metal and therefore require no pre-reduction prior to use, unlike conventional catalysts, the precursors of which are oxides of the active metal supported on a carrier.

Fused catalysts are particularly used as alloy catalysts. The synthesis from a homogeneous melt by rapid cooling may yield metastable materials with compositions that can otherwise not be achieved [232]. Amorphous metal alloys have also been prepared (metallic glasses) [232,233].

Oxide materials can also be fused for catalytic applications [232]. Such oxides exhibit a complex and reactive internal interface structure which may be useful either for direct catalytic application in oxidation reactions or in predetermining the micromorphology of resulting catalytic materials when the oxide is the catalyst precursor. The prototype of such a catalyst is the multiply promoted iron oxide precursor of catalysts used for ammonia synthesis [48,234].

4.1.3. Carbides and Nitrides [48,235]

Monometallic carbides and nitrides of early transition metals often adopt simple crystal structures in which the metal atoms are arranged in cubic close-packed (ccp), hexagonal close-packed (hcp), or simple hexagonal (hex) arrays. C and N atoms occupy interstitial positions between metal atoms (interstitial alloys). The materials have unique properties in terms of melting point (> 3300 K), hardness (> 2000 kg mm^{-2}), and strength ($> 3 \times 10^5$ MPa). Their physical properties resemble those of ceramic materials, although their electronic and magnetic properties are typical of metals. Carbon in the carbides donates electrons to the d band of the metal, thus making the electronic characteristics of, e.g., tungsten and molybdenum resemble more closely those of the platinum group metals.

Bulk carbides and nitrides, e.g., of tungsten and molybdenum, can be prepared with surface areas between 100 and 400 $m^2\ g^{-1}$ by advanced synthetic procedures [235], so that they can be applied as bulk catalysts. They catalyze a variety of reactions for which noble metals are still preferentially used. Carbides and nitrides are exceptionally good hydrogenation catalysts, and they are active in hydrazine decomposition. Carbides of tungsten and molybdenum are also highly active for methane reforming, Fischer – Tropsch synthesis of hydrocarbons and alcohols, and hydrodesulfurization, and the nitrides are active for ammonia synthesis and hydrodenitrogenation [234]. The catalytic properties of carbides can be fine tuned by treatment with oxygen, which leads to the formation of oxycarbides [236]. While clean molybdenum carbide is an excellent catalyst for C – N bond cleavage (cracking of hydrocarbons), molybdenum oxide carbide is selective for skeletal isomerization [236].

In conclusion, carbides and nitrides, especially those of tungsten and molybdenum, may well be considered as future substitutes for platinum and other metals of Groups 8 – 10 as catalysts.

4.1.4. Carbons [237]

Although carbons are frequently used as catalyst supports, they may also be used as catalysts in their own right [238,239]. Carbons exist in a variety of thermodynamic phases (allotropes of carbon) and metastable structures, which are often ill defined (see also → Carbon,

1. General). The surface chemistry of carbons is rather complex [174,237]. Carbon surfaces may contain a variety of functional groups, particularly those containing oxygen, depending on the provenience and pretreatment of the carbon. At a single adsorption site several chemically inequivalent types of heteroatom bonds may form. Strong interactions between surface functional groups further complicate the variety of surface chemical structures derived for the most important carbon – oxygen system. Two functions of the carbon surface act simultaneously during a catalytic reaction. Firstly, the reactants are chemisorbed selectively on the carbon surface by ion exchange via oxygen functional groups or directly by dispersion forces involving the graphite valence-electron system. The second function is the production of atomic oxygen occurring on the graphene basal faces of all sp^2 carbon materials [237].

Carbon can already be catalytically active under ambient conditions and in aqueous media. Therefore efforts have been made to apply carbons as catalysts in condensed phases. Its application in the gas phase under oxidizing conditions is severely limited by its tendency to irreversible oxidation.

Catalytic applications of carbons include the oxidation of sulfurous to sulfuric acid, the selective oxidation of hydrogen sulfide to sulfur with oxygen in the gas phase at ca. 400 K, the reaction between phosgene and formaldehyde, and the selective oxidation of creatinine by air in physiological environments.

A potential technological application of carbon catalysts involves the catalytic removal of NO by carbon [237].

More recently, carbon nanotubes (CNT) and nanofibers (CNF) have found significant interest as catalysts and catalyst supports [237,240]. These materials, especially nanotubes, exhibit interesting electronic, mechanical and thermal properties that are clearly different from those of activated carbons. High mechanical strength and resistance to abrasion in combination with high accessibility of active sites are advantages of CNT-based catalysts which make them very attractive for liquid-phase reactions, where the microporosity of activated carbons often limits the catalytic performance. Due to their high electrical conductivity and oxidation stability, CNTs are also highly interesting carrier materials for proton-exchange membrane fuel cell (PEMFC) and direct methanol fuel cell (DMFC) catalysts [241].

4.1.5. Ion-Exchange Resins and Ionomers

Ion-exchange resins (→ Ion Exchangers) are strongly acidic organic polymers which are produced by suspension copolymerization of styrene with divinylbenzene and subsequent sulfonation of the cross-linked polymer matrix [242]. This matrix is insoluble in water and organic solvents. Suspension polymerization yields spherical beads which have different diameters in the range 0.3 – 1.25 mm. The Gaussian size distribution of the beads can be influenced by the polymerization parameters.

A network of micropores is produced during the copolymerization reaction. The pore size is inversely proportional to the amount of cross-linking agent. In the presence of inert solvents such as isoalkanes during the polymerization, which dissolve the reactive monomers and precipitate the resulting polymers, beads with an open spongelike structure and freely accessible inner surface are obtained. The matrix is then a conglomerate of microspheres which are interconnected by cavities or macropores. Macroporous resins are characterized by micropores of 0.5 – 2 nm and macropores of 20 – 60 nm, depending on the degree of cross-linking.

Strongly acidic polymeric resins are thermally stable at temperatures below 390 – 400 K. Above 400 K, sulfonic acid groups are split off and a decrease in catalytic activity results.

Industrially, acidic resins are used in the production of methyl *tert*-butyl ether [243].

The ionomer *Nafion* is a perfluorinated polymer containing pendant sulfonic acid groups which is considered to develop superacidic properties. It can be used as a solid acid catalyst for reactions such as alkylation, isomerization, and acylation [244].

4.1.6. Molecularly Imprinted Catalysts [245]

Molecular imprinting permits heterogeneous *supramolecular catalysis* to be performed on surfaces of organic or inorganic materials with

substrate recognition. Heterogeneous catalysts with substrate specificity based on molecular recognition require a material having a shape- and size-selective footprint on the surface or in the bulk. The stabilization of transition states by imprinting their features into cavities or adsorption sites by using stable transition-state analogues as templates is of particular interest.

Imprinted materials can be prepared on the basis of Al^{3+}-doped silica gel [246] and of cross-linked polymers [247,248]. Chiral molecular footprint cavities have also been designed and imprinted on the surface of Al^{3+}-doped silica gel by using chiral template molecules.

When transition-state or reaction-intermediate analogues are used as templates for molecular imprinting, specific adsorption sites are created. Such molecular footprints on silica gel consist of a Lewis site and structures complementary to the template molecules. These structures can stabilize a reacting species in the transition state and lower the activation energy of the reaction, thus mimicking active sites of natural enzymes and catalytic antibodies.

Although this approach seems to have a high potential for heterogeneous catalysis, the real application of imprinted materials as catalysts still remains to be demonstrated.

4.1.7. Metal – Organic Frameworks [249,250]

Metal – organic frameworks (MOFs) are highly porous, crystalline solids consisting of a three-dimensional network of metal ions attached to multidentate organic molecules. Similar to zeolites, the spatial organization of the structural units gives rise to a system of channels and cavities on the nanometer length scale. A milestone for the development of MOFs was the synthesis of MOF-5 in 1999 [251]. This material consists of tetrahedral Zn_4O^{6+} clusters linked by terephthalate groups and has a specific surface area of 2900 $m^2\ g^{-1}$. MOF-177 has an even larger specific surface area of 4500 $m^2\ g^{-1}$ [252]. By selection of the linker length, the size of the resulting pores can be tailored.

Due to their extremely high surface areas and their tunable pore structure with respect to size, shape, and function, MOFs are highly interesting materials for various applications. Examples are the adsorption of gases such as hydrogen or methane targeted at the replacement of compressed-gas storage, removal of impurities in natural gas, pressure-swing separation of noble gases (krypton, xenon), and use as catalysts [253]. Despite their higher metal content compared to zeolites, the use of MOFs in heterogeneous catalysis is restricted due to their relatively low stability at elevated temperature and in the presence of water vapor or chemical reagents. In addition, the metal ions in MOFs are often blocked by the organic linker molecules and are therefore not accessible for catalytic reactions. However, successful applications of especially stable Pd MOFs in alcohol oxidation, Suzuki C–C coupling and olefin hydrogenation have been reported [254]. It can be expected that the number of successful catalytic studies using MOFs will grow considerably.

4.1.8. Metal Salts

Although salts can be environmentally harmful, they are still used as catalysts in some technologically important processes. $FeCl_3$ – $CuCl_2$ is a catalyst for chlorobenzene production, and $AlCl_3$ is still used for ethylbenzene synthesis and *n*-butane isomerization.

4.2. Supported Catalysts

Supported catalysts play a significant role in many industrial processes. The support provides high surface area and stabilizes the dispersion of the active component (e.g., metals supported on oxides). Active phase – support interactions, which are dictated by the surface chemistry of the support for a given active phase, are responsible for the dispersion and the chemical state of the latter. Although supports are often considered to be inert, this is not generally the case. Supports may actively interfere with the catalytic process. Typical examples for the active interplay between support and active phase are bifunctional catalysts such as highly dispersed noble metals supported on the surface of an acidic carrier.

To achieve the high surface areas and stabilize the highly disperse active phase, supports are typically porous materials having high

thermostability. For application in industrial processes they must also be stable towards the feed and they must have a sufficient mechanical strength.

4.2.1. Supports

Many of the bulk materials described in Section Unsupported (Bulk) Catalysts may also function as supports. The most frequently used supports are *binary oxides* including transitional aluminas, α-Al_2O_3, SiO_2, MCM-41, TiO_2 (anatase), ZrO_2 (tetragonal), MgO etc., and ternary oxides including amorphous $SiO_2 - Al_2O_3$ and zeolites. Additional potential catalyst supports are aluminophosphates, mullite, kieselguhr, bauxite, and calcium aluminate. *Carbons* in various forms (charcoal, activated carbon) can be applied as supports unless oxygen is required in the feed at high temperatures. Table 7 summarizes important properties of typical oxide and carbon supports.

Silicon carbide, SiC, can also be used as a catalyst support with high thermal stability and mechanical strength [255]. SiC can be prepared with porous structure and high surface area by biotemplating [256]. This procedure yields ceramic composite materials with biomorphic microstructures. Biological carbon preforms are derived from different wood structures by high-temperature pyrolysis (1100 – 2100 K) and used as templates for infiltration with gaseous or liquid Si to form SiC and SiSiC ceramics. During high-temperature processing the microstructural details of the bioorganic preforms are retained, and cellular ceramic composites with unidirectional porous morphologies and anisotropic mechanical properties can be obtained. These materials show low density, high specific strength, and excellent high-temperature stability. Although they have not yet found application in catalysis, the low-weight materials may well be advantageous supports for high-temperature catalysis processes.

Monolithic supports with unidirectional macrochannels are used in automotive emission control catalysts (→ Automobile Exhaust Control) where the pressure drop has to be minimized [257]. The channel walls are nonporous or may contain macropores. For the above application the monoliths must have high mechanical strength and low thermal expansion coefficients to give sufficient thermal shock resistance. Therefore, the preferred materials of monolith structures are ceramics (cordierite) or high-quality corrosion-resistant steel. Cordierite is a natural aluminosilicate ($2\ MgO \cdot 2\ Al_2O_3 \cdot 5\ SiO_2$). The accessible surface area of these materials corresponds closely to the geometric surface area of the channels. High surface area is created by depositing a layer of a mixture of up to 20 different inorganic oxides, which include transitional aluminas as a common constituent. This so-called *washcoat* develops internal surface areas of 50 to 300 m^2/g [258,259].

Silica, *MCM-41*, and *polymers* can be functionalized for application as supports for the preparation of immobilized or hybrid catalysts [174,177,260–266]. The functional groups may serve as anchoring sites (surface bound ligands) for complexes and organometallic compounds. Chiral groups can be introduced for the preparation of enantioselective catalysts (see Section Hybrid Catalysts).

4.2.2. Supported Metal Oxide Catalysts

Supported metal oxide catalysts consist of at least one active metal oxide component dispersed on the surface of an oxide support

Table 7. Properties of typical catalyst supports

Support	Crystallographic phases	Properties/applications
Al_2O_3	mostly α and γ	SA up to 400; thermally stable three-way cat., steam reforming and many other cats.
SiO_2	amorphous	SA up to 1000; thermally stable; hydrogenation and other cats.
Carbon	amorphous	SA up to 1000; unstable in oxid. environm., hydrogenation cats.
TiO_2	anatase, rutile	SA up to 150; limited thermal stability; SCR cats.
MgO	fcc	SA up to 200; rehydration may be problematic; steam reforming cat.
Zeolites	various (faujasites, ZSM-5)	Highly defined pore system; shape selective; bifunctional cats.
Silica/alumina	amorphous	SA up to 800; medium strong acid sites; dehydrogenation cats.; bifunctional catalysts.

SA = surface area in m^2/g

[52,267,268]. The active oxides are often transition metal oxides, while the support oxides typically include transitional aluminas (preferentially γ-Al_2O_3), SiO_2, TiO_2 (anatase), ZrO_2 (tetragonal), and carbons.

Supported vanadia catalysts are extremely versatile oxidation catalysts. V_2O_5/TiO_2 is used for the selective oxidation of *o*-xylene to phthalic anhydride [269,270] and for the ammoxidation of alkyl aromatics to aromatic nitriles [270]. The latter reaction is also catalyzed by V_2O_5/Al_2O_3 [270]. The selective catalytic reduction (SCR) of NO_x emissions with NH_3 in tail gas from stationary power plants is a major application of $V_2O_5 - MoO_3 - TiO_2$ and $V_2O_5 - WO_3 - TiO_2$ [271,272]. $MoO_3 - Al_2O_3$ and $WO_3 - Al_2O_3$ (promoted by oxides of cobalt or nickel) are the oxide precursors for sulfided catalysts (see Section Supported Sulfide Catalysts) for hydrotreating of petroleum (hydrodesulfurization, hydrodenitrogenation, hydrocracking) [49,273,274]. $WO_3 - ZrO_2$ develops acidic and redox properties [275,276]. When promoted with Fe_2O_3 and Pt it can be applied as a highly selective catalyst for the low-temperature isomerization of n-alkanes to isoalkanes [277]. $Re_2O_7 - Al_2O_3$ is an efficient metathesis catalyst [278]. $Cr_2O_3 - Al_2O_3$ and $Cr_2O_3 - ZrO_2$ are catalysts for alkane dehydrogenation and for dehydrocyclization of, e.g., *n*-heptane to toluene [279].

The above-mentioned transition metal oxides have lower surface free energies than the typical support materials [52,280]. Therefore, they tend to spread out on the support surfaces and form highly dispersed active oxide overlayers. These supported oxide catalysts are thus frequently called *monolayer catalysts*, although the support surface is usually not completely covered, even at loadings equal to or exceeding the theoretical monolayer coverage. This is because most of the active transition metal oxides (particularly those of V, Mo, and W) form three-dimensional islands on the support surface which have structures analogous to molecular polyoxo compounds [52,267].

4.2.3. Surface-Modified Oxides

The surface properties, that is acidity and basicity, of oxides can be significantly altered by deposition of modifiers. The acid strength of aluminas is strongly enhanced by incorporation of Cl^- into or on the surface. This may occur during impregnation with solutions containing chloride precursors of an active component [169] or by deposition of $AlCl_3$. Chlorinated aluminas are also obtained by surface reaction with CCl_4 [174]. The presence of chlorine plays an important role in catalytic reforming with $Pt - Al_2O_3$ catalysts [50].

Strongly basic materials are obtained by supporting alkali metal compounds on the surface of alumina [281]. Possible catalysts include KNO_3, $KHCO_3$, K_2CO_3, and the hydroxides of the alkali metals supported on alumina.

Sulfation of several oxides, particularly tetragonal ZrO_2, yields strong solid acids, which were originally considered to develop superacidic properties [282,284], because, like tungstated ZrO_2 (see Section Supported Metal Oxide Catalysts), they also catalyze the isomerization of *n*-alkanes to isoalkanes at low temperature.

4.2.4. Supported Metal Catalysts

Metals typically have high surface free energies [280] and therefore a pronounced tendency to reduce their surface areas by particle growth. Therefore, for applications as catalysts they are generally dispersed on high surface area supports, preferentially oxides such as transitional aluminas, with the aim of stabilizing small, nanosized particles under reaction conditions [169, 285]. This can be achieved by some kind of interaction between a metal nanoparticle and the support surface (*metal – support interaction*:), which may influence the electronic properties of the particles relative to the bulk metal. This becomes particularly significant for raftlike particles of monatomic thickness, for which all atoms are surface atoms. Furthermore, the small particles expose increasing numbers of low-coordinate surface metal atoms. Both electronic and geometric effects may influence the catalytic performance of a supported metal catalyst (*particle-size effect*). Aggregation of the nanoparticles leads to deactivation.

Model supported metal catalysts having uniform particle size and structure can be prepared by anchoring molecular carbonyl clusters on support surfaces, followed by decarbonyla-

tion [286,287]. Examples are Ir_4 and Ir_6 clusters on MgO and in zeolite cages.

Bimetallic supported catalysts contain two different metals, which may either be miscible or immiscible as macroscopic bulk alloys. The combination of an active and an inactive metal [e.g., Ni and Cu (miscible) or Os and Cu (immiscible)] dilutes the active metal on the particle surface. Therefore, the catalytic performance of reactions requiring ensembles of several active metal atoms rather than single isolated atoms is influenced [288,289]. Selectivities of catalytic processes can thus be optimized. Typically, the surface composition of binary alloys differs from that of the bulk. The component having the lower surface free energy is enriched in the surface layer. For example, Cu is largely enriched at the surface of Cu – Ni alloys, even at the lowest concentration. Also, surface compositions of binary alloys may be altered by the reaction atmosphere.

In industrial application, supported metal catalysts are generally used as macroscopic spheres or cylindrical extrudates. By special impregnation procedures, metal concentration profiles within the pellet can be created in a controlled way. Examples are schematically shown in Figure 13 [169]. The choice of the appropriate concentration profile may be crucial for the selectivity of a process because of the interplay between transport and reaction in the porous mass of the pellet. For example for the selective hydrogenation of ethyne impurities to ethene in a feed of ethene, eggshell profiles are preferred.

Applications of supported metal catalysts, such as noble (Pt, Pd, Rh) or non-noble (Ru, Ni, Fe, Co) metals supported on Al_2O_3, SiO_2, or active carbon include hydrogenation and dehydrogenation reactions. Ag on Al_2O_3 is used for ethene epoxidation. Supported Au catalysts are active for low-temperature CO oxidation.

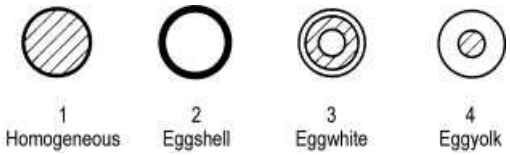

Figure 13. The four main categories of macroscopic distribution of a metal within a support

Multimetal catalysts Pt – Rh – Pd on Al_2O_3 modified by CeO_2 as oxygen storage component are used on a large scale in three-way car exhaust catalysts [259]. Pt supported on chlorinated Al_2O_3 is the bifunctional catalyst used for catalytic reforming, isomerization of petroleum fractions, etc.

Modification of supported Pt catalysts by cinchona additives yields catalysts for the enantioselective hydrogenation of α-ketoesters [290].

4.2.5. Supported Sulfide Catalysts

Sulfided catalysts of Mo and W supported on γ-Al_2O_3 or active carbons are obtained by sulfidation of oxide precursors (supported MoO_3 or WO_3; see Section Supported Metal Oxide Catalysts) in a stream of H_2/H_2S. They are typically promoted with Co or Ni and serve (in large tonnage) for hydrotreating processes of crude oil, including hydrodesulfurization (HDS) [49,273,274], hydrodenitrogenation HDN [274], and hydrodemetalation HDM [291]. Currently, the CoMoS and NiMoS models are most accepted for describing the active phase. These phases consist of a single MoS_2 layer or stacks of MoS_2 layers in which the promoter atoms are coordinated to edges [49,274], as shown in Figure 14. This figure also indicates that Co may simultaneously be present as Co_9S_8 and as a solid solution in the Al_2O_3 support matrix. It is inferred that the catalytic activity of the MoS_2 layers is related to the creation of sulfur vacancies at the edges of MoS_2 platelets. These vacancies have recently been visualized on MoS_2 crystallites by scanning tunneling microscopy (STM) [292].

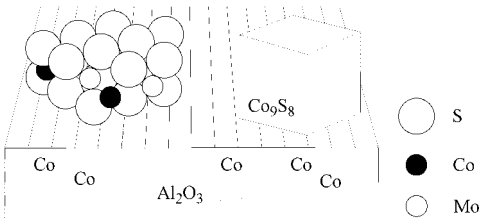

Figure 14. Three forms of Co present in sulfided Co – Mo/Al_2O_3 catalysts: as sites on the MoS_2 edges (the so-called Co – Mo – S phase), as segregated Co_9S_8, and as Co^{2+} ions in the support lattice.

4.2.6. Hybrid Catalysts [260,262,263,265,266]

Hybrid catalysts combine homogeneous and heterogeneous catalytic transformations. The goal of the approach is to combine the positive aspects of homogeneous catalysts or enzymes in terms of activity, selectivity, and variability of steric and electronic properties by, e.g., the appropriate choice of ligands (including chiral ligands [293]) with the advantages of heterogeneous catalysts such as ease of separation and recovery of the catalyst. This can be achieved by *immobilization* (*heterogenization*) of active metal complexes, organometallic compounds, or enzymes on a solid support.

There are several routes for the synthesis of immobilized homogeneous catalysts:

1. Anchoring the catalytically active species via covalent bonds on the surface of suitable inorganic or organic supports such as SiO_2, mesoporous MCM-41, zeolites, polystyrenes, and styrene – divinylbenzene copolymers [260–262,266]. The polymerization or copolymerization of suitably functionalized monomeric metal complexes is also known.
2. Chemical fixation by ionic bonding using ion exchange.
3. Deposition of active species on surfaces of porous materials by chemi- or physisorption, or chemical vapor deposition (CVD). The "ship-in-bottle" principle belongs to this synthetic route, but is treated separately in Section Ship-in-a-Bottle Catalysts.
4. Molecularly defined surface organometallic chemistry may also yield immobilized active organometallic species.

The reagents for covalent bonding on siliceous materials (SiO_2, MCM-41) are often alkoxy- or chlorosilanes which are anchored to the surface by condensation reactions with surface hydroxyl groups [260–262,266]. Functional groups thus created on the surface can include phosphines, amines etc., which serve as anchored ligands for active species that undergo ligand-exchange reactions. Careful control of the density of functional groups leads to spatial separation of active complexes (site isolation) and thus helps to avoid undesired side reactions [294].

Immobilized enzymes (→ Immobilized Biocatalysts) are frequently used in biocatalysis and in organic synthesis. The synthesis and catalytic performance of this class of heterogenized materials is discussed in several review articles [266,295].

Dendrimers [296] which are functionalized at the ends of the dendritic arms can be used for immobilization of metal complexes. A catalytic effect is thus generated at the periphery of the dendrimer. Dendrimers with core functionalities have also been synthesized. The resemblance of the produced structures to prosthetic groups in enzymes led to the introduction of the word *dendrizymes* [297]. Dendrimers have found application, e.g., in membrane reactors.

Immobilized homogeneous catalysts are used for selective oxidation reactions, for hydrogenation, and for C – C coupling reactions. They have proved very efficient in asymmetric synthesis [262,265,298].

Special processes with immobilized catalysts are *supported (solid) liquid-phase catalysis* (SLPC) [299] and *supported (solid) aqueous-phase catalysis* (SAPC) [300]. In SLPC a solution of the homogeneous catalyst in a high-boiling solvent is introduced into the pore volume of a porous support by capillary forces, and the reactants pass the catalyst in the gas phase. For example, the active phase — a mixture of vanadium pentoxide with alkali metal sulfates or pyrosulfates — is present as a melt in the pores of the SiO_2 support under the working conditions of the oxidation of SO_2 [301]. In SAPC hydrophobic organic reactants are converted in the liquid phase. The catalyst consists of a thin film of water on the surface of a support (e.g., porous SiO_2) and contains an active hydrophilic organometallic complex [300]. The reaction takes place at the interface between the water film and an organic liquid phase containing the hydrophobic reactant. The nature of these catalyst systems is schematically shown in Figure 15.

A new and improved version of SLPC uses ionic liquids for immobilization of homogeneous catalysts in *supported ionic liquid phase* (SILP) systems. The advantage of ionic liquids over the previously used solvents is their extremely low vapor pressures that allow for long-term immobilization of homogeneous catalysts. A variety of reactions have already been successfully

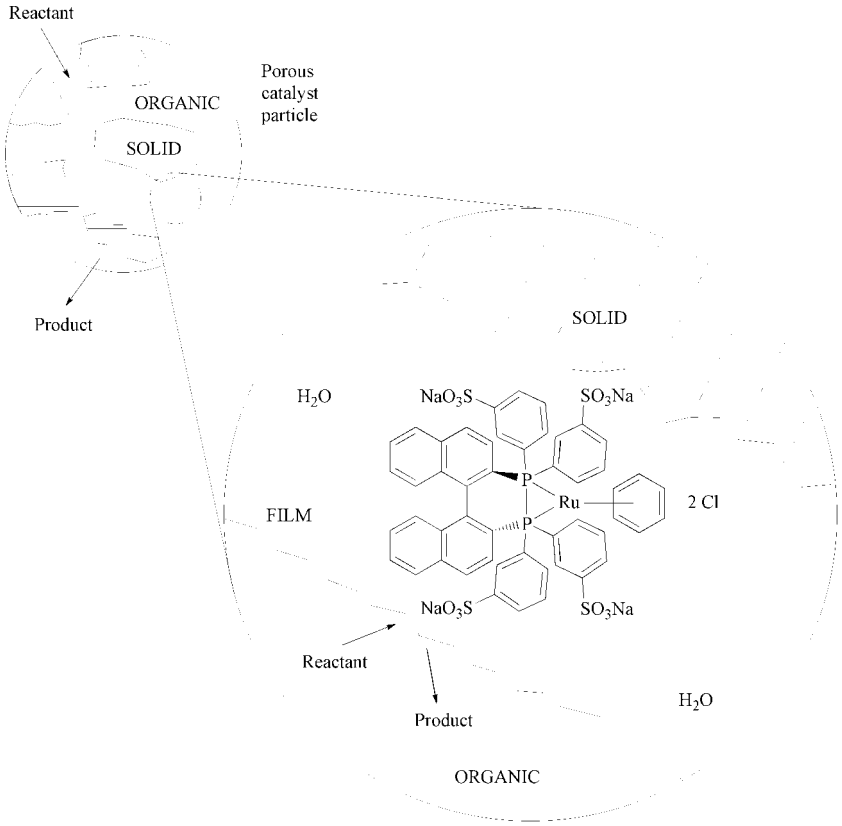

Figure 15. Schematic representation of SAP catalysis

studied [302,303]. A related novel concept uses *solid catalysts with ionic liquid layer* (SCILL) as a method to improve the selectivity of heterogeneous catalysts. The sequential hydrogenation of cyclooctadiene to cyclooctene and cyclooctane on a commercial Ni catalyst coated with an ionic liquid was tested as model system. Compared to the original catalyst, the coating of the internal surface with the ionic liquid strongly enhanced the maximum intrinsic yield of the intermediate product [304].

4.2.7. Ship-in-a-Bottle Catalysts [305]

Metal complexes which are physically entrapped in the confined spaces of zeolite cages (*confined catalysts*) are known as *ship-in-a-bottle catalysts* or *tea-bag catalysts*. The entrapped complexes are assumed to retain many of their solution properties. The catalytic performance can be modified in a synergistic manner by shape selectivity, the electrostatic environment, and the acid-base properties of the zeolite host. Ligands for metal centers in the zeolite cages include ethylenediamine, dimethylglyoxime, various Schiff bases, phthalocyanines, and porphyrins [305,306]. The entrapped complexes can be obtained via three principal routers [305]:

1. Reaction of the preformed flexible ligand with transition metal previously introduced into the zeolite cages (flexible ligand method). The synthesis of a zeolite entrapped metal salen complex is schematically shown in Figure 16.
2. Assembling the ligand from smaller species inside the zeolite cavities (ship-in-a-bottle technique). For example, the synthesis of a zeolite-entrapped metal phthalocyanine is schematically shown in Figure 17.

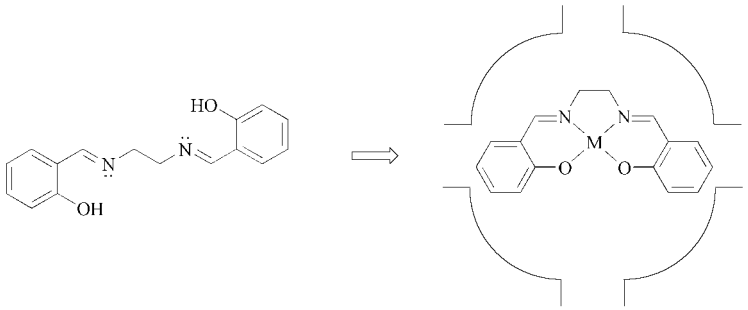

Figure 16. Synthesis of zeolite-entrapped metal salen complexes by the flexible ligand method

3. Synthesis of the zeolite structure around the preformed transition metal complex (zeolite synthesis technique).

The success of ship-in-a-bottle catalysts in catalytic processes has still to be demonstrated.

Zeolite-encapsulated complexes have also been suggested as model compounds for mimicking enzymes. These zeolite-based enzyme mimics are called *zeozymes* to describe a catalytic system, in which the zeolite replaces the protein mantle of the enzyme, and the entrapped metal complex mimics the active site of the enzyme (e.g., an iron porphyrin) [307].

Host – guest supramolecular compounds may also be mentioned in this context [245,308].

4.2.8. Polymerization Catalysts

Ziegler – Natta (→ Polyolefins – Ziegler Catalysts) catalysts are mixtures of solid and liquid compounds containing a transition metal such as Ti or V [309,310]. $TiCl_4$ combined with Al $(C_2H_5)_3$ or other alkyl aluminum compounds were found to be active for olefin polymerization. More active catalysts were produced commercially by supporting the $TiCl_4$ on solid $MgCl_2$, SiO_2 or Al_2O_3 to increase the amount of active titanium. Currently, Ziegler – Natta catalysts are produced by ball milling $MgCl_2$ with about 5 % of $TiCl_4$, and the cocatalyst is Al $(C_2H_5)_3$.

The *Phillips catalyst* (→ Polyolefins – Phillips Catalysts) consists of hexavalent surface chromate on high surface area silicate supports. Cr^{6+} is reduced by ethylene or other hydrocarbons, probably to Cr^{2+} and Cr^{3+}, the catalytically active species [309,310].

More recently, so-called single-site catalysts using metallocenes as active species were developed (→ Metallocenes, → Polyolefins) [310,311]. The activity of these materials is dramatically enhanced by activation with methylaluminoxane (MAO), obtained by incomplete

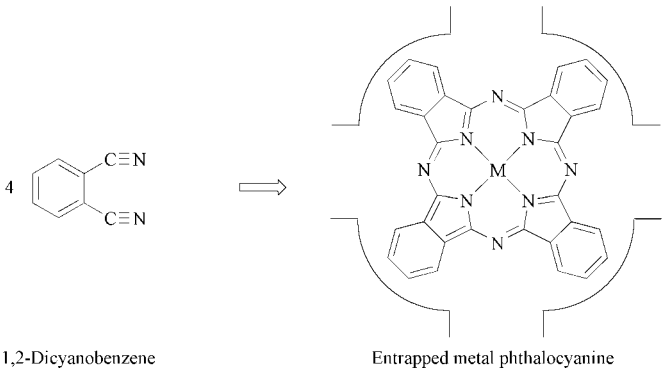

Figure 17. Ship-in-a-bottle synthesis of zeolite-encaged metal phthalocyanines

hydrolysis of $Al(CH_3)_3$, the catalytic performance of which is significantly more versatile than that of the classical Ziegler – Natta or Phillips catalysts. Activities and the nature of the polymeric product can be tailored by the choice of the metal and ligands.

4.3. Coated Catalysts

In addition to bulk and supported catalysts, coated catalysts can be considered as a third class of catalysts. In contrast to traditional catalyst geometries such as powders, tablets, spheres, and rings, coated catalysts are catalytically active layers applied on inert structured surfaces. These active layers consist of bulk or supported catalysts. The use of coated catalysts has recently become increasingly popular. Examples for such systems are:

- Egg-shell catalysts deposited on an inert carrier
- Monolithic honeycombs for environmental applications or for multiphase reactions [312,313]
- Structured packings [314]
- Foams and sponges [315]
- Fibers and cloths [316]
- Catalytic-wall reactors
- Catalytic filters for flue gas treatment and diesel exhaust after-treatment [317]
- Membrane – electrode assemblies for fuel cells [318]
- Microstructured reactors with coated channels [319]

Advantages of coated catalysts are optimal usage of the active mass, high selectivity at low diffusion lengths, highly efficient mass transfer from fluid phases to the solid catalyst layer, and low pressure drop.

5. Production of Heterogeneous Catalysts

The development of heterogeneously catalyzed reactions for the production of chemicals initiated the preparation of the required catalysts on a technical scale. Up to the end of World War II, solid catalysts were produced predominantly in process companies such as IG Farben and BASF in Germany, and Standard Oil Company and UOP in the USA [320,321]. About ten years later some independent catalyst producing companies were founded in the USA, Western Europe, and Japan [320]. At present more than 15 international companies [320,322] are producing solid catalysts on multitonne scale; for example:

- Synetix (ICI Catalysts and ICI Catalco)
- Davison Chemicals and Grace
- SÜD-Chemie Catalyst Group (incl. UCI, Houdry, Prototec in the USA, NGC, CCIFE in Japan, UCIL in India and AFCAT, SYNCAT in South Africa)
- UOP and Katalystiks
- BASF (incl. Engelhard Corp., Calsicat)
- Monsanto
- Shell and Criterion Catalysts
- Akzo Chemicals
- Johnson Matthey
- Haldor Topsøe
- Evonik Degussa
- Nippon Shokubai
- Nikki Chemical

In 1991 the catalyst world market achieved a turnover of about $\$ 6 \times 10^9$ [320,321,323], grew to $\$ (8 - 9) \times 10^9$ in 1996, and reached $\$ 13 \times 10^9$ in 2008.

Approximately 24 – 28 % of produced catalysts were sold to the chemical industry and 38 – 42 % to petrochemical companies including refineries. 28 – 32 % of solid catalysts were used in environmental protection, and 3 – 5 % in the production of pharmaceuticals [320,323].

The catalytic properties of solid catalysts are strongly affected by the preparation method, production conditions, and quality of source materials. Therefore, it is necessary to control each production step and the physical or mechanical properties of all intermediates. To attain a better reproducibility of catalyst production, batch procedures were mainly replaced by continuous operations, such as precipitation, filtration, drying, calcination, and forming.

Automation of various operations and computer control of different equipments were installed in catalyst production lines [320]. Recently, SPC (statistic process control) and QA (quality assurance) were integrated into the

catalyst production process. Some companies, especially in Western Europe and in the USA, produce solid catalysts according to ISO Standard which guarantees a standard catalyst quality to the customer [320,324].

Catalysts applied in several industrial processes can be subdivided into the following categories:

- Unsupported (bulk) catalysts
- Supported catalysts

5.1. Unsupported Catalysts

Unsupported catalysts represent a large category and are applied in numerous industrial processes. Various preparation methods were adopted in the past decades in the commercial production of unsupported catalyst, such as mechanical treatment or fusion of catalyst components, precipitation, coprecipitation, flame hydrolysis, and hydrothermal synthesis[232,322,325–329].

Mechanical treatment, for example, mixing, milling, or kneading of catalytic active materials or their precursors with promoters, structure stabilizers, or pore-forming agents, is one of the simplest preparation methods [322,325–327]. In some cases, however, the required intimate contact of catalyst components could not be achieved and therefore the activity, selectivity, or thermal stability of catalysts prepared in this way was lower than of those prepared by other methods. However, recent improvements in the efficiency of various aggregates for the mechanical treatment of solids resulted in activity enhancement. An important advantage of these methods is that formation of wastewater is avoided.

Industrial catalysts produced by mechanical treatment are summarized in Table 8.

Fusion of components or precursors is used for the production a small group of unsupported catalysts. The fusion process [232] permits the synthesis of alloys consisting of elements which do not mix in solution or in the solid state. However, preparation of unsupported catalysts by fusion is an energy-consuming and quite expensive process.

The most important application of this method is the production of ammonia synthesis catalysts based on the fusion of magnetite (Fe_3O_4) with promoters such as oxides of K, Al, Ca, and Mg [232]. Another example is the preparation of SO_2 oxidation catalysts by fusion of V_2O_5 with K pyrosulfate ($K_2S_2O_7$) [232]. Some producers incorporate Cs oxide as an activity promoter in this catalyst.

Quite recently, amorphous alloys composed, e.g., of Pd and Zr, so-called *metallic glasses* were found to be active in catalytic oxidations [232,233].

Industrial catalysts produced by the fusion process are listed in Table 8.

Table 8. Unsupported catalysts prepared by mechanical treatment (MT) or by fusion (F)

Catalyst*	Preparation method	Application
Fe_2O_3(K, Cr, Ce, Mo)	MT	ethylbenzene dehydrogenation (styrene production)
Fe_2O_3(K)	MT	Fischer – Tropsch synthesis
ZnO – Cr_2O_3	MT	hydrogenation of carbonyl compounds
Fe_3O_4(K, Al, Ca, Mg)	F	NH_3 synthesis
V_2O_5 – $K_2S_2O_7$	F	SO_2 oxidation (H_2SO_4 production)
Pt/Rh grid	F	NH_3 oxidation (HNO_3 production)

*Elements in parentheses are promoters.

Precipitation and coprecipitation are the most frequently applied methods for the preparation of unsupported catalysts or catalyst supports [322,325–329]. However, both methods have the major disadvantage of forming large volumes of salt-containing solutions in the precipitation stage and in washing the precipitate.

Source materials are mainly metal salts, such as sulfates, chlorides, and nitrates. Acetates, formates, or oxalates are used in some cases. In industrial practice nitrates or sulfates are preferred. Basic precipitation agents on an industrial scale are hydroxides, carbonates, and hydroxocarbonates of sodium, potassium, or ammonium.

Alkali metal nitrates or sulfates formed as precipitation byproducts must be washed out of the precipitate. Thermally decomposable anions, such as carbonates and carboxylates and cations like NH_4^+ are especially favored in catalyst production.

Coprecipitation of two or more metal cations is a suitable operation for the homogeneous dispersion of the corresponding oxides, especially if the catalyst precursors have a defined crystalline structure, for example, Cu(OH) NH_4CrO_4 or $Ni_6Al_2(OH)_{16}CO_3$. After thermal treatment, binary oxides such as CuO – Cr_2O_3 and NiO – Al_2O_3 are formed [322,325–329].

Precipitation and coprecipitation can be carried out in batch or continuous operations.

If the metal salt solution is placed in the precipitation vessel and the precipitating agent is added, then the pH changes continuously during the precipitation. Coprecipitation should be carried out in the reverse manner (addition of the metal salt solution to the precipitation agent) to avoid sequential precipitation of two or three metal species.

If the metal salt solution and the precipitating agent are simultaneously introduced into the precipitation vessel, then it is possible to keep the pH constant. However, the residence time of the precipitate in the vessel changes continuously.

Finally, if the metal salt solution and the precipitating agent are continuously introduced in the precipitation vessel, and the reaction products are removed continuously, then pH and residence time can be kept constant [322,325–329].

Besides pH and residence time, other precipitation parameters, such as temperature, agitation, and concentration of starting solutions, affect the properties of the precipitate. The choice of anions, the purity of raw material, and the use of various additives also play an important role [322,325–329].

In general, highly concentrated solutions, low temperatures and short ageing times result in finely crystalline or amorphous materials which are difficult to wash and filter. Lower concentrations of the solutions, higher temperatures, and extended ageing provide coarse crystalline precipitates which are easier to purify and separate [322,325–329].

The industrial production of precipitated catalysts usually involves the following steps:

- Preparation of metal salt solution and of precipitating agent (dissolution, filtration)
- Precipitation
- Ageing of the precipitate
- Washing of the precipitate by decantation
- Filtration
- Washing of the filter cake (spray drying)
- Drying
- Calcining
- Shaping
- Activation

Operations such as filtration, drying, calcination etc. are discussed in Section Unit Operations in Catalyst Production.

Typical unsupported industrial catalysts produced by precipitation or coprecipitation are compiled in Table 9.

The sol – gel process [330] involves the formation of a sol, followed by the creation of a gel. A sol (liquid suspension of solid particles smaller than 1 μm) is obtained by the hydrolysis and partial condensation of an inorganic salt or a metal alkoxide. Further condensation of sol particles into a three-dimensional network results in the formation of a gel. The porosity and the strength of the gel are strongly affected by conditions of its formation. For example, slow coagulation, elevated temperature, or hydrothermal posttreatment increase the crystalline fraction of the gel.

Table 9. Catalysts (their precursors) or supports prepared by precipitation or coprecipitation

Catalysts (precursors) or supports	Source materials	Application
Alumina	Na aluminate, HNO_3	support, dehydration, Claus process
Silica	Na silicate (water glass), H_2SO_4	support
Fe_2O_3	$Fe(NO_3)_3$, NH_4OH	ethylbenzene dehydrogenation (styrene production)
TiO_2	Fe titanate, titanyl sulfate, NaOH	support, Claus process, NO_x reduction
CuO – ZnO – (Al_2O_3)	Cu, Zn, (Al) nitrates, Na_2CO_3	LTS, methanol synthesis
Fe molybdate	$Fe(NO_3)_3$, $(NH_4)_2MoO_4$, NH_4OH	methanol oxidation to formaldehyde
Vanadyl phosphate	vanadyl sulfate, $NaHPO_4$	butane oxidation to maleic acid anhydride
NiO – Al_2O_3	Ni, Al nitrates, Na_2CO_3	hydrogenation of aromatics
NiO – SiO_2	Ni nitrate, Na silicate, Na_2CO_3	hydrogenation of aromatics

Alumina and silica can be produced from sodium aluminate or sodium silicate by treatment with nitric, hydrochloric, or sulfuric acid. In this process, first sols and then gels are formed. Washing the sodium from the gels is essential [327,328,330].

Spherical silica or silica-alumina gels are produced directly by injecting drops of a gelling mixture into oil at a proper rate to allow setting of the gel. To avoid bursting during drying, the gel beads are washed to reduce the salt content ($NaNO_3$, NaCl, or Na_2SO_4). Finally, the beads are dried and calcined [327,328].

Based on the sol – gel process, high-purity materials such as alumina, TiO_2, ZrO_2 are produced on an industrial scale. Raw materials are the corresponding metal alkoxides, e.g., Al(C_{12} – C_{18} alkoxide)$_3$ and Ti(n-$C_4H_9O)_4$ [330].

Flame Hydrolysis In flame hydrolysis [331] a mixture of the catalyst or support precursor, hydrogen, and air is fed into the flame of a continuously operating reactor. Precursors (mainly chlorides such as $AlCl_3$, $SiCl_4$, $TiCl_4$ or $SnCl_4$) are hydrolyzed by steam (formed by H_2 oxidation). The products of flame hydro1ysis are oxides. More than 100 000 t/a of so-called fumed silica, alumina, or titania are produced by Degussa, Wacker (both Germany), and Cabot (USA).

Thermal decomposition of metal – inorganic or metal – organic catalyst precursors is sometimes used in industrial catalyst production. For example, mixtures of Cu- and Zn $(NH_3)_4(HCO_3)_2$ decompose at 370 K to form binary Cu – Zn carbonates, which are transformed during calcination into the corresponding binary oxides, used as low temperature water gas shift catalysts [327].

Industrial production of Cu – Cr oxides (copper chromites), used in the hydrogenation of carbonyl compounds, is based on the thermal decomposition of a basic copper ammonium chromate [$CuNH_4(OH)CrO_4$] at 620 – 670 K [327,328].

Highly active Ni catalysts for the hydrogenation of fats and oils are obtained by the thermal decomposition of Ni formate [$(HCOO)_2Ni$] at 390 – 420 K. The decomposition is usually carried out in hard fat, which protects Ni against oxidation [327].

Catalysts or supports produced by flame hydrolysis or thermal decomposition of inorganic complexes are summarized in Table 10.

Hydrothermal synthesis [180,216] is a very important preparation method for zeolites and other molecular sieves.

Currently, the importance of zeolites in industrial catalysis is still increasing. They are used as catalysts or supports not only in petrochemical operations but also in the production of fine chemicals.

In hydrothermal synthesis (see also → Zeolites–Zeolite Synthesis: Routes and Raw Materials) a mixture of silicon and aluminum compounds containing alkali metal cations, water, and in some cases organic compounds (so-called templates) is converted into microporous, crystalline aluminosilicates [328,333].

Common sources of silicon are colloidal silica, water glass, fumed silica, and silicon alkoxides. Aluminum can be introduced as aluminum hydroxide, metahydroxide, or aluminate salts. Common templates are tetrapropyl- or tetraethylammonium bromides or hydroxides [328,333].

Hydrothermal synthesis is a complex process consisting of three basic steps: achievement

Table 10. Catalysts (their precursors) or supports prepared by sol – gel process (SG), flame hydrolysis (FH), or thermal decomposition (TD) of inorganic metal complexes

Catalyst (precursor) or support	Source material	Preparation method	Application
Alumina (high-purity)	Al alkoxides	hydrolysis, SG	support for noble metals
Alumina (acidic, low bulk density)	$AlCl_3$	FH	support or additive
Silica (low bulk density)	$SiCl_4$	FH	support or additive
TiO_2	Ti(n-$C_4H_9O)_4$	hydrolysis, SG	support
TiO_2 (low bulk density)	$TiCl_4$	FH	support or additive
CuO – ZnO	Cu, Zn $(NH_3)_4HCO_3$	TD	low-temperature shift, methanol
CuO – Cr_2O_3	$Cu(NH_4)OHCrO_4$	TD	hydrogenation of carbonyl compounds
Ni (kieselguhr)	Ni formate	TD	hydrogenation of fats and oils

of supersaturation, nucleation, and crystal growth. It is affected by the hydrogel molar composition, a1kalinity, temperature, and time [328,333].

In general, synthesis is carried out at 360 – 450 K under atmospheric or autogenous water pressure (0.5 – 1 MPa) with residence times of 1 – 6 d. After synthesis, the crystalline product is separated by filtration or centrifugation, washed, dried, and calcined. Sodium-containing zeolites, which are the products of the hydrothermal synthesis, are converted into acidic forms by exchange of sodium ions with the ammonium, followed by thermal treatment [328,333].

Zeolites used in the industrial catalysis are above all Y zeolite, mordenite, ZSM-5, ZSM-11, and zeolite β [180,215].

To improve the thermal stability of zeolites, especially of Y zeolite, Al ions are extracted from the lattice by steaming or acid treatment. For example, fluid-cracking catalysts (amorphous aluminosilicates) contain 10 – 50 % of ultrastable Y zeolites [328,333].

Related to zeolites are other molecular sieves such as aluminum phosphates (AlPO) and silico-aluminum phosphates (SAPO), the importance of which in industrial catalysis is growing. SAPO-11 was applied recently in the isomerization of cyclohexanone oxime to ϵ-caprolactam, instead of sulfuric acid in a demonstration unit [180].

Other preparation methods include condensation of more than two kinds of oxo anions, such as MoO_4^{2-}, WO_4^{2-}, HPO_4^{2-}, etc. to give heteropolyacids such as $H_3PW_{12}O_{40}$ or $H_3PMo_{12}O_{40}$ [222].

In industrial practice, the source materials are Na_2HPO_4, Na_2WO_4, or Na_2MoO_4 solutions. Hydrolysis and subsequent condensation are carried out with HCl. The heteropolyacids are extracted with organic solvents. Heteropolyacids are very strong acids with Hammett acidity function $H_o < -8$. They have found industrial application in acid-catalyzed reactions conducted in the liquid phase, such as hydration, esterification, and alkylation. Their activity is evidently higher than that of inorganic acids [222]. Their K or Cs salts are used as catalysts in the selective vapor phase oxidation of propene to acrolein or isobutene to methacrolein [222].

Another preparation method is based on the treatment of alumina or aluminosilicate with gases such as HF, HCl, BF_3, $AlCl_3$ to create highly acidic centers. Such catalysts are active in the skeletal isomerization of hydrocarbons, e. g., n-C_4 or n-C_5 [328].

Skeletal catalysts, also called porous metals, consist of the metal skeleton remaining after the less noble component of an alloy was removed by leaching with alkali, preferentially NaOH. Skeletal catalysts were discovered in 1925 and introduced into chemistry by Raney, and therefore some bear his name, e.g., Raney Ni or Co.

The group of skeletal catalysts [231] includes Ni, Co, Cu, Fe, Pt, Ru, and Pd. The second alloy component can be Al, Si, Zn, or Mg, with Al being used preferentially.

Small amounts of a third metal such as Cr or Mo have been added to the binary alloy as activity promoter.

Ni – Al, Cu – Al, and Co – Al alloys with different grain sizes are commercially available and can be leached out before use. Davison-Grace and Degussa provide finished extremely pyrophoric Ni or Co skeletal catalysts protected by water in commercial quantities. Skeletal Ni found technical application in the hydrogenation of aliphatic or aromatic nitro compounds and nitriles.

5.2. Supported Catalysts

The main feature of supported catalysts is that the active material forms only a minor part and is deposited on the surface of the support [326,328,332].

In some cases, the support is more or less inert, e.g., α-alumina, kieselguhr, porous glass, ceramics. In other cases the support takes part in the catalytic reaction, as in the case of bifunctional catalytic systems, e.g., alumina, aluminosilicate, zeolites, etc. [326,328,332].

Additionally, some supports can alter the catalytic properties of the active phase. This so-called strong metal – support interaction (SMSI) can decrease, for example, the chemisorption capacity of supported metals (Pt – TiO_2) or can hinder the reduction of supported metal oxides (Ni silicate, Ni and Cu aluminates, etc.) [326,328].

5.2.1. Supports

Currently, various industrial supports are available in multitonne quantities possessing a wide range of surface areas, porosities, shapes, and sizes.

Widely used supports include alumina, silica, kieselguhr, porous glass, aluminosilicates, molecular sieves, activated carbon, titania, zinc oxide, silicates such as cordierite ($2\ MgO \cdot Al_2O_3 \cdot 5\ SiO_2$) and mullite ($3\ Al_2O_3 \cdot 2\ SiO_2$), and Zn and Mg aluminates [326,328].

The supports are produced by specialized producers or directly by catalyst producers. Well known support manufacturers are:

- Grace Davison (USA, UK, Germany)
- Alcoa (USA)
- Sasol (former CONDEA) (Germany)
- BASF (former Engelhard) (USA)
- Saint Gobain Norpro (USA)
- Evonik Degussa (Germany)
- Cabot Corp. (USA)
- Corning (USA)

In the past, mostly natural supports, e.g., bauxite, pumice and kieselguhr, were used in catalyst production. At present (with the exception of kieselguhr) mainly synthetic supports with "tailored" physical properties are preferred in industrial catalysis.

Because the majority of supports also have catalytic properties (e.g., alumina, aluminosilicates, zeolites) their production methods are described in Section Unsupported Catalysts.

5.2.2. Preparation of Supported Catalysts

The broad application of supported catalysts in industrial catalysis led to the development of numerous preparation methods applicable on a technical scale. Some of these methods are identical with those used in the production of unsupported catalysts, e.g., mechanical treatment, precipitation, thermal decomposition of metal – inorganic or metal – organic complexes and therefore they will be discussed here very briefly.

Mechanical treatment, e.g., kneading of a catalyst precursor with a support is applied, e.g., in the production of kieselguhr-supported Ni (precursor $NiCO_3$) [325,327,328]. Also, MoO_3 supported on Al_2O_3 is sometimes produced by this process. However, the distribution of the active phase on the support is in some cases not sufficient [325].

Better results are obtained by the combination of mechanical and thermal treatment which, results in spreading [52] of, e.g., MoO_3 on Al_2O_3 or of V_2O_5 on Al_2O_3 or TiO_2.

Impregnation by pore filling of a carrier with an active phase is a frequently used production method for supported catalysts [169,325]. The object of this method is to fill pores of the support with a solution of the catalyst precursor, e.g., a metal salt of sufficient concentration to achieve the desired loading. If higher loadings with active phases are required, it is mostly necessary to repeat the impregnation after drying or calcination of the intermediate. Examples of catalysts prepared by the pore filling method are Ni or Co on Al_2O_3 – MoO_3, MoO_3 on aluminosilicates including zeolites, Ni or Ag on α-alumina, noble metals on active carbon, etc. [322,325–328].

Adsorption is a very good method to achieve uniform deposition of small amounts of active component on a support. Powders or particles exposed to metal salt solutions adsorb equilibrium quantities of salt ions, in accordance with adsorption isotherms. Adsorption may be either cationic or anionic, depending on the properties of the carrier surface. For example, alumina (depending on the adsorption conditions, mainly on the pH of the solution) adsorbs both cations and anions. Silica weakly adsorbs cations, while magnesia strongly adsorbs anions [322].

Adsorption of $PdCl_2$ from aqueous solution on different aluminas is very fast, and a high equilibrium concentration (ca. 2 wt %) can be obtained. The Pd deposition takes place mainly in an outer shell (egg shell profile) of shaped particles [322,328].

With $H_2[PtCl_4]$ only 1 wt % Pt loading on alumina is possible owing to from the flat adsorption isotherm [322,328].

The addition of oxalic, tartaric, and citric acid to the metal salt solution changes the profiles of active component on the carrier. In

general, with increasing acid strength the metal ions are forced deeper into the support particles [322].

Ion exchange [169,322] is very similar to ionic adsorption but involves exchange of ions other than protons. Lower valence ions, such as Na^+ or NH_4^+ can be exchanged with higher valence ions, for example, Ni^{2+} or Pt^{4+}. This method is used mainly in the preparation of metal-containing zeolites, e.g., Ni- or Pd-containing Y zeolites or mordenites used in petroleum-refining processes.

Thermal decomposition of inorganic or organic complexes in the presence of a support. This method is identical with that used in the preparation of unsupported catalysts by thermal decomposition of precursors. Supports can be used either as powder or preshaped. For example, Ni or Co deposited on kieselguhr or silica is produced by this method [327].

Precipitation onto the support is carried out in a similar way as in the case of unsupported catalysts [322,325,332]. Supports, mainly as powders, are slurried in the salt solution, and alkali is added. Rapid mixing is essential to avoid precipitation in the bulk.

Uniform precipitation can be achieved by using urea rather than conventional alkalis [332]. An appropriate amount of urea is added to the metal salt – support slurry and the mixture is heated while stirring. At 360 K urea decomposes slowly to NH_3 and CO_2, and precipitation takes place homogeneously over the surface and in pores of the support. This method is called *deposition – precipitation* [332] and is used especially in the production of highly active Ni – SiO_2 or Ni – Al_2O_3 catalysts.

Reductive deposition is a preparation method in which especially precious metals are deposited on the carrier surface by reduction of aqueous metal salts, mainly chlorides or nitrates, with agents such as H_2, Na formate, formaldehyde, and hydrazine. Examples of commercial catalysts produced by this method are precious metals on active carbon, SiO_2 or α-Al_2O_3. Reductive deposition is preferred especially in the case of bimetallic supported catalysts such as Pt – Re or Pd – Rh [334].

Heterogenization of homogeneous catalysts is based on the binding of metal complexes to the surface or entrapment in pores of the inorganic or organic support [266]. Such catalysts are used mainly in stereospecific hydrogenations in the production of fine chemicals or pharmaceuticals.

Enzymes [266] can also be heterogenized. They found industrial application in biochemical processes. A prominent example is the isomerization of glucose to fructose in the production of soft drinks.

5.3. Unit Operations in Catalyst Production

As in other branches of the chemical industry, unit operations have also been established in catalyst production in the past few decades, for example, in operations such as filtration, drying, calcination, reduction and catalyst forming [322,324,328]. Continuous operations are favored because of larger throughputs, lower operating costs, and better quality control. Additionally, factors such as environmental pollution and hazards to human health can be minimized more easily.

Filtration, Washing The main purpose of these operations is to separate precipitates and to remove byproducts and possible impurities. In batch operations mainly plate-and-frame filter presses are used [322,328]. The washing of the filter cake proceeds in countercurrent to the direction of the filtration.

Continuous vacuum rotary filters are widely used. By changing the speed of the filter drum (covered with filter cloth), the quantity of slurry filtered and the thickness of the filter cake can be varied over a broad range. As the drum rotates, there is a washing phase in which water is sprayed against the moving filter cake. Finally, the filter cake is scraped or blown to remove it from the drum [328].

Another filtration equipment is the centrifuge. However, its application is possible only when the filtered material is grainy or crystalline, e.g., zeolites. Washing can be carried out by introducing washing water into the centrifuge. Centrifuges can operate either in a discontinuous or continuous manner [328].

Drying Because drying conditions such as rate, temperature, duration, or gas flow rate can change the physical properties of the resulting material, it is important to measure and keep these parameters constant. For example the porosity of precipitated catalysts depends on the drying procedure. The drying of impregnated supports can change the distribution of active components. Their uniform distribution can be obtained only if all the liquid is evaporated spontaneously [322,325,328]. Usually, drying proceeds up to 400 K.

For the drying of filter cake, various tools are used, e.g., box furnaces with trays, drum dryers, rotary kilns, and spray dryers [322,325,328].

The main problems with drums and rotary dryers are the feeding of the wet filter cake and removal of adhering material from the walls. Because lumps are usually formed in the drying process, the resulting material must pass a granulator equipped with a sieve [328].

Spray dryers provide microspherical materials with a narrow particle-size range. Spray dryers are equipped with a nozz1e or a rotating disk to disperse the watery slurry of the filter cake in a stream of hot air [322,328,335].

All the above drying equipment operates in continuous mode.

Small batches of catalyst precursors are dried in box furnaces with trays [325].

For the drying of extrudates, continuously operating belt dryers have found technical application [328].

Calcination The main object of calcination (thermal treatment in oxidizing atmosphere) is to stabilize physical and chemical properties of the catalyst or its precursor. During calcination, thermally unstable compounds (carbonates, hydroxides, or organic compounds) decompose and are usually converted to oxides. During calcination new compounds may be formed, especially if the thermal treatment is carried out at higher temperatures [268]. For example, in the thermal decomposition of Cu or Ni nitrate deposited on alumina, not only CuO or NiO but also Cu or Ni aluminate is additionally formed [268].

Furthermore amorphous material can become crystalline. Various crystalline modifications can undergo reversible or irreversible changes.

Physical and mechanical properties and pore structures can also change. The calcination temperature is usually slightly higher than that of the catalyst operating temperature [322,325,328,335].

For the calcination of powder or granulate, rotary kilns are preferably used [325,328]. Smaller batches of powdered catalysts are calcined in box or muffle furnaces with trays, as in the case of drying. The gases that are mainly used for heating are in direct contact with the material being calcined [322,325,328].

Pellets or extrudates are calcined in belt or tunnel furnaces. The tunnel-type calciner can operate at substantially higher temperatures (close to 1270 – 1470 K) than the belt type (870 – 1070 K). The tunnel calciner is especially suitable for firing ceramic carriers. The material being calcined is taken in boxes or carts which are recycled to the entrance via a continuous chain or belt [328].

Reduction, Activation, and Protection Reduction, activation, or passivation, is in several cases the last step in catalyst production. These operations are performed by the catalyst producer or in the plant of the client.

For example, in the production of Ni catalysts for the liquid-phase hydrogenation of fats and oils, the reduction of NiO deposited on kieselguhr is carried out exclusively by the catalyst producer. The reduction of powders (50 – 500 μm particle size) is performed on an industrial scale in fluid-bed reactors. The reduced material is pyrophoric and must be protected with a hard fat such as tallow, to make its handling easy and safe. The finished catalyst is supplied in the form of flakes or pastilles [322,328,336].

The reduction of metal oxides such as NiO, CuO, CoO, or Fe_2O_3 is carried out with H_2 at elevated temperature (> 470 K) and has two steps. In the first step metal nuclei are formed. In the second, nuclei accumulate to form metal crystallites. The rates of both processes depend on temperature and on the nature of the substrate [322]. Reduction at lower temperatures (< 570 K) provides a narrow distribution of small metal crystallites. Reduction at higher temperatures (> 670 K) gives a broader distribution and larger metal crystallites [322].

Reduction of some oxides, such as those of Cu and Fe, is exothermic and needs to be carried out carefully with H_2 diluted with N_2.

Water, the reduction product, has negative effects on the rate and on the extent of reduction [322]. In industrial practice, where H_2 is recycled, the removal of water by freezing out (below 270 K) and by adsorption on molecular sieve is essential.

To achieve optimal activity, partial reduction of oxidic catalysts is common [322,337]. For example, Ni catalysts for fat and oil hydrogenation contain about 50 – 60 wt % of metallic Ni, 45 – 35 wt % NiO, and about 5 wt % Ni silicate.

When the reduction of shaped oxidic catalysts is conducted by the catalyst producer, then the active material is protected either with a high-boiling liquid such as higher aliphatic alcohols or C_{14} – C_{18} paraffins [337] or it is passivated. In this procedure, chemisorbed hydrogen is removed in a gas stream composed of N_2 and about 0.1 – 1.0 vol % of O_2 at ambient temperature. After this treatment catalysts can be handled in air without any precautions [336]. The activity is restored in the client's plant by treatment with H_2 [322].

The activation of hydrotreating catalysts composed of Ni- or Co-promoted MoO_3 – Al_2O_3 is carried out with H_2 containing 10 vol % of H_2S [268]. In the past, this activation was performed exclusively in the hydrodesulfurization plants. However, presulfiding at catalyst producers is becoming more common [322].

Mainly electrical or gas-heated shaft reactors are used for the reduction of extrudates, spheres, or pellets in plants of catalyst producers.

Catalyst Forming The size and shape of catalyst particles depend on the nature of the reaction and on the type of applied reactor.

Reactions in the *liquid phase* require small particles or even powders (50 – 200 μm). Such materials are made by grinding of a dried or calcined precursor, e.g., filter cake, using granulators equipped with sieves to give uniform particle size [322,328,335,337].

Catalysts for *fluidized bed reactors* (0.05 – 0.25 mm) are usually made by spray drying or by cooling molten material droplets (V_2O_5) in an air stream [322,328,335].

Spheres consisting of Al_2O_3, SiO_2, or aluminosilicate with 3 – 9 mm diameter are used preferentially as a support for catalysts in *moving-bed* or *ebullating-bed reactors*. They are produced by the so-called oil-drop method (see Section Unsupported Catalysts). Spheres prepared in this way possess sufficient abrasion resistance [322,328,335].

Another method for producing spheres is based on agglomeration of powder by moistening on a rotating disk (spherudizer) [322,328,335]. As the spheres reach the desired diameter they are removed automatically and transported to the dryer and calciner. Such spheres are suitable for *fixed bed reactors*.

Other methods for forming spherical particles include tumbling short, freshly extruded cylinders in a rotating drum [328].

In the briquetting technique, the plastic mixture of catalyst powder with a binder is fed between two rotating rolls provided with hollowed-out hemispheres [328].

Extrusion of pastes containing catalyst powder, binders and lubricants is a frequently used industrial shaping method [322,328,335]. Depending on the properties of the paste, press or screw extruders are applied. Press extruders are principally suitable for viscous pastes. Screw extruders are preferred for thixotropic masses. In both cases, pastes are forced through a die, and the extruded material is cut with a special device to a desired length and falls onto a moving belt that transports it through a drier or calciner [322,328,335]. Poly(vinyl alcohol), powdered stearine, and Al stearate are used as lubricants. If the mass being extruded contains alumina, then peptizing agents such as nitric acid are added mainly to improve the mechanical strength [322,327,328].

Another type of binder is calcium aluminate cement, which sets up by treatment with steam [322,328].

The extruded material can have different shapes, such as cylinders (noodles), hollow cylinders (macaroni), or ribbed cylinders. The sizes depend on the shape and are in the range of 1.5 – 15 mm diameter [328,337].

Added organic lubricants and pore-forming agents can be removed by calcination in a stream of air.

Special extrusion techniques and equipment are necessary to produce honeycombs.

Extruding is less expensive than pelletizing, but extrudates have less resistance to abrasion than pellets. Extrudates are suitable for different types of *fixed-bed reactors* operating in the gas or trickle phase.

Pelletizing is a very common method for catalyst forming. It is based on compression of a certain volume of powder in a die between two moving punchers, one of which also serves to eject the formed pellet [322,328,335]. Depending on the size and the shape of the prepared pellets, the material being pelletized must be crushed and forced through a corresponding sieve [328]. Furthermore, lubricants such as graphite, Al stearate, pol(vinyl alcohol), kaolin, and bentonite are added before the material enters the tabletting machine. The fluidity of the material is required to assure homogeneous filling of the die [322,328,335]. As in the case of extrudates, organic lubricants can be removed by calcination of the pellets.

Industrial pelleting machines are equipped with around thirty dies and produce about 10 liter of pellets per hour or more, depending on their shape and size. Pressures in the range 10 – 100 MPa in the pelleting machine are common [322,328,335].

Commercially, cylindrical pellets with sizes such as 3×3, 4.5×4.5, 5×5, or 6×6 mm are offered [322,328,335]. Production of 3×3 mm pellets is more expensive than that of larger sizes. Besides cylindrical pellets, various companies provide rings, cogwheels, spoked wheels, multihole pellets, etc. [336,337].

Pellets of different shapes and sizes are suitable for various types of fixed-bed reactors.

Coating of inert supports [338] with a thin layer of catalytically active material is required for manufacture of coated catalysts. A variety of methods for coating with catalysts are available. One can distinguish between material-dependent methods for the preparation of thin catalytically active layers on supports and material-independent coating methods [319]. Material-dependent methods are anodic oxidation of aluminum or aluminum alloys, which gives rise to a layer with a one-dimensional and unidirectional pore system with adjustable properties [339], and formation of porous layers on FeCrAl alloys by heat treatment. Material-independent coating technologies can be grouped according to the state of aggregation of the catalyst precursor [338].

Gaseous catalyst precursors can be transformed into coatings by chemical vapor deposition (CVD) or physical vapor deposition (PVD). Coating methods based on a liquid phase comprise sol – gel methods, deposition of catalyst suspensions, and combinations of both techniques. Depending on the adjusted viscosity of the sols or suspension, the liquid precursors may be applied on surfaces by dip coating, spraying, printing, or rolling. Solid catalyst powders can be applied, e.g., by flame spray deposition or powder plasma spraying.

A coating procedure that has been intensively studied is the manufacture of monoliths, e.g., as catalysts for pollution control [340]. Oxides such as Al_2O_3, CeO_2, and ZrO_2 (washcoat) are deposited on monoliths with a honeycomblike structure by dipping into an aqueous slurry containing primary particles (about 20 nm in diameter) of these materials [259]. The excess slurry is blown out, and after drying and calcination a thin catalyst layer is obtained, the thickness of which can be tailored by adjusting the slurry properties and repetition of the dip-coating step.

6. Characterization of Solid Catalysts

Catalytic activity and selectivity critically depend on the morphology and texture, surface chemical composition, phase composition, and structure of solid catalysts. Therefore, many physical and chemical methods are used in catalysis research to characterize solid catalysts and to search for correlations between structure and performance of catalysts. These methods include classical procedures [341] as well as techniques developed more recently for the study of the chemistry and physics of surfaces [341].

6.1. Physical Properties

6.1.1. Surface Area and Porosity [342,343]

The specific surface area of a catalyst or support (in m^2/g) is determined by measuring the vol-

ume of gas, usually N_2, needed to provide a monomolecular layer according to the Brunauer – Emmett – Teller (BET) method.

In this approach, the determination of the monolayer capacity is based on the physisorption of the test gas. The volume adsorbed at a given equilibrium pressure can be measured by static methods, namely, volumetric or gravimetric measurements. Flow or dynamic techniques are also applied.

The *total surface area* of a porous material is given by the sum of the *internal* and *external* surface areas. Pores are classified as *micropores* (pore width < 2 nm), *mesopores* (pore width 2 – 50 nm), and *macropores* (pore width > 50 nm) according to IUPAC definitions [344].

The *specific pore volume*, *pore widths*, and *pore-size distributions* for micro- and mesopores are determined by gas adsorption. For mesopores, the method is based on the dependence of the pressure of capillary condensation on the radius of a pore in which condensation takes place, which is given by the Kelvin equation:

$$\ln(p/p_o) = \frac{V}{RT}\left(\frac{2\sigma\cos\theta}{r\kappa}\right) \qquad (18)$$

where p/p_o = pressure/saturation pressure, V is the molar volume, σ the surface tension of the liquid adsorbate, Θ the contact angle between adsorbate and adsorption layer on pore walls (hence, $\Theta = 0$ is a good approximation), and r_K is Kelvin radius of a pore assuming cylindrical shape. Since an adsorption layer is typically formed before capillary condensation occurs, the geometric radius r_p of a pore is given by the sum of the Kelvin radius r_K and the thickness of the adsorption layer t: $r_p = r_K + t$. *Mesopore size distributions* can be calculated when adsorption and desorption isotherms are available in the full pressure range up to $p/p_o = 0.95$. The mesopore volume V_p is assumed to be completely filled at this relative pressure, which corresponds to $r_p \approx 20$ nm.

In the *micropore* range (pore width < 2 nm), where the pore dimensions are comparable to molecular dimensions, *pore filling* occurs rather than condensation [343]. The Dubinin – Radushkevich and the Dubinin – Stoeckli theories then permit the estimation of pore dimensions from physisorption data. In addition, several empirical methods exist, such as the t-method [345] and the α_s-method [346]. In the original t-method the amount of nitrogen adsorbed at 77 K was plotted against t, the corresponding multilayer thickness calculated from a universal N_2 isotherm, while in the α_s method the multilayer thickness t is replaced by the reduced adsorption α_s. Here, α_s is defined as the dimensionless adsorption n^a/n_x^a such that $\alpha_s = 1$ at $p/p_o = 0.4$, and n^a is the adsorbed amount in moles of the adsorbate (e.g., N_2) at a given relative pressure and n_x^a is the amount adsorbed (in moles) at a relative pressure of 0.4.

For meso- and macroporous materials (pore width > 2 nm), the pore size distribution is determined by measuring the volume of mercury (or another nonwetting liquid) forced into the pores under pressure [322]. The measurement, carried out with a *mercury pressure porosimeter*, depends on the following relation:

$$P = \frac{2\pi\sigma\cos\alpha}{r_p} \qquad (19)$$

where P is pressure, σ is surface tension of mercury, and α is the contact angle of mercury with solid. At pressures of 0.1 – 200 MPa, pore size distributions in the range of 3.75 – 7500 nm can be measured. Because the actual shape of the pores is not exactly cylindrical as assumed in the derivation of the above equation, the calculated pore sizes and distributions can deviate appreciably from the actual values shown by electron microscopy.

For pore systems with narrow pore size distributions, the *average pore radius* can be approximated by using

$$r_p = 2\,V_p/S_p \qquad (20)$$

where V_p is pore volume, and S_p is the surface area. The pore volume of a catalyst or support is given by

$$V_p = 1/\varrho_p - 1/\varrho \qquad (21)$$

where ϱ_p and ϱ are the *particle* and *true densities*, respectively. The former is determined by a pycnometer using a nonpenetrating liquid, such as mercury, whereas the true density is obtained by measuring the volume of the solid part of a weighed sample by helium displacement.

In certain instances, pore dimensions can be determined by high-resolution electron microscopy (HREM) [347].

6.1.2. Particle Size and Dispersion [348]

The surface area of active metals dispersed on a support deserves particular consideration since the metal surface area and particle size (which are interrelated quantities) determine the catalytic properties of supported metal catalysts. The metal *dispersion D* is given by $D = N_S/N_T$, where N_S is the number of metal atoms exposed at the surface and N_T is the total number of metal atoms in a given amount of catalyst. The fraction of surface atoms D can be determined if N_S is experimentally available. It can be determined by chemisorption measurements with adsorptives that strongly bind to the metal but which interact negligibly with the support at the chosen temperatures and pressures. H_2, CO, NO, and N_2O have been used for this purpose at or above room temperature [348], and static, dynamic, and desorption methods have been applied. Saturation values of the chemisorbed amounts permit N_S to be calculated if the chemisorption stoichiometries are known.

Dispersion is directly related to particle size and particle size distribution. Assuming reasonable model shapes for the metal particles, average particle sizes can be calculated from the chemisorption data.

Average crystallite size distributions can be determined independently from X-ray diffraction line broadening [348,350], and small-angle X-ray scattering (SAXS) permits the determination of particle sizes and particle size distributions, but also of the specific surface area of the metal and of the support [348,350].

Electron microscopy offers the unique opportunity to observe catalyst morphologies over the entire range of relevant particle sizes [347,348,351–353]. Particle shapes and sizes of the support or active phase and their size distributions can be extracted from micrographs, but structural information can be also obtained by electron-diffraction and lattice-imaging techniques [347].

6.1.3. Structure and Morphology

X-ray powder diffraction (see also → Structure Analysis by Diffraction – Diffraction by Polycrystalline Specimens) (XRD) is a routine technique for the identification of phases present in a catalyst [349,354]. It is based on the comparison of the observed set of reflections of the catalyst sample with those of pure reference phases, or with a database (Powder Diffraction File (PDF) distributed by ICDD, the International Centre for Diffraction Data). XRD studies can now be carried out in situ on the working catalyst [354], and the use of synchrotron radiation permits dynamic experiments in real time [355]. Time-resolved studies on a timescale of seconds are now becoming possible. Quantification of phase compositions can also be performed.

More sophisticated analysis of the diffraction patterns of crystalline materials provides detailed information on their atomic structure. The Rietveld method is used for structure refinements. Perhaps more importantly for catalytic materials, the local atomic arrangement of amorphous catalysts is based on the Debye equation, which gives the intensity scattered by a collection of randomly distributed atoms. The Fourier transform of the Debye equation gives the radial distribution function (RDF) of electrons, from which the number of atoms (electrons) located in the volume between two spheres of radius r and $r + \mathrm{d}r$ around a central atom, i.e., the radial density of atoms, can be obtained [354]. This approach has been applied for the structural analysis of amorphous or poorly crystalline catalyst materials and of small metal particles.

X-ray Absorption Spectroscopy (XAS) [356,358], is the method of choice where the applicability of XRD for structure analyses ceases to be possible. Because of their high photon flux, synchrotron facilities are the preferred sources for XAS experiments. The physical principle of XAS is the ejection of a photoelectron from a core level of an atom by absorption of an X-ray photon. The position of the absorption edge gives the binding energy of the electron in the particular core level and is thus characteristic of the respective element and its chemical state (see also → Surface and Thin-Film Analysis) and the shape of the absorption edge provides information on the distribution of the local density of states (LDOS).

The ejected photoelectron wave is backscattered at neighboring atoms, and the scattered wave interferes with the outgoing primary wave. This interference results in a modulation of the

absorption coefficient at energies between 50 and 1000 eV beyond the absorption edge (extended X-ray absorption fine structure, EXFAS). Analysis of these oscillations provides information on the chemical nature of atoms at well-defined distances from the central (ionized) atom and gives coordination numbers. Qualitative information on coordination of the central atom may also be obtained from the observation of pre-edge peaks. Information on dynamic and static disorder can also be extracted from the EXAFS. Hence, a detailed microscopic picture of the structure of a catalyst can be derived. XAS is particularly attractive for studies of catalysts under working conditions, although there are limitations regarding temperature [356]. The combined application of XAS and XRD on the same sample using synchrotron radiation for in situ studies is an ideal tool in catalysis research [359].

Electron Microscopy and Diffraction [347,351–353], (see also → Microscopy–Electron Microscopy). When electrons penetrate through matter in an electron microscope, contrast is formed by differential absorption (amplitude contrast) or by diffraction phenomena (phase contrast). Electron micrographs of catalyst materials can provide for identification of phases, images of surfaces and their morphologies, and elemental compositions and distributions. Image interpretations are often not straightforward and need expert analysis. Several variants of electron microscopy use different electron optics and working principles and therefore have to be chosen according to the problem to be solved.

Conventional transmission electron microscopy (CTEM) operates in the 100 – 200 kV range of electron energies, and imaging is based on amplitude contrast in the bright-field mode. Point resolutions of 0.2 – 0.3 nm can be achieved in favorable cases. A typical application of CTEM in catalysis research is the examination of metal particle sizes and their distributions in supported catalysts.

Dark-field images are produced when the directly transmitted electron beam is excluded by the objective aperture, and only diffracted electrons are used for imaging. This mode of operation selectively detects crystallites with crystallographic spacings within a narrow range.

High-resolution electron microscopy (HREM) can be performed in CTEM instruments by modifying the mode of imaging, or in dedicated instruments operating at electron energies of 0.5 – 1.0 MeV. HREM images can be directly related to the atomic structure of the material [360]. Lattice fringes can be resolved, and the determination of the spacings of atomic planes is enabled. Support particles can thus be identified, and the crystal structure of heavy metal particles having sizes in the range down to 1 nm can be investigated.

In dedicated *scanning transmission electron microscopes* (STEM) an annular detector provides the image formed from diffracted beams, while the central transmitted beam can be further analyzed by using an electron spectrometer to simultaneously provide elemental analysis. The intensity distribution of electrons scattered at high angles (40 – 150 mrad) depends on the square of the atomic number Z according to the Rutherford scattering cross section. The STEM images are therefore also called Z-contrast images, and they are particularly useful for the study of catalysts containing small metal particles [347].

In *scanning electron microscopy* (SEM) the image is produced by scanning a finely focused probe beam in a raster pattern across the specimen surface. Emitted signals such as backscattered and secondary electrons are detected and used for image formation. Secondary electrons are most commonly used. The best resolutions that can be achieved with current generation SEM instruments are approximately 1 nm. SEM is most useful for studying sample topographies, and it can be applied with a significant background pressure of a reactive gas while the sample is observed (environmental SEM or ESEM).

Selected area electron diffraction (SAED) provides information on phase compositions and structures at a microscopic level. The combination of microdiffraction patterns and bright-field images enables the determination of shapes and exposed facets in dispersed phases in solid catalysts.

Analytical electron microscopy (AEM) permits the determination of the elemental composition of a solid catalyst at the microscopic level by energy dispersive detection of the electron-induced X-ray emission. Energy dispersive

spectroscopy (EDS) is sensitive for elements with atomic numbers $Z > 11$. For lighter elements ($Z < 11$), electron energy loss spectroscopy EELS is applied.

Controlled atmosphere electron microscopy (CAEM) [347,361] is arousing considerable interest as it will permit the observation of changes in the catalyst structure and morphology under reaction conditions.

Vibrational Spectroscopy [362] (→ Infrared and Raman Spectroscopy). Vibrational spectroscopy is one of the most promising and most widely used methods for catalyst characterization, since it provides detailed structural information on the solid catalyst material and on surface groups and adsorbates. Several vibrational spectroscopic methods can be applied in situ, and they can be successfully used for studies on ill-defined high surface area porous materials. In situations where X-ray diffraction techniques are not applicable, vibrational spectroscopy can often provide information on phase transitions and changes in compositions of bulk catalyst materials, on their crystallinity, and on the nature of surface functional groups. Most vibrational spectroscopic methods are not surface-sensitive, but they become surface-sensitive when vibrational spectra are recorded for groups or adsorbates that are present exclusively at the material's surface. Representative examples for the structural characterization of solid catalysts by vibrational spectroscopy are bulk oxides (including simple binary oxides, multicomponent materials such as oxidation catalysts, and zeolites and molecular sieves), and supported oxides (e.g., monolayer-type catalysts), and sulfides. The vibrational analysis of surface groups, particularly of hydroxyl groups, can also be addressed. In many cases surface hydroxyl groups (e.g., on oxides) are simply formed by dissociative chemisorption of water molecules, which reduces the surface free energy. Hydroxyl groups can also be constituents of the solid-state structure, for example as in zeolites.

There are several methods and techniques of vibrational spectroscopy which are particularly suitable in catalysis research. *Infrared transmission – absorption spectroscopy* is the most commonly used technique. The KBr disk technique is routine for transmission spectroscopy of powder samples. However, for in situ investigations pressed self-supporting wafers have to be used. Samples which exhibit only weak bulk absorption, and the average particle size d of which is smaller than the wavelength of the infrared radiation ($d < \lambda$) are optimally suited for the transmission mode. Transmission – absorption infrared spectroscopy has been particularly successful in elucidating the structure of hydroxyl groups [174,362]. More strongly absorbing materials, and particularly those having average particle sizes greater than the wavelength of the infrared radiation, which therefore cause significant scattering losses in transmission, may preferentially be studied by *diffuse reflectance spectroscopy* (DRS, DRIFT). A powerful technique for structural studies on catalytic materials under extreme temperature and pressure conditions is *laser Raman spectroscopy* (LRS), although laser heating and laser-induced fluorescence may cause serious problems. One way, among others [362], to avoid fluorescence is to use of UV light instead of visible radiation for spectral excitation [363]. LRS has been successfully applied for the structural characterization of complex oxides, zeolites, and supported oxides and sulfides [362]. *Surface-enhanced Raman spectroscopy* (SERS) has found some application in studies of finely divided metal catalysts, particularly silver [364]. *Second harmonic generation* (SHG) and *sum frequency generation* (SFG) [365,366] are nonlinear optical techniques with high surface sensitivity which will probably find increasing application in studies relevant to catalysis.

Neutron techniques [367] include *neutron diffraction* and *inelastic neutron scattering* (INS). Both techniques are particularly sensitive to light elements (such as H or D) and provide complimentary structural information to XRD.

6.1.4. Local Environment of Elements

Nuclear spectroscopic methods provide information on the local environment of several selected elements.

Mössbauer spectroscopy and time differential perturbed angular correlation (TDPAC) belong to the class of techniques which detect solid-state properties mediated by

hyperfine interactions via nuclear spectroscopy [368]. Both techniques are **γ** spectroscopies; they are bulk techniques and can be applied under in situ conditions, although Mössbauer spectroscopy requires low temperatures.

Mössbauer spectroscopy (Mössbauer Spectroscopy) [368,369] provides information on oxidation states, phases, lattice symmetry, and lattice vibrations. Its application is limited to elements which exhibit the Mössbauer effect, such as iron, cobalt, tin, iridium, ruthenium, antimony, and platinum. Particularly valuable information on catalyst structures has been obtained for iron catalysts for Fischer-Tropsch and ammonia synthesis, and for cobalt-molybdenum hydrodesulfurization catalysts.

The time differential observation of the perturbed angular correlation of **γ** rays emitted from radioactive nuclei (TDPAC) [368,370,371] is a **γ**-spectroscopic technique which also allows the determination of hyperfine interactions such as nuclear electric quadrupole interactions (NQI). The NQI parameters enable local structural information around the **γ** emitter to be extracted. The technique has been successfully applied in studies on molybdenum-containing catalysts, and its application to tungsten seems promising.

Solid State Nuclear Magnetic Resonance [372–374] (see also → Nuclear Magnetic Resonance and Electron Spin Resonance Spectroscopy – NMR of solids and Heterogeneous Systems). NMR spectroscopy in heterogeneous catalysis principally allows the characterization of the chemical and structural environment of atoms in the catalysts (or in species adsorbed on catalyst surfaces). NMR studies on catalysts can be carried out over a wide range of temperatures and pressures, as well as in the presence of gases and liquids. Information can therefore be derived about the structures of catalysts and their thermal or chemical transformations. In addition, specific adsorbent – adsorbate interactions, the nature of chemically bonded surface species, and chemical reactions occurring at the catalyst surface can be studied. Most elements of interest in catalysis have isotopes that can be studied with modern NMR spectrometers. Isotope enrichments may be desirable or even necessary for certain elements, for example, ^{17}O.

NMR spectra of solids are often complex since structure-dependent interactions such as dipolar interactions, chemical shift interactions, quadrupolar interactions (for nuclei with spin $I > 1/2$) contribute strongly to the shape and position of NMR lines. Because of their structure-dependence these interactions are the main source of information on the structural environment of the nucleus in question. The selective determination of the related interaction parameters of structurally inequivalent nuclei is the major goal of an NMR experiment. In well-crystallized samples, the interaction parameters adopt unique values, while in poorly crystallized or amorphous powders they must be described by distribution functions.

The anisotropy of the above-mentioned interactions results in line broadening, and the spectra of polycrystalline samples consist of a broad superposition of signals arising from different orientations of the crystallites relative to the direction of the external magnetic field B_o, weighted by the statistical probability with which each orientation occurs (powder patterns). Special techniques have been developed which remove or at least reduce substantially these line-broadening effects and permit highly resolved NMR spectra of powders with individual lines for inequivalent nuclei to be recorded. The most important of these techniques are *dipolar decoupling*, *magic-angle spinning* (MAS), and *double oriented rotation* (DOR). *Cross-polarization* (CP) improves the sensitivity for nuclei with low natural abundance and allows the spatial proximity of nuclei to be monitored.

Typical examples for structural characterizations by solid-state NMR [372] are studies on zeolites using ^{27}Al and ^{29}Si NMR. Information on the distribution of Al in the environment of Si atoms and on the possible presence of nonframework Al species has been obtained. The location of exchangeable alkali metal ions has been studied by ^{23}Na and ^{133}Cs NMR. Vanadium- and molybdenum-based catalysts have successfully been characterized by ^{51}V and ^{95}Mo NMR.

6.2. Chemical Properties

6.2.1. Surface Chemical Composition

The atomic composition of a catalyst surface plays a decisive role for the catalytic properties.

Electron and ion spectroscopies [375] are surface-sensitive analytical tools which provide information on the atomic composition within the topmost atomic layers. The information depth, i.e., the number of atomic layers contributing to the measured signal, depends on the method. Concentration profiles can be obtained by sputter etching of the surface by ion bombardment. The application of these particle spectroscopies requires ultrahigh-vacuum (UHV) conditions.

The basis for the identification of atoms on surfaces of solid materials by electron spectroscopies, such as *Auger electron spectroscopy* (AES) and *X-ray photoelectron spectroscopy* (XPS) are the electronic binding energies. With ion spectroscopies, such as *low-energy ion scattering* (LEIS) and *Rutherford backscattering* (RDS), surface atoms are identified by their nuclear masses. Ion bombardment of surfaces is accompanied by sputtering processes (surface etching) which lead to the removal of secondary ionic and neutral particles. These are analyzed by mass spectroscopic techniques, such as *secondary ion mass spectroscopy* (SIMS), and *secondary neutral mass spectroscopy* (SNMS). Less frequently used is *laser microprobe mass analysis* (LAMMA). Relevant information on the properties of the various surface analytical techniques is summarized in Table 11.

The physical principles of the various techniques have been discussed in several articles and monographs [375,376].

Electron Spectroscopy (AES, XPS) (see also → Surface and Thin-film Analysis – Auger Electron Spectroscopy (AES)). These techniques use electrons as information carriers. The electrons can be produced by the absorption of photons resulting in photoemission. In XPS, X-ray photons are used to ionize core levels, and the kinetic energy E_k of the emitted photoelectrons is measured. The energy balance is given by:

$$E_k = h\nu - E_b - \Phi \qquad (22)$$

This equation permits the electron binding energy E_b (relative to the Fermi level) to be measured when the photon energy $h\nu$ and the work function Φ of the spectrometer are known. The binding energies are characteristic for a particular element.

As a result of the photoionization a singly ionized atom is formed, which can also be produced by electron impact. The core hole (e.g., in the K shell) can be filled by an electron from a higher shell (e.g., the L_1 shell) and the energy of this de-excitation process can be released by emission of an X-ray photon (*X-ray fluorescence*, XRF) or can be transferred to another electron (e.g., in the L_2 shell) which is then emitted with a well-defined kinetic energy (Auger process). This kinetic energy is determined by the orbital energies E_K, E_{L1}, and E_{L2} of the three orbitals involved. The Auger energy E_{KLL} is then given by:

$$E_{KLL} = E_K - E_{L_1} - E_{L_3} - \delta E - \Phi \qquad (23)$$

where δE is a relaxation energy, and Φ the spectrometer work function. Clearly, E_{KLL} is characteristic for an element and independent of the initial ionization process. Thus, both techniques permit the elemental constituents of a surface to be identified.

The information depth of both electron spectroscopies is determined by the mean free path of the emitted electrons, which depends on the kinetic energy of the electron in the solid matrix. This dependence is known [375–377]. The electron mean free path is typically larger in oxides than in metals at equal energy, and it is particularly large for zeolites because of their low

Table 11. Characteristics of surface analytical techniques in standard applications (adapted from ref. [375])

Information	Technique					
	AES	XPS	LEIS	RBS	SIMS	SNMS
Surface sensitivity (monolayers)	2 – 5	5 – 10	1 – 2	20 – 50	2 – 4	2 – 4
Detection limits (monolayers)	10^{-2} – 10^{-3}	10^{-2}	10^{-3}	10^{-3}	10^{-6}	10^{-6}
Quantification*	+	++	+	+++	–	+
Chemical information*	(+)	+	–	–	+	–
Structural information*	–	(+)	(+)	+	(+)	–

*Increasing number of positive signs indicates better capabilities; parentheses indication of restriction to special conditions.

density. Together with reported ionization cross sections and, in the case of AES, Auger decay probabilities, quantitative surface analysis is possible. The ratios of integral peak areas are proportional to concentration ratios. These can be analyzed as a function of preparation and treatment conditions of a given catalyst system (e.g., supported metal, oxide, or sulfide catalysts) and compared with model calculations [376]. Information on the elemental distributions and on dispersions of active components thus becomes available.

Ion-scattering Spectroscopies [375] (see also → Surface and Thin-Film Analysis). In ion-scattering spectroscopies solid surfaces are bombarded with monoenergetic ions, which are scattered on the top atomic layer (ion energies of about 0.5 – 5 keV, *low-energy ion scattering* (LEIS) [378,379]) or within near-surface regions (ion energies of about 0.1 – 23 MeV, *Rutherford backscattering* (RBS) [380,381]). In both cases the collision kinematics can be described as simple binary collisions, so that the kinetic energy of the backscattered ion is directly dependent on the ratio of the masses of the projectile and the scattering target atom and on the scattering angle. The mass of the projectile is known and the scattering angle is fixed and determined by the geometry of the spectrometer. Thus, the mass, and hence the identity, of the scattering target atoms can be determined unequivocally.

The LEIS technique provides information on the nature of the atomic constituents of the topmost atomic layers. Quantitative analysis, however, is difficult since neutralization probability, which makes the technique surface sensitive, is not easily available. Only a few percent of the primary ions are backscattered as ions in the case of noble gas ion (e.g., He^+). The technique can be applied for the characterization of real catalyst surfaces, although surface roughness reduces the signal intensity.

In contrast, in the energy regime of RBS the scattering cross sections can be calculated exactly. As a consequence, quantitative analysis is possible by RBS, but the surface sensitivity is lower than for LEIS. In optimal cases an information depth of 1 – 5 nm can be achieved. A combined application of LEIS, RBS, and perhaps XPS is often most informative [375].

Secondary Particles Ion bombardment of a surface leads to ion etching with the release of atoms and molecular fragments with varying charges (anions, cations, and neutrals) and excitation states. The mass analysis of secondary ions by mass spectrometry [*secondary ion mass spectroscopy* (SIMS)] has been developed as a highly sensitive and powerful surface analytical method (→ Surface and Thin-Film Analysis – Secondary ion Mass Spectrometry) [382,383]. Although destructive because of the need for sputtering, the sputtering rate can be kept low in the so-called static mode (low primary-ion current density) so that the surface remains essentially unchanged. Since the sputtered particles are preferentially released from the first two atomic layers, the SIMS technique is surface-sensitive. In contrast to the ion-scattering techniques, not only atomic constituents of a surface can be detected but information on the local environment of an atom in the surface can be obtained by analysis of molecular fragments. The detection of light elements, particularly hydrogen, is also possible. Quantification of the method is difficult, although not entirely impossible.

A high percentage of the sputtered secondary particles are neutral and must be postionized for mass spectroscopic analysis [*secondary neutral mass spectroscopy* (SNMS), → Surface and Thin-Film Analysis – Secondary Natural Mass Spectrometry (SNMS)] [384,173]. Post-ionization can be achieved by electron impact in a plasma or by an electron beam. Alternatively, resonant and nonresonant laser ionization can be applied. Applications of SNMS for catalyst characterization have still not been reported.

6.2.2. Valence States and Redox Properties

Electron Spectroscopies *X-ray photoelectron spectroscopy* (XPS) and *Auger electron spectroscopy* (AES), in addition to elemental analysis, permit information to be obtained on the valence and bonding states of a given element. This is due to the fact that the core-level binding energies and Auger kinetic energies are dependent on the chemical state, which leads to characteristic chemical shifts. In solids, the Madelung potential also plays an important role [376,385,386]. In addition, the ionization

of an atom leads to relaxation phenomena which provide a relaxation energy that is carried on by the emitted photoelectron. The binding energy of a core electron in level C of an atom is given by:

$$E_b(C) = \text{const.} + \sum_j (q_j/R_j) + \kappa q - R_{ea} \quad (24)$$

where q_j are the charges of all other atoms and R_j their distances from the core-ionized atom. The constant is the Hartree – Fock energy of the core electron in the atomic level C for the free atom, k is the change of the core potential resulting from the removal of an electron, and R_{ea} represents the extra-atomic polarization energy.

For an Auger transition involving the atomic levels C, C′, and C″, the kinetic energy E_k(C, C′, C″) of the Auger electron is related to the photoelectron binding energy E_b(C) in good approximation by:

$$\alpha' = E_b(C) + E_k(C, C'.C'') = \text{const.} + R_{ea} \quad (25)$$

where α' is the so-called Auger parameter.

Chemical shifts and the Auger parameter provide detailed information on the chemical state of an element as regards its oxidation state and its local environment. The latter is reflected in the Auger parameter, which is dependent on the extra-atomic polarization energy and hence, on the structural and bonding characteristics of the atom under consideration. So-called Wagner plots [386,387] in which the XP binding energy, the Auger energy, and the Auger parameter are correlated for families of compounds often permit the analysis of a compound of unknown structural and bonding characteristics.

Optical Spectroscopy and Electron Paramagnetic Resonance Optical excitations in the UV, VIS, and NIR regions and electron paramagnetic resonance (EPR) are classical techniques which provide information on the electron configuration (oxidation state) of a metal center and on the symmetry of the ligand sphere [388–391]. While optical spectroscopy is applicable to practically all systems, EPR is limited to paramagnetic species, i.e. those which contain one or more unpaired electrons.

UV – VIS – NIR spectroscopy covers a wide range of energies (typically 0.5 – 6 eV or 4000 to 50 000 cm^{-1} or wavelengths (2500 to 200 nm) as shown in Figure 18. Several types of transitions occur in this range, namely, charge-transfer (CT) and $d - d$ transitions, as also indicated in Figure 18. The first class of excitations involves two adjacent atoms, one of which is typically a metal center and the other a ligand or another metal atom. Electromagnetic radiation can promote charge transfer from the ligand (L) to the metal (M), from the metal (M) to the ligand (L) or from one metal center to another. These transitions are therefore called ligand-to-metal CT (LMCT), metal-to-ligand CT (MLCT), and metal-to-metal CT (MMCT), respectively. Such transitions occur in molecular complexes and in nonmolecular solids, such as metal oxides. The energy of CT transitions depends on the symmetry and oxidation state of the metal center and on the nature of the ligand or of the second metal atom [392]. Hence, information on these properties can be extracted from CT spectra. These spectra are relatively intense since they are dipole-allowed. In contrast, metal-centered or intra-atomic transitions in transition metal atoms or ions (ligand-field or $d - d$ transitions) are of moderate or weak intensity because they are forbidden by the Laporte (orbital) selection rule (and also by the spin selection rule) unless the selection rules are relaxed by vibronic or spin – orbit coupling. The $d - d$ transitions also provide information on the electron configuration and on the symmetry of a complex (or local environment in a

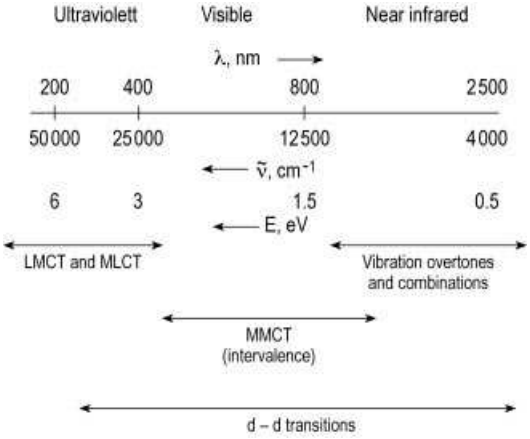

Figure 18. Energy ranges of different types of electronic transitions (adopted from [388])

solid). Typical systems that have been studied by optical spectroscopy are transition metal and base metal oxides, transition metal ions or complexes grafted on support surfaces, and transition metal ion-exchanged zeolites.

While spectra of liquid samples can be recorded in the transmission mode, catalyst powders must be studied by the diffuse reflectance technique (DRS) [389,390,393]. The measured diffuse reflectance can be converted into the so-called Schuster – Kubelka – Munk (SKM) function, which is directly proportional to the absorption coefficient. The wavelength dependence of the SKM function is thus equivalent to an absorption spectrum, provided the scattering coefficient is independent of the wavelength. This condition is often fulfilled in the UV and VIS spectral regions. Simple quartz cells for in situ treatments can be designed, to which an EPR tube can also be connected for simultaneous optical spectroscopy and EPR on the same sample [388].

Luminescence spectroscopy [394,395] has proved to be a valuable addition to the spectroscopy techniques for characterization of solid catalysts under well-defined conditions.

As mentioned above, *electron paramagnetic resonance* (EPR) is used to study paramagnetic species in catalytic materials. Besides the simple qualitative (and quantitative) detection of the presence of paramagnetic sites, the spin density distribution at the paramagnetic center and on the neighboring atoms can be deduced from the spectra. Simulations of EPR spectra are often useful for full interpretation. The extremely high sensitivity of the EPR technique can be an advantage but also a drawback because the importance of minority radical species may be overemphasized. EPR is not surface-sensitive. However, radical species in the surface can easily be identified by exposing the sample to paramagnetic O_2, which leads to significant broadening or disappearance of signals of surface species because of dipole – dipole interactions.

Several reviews on the use of EPR in catalyst characterization have been published [388,396,397]. Typical applications of EPR are the detection of paramagnetic states of transition metal ions and analysis of the symmetry of their ligand sphere and/or their coordination, redox properties of catalytic materials and their surfaces, and surface anion or cation radicals deliberately produced by organic molecules as probes for the redox properties of the solid catalyst. Radical species (e.g., in connection with coke formation) formed during catalytic reactions have also been detected.

Thermal Analysis Thermoanalytical techniques such as *differential thermal analysis* (DTA), *thermogravimetry* (TG), and *differential scanning calorimetry* (DSC) are well-established methods (→ Thermal Analysis and Calorimetry) in solid-state chemistry [398,399] which have successfully been applied to investigating the genesis of solid catalytic materials. They can also be used to follow reduction and oxidation processes by measuring either thermal effects and/or weight changes. When combined with an on-line mass spectrometer, changes in the gas-phase composition occurring during chemical transformations of the solid sample can be monitored simultaneously.

In temperature-programmed reduction (TPR), as first described by Robertson et al. [400], a stream of inert gas (N_2 or Ar) containing ca. 5 vol % H_2 is passed through the catalyst bed of a flow reactor containing a reducible solid catalyst [401]. By monitoring continuously the H_2 concentration in the gas stream and its eventual consumption with a thermal conductivity detector while heating the sample with a linear temperature ramp of ca. 10 K/min, the rates of reduction are obtained as a function of time (or temperature). The total amount of H_2 consumed determines the reduction equivalents present in the catalyst, and detailed analysis of the experiment permits the kinetic parameters of the reduction process to be determined and provides information on reduction mechanisms. Characteristic numbers which depend on the experimental parameters (amount of reducible species present, H_2 concentration, flow rate, and temperature ramp) have been defined [328,329]. These numbers must be kept in certain ranges for optimal performance of the experiment.

TPR experiments have been used to investigate the reduction behavior of bulk and supported reducible species, solid solutions, promoted metal catalysts, metals in zeolites, and of supported sulfides and of nitrides [401].

Temperature-programmed oxidation (TPO) is an equally valuable technique for investigat-

ing the oxidation kinetics and mechanisms of reduced materials [401]. Cyclic application of TPR and TPO provides information on the redox behavior of catalytic materials, e.g., of catalysts for selective catalytic oxidations.

6.2.3. Acidity and Basicity

Acid-catalyzed reactions are among the industrially most important hydrocarbon conversions. Acid sites can be classified as Lewis acidic sites, such as coordinatively unsaturated cations (e.g., Al^{3+} on the surface of partially dehydroxylated alumina, and Brønsted acidic sites, which are typically surface OH groups as, e.g., in H forms of zeolites. Carbenium and carbonium ions are thought to be formed by protonation of hydrocarbons on these groups. Surface oxygen ions may function as Lewis basic centers, and if strong enough they may abstract protons from hydrocarbon molecules to form carbanion intermediates. A typical solid base is MgO.

For characterization of acid and base properties, the nature (Lewis or Brønsted) of the sites, the acid or base strength, and the number of sites per unit surface area of a solid catalyst must be determined. Brønsted acidity is almost certainly required for all acid-catalyzed reactions. However, the mechanistic details on surfaces are significantly different from the well-known carbenium and carbonium ion chemistry in solution, because of the lack of the stabilizing effect of solvation in heterogeneously catalyzed gas-phase reactions. As shown by KAZANSKY [404], the electronic ground state of surface acidic OH groups of oxides and in H forms of zeolites is essentially covalent. The main differences in their acid strength are thought to be due to the energetic positions of their electronically excited heterolytic terms. Similarly, the interaction of acid groups with alkenes does not result in the formation of adsorbed carbenium ions but rather in the formation of more stable covalent alkoxides. Basic sites (surface O^{2-} ions) in the vicinity of OH groups could be involved in this process. Carbenium ions (and even more so carbonium ions) are therefore not considered to be reaction intermediates in solid acid catalysis, but rather excited unstable ion pairs or transition states resulting from electronic excitation of covalent surface alkoxy species. Because of the proposed bifunctional nature of active acid sites in heterogeneous acid catalysis, it is necessary to characterize both the acidic and basic properties of solid catalysts. Many different methods have been developed for the characterization of acidity, but only little is known about the basic character, particularly of materials that are typically considered to be acid catalysts.

Chemical Characterization [405]. Titration methods in aqueous medium are not very informative, because H_2O tends to strongly modify surface properties by molecular or dissociative chemisorption. Therefore, nonaqueous methods have been proposed, in which the solvent (e.g., benzene or isooctane) does not or only weakly interact with the catalyst surface. Hammett indicators were used to determine the acid strength in terms of the Hammett – Deyrup H_0 function:

$$H_0 = -\log a_{H^+}(f_B/f_{BH^+}) \qquad (26)$$

where a_H^+ is the proton activity and f_B and $f_{BH}{}^+$ are the activity coefficients of the basic probe and its protonated form, respectively. A series of Hammett indicators covers the range of $-18 < H_0 < 4$, where $H_0 = -12$ corresponds to 100 % H_2SO_4.

Site densities and acid strength distributions were determined by the *n*-butylamine titration method [406]. As these titration and indicator methods can yield erroneous results [407], they are not frequently used today.

Isosteric heats of adsorption of strong bases (e.g., pyridine) may be considered as measures of acid strength. However, a discrimination between Lewis and Brønsted sites is not possible.

Temperature-programmed desorption [also called *thermal desorption spectroscopy* (TDS)] of basic probe molecules has been developed as a powerful tool for the characterization of solid acids [408,409]. In this method, a strong base is isothermally pre-adsorbed on an acidic catalyst and then exposed to a stream of inert gas (e.g., He). Heating by a temperature ramp (ca. 10 K/min) leads to desorption of the base. The integral area of the desorption peak gives the total acid site density, and the position of the peak maximum provides the activation energy of

desorption (which may be close or identical to the heat of adsorption), which can be considered to be a measure of the acid strength. This approach has been applied for investigations of H forms of zeolites using ammonia as the probe [410,411]. However, discrimination between Lewis and Brønsted acid sites is again only possible with the assistance of, e.g., vibrational spectroscopy.

Microcalorimetry [408]. Differential heats of adsorption of probe molecules can be measured with high accuracy by heat-flow calorimetry and differential scanning calorimetry. These data provide information on the acid (or base) strength distribution. Ammonia and other amines have been used as probes for acid sites on oxides [412] and in H forms of zeolites [413,414], and carbon dioxide and sulfur dioxide were adsorbed as acidic probes on several oxides [412].

Vibrational spectroscopy [415,420]. *Transmission infrared spectroscopy* is the most frequently applied technique for investigations into acidic and basic properties of solid catalysts. Surface hydroxyl groups can easily be detected since they function as dipolar oscillators. However, the stretching frequency of unperturbed OH groups can not be taken as a measure of the acid strength. Lewis acidic and basic centers can only be detected by vibrational frequencies with the adsorption of suitable probe molecules. Criteria for the selection of optimal probe molecules have been defined by KNOEZINGER et al. [415,420].

The use of basic probe molecules permits a discrimination between Brønsted and Lewis acid sites. When a base B is adsorbed on an acidic OH group, hydrogen bonding followed eventually by protonation of the base may occur (Eq. 20):

$$\mathrm{OH}+\mathrm{B} \rightleftharpoons \mathrm{OH}\cdots\mathrm{B} \rightleftharpoons \mathrm{O}^{-}\cdots\mathrm{H}^{+}\mathrm{B} \qquad (27)$$

The strength of the hydrogen bond and the ability of the OH group to protonate the base is determined by the acid strength of the surface OH group and by the base strength (or proton affinity) of B. When hydrogen bonding occurs, the induced frequency shift of the O – H stretching mode $\Delta\nu_{\mathrm{OH}}$ is a measure of the strength of the hydrogen bond ΔH_{B} (Eq. 28) [421] and hence, of the acidity of the OH group.

$$|\Delta\nu_{\mathrm{OH}}|^{1/2} \sim \Delta H_{\mathrm{B}} \qquad (28)$$

Simultaneously, internal molecular modes of the base B are modified, particularly when protonation occurs. These changes can also be used for the interpretation of the bonding type of the probe. Strong bases such as the traditional probe molecules ammonia and pyridine are protonated by even very weak Brønsted sites which may not be at all relevant in acid catalysis. Weaker bases such as nitriles, carbon monoxide, and even dinitrogen and dihydrogen only undergo hydrogen bonding (hydrogen bonding method [416]), but due to their weak interactions they are very specific and can provide very detailed information on the properties of acidic surfaces.

The same bases can be used for the detection of Lewis acid sites L, with which they form surface coordination compounds:

$$\mathrm{L}+\mathrm{B} \rightleftharpoons \mathrm{L}\leftarrow\mathrm{B} \qquad (29)$$

The frequency shifts of the internal B modes are a measure of the nature and strength of the coordinative bond. For example, carbon monoxide when coordinated to L sites undergoes very typical shifts of the C – O stretching frequency which provide information on the nature of the element and of the coordinative bond, on the oxidation state, and on the coordination of the L site [415,420].

The investigation of basic sites O^{2-} by acidic probe molecules AH with analysis of the vibrational spectra is much less advanced than that of acid sites. The hydrogen-bond method can in principle be applied:

$$\mathrm{O}^{2-}+\mathrm{H}-\mathrm{A} \rightleftharpoons \mathrm{O}^{2-}\cdots\mathrm{H}-\mathrm{A} \qquad (30)$$

Here the shift of the H–A stretching mode is a measure of the hydrogen-bond strength and hence, the basic character (proton affinity) of the surface O^{2-} site. Recently, CH compounds such as trichloromethane [416], acetylene and substituted acetylenes [420,422] and even methane [423] were proposed and successfully tested as acidic probe molecules. Pyrrole [419] and several Lewis acids [415] have also been used.

Surface chemical transformations of, e.g., CO_2, alcohols, ketones, acetonitrile, and

pyridine gave detailed information on the bifunctional acid – base pair character of several oxides, particularly of alumina [415,424].

Nuclear Magnetic Resonance [425,427]. Solid-state ^{1}H magic-angle spinning (MAS) NMR spectroscopy measures proton chemical shifts, which were thought to reflect the deprotonation energies of surface OH groups. However, proton chemical shifts are also very sensitive to hydrogen bonding. Therefore, changes in proton chemical shifts induced by hydrogen bonding of probe molecules can also be used for the characterization of protic acidity.

Dissociative chemisorption of CH_3I was proposed for characterization of surface basicity by ^{13}C NMR spectroscopy [428].

6.3. Mechanical Properties [429]

Catalyst particles are exposed to diverse mechanical strains during transportation, charging to the reactor, and operation. In fixed bed reactors catalyst particles must withstand pressure caused by the mass of the catalyst charge and erosion by high-velocity gas streams. In fluidized- and moving-bed reactors, the particles must resist attrition from rubbing against each other and from colliding with the walls of the reactor system. The technical performance of catalysts depends on their mechanical strength to maintain integrity for a reasonable time in spite of these strains.

There are three types of methods for determining the strength of catalysts used under static conditions [430]. For pellets and rings with no areas of distortion (preferably sized 1 cm or larger), the *crushed* (or crush) *strength* is determined by exerting pressure on the specimen placed between two horizontal plates of a hydraulic press. The upper plate moves down until the specimen is crushed, at which point the pressure is recorded. The test is repeated for several particles, and the values are averaged. In the knife-edge hardness test, the upper plate of the press is replaced by a knife with a 0.3 mm edge. A mass of 1 kg is applied to the knife and the percentage of broken samples is recorded. The mass is then raised in increments of 1 kg, and the test is repeated until 100 % of the particles are broken or until a mass of 10 kg is reached. Catalyst particles of irregular form are tested in a cylinder provided with a ram. After a definite pressure is applied, the sample is discharged, and the weight percent of fines formed during the test is determined by screening.

Tests for impact strength and resistance against abrasion or attrition are carried out under dynamic conditions. For *impact testing* of very strong catalysts (e.g., ammonia synthesis catalysts), a mass of 500 – 1000 g is dropped on the particle from a standard height and the percentage of unbroken, split, and broken samples out of 20 or more is recorded. *Abrasion tests* on tableted and extruded catalysts are carried out in a rotating horizontal steel cylinder provided with one baffle. The percent of fines (based on the mass of the catalyst tested) formed after 1 h is reported as attrition loss. The *attrition loss* of fluid catalysts is measured by exposing the catalyst particles to a high-velocity air stream in a glass pipe. The fines formed during the test (prevented from escaping by a filter) are reported as attrition loss expressed as the percentage of the sample charged [431].

6.4. Characterization of Solid Catalysts under Working Conditions

The best description of a catalytic mechanism is the corresponding catalytic cycle. As a first step, a detailed product analysis is required to differentiate between a single clean reaction and systems undergoing parallel and/or consecutive reactions. The microkinetic approach, as outlined in Section Kinetics of Heterogeneous Catalytic Reactions, for the prediction of the overall rate of a catalytic reaction taking into account the surface chemistry of the catalyst and the elementary reactions involved, is the most promising procedure to predict a mechanism. However, the results of microkinetic analyses may not always be unequivocal, and discrimination between different kinetic models may not be straightforward. Therefore, additional information is necessary to prove or disprove the sequence of elementary steps (catalytic cycle) that represents the mechanism of a catalyzed reaction at the molecular level.

Quantum chemical calculations at various levels of sophistication and computer modeling procedures now permit structures of adsorbed

intermediates and transition states to be elucidated and reaction energy diagrams to be computed (see Section Molecular Modeling in Heterogeneous Catalysis).

6.4.1. Temporal Analysis of Products (TAP Reactor)

Transient kinetics measurements can also provide quantitative values of kinetic parameters and elucidate individual reaction steps [432,433]. Pulse reactors are one type of transient reactors. A valuable laboratory pulse reactor (transient operation) is the *TAP reactor* (TAP = temporal analysis of products). Pulses containing small amounts of reactants (10^{13} – 10^{17} molecules per pulse) are injected into the evacuated reactor containing the catalyst bed. The reactant/product molecules leaving the reactor (response signal) are analyzed by mass spectroscopy with a time resolution of less than 100 ms. This approach permits surface processes on solid catalysts such as adsorption, reaction, and desorption to be studied, and reaction mechanisms and kinetic models to be established [434,436].

In another kind of transient experiment, step changes in concentrations are effected, and the response of product concentration is measured as a function of time. The analysis of this response provides details of the course of reaction and permits kinetic parameters to be determined.

6.4.2. Use of Isotopes

A powerful technique for the kinetic and mechanistic study of heterogeneous catalytic reactions is steady-state isotopic-transient kinetic analysis (SSITKA) [433,437]. The technique is based on the detection of isotopic labels in the reactor effluent species versus time following a step change in the isotopic labeling of one of the reactants in the reactor feed. Reactant and product concentrations and flow rates remain undisturbed during the step change and — in the absence of isotopic mass effects — steady-state conditions are maintained under isotopic-transient operation. In contrast to other transient experiments, the steady-state kinetic behavior of the catalyst surface can be studied. Steady-state kinetic and mechanistic information which can be obtained from SSITKA includes concentrations of different types of adsorbed reaction intermediates, coverages, surface lifetimes, site heterogeneity, activity distributions, and identification of possible mechanisms [433].

The use of isotopes can greatly aids the elucidation of catalytic mechanisms [438]. The most frequently used isotopes are ^{2}H, ^{13}C, ^{14}C, and ^{18}O. Deuterium-exchange reactions with organic reactants yield isotopic distribution patterns which are often specific enough to eliminate a number of conceivable mechanisms. When carried out in conjunction with structure variations, isotopic distribution patterns may be effective in narrowing the range of possible mechanisms, even though such studies cannot give "the mechanism" [34]. Deuterium labeling is also used to determine which carbon atoms end up where or whether a reaction is inter- or intramolecular [34]. ^{13}C labeling can be used for the same purpose. Although nonradioactive labels are preferred, radioactive tracers such as ^{14}C have also been used [439]. ^{18}O labeling has been applied to elucidate the relative rates of CO and CO_2 in methanol synthesis [440].

Kinetic isotope effects [441,442] are due to the different masses of a given element and its corresponding isotope. The resulting difference in zero-point energy may lead to an increase in activation energy of the labeled molecule and therefore a reduction of the rate. Whether a kinetic isotope effect occurs or not when an atom in a certain position or group is isotopically labeled (i.e., an X−H bond is replaced by X−D) for a catalytic reaction of interest provides information on whether weakening or rupture of the X−H bond is involved in a kinetically significant elementary step.

6.4.3. Use of Substituents, Selective Feeding, and Poisoning

Modification of organic molecules with suitable substituent groups may provide valuable information on reaction mechanisms from the stereochemistry of the reaction of interest [34,443,13]. Substituents generally also have electronic effects on the reactivity of a

parent reactant (substituent effects). Resulting linear free-energy relationships for a series of substituents also assist the determination of kinetically significant reaction steps of a conceivable reaction mechanism [444,445,14,18], since the substituents directly affect the relative energy of the transition state and hence the activation barrier of a kinetically significant step.

Modification of molecules by substituents may also cause intra- or intermolecular steric effects [34], and steric interactions between adsorbate and catalyst surface can be studied. The latter studies provide almost the only way to directly probe the steric nature of active catalytic sites without confusion with adsorption sites that are not catalytic sites [34].

Selective feeding and scavenging have been proposed for the characterization of reaction intermediates [34]. Suppose Q is a suspected intermediate for a particular reaction. This hypothesis can be tested by adding (feeding) a compound to the reaction feed which is supposedly adsorbed to form the suspected intermediate Q, and by testing whether the added compound is indeed converted to the expected product. In scavenging, a compound is added which should react with the intermediate Q to form another compound which is not normally a product.

The nature of catalytic sites can be tested and their density estimated by selective poisoning [446].

6.4.4. Spatially Resolved Analysis of the Fluid Phase over a Catalyst

Analysis of the temperature and concentration profiles in the fluid phase over a working catalyst often provides valuable information on the functional behavior of the catalyst. Since, at high temperatures, conversion of reactants can also proceed via homogeneous reactions in the fluid phase aside from catalytic conversion, interaction of homogeneous and heterogeneous chemical reactions and mass and heat transfer in the catalyst-containing reactor becomes important to fully understand the function of the catalyst. In particular in these cases, temporally and spatially resolved profiles provide a more stringent test for model development and evaluation.

Useful data arise from the experimental resolution of local velocity profiles by laser Doppler anemometry/velocimetry (LDA, LDV) [447,449] and of spatial and temporal species profiles by in situ, noninvasive methods such as Raman and laser-induced fluorescence (LIF) spectroscopy. For instance, an optically accessible catalytic channel reactor can be used to evaluate models for heterogeneous and homogeneous chemistry as well as transport by the simultaneous detection of stable species by Raman measurements and OH radicals by planar laser-induced fluorescence (PLIF) [450,451]. For example, the onset of homogeneous ignition of methane oxidation in a platinum-coated catalytic channel can be monitored by means of the distribution of OH radicals. While catalytic oxidation of methane along the channel walls releases some OH radicals, at a certain point in the reactor a transition to homogeneous oxidation occurs accompanied by high concentrations of OH radicals in the flame region. Since transient phenomena such as ignition, extinction, and oscillations of reactions are very sensitive to transport and kinetics, they can serve as measures for critical evaluation of theoretical models. For instance, the reliability of different heterogeneous and homogeneous reaction schemes proposed in the literature was investigated by comparison of the experimentally derived ignition distances with numerical elliptic two-dimensional simulations of the flow field by using combinations of a variety of schemes [452,453].

6.4.5. Spectroscopic Techniques

Any spectroscopic technique which is surface-sensitive, has sufficiently high sensitivity, and can be applied under catalytic working conditions can provide valuable information on the nature of sufficiently long lived intermediates. However, spectroscopy often detects spectator species rather than reaction intermediates. Therefore, it is mandatory to demonstrate that true intermediates are in fact seen. This can be done by varying critical reaction parameters and monitoring the response of spectroscopic signal intensities as a function of time. Sufficiently high temporal resolution of the applied spectroscopic technique is therefore required.

7. Design and Technical Operation of Solid Catalysts

7.1. Design Criteria for Solid Catalysts [454]

Solid catalysts are used in a surprising variety of shapes including powders and irregularly shaped particles, regular particles such as spheres and cylinders, and more complex geometries like monolithic honeycombs, gauzes, and fibers. The most suitable geometry must be carefully selected and adjusted according to the properties of the catalytically active material and specific requirements of the chemical reaction and catalytic reactor. Only rarely is the catalytic reaction so fast that the outer geometric surface area of a nonporous catalytic body is sufficiently large. Hence, porous catalysts are mainly used in which the catalytically active surface area inside the structure often exceeds the geometric surface area by several orders of magnitude. In these cases, the pore structure must be accessible to the reactants while products are allowed to leave. Design criteria for solid catalysts comprise the choice of appropriate geometries with respect to highest possible catalyst utilization and product selectivity in a given reactor. These goals should be achieved at the lowest possible pressure drop over the reactor.

Diffusion, Mass- and Heat-Transfer Effects [89,455,456]. Heterogeneous catalytic reactions take place on the external and internal surfaces (pores) of the catalyst. External and internal concentration and temperature gradients can build up in the fluid (gas or liquid) boundary layer around the catalyst particles and inside the pores if mass and heat transfer between the bulk of the fluid and the active surfaces are not sufficiently fast. Such gradients tend to exist (1) in fixed-bed reactors charged with large, porous catalysts; (2) during operation at low mass flow velocities (mass flow rate per unit cross-sectional area); or (3) in the case of highly exothermic reactions. On the other hand, gradient effects usually are absent when small catalyst particles are used in fluidized-bed reactors.

Because such internal and external gradients can substantially reduce the activity and selectivity of the catalyst, conditions have been delineated under which their adverse effects can be minimized [89,455,456]. By carefully matching operating conditions, catalyst, and reactor, optimum catalyst performance can be ensured.

Mass and heat transfer in heterogeneous catalytic reactions occur in two ways. *External transport* to the external surface involves diffusion through the more or less stationary hydrodynamic boundary layer that surrounds the catalyst particle. The thickness of this layer depends on the characteristics of the fluid and its flow rate past the particle, and affects the rate of mass and heat transfer. *Internal transport* to the stationary fluid in the pores of catalyst particle is controlled by diffusion alone.

Depending on the relative rates of the transport processes and the catalytic reaction, three or four types of regimes can be distinguished. In the *kinetic regime* the rates of external and internal mass transport are much higher than the rate of the chemical reaction. Therefore, concentration and temperature gradients between the fluid and the center of a catalyst particle are negligible, and the catalyst is fully utilized.

In the *internal diffusion regime*, mass transport in the catalyst pores is about as fast as, or slower than, the chemical reaction. In this case there are considerable concentration gradients along the length of the pores, the effectiveness of the catalyst is impaired, and the apparent energy of activation is lower than that observed in the kinetic regime.

At an even lower ratio of rates of transport and conversion, there is an *intermediate regime* in which the reaction takes place only on the external surface of the catalyst particles while the internal surface area in the pores is inactive. Because of the limited heat transfer in this regime, exothermic reactions can overheat the catalyst, and this results in a higher activity than that corresponding to the temperature of the fluid.

Finally, on further decreasing the ratio of the rates of transport and conversion (e.g., by raising the temperature of the fluid), the *external mass transfer regime* is reached in which the reaction rate is controlled by mass transfer, and the concentration of the reactants at the surface of the catalyst particles drops. Raising the

reactor temperature in this regime has little effect on the reaction rate, and the apparent activation energy drops.

Effectiveness Factor [89,455,456] The effectiveness factor η is the ratio of the actual reaction rate observed on a porous catalyst particle to the rate that would be obtained if the inside of the particle were exposed to the temperature and reactant concentrations of the fluid. Mathematical analysis [89,457–466] of mass transfer in porous particles of different shapes has shown that the effectiveness factor is a function of a dimensionless quantity, called the *Thiele modulus* φ [457]: for a sphere of radius R and for a plate sealed on one side and on the edges the thickness of which is L, φ is defined by the following equations:

$$\text{sphere} : \varphi_s = R\left(\frac{k_v c_s^{m-1}}{D_{eff}}\right)^{1/2} \qquad (31)$$

$$\text{plate} : \varphi_L = L\left(\frac{k_v c_s^{m-1}}{D_{eff}}\right)^{1/2}$$

where k_v is the reaction rate constant per unit of gross catalyst volume, c_s is the concentration on the surface, m is the reaction order, and D_{eff} the effective diffusion coefficient, given by

$$D_{eff} = D\frac{\Theta}{\tau} \qquad (32)$$

where D is the diffusion coefficient for a pair of fluids taking into account binary and Knudsen diffusion, Θ the void fraction of the porous mass, and τ a factor allowing for tortuosity and varying cross sections of the pores.

Equation (31) for the plate can also be used for arbitrary catalyst geometry if L is interpreted as *characteristic diffusion length*, i.e. the ratio of catalyst particle volume and its external surface area.

For first-order reactions ($m = 1$), the effectiveness factors are as follows (tan is hyperbolic tangent):

$$\text{Sphere} : \eta = \frac{3}{\varphi_s}\left(\frac{1}{\tanh \varphi_s} - \frac{1}{\varphi_s}\right) \qquad (33)$$

$$\text{Plate} : \eta = \frac{\tanh \varphi_L}{\varphi_L}$$

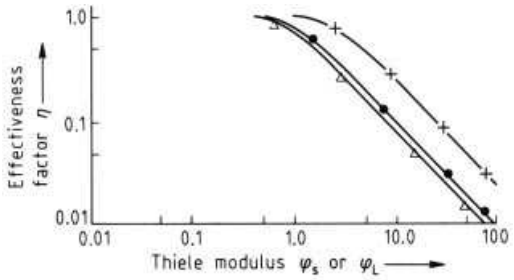

Figure 19. Effectiveness factor φ as a function of the Thiele modulus φ_s or σ_L
Flat plate sealed on one side and on edges, first-order reaction; Δ Same, second-order reaction; + Spherical particle, first-order reaction
* Reproduced with permission [462]

Correlation between the effectiveness factor and the Thiele modulus for nonexothermic reactions is shown in Figure 19 [462]. The effectiveness factor is about unity for $\varphi < 1$ and inversely proportional to φ for $\varphi > 3$.

If the intrinsic velocity rate constant k_v (Eq. 32) cannot be determined directly, another dimensionless modulus Θ has been derived [460,462]. For first-order reactions occurring in a sphere, it is defined by

$$\Theta \equiv \varphi^2 \eta = \left(\frac{R^2}{D_{eff} V_c C_s}\right)\left(\frac{dn}{dt}\right) \qquad (34)$$

where dn/dt is the conversion rate in moles per second of the reactant in the catalyst volume V_c. The effectiveness factor as a function of Θ is shown in Figure 20 for a moderate energy of activation ($E = 10\ RT$; first-order reaction in a spherical particle) and variable enthalpy change ΔH (λ is the thermal conductivity of the catalyst). For exothermic reactions ($\beta > 0$), the effectiveness factor goes through a maximum value exceeding unity because of the interaction of two opposing effects. Poor mass transfer lowers the efficiency of the catalyst, whereas insufficient heat transfer raises catalyst temperature and reaction rate.

Effects on Selectivity [89,455,456] The effect of mass- and heat-transport processes on the selectivity of reactions yielding more than one product depends on the *selectivity type*. In a type I reaction at low effectiveness factors, the observed selectivity factor changes from k_1/k_2 to

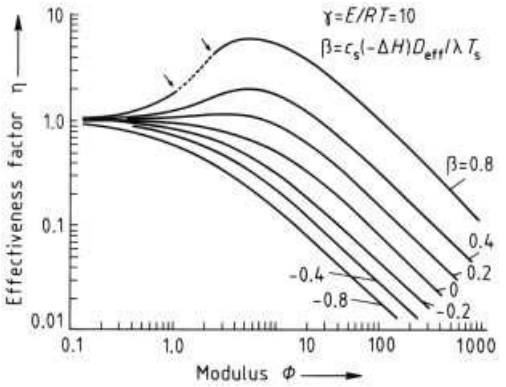

Figure 20. Effectiveness factor as a function of modulus (Eq. 34)
--- Unstable region
* Reproduced with permission [467]

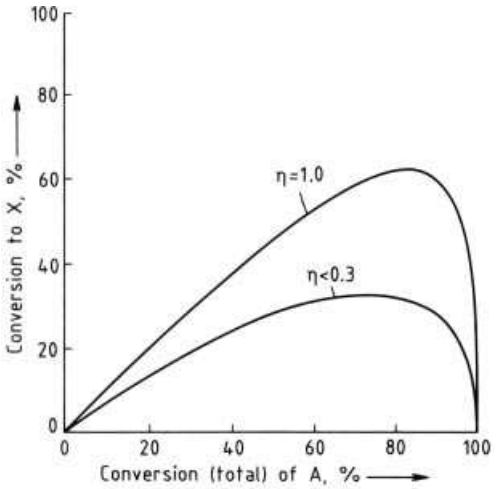

Figure 21. Effect of the effectiveness factor on catalyst selectivity
* Reproduced with permission [468]

$(k_1 D_{\mathrm{Aeff}} k_2^{-1} D_{\mathrm{Beff}}^{-1})^{1/2}$, provided the order of the two reactions (A → X and B → Y) is the same. If, as usual, the ratio of the effective diffusivities is smaller than k_1/k_2, the selectivity will drop at low effectiveness factors. However, if the diffusivity ratio is high, the selectivity can increase in a porous catalyst. This is the situation in the so-called shape-selective zeolites [89]. If the reaction orders are different, the reaction with the lower order is favored in the porous catalyst at low η values.

In reaction type II, the effectiveness factor has no influence on the selectivity if the orders of the two reactions are equal. Otherwise, the effect of different orders is the same as in type II reactions [456,467].

For an isothermal first-order reaction of type III occurring at low effectiveness factor on a porous plate, the observed selectivity is approximately the square root of the intrinsic rate constant ratio k_1/k_2 [468]. Figure 21 shows comparative conversions of A to X for type III at effectiveness factors $\eta = 1$ and $\eta < 0.3$, for $k_1/k_2 = 4$; the maximum yield and selectivity both drop by ca. 50 % at the low effectiveness factor [468].

Temperature gradients caused by exothermic reactions favor reactions with higher apparent *energies of activation*. Because such undesired side reactions as decomposition and oxidative degradation generally have high energies of activation, large catalysts having narrow pore structure can have an unfavorable effect on the selectivity and product yield.

In the regime of external mass transfer, resistance of the boundary layer to *diffusion* has similar effects on the selectivity of parallel and consecutive reactions as does diffusion in pores.

Catalyst Geometries and Transfer Processes Industrial processes that occur in the kinetic regime include reactions conducted in fluidized-bed reactors using catalysts 0.05 – 0.25 mm in size [89,456]. Because diffusion coefficients in liquids are smaller by several orders of magnitude than those in the gaseous phase, liquid-phase operation in the kinetic regime requires a finely powdered catalyst.

Because the resistance to flow of catalysts increases steeply with decreasing size, use of catalysts smaller than 2 – 3 mm in fixed-bed reactors is restricted to radial-flow reactors with small bed length. Ring-shaped and tablet catalysts show relatively favorable pressure drop and diffusion characteristics.

In various partial oxidation processes (e.g., *o*-xylene to phthalic anhydride), good results have been obtained with so-called *eggshell catalysts* in which the active catalyst mass is applied in a thin layer of a few tenths of a millimeter to the external surface of an inert, nonporous support.

If the reaction rate is higher and the regime of *internal diffusion* cannot be avoided, it is often advantageous to use catalysts with a bimodal pore system in which micropores (< 2 nm) are

connected by macropores (> 50 nm) to the external surface area of the catalyst particle. The micropores provide the needed high active surface area, whereas the macropores facilitate mass transport to and from the micropores. Such catalysts are especially suitable for operation at process pressures below 3 MPa. At these pressures mass transport into pores smaller than 100 – 1000 nm occurs increasingly through *Knudsen diffusion* involving molecular collisions with the pore wall rather than between molecules [89,456].

In fast processes occurring in the regime of *external mass transfer*, the overall conversion rate is independent of the porosity of the catalyst and is essentially proportional to its external surface area [463]. Examples of such reactions are oxidation of ammonia to nitric acid and ammoxidation of methane to hydrogen cyanide carried out at 1070 – 1270 K on stacks of fine-mesh Pt – Rh gauze.

7.2. Catalytic Reactors [469–473]

7.2.1. Classification of Reactors [167,469,471]

Catalytic reactors can be classified by their mode of operation under steady-state or transient conditions or on their mode of contacting/mixing of reactants and solid catalyst.

Typical *steady-state reactors* are packed-bed tubular reactors under continuous flow conditions, either plug flow or mixed flow. In an ideal tubular reactor ideal mixing takes place in the radial direction, but there is no mixing in the axial direction. Plug flow is attained in this case. *Plug flow reactors* can be operated either in integral or differential mode. In the latter case, single-pass experiments in small-scale reactors provide the data for differential conditions required for analysis of the reaction kinetics. As an alternative, the effluent from the differentially operating reactor can also be recycled externally or internally, thus approaching a well-mixed reactor system, the continuous-flow *stirred tank reactor* (CSTR). Without inlet and outlet feed a continuous recycle flow results, characteristic of a *batch reactor* in which the feed composition changes with time (transient conditions as opposed to steady-state conditions). The catalyst must not necessarily be kept in a packed bed but can be suspended in the liquid or gaseous fluid reactant mixture. In the fluidized-bed mode, the solid catalyst consisting of fine powder (particle diameter 10 – 200 μm) is kept in motion by an upward gas flow (*fluidized-bed reactor*, see Section Industrial Reactors). If the fluid is a liquid the catalyst can be suspended easily in a CSTR by efficient stirring (*slurry reactor*, see Section Industrial Reactors). In so-called *riser reactors*, catalyst material is continuously introduced into and removed from the reactor with the reactant and product feeds.

Batch and semi-batch reactors operate under transient conditions. Discontinuous step or pulse operation necessarily results in transient conditions.

Several catalytic reactor types are schematically shown in Figure 22. *Tubular fixed bed reactors* (A) have an inlet flow n_0 and an outlet flow n of the reactant-product mixture. The *adiabatic fixed-bed reactor* is shown in Figure 22 B. *Multitube fixed-bed reactors* (C) are used for highly exothermic reactions such as the oxidation of *o*-xylene to phthalic anhydride. The principle of a CSTR is demonstrated as D. A *fluidized-bed reactor* with catalyst recirculation is sketched in E. A *slurry CSTR reactor* is schematically shown in F. An alternative for three-phase reactions (gas – liquid – solid) is the *packed bubble column* or *slurry reactor* (G). Discontinuous batch reactors with internal and external recycling operating under transient conditions are depicted as H and I, respectively.

7.2.2. Laboratory Reactors [469,470]

A compilation of laboratory reactors and their operation mode is given in Figure 23.

Laboratory reactors are small-scale reactors. Steady-state fixed-bed tubular flow reactors are most frequently used for catalyst testing and determination of the reaction kinetics on the laboratory scale. These reactors are favored because of the small amounts of catalyst required, the ease of operation, and the low cost. Stirred tank reactors (e.g., with fixed or rotating basket) and batch suspension reactors are less frequently used. Provided that heat- and mass-transfer limitations can be neglected under the

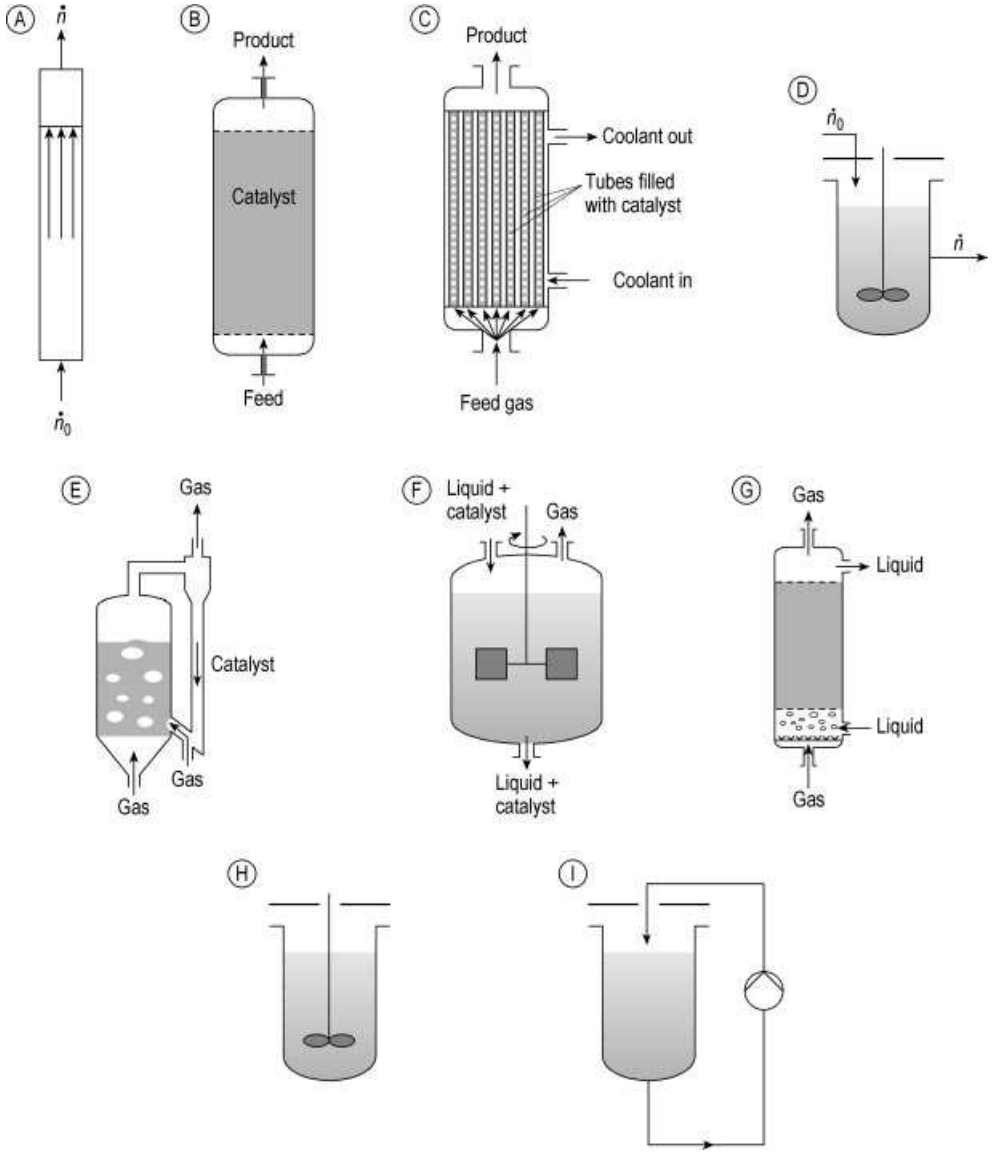

Figure 22. Schematic representation of several types of catalytic reactors
A) Tubular fixed bed reactor; B) Adiabatic fixed-bed reactor; C) Multitube fixed-bed reactor; D) CSTR; E) Fluidized-bed reactor with catalyst recirculation; F) Slurry CSTR reactor; G) Packed bubble column or slurry reactor; H), I) Discontinuous batch reactors

operating conditions in a tubular flow reactor, the catalyst bed is isothermal, and the pressure drop across the catalyst bed is negligible, the reaction rate can be determined from the mass balance for a component *i*. This is usually verified in microreactors operating under differential conditions. The *reaction rate* per unit mass r_W (mol s^{-1} kg^{-1}) is then given by Equation (35):

$$\frac{dx_i}{d\left(\frac{W}{F_i^0}\right)} = -\nu_i r_W, \qquad (35)$$

where X_i is the conversion of component *i*, ν_i its stoichiometric coefficient, *W* the catalyst mass (kg), and F_i^o the molar rate of component *i* at the

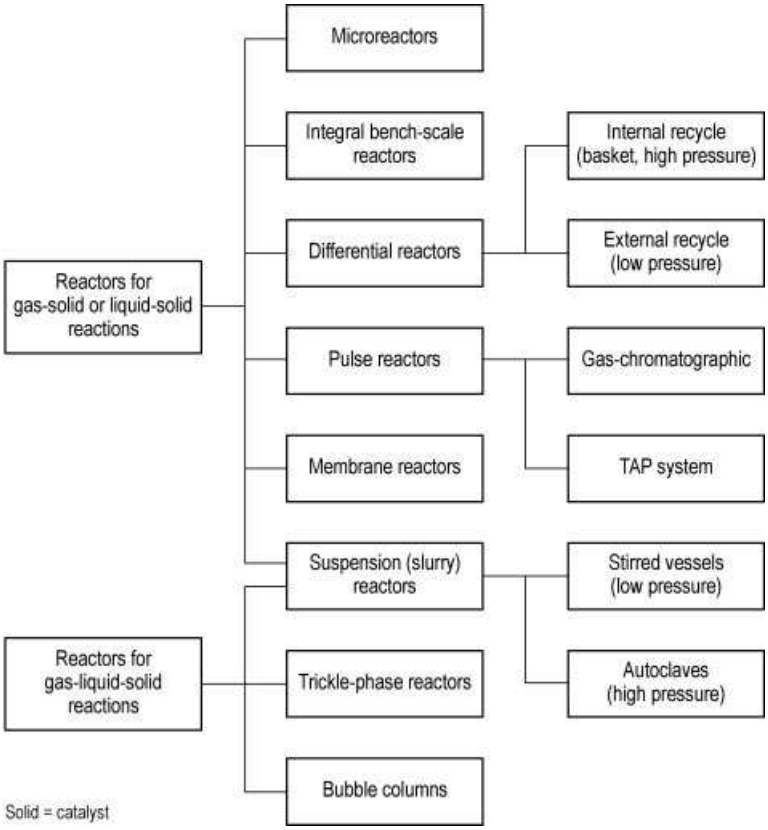

Figure 23. Classification of laboratory reactors

reactor inlet (mol s^{-1}). The ratio W/F_i^o is the space – time.

Ancillary techniques in laboratory units for catalyst testing such as generation of feed streams and product sampling are discussed in [474].

The TAP reactor, a laboratory pulse reactor, is described in Section Temporal Analysis of Products (TAP Reactor).

7.2.3. Industrial Reactors [167,471]

Various types of industrial reactors and their operation mode are listed in Figure 24.

Catalytic Fixed-Bed Reactors [475,477]
In the chemical industry fixed-bed reactors are the standard type of reactors for heterogeneously catalyzed gas-phase reactions (two-phase reactors). Fixed catalyst beds can be realized in various ways. Randomly packed beds (deep beds) require catalyst particles having different shapes such as spheres, cylinders, rings, flat disk pellets, or crushed material of a defined sieve fraction. The geometries and dimensions of the catalyst particles are dictated by pressure drop and heat- and mass-transfer considerations. The use of monolithic catalysts significantly reduces the pressure drop across the catalyst bed. This type of catalyst is employed for example for automobile exhaust gas purification and for the removal of nitrogen oxides from tail gases of power stations.

Fixed-bed reactors can be operated under adiabatic or nonadiabatic conditions. Adiabatic reactors can be applied for reactions with low heats of reaction such as gas purification. They consist of a cylindrical tube in which the catalyst is packed on a screen and is traversed in axial direction (Fig. 22 B). This design is particularly suitable when short residence times and high

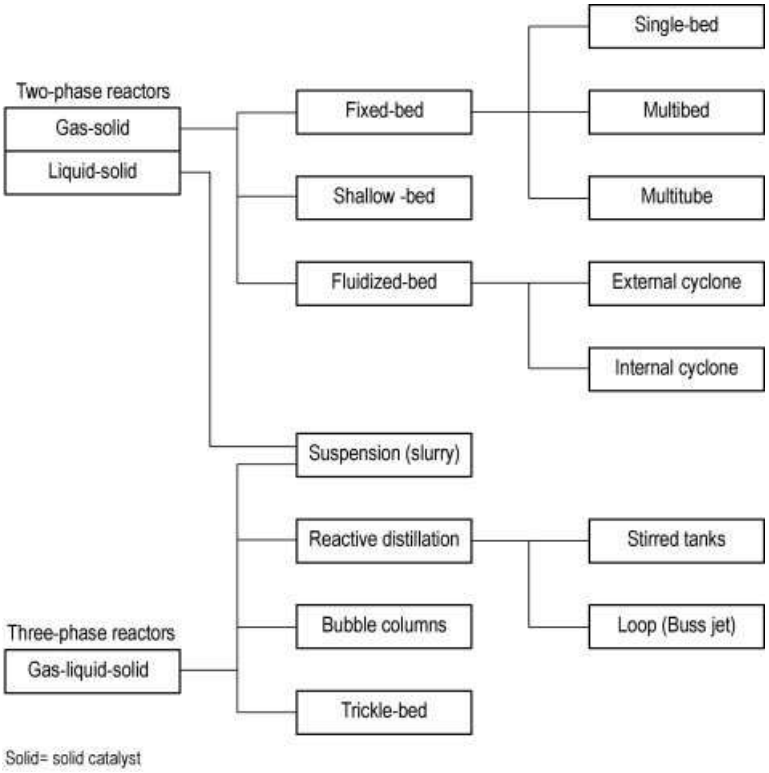

Figure 24. Classification of industrial reactors

temperatures are required. In this case a fixed bed of large diameter and small height (5 – 20 mm) is used (shallow bed). As an example, for ammonia oxidation in nitric acid plants the fixed bed consists of several layers of platinum wire gauze with bed diameters up to several meters. This type of reactor is limited to small catalyst volumes. The radial flow concept is preferred when large amounts of catalyst are required [475]. In this reactor type, the catalyst is charged in the annular space around an axially located tube. The reactants are traversing radially, either from the inside or from the outside of perforated plate rings. Because of the low pressure drop, smaller catalyst pellets (4 × 4 or 3 × 3 mm) can be used in this reactor type.

Only limited conversions can be achieved by adiabatic reactors because of the necessary control of the adiabatic temperature change. Multistage reactors consisting of several sequential adiabatic stages which are separated by interstage heat exchangers have therefore been introduced.

Nonadiabatic operation can be achieved with fixed-bed reactors which are cooled or heated through the reactor walls. Efficient heat exchange results in so-called isothermal reactors. A typical example is the multitubular reactor schematically shown in Fig. 22 C, which is used for highly exothermic and temperature sensitive reactions (e.g., *o*-xylene oxidation) with, e.g., salt melts as heat-transfer media. In a *multitube reactor*, the pressure drop must be the same in each tube so that the gas flow is distributed uniformly over the tubes. Small changes in the packing density in the tubes can cause uneven heat transfer and, in the case of highly exothermic reactions, hot spots and selectivity loss. For these reasons multitube reactors are filled by special equipment that charges each tube with the same amount of catalyst at a definite rate. After filling, the tubes are checked for pressure drop, and if necessary, the charge is adjusted.

Autothermal reactors can favorably be applied for exothermic and temperature sensitive

reaction systems. The conventional reactor design consists of an adiabatic packed-bed reactor coupled with a countercurrent heat exchanger in which the cold reactant feed is brought to reaction temperature.

Multifunctional reactors are being developed [478] with the goal of improving operation conditions which are not necessarily optimally determined in standard fixed-bed reactor configurations.

The following industrial processes are performed in various types of fixed-bed reactors:

i. "deep-bed" adiabatic system:
- Isomerization of C_4 – C_6 alkanes or of light gasoline at 620 – 770 K, 20 – 40 bar on Pt-alumina (HCI activated) or on Pt-H-mordenite.
- Catalytic reforming of heavy gasoline using a cascade of single bed reactors at 700 – 820 K, 20 – 25 bar on K-promoted Cr_2O_3-Al_2O_3 catalyst.
- Hydrocracking of vacuum gas oil at 670 – 770 K, 20 – 40 bar, using single or two stage processes on Ni-MoO_3-Y-zeolite-alumina and Pt-mordenite-alumina, respectively.

ii. "multibed" adiabatic system:
- Ammonia synthesis at 670 – 770 K, 200 – 300 bar on K-, Mg-, Al-promoted iron catalysts.
- Oxidation of SO_2 in the sulfuric acid production at 720 – 770 K, atmospheric pressure on K_2SO_4-V_2O_5 catalysts. Reactor with externally located heat exchangers are in operation.

iii. "radial flow" system:
- Water gas shift (HTS) at 620 – 670 K, 25 – 50 bar on Cr_2O_3-Fe_2O_3 catalysts.

iv. "shallow-bed" system:
- Methanol dehydrogenation to formaldehyde at 870 K, atmospheric pressure on metallic Ag (granulate).
- Ammonia oxidation to NO_x at 1170 K atmospheric pressure on Pt/Rh-grids.

v. "quench" system:
- Methanol synthesis at 490 – 520 K, 50 – 100 bar on Cu-ZnO-Al_2O_3 catalysts.

vi. "multitube" system:
- Methanol synthesis at 490 – 520 K, 50 – 100 bar on Cu-ZnO-Al_2O_3 catalysts.
- Oxidation of ethylene to ethylene oxide at 470 – 520 K, atmospheric pressure on Ag-α-alumina.
- Oxidation of *o*-xylene to phthalic anhydride at 640 – 680 K, at atmospheric pressure on V_2O_5-TiO_2 catalysts.
- Hydrogenation of benzene to cyclohexane at 470 – 520 K, 35 bar on Ni-SiO_2 catalysts.
- Dehydrogenation of ethylbenzene to styrene at 770 – 870 K, atmospheric or reduced pressure on promoted (K, Ce, Mo) Fe-oxide.

Fluidized Bed Reactors [479–482] Fluidized-bed reactors are preferred over fixed-bed reactors if rapid catalyst deactivation occurs or operation in the explosive regime is required. In this type of reactor, an initially stationary bed of catalyst is brought to a fluidized-state by an upward stream of gas or liquid when the volume flow rate of the fluid exceeds a certain limiting value, the minimum fluidization volume flow rate. The catalyst particles are held suspended in the fluid stream at this or higher flow rates. The pressure drop of fluid passing through the fluidized bed is equal to the difference between the weight of the solid catalyst particles and the buoyancy divided by the cross-sectional area of the bed. Major advantages of fluidized-bed reactors are excellent gas – solid contact, good gas – solid heat and mass transfer, and high bed-wall heat transfer coefficients.

The gas distribution in the fluidized bed is performed industrially by, for example, perforated plates, nozzles, or bubble caps which are mounted at the reactor bottom.

Depending on the volume flow rate of the fluid different types of fluidized beds form. Fluidization with a liquid feed leads to a uniform expansion of the bed. In contrast, solid-free bubbles form when fluidization is carried out in a gas stream. These bubbles move upwards and tend to coalesce to larger bubbles as they reach increasing heights in the bed. At high gas volume flow rates, solid particles are carried out of the bed. To maintain steady-state operation of

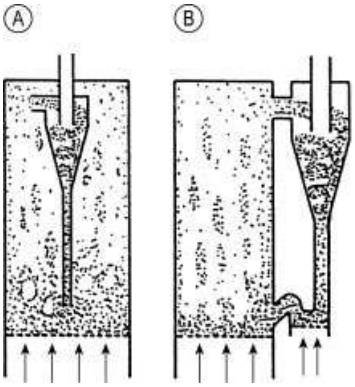

Figure 25. Schematic representation of two forms of gas – solid fluidized beds under turbulent flow conditions

such a turbulent fluidized bed, the solid catalyst particles entrained in the fluidizing gas must be collected and transported back to the reactor bed. This can be achieved most easily with an integrated cyclone, as schematically shown in Figure 25 A. A circulating fluidized bed is finally formed at still higher gas volume rates. An efficient external recycle system, as shown in Figure 25 B, is required for such operating conditions because of the high solids entrainment.

Catalytic cracking is carried out in fluidized-bed reactors because the solid acid catalysts are rapidly deactivated by coke deposition. The catalyst must therefore continuously be discharged from the reactor and regenerated in an air-fluidized regenerator bed where the coke is burned off. The regenerated catalyst is then returned to the fluidized-bed reactor. The heat of combustion of the coke can be used for preheating of the reactant feed.

The main advantages of *fluidized-bed* reactors are:

- Uniform temperature distribution (due to intensive solid mixing)
- Large solid-gas exchange area
- High heat-transfer coefficient between bed and immersed heating or cooling surfaces.

However, these reactors have also some disadvantages, e.g.:

- Expensive catalyst separation and purification of reaction products (installation of cyclones and filters)
- Undesired bypass of reactants due to bubble development
- Catalyst attrition
- Erosion of internals resulting from high solids velocities

Fluidized-bed reactors found very broad application in the petroleum refining and production of chemicals, for example:

- Catalytic cracking of vacuum gas oil to gasoline at 720 – 820 K on aluminosilicates containing ultrastable Y-zeolites.
- Fischer – Tropsch synthesis (Synthol process) from CO und H_2 at 620 – 670 K and 15 – 30 bar on promoted Fe-oxide catalysts.
- Ammoxidation of propylene to acrylonitrile (SOHIO-process) at 670 – 770 K, 1 – 2 bar on promoted Bi-MoO_x catalysts.
- Oxidation of naphthalene or *o*-xylene to phthalic anhydride at 620 – 650 K, at atmospheric pressure on V_2O_5–SiO_2 catalysts.

A special type of the fluidized-bed reactor is the so-called riser reactor. This reactor consists of a vertical tube in which the reaction takes place in the presence of the entrained catalyst. Catalyst coming from the riser tube is collected in the vessel, before passing through the stripper to the regenerator (fluidized-bed type). The riser reactor is mainly used in the catalytic cracking of heavy oils on highly active zeolitic catalysts.

The *moving-bed* reactor [479] operates with spherical catalyst particles larger (2 – 6 mm) than those used in the fluid-bed system. In the standard arrangement, catalyst particles are moving slowly through the agitated bed. Catalyst reaching the reactor top is transported into the regenerator. Using mechanical or pneumatic conveyer the regenerated catalyst is returning to the bottom of the reactor.

The main advantage of the moving-bed reactor is lower catalyst attrition than in the fluidized-bed system. The disadvantage is a poor heat transfer, and therefore this reactor is not suitable for exothermic reactions.

The moving-bed reactor found application mainly in petroleum cracking.

Slurry Reactors [483] The aim of slurry reactors is intimate contact between a gas

phase component (which is to be dissolved in a liquid-phase component) and a finely dispersed solid catalyst (three-phase reactors). The particle size of the solid catalyst is kept sufficiently small (< 200 μm) that it remains suspended by the turbulence of the liquid in the slurry reactor. This is in contrast to three-phase fluidized-bed reactors, in which an upward liquid flow is required to suspend the larger catalyst particles.

On the basis of the contacting pattern of the phases and the mechanical devices that achieve contact and the mass transfer, nine types of slurry reactors can be distinguished [483]:

1. Slurry bubble column
2. Countercurrent column
3. Cocurrent upflow
4. Cocurrent downflow
5. Stirred vessel
6. Draft-tube reactor
7. Tray column
8. Rotating-disk or multiagitator column
9. Three-phase spray column

Slurry reactors are industrially applied for a multitude of processes [484], many of which are heterogeneously catalyzed processes for hydrogenation of edible oils. A new development is the continuous Fischer – Tropsch slurry synthesis process of SASOL in South Africa [485].

Three-phase reactors are classified as fixed-bed or suspension reactors depending on the catalyst arrangement and shape:

Fixed-bed reactors operate either in the trickle-bed or in the bubble-flow mode [483]. In the first case, liquid reactants or reactants dissolved in a solvent are flowing downward through the catalyst bed and the gaseous reactants are conducted in the countercurrent or concurrent direction.

In the bubble-flow reactors, liquid and gaseous reactants are fed into the bottom of the column and are flowing upward through the catalyst fixed-bed.

The trickle-bed arrangement has some advantages such as:

- Fast diffusion of gases through the liquid film to the catalyst surface
- Lower back-mixing
- No problems with catalyst separation
- Selective removal of catalytic poison in the entrance zone of the bed
- Simple catalyst regeneration

Drawbacks of trickle-bed reactors are:

Poor heat transfer
Partial utilization of the catalyst in case of the incomplete wetting
Possibility of "brooks" formation

The successful performance of the trickle-phase reactors depends on the suitable diameter/length ratio, catalyst shape and size, and the liquid flow distribution through the catalyst bed. The catalyst particle size is limited by the allowed pressure drop. Larger sizes (6 – 10 mm diameter) are therefore preferred, which, however, can bring diffusion problems.

The "bubble-flow" version is favored in particular for reactions with a low space velocity. A good heat transfer and no problems with an incomplete catalyst wetting are the main advantages of the "bubble-flow" reactors.

Both types of the three-phase reactors have found numerous industrial applications, e.g.:

- Hydrotreating of petroleum fractions at 570 – 620 K, 30 – 60 bar on Ni–MoO_3–Al_2O_3 catalysts.
- Hydrocracking of high boiling distillates at 570 – 670 K, 200 – 220 bar on Ni–MoO_3–Y–zeolite–alumina catalysts.
- Selective hydogenation of C_4-fractions (removal of dienes and alkines) at 300 – 325 K, 5 – 20 bar on Pd-Al_2O_3 catalysts.
- Hydrogenation of aliphatic carbonyl compounds to alcohols at 370 – 420 K, 30 bar on CuO–Cr_2O_3 catalysts.

Suspension reactors [483,484] are operated successfully in the chemical industry because of their good heat transfer, temperature control, catalyst utilization, and simple design. Because of the small catalyst particle size, there are no problems with internal diffusion. Suspension reactors operate either in the discontinuous or in the continuous mode. One serious disadvantage is the difficult catalyst separation, especially if fine particles have to be removed from the viscous liquid.

Currently two types of suspension reactors are in use: stirred vessels and three-phase bubble columns.

In the case of *stirred vessels* the catalyst particles (mainly smaller than 200 μm) are suspended in the liquid reactant or solutions of reactants, whereas gaseous reactants are introduced at the bottom of the vessel through perforated tubes, plates or nozzles. The vessels are equipped with different types of stirrers or turbines keeping the catalyst suspended. Cooling and heating coils as well as the gas recycle system belong to the standard equipment. Stirred vessels operate mostly discontinuously. However, if continuous operation is favored, then stirred vessels are arranged in a cascade to complete the required conversion.

Bubble columns are mainly continuously operating three-phase reactors. The gas is introduced at the bottom of the column through nozzles, perforated plates or tubes. In the standard arrangement the liquid reactant flows in the cocurrent direction with the gas. In some cases stirrers are installed to keep powdered catalysts in the suspension.

The gaseous reactants can be recycled by an external loop or by an internal system, such as a Venturi jet tube. This equipment is driven by a recycle of the slurry using a simple pump. The Venturi tube is sucking the gas from the free board above the reactor back into the slurry. Heat exchangers can be installed in the loop in both cases.

The main advantages of bubble columns are simple and low-priced construction, good heat transfer, and good temperature control.

Suspension reactors are used predominantly for fat and oil hydrogenation 420 – 470 K, at 5 – 15 bar using various Ni–kieselguhr catalysts.

Also, hydrogenolysis of fatty acid methyl esters to fatty alcohols is performed in suspension reactors at 450 – 490 K, 200 – 300 bar on promoted copper chromites ($CuO–Cr_2O_3$).

Further applications are: syntheses of acetaldehyde and of vinyl acetate according to the Wacker process.

7.2.4. Special Reactor Types and Processes

Microstructured Reactors [486–491] A microstructured reactor can be defined as a series of interconnecting channels having diameters between 10 and 1000 μm that are formed in a planar surface in which small quantities of reagents are manipulated (see also → Microreactors – Modeling and Simulation). Among the advantages of microstructured reactors over conventional catalytic reactors are high heat-transfer coefficients, increased surface-to-volume ratios of up to 50 000 $m^2\ m^{-3}$, as opposed to 1000 $m^2\ m^{-3}$ for conventional catalytic laboratory reactors, shorter mixing times, and localized control of concentration gradients. The small scales reduce exposure to toxic or hazardous materials, and the enclosed nature of the microstructured reactors permits greater ease of containment in the event of a runaway reaction. Furthermore, the highly efficient heat transfer as well as high surface areas available for adsorption of radicals allow reactions to be carried out beyond the explosion limit [488,492,493].

Despite their small size, microstructured reactors can be used for synthetic chemistry [494], since as few as 1000 microchannels operating continuously could produce 1 kg of product per day. While several types of laboratory-scale microstructured reactors are already commercially available, further developments are still required to make microstructured reactors mature for industrial application. One of the most advanced designs targeted at large-scale applications for exothermic gas-phase reactions is the DEMiS project of Degussa and Uhde [495]. The state of development of microstructured reactors for heterogeneously catalyzed gas-phase and liquid-phase reactions has been summarized [319]. Coating of wall materials with catalysts, strategies for replacement of spent catalysts, and the reduction of overall apparatus size appear to be the most challenging obstacles to be overcome. It is also evident that in many cases more active catalysts are required for full utilization of microstructured reactors.

Unsteady-State Reactor Operation [496] Forced unsteady-state reactor operation has been applied to continuous catalytic processes in fixed and f1uidized-bed reactors. This operating mode can lead to improved reactor performance. Nonlinearity of chemical reaction rates and complexity of reaction systems are responsible for conversion or selectivity

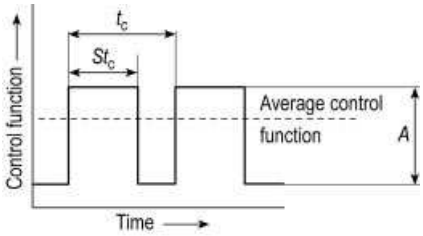

Figure 26. Stepwise variation of inlet parameters to create unsteady state conditions

improvements under forced unsteady-state conditions [497].

An unsteady-state in a fixed-bed reactor can be created by oscillations in the inlet composition or temperature (control function) such as schematically shown in Figure 26. The most widely applied technique in a fixed-bed reactor is periodic flow reversal. Examples of this operation mode in industrial applications are SO_2 oxidation, NO_x reduction by NH_3, and oxidation of volatile organic compounds (VOC). In fluidized-beds for exothermic reactions, favorable unsteady-state conditions of the catalyst can be achieved by catalyst circulation inside the reactor. The unsteady-state operation in the fluidized-bed is applied for example for the partial oxidation of *n*-butane to maleic anhydride on vanadyl pyrophosphate catalysts developed by DuPont. In the first step, *n*-butane diluted with an inert gas is contacted in the riser reactor (residence time 10 – 30 s) with spherical catalyst particles (100 μm). The partial oxidation of *n*-butane proceeds on account of the lattice oxygen in the surface layer of vanadyl pyrophosphate. In the second step, the partially reduced catalyst is transported into the fluidized-bed reactor where the catalyst reoxidation takes place. The obtained selectivity was about 10 % higher than that in the multitubular fixed-bed reactor, operating under steady-state conditions. A further group of forced unsteady-state processes uses the combination of a chemical reaction with the separation of products (chromatographic reactor). Systems applied till today operating on the principle of chromatographic columns are filled with a catalyst possessing suitable adsorption properties, such as Pt - Al_2O_3. Pulses of reactant are periodically injected into this reactor which is purged by carrier gas during periods between the pulses. This operation can provide a higher conversion for reversible reactions if one of the reaction products is adsorbed on the catalyst more strongly than the other one. The feasibility of this principle was tested in the dehydrogenation of cyclohexane to benzene on pilot scale.

Membrane Reactors [498–500] In membrane reactors (→ Membrane Reactors) catalytic conversion is coupled with a separation effect provided by the integrated membrane. High conversions can be achieved for equilibrium-restricted reactions when one of the reaction products can be removed from the reaction mixture by diffusion through a permselective membrane. Hydrocarbon dehydrogenation reactions are the best example for this application. In addition, catalytic membrane reactors have been proposed for improved control of the selectivity of some catalytic reactions. For example, controlled introduction of a reactant into the reactor by selective or preferential permeation may limit possible secondary reactions of the target product.

Two types of membranes can be distinguished: dense membranes and porous membranes. Dense metallic membranes consist of thin metal foils. Palladium and palladium alloys (PdAg, PdRu) are specific for hydrogen permeation. Dense oxide membranes are usually solid electrolytes such as ZrO_2 and CeO_2, which are permeable for O_2 [500]. Porous membranes are typically made of oxides, although carbon membranes have also been used [501]. Ceramic membranes consist of several layers of material with progressively decreasing pore size. The top layer with the smallest pore size controls the separation. Most of these membranes are produced by sol – gel techniques. Intrinsic catalytic properties can be introduced into these membranes, which can be produced as cylindrical tubes forming the basis for tubular reactors. Zeolite membranes can also be prepared, and the structure of the zeolite should permit high selectivity in separation processes.

Despite the potential of membrane reactors, their development is still not mature for industrial application.

Reactive Distillation [502–504] In reactive distillation (→ Reactive Distillation) fractional distillation and chemical reaction are

performed simultaneously, e.g., for a reaction of the type

$$A+B \rightarrow C+D$$

in which at least one of the products has a volatility which is different form those of the other compounds. The most attractive features of reactive distillation are:

1. The separation of at least one of the products by distillation drives reactions to completion which are otherwise equilibrium-limited.
2. Reactions in which high concentrations of a product or one of the reactants lead to undesired side reaction, can be carried out.

Despite these advantages, several chemical and physical limitations exist in practice for its use in chemical processes, so that reactive distillation has found application for only a few important reactions. Industrially important processes are various etherification, esterification, alkylation, and isomerization reactions.

IFP, Mobil, Neste Oy, Snamprogetti, Texaco, and UOP are providing licenses for plants to produce *tert*-butyl and *tert*-amyl ethers from the corresponding olefins and methanol or ethanol using strong acidic resins as solid catalysts.

Reactions under Supercritical Conditions [505–508] The major advantage of supercritical fluids as solvents in catalytic reactions is the fact that carbon dioxide and water can be used as environmentally benign solvents. When in their supercritical state, these nontoxic compounds are good solvents for many organic compounds. A multicomponent system under supercritical conditions may behave like a single gaslike phase with advantageous physical properties. Under reaction conditions this leads to [505]:

1. Higher reactant concentrations
2. Elimination of contact problems and diffusion limitations in multiphase reaction systems
3. Easier separations and downstream processing
4. In situ extraction of coke precursors
5. Strongly pressure and temperature dependent solvent properties near the critical point
6. Higher diffusivities than in liquid solvents
7. Better heat transfer than in gases
8. Use of clustering to alter selectivities

Hence, supercritical fluids offer strategies for more economical and environmentally benign process design, mainly because of enhanced reaction rates, prolongation of catalyst lifetime, and simplification of downstream processing.

7.2.5. Simulation of Catalytic Reactors [122]

Catalytic reactors are generally characterized by a complex interaction of various physical and chemical processes. Therefore, the challenge in catalysis is not only the development of new catalysts to synthesize a desired product, but also the understanding of the interaction of the catalyst with the surrounding reactive flow field. Sometimes, the exploitation of these interactions can lead to the desired product selectivity and yield. This challenge calls for the development of reliable simulation tools that integrate detailed models of reaction chemistry and computational fluid dynamics (CFD) modeling of macroscale flow structures. The consideration of detailed models for chemical reactions, in particular for heterogeneous reactions, however, is still very challenging due to the large number of species mass-conservation equations, their highly nonlinear coupling, and the wide range of timescales introduced by the complex reaction networks.

Currently available multipurpose commercial CFD codes can simulate very complex flow configurations including turbulence and multicomponent species transport. However, CFD codes still have difficulties in implementing complex models for chemical processes, in which an area of recent development is the implementation of detailed models for heterogeneous reactions. Several software packages have been developed for modeling complex reaction kinetics in CFD such as CHEMKIN [509], CANTERA [510], DETCHEM [511], which also offer CFD codes for special reactor configurations such as channel flows and monolithic reactors. These kinetic packages and also a variety of user written subroutines for modeling complex reaction kinetics have meanwhile been coupled to several commercial CFD codes. Aside from

the commercially widespread multipurpose CFD software packages such as FLUENT [512], STAR-CD [513], FIRE [514], CFD-ACE+ [515], and CFX [516], a variety of multipurpose and specialized CFD codes have been developed in academia and at research facilities such as MP-SALSA [517].

From a reaction-engineering perspective, computational fluid dynamics simulations have matured to a powerful tool for understanding mass and heat transport in catalytic reactors. Initially, CFD calculations focused on a better understanding of mixing, mass transfer to enhance reaction rates, diffusion in porous media, and heat transfer. Later, the flow field and heat transport models were also coupled with models for heterogeneous chemical reactions. So far, most of these models are based on the mean-field approximation as discussed in Section Mean-Field Approximation, in which the local state of the surface is described by its coverage with adsorbed species averaged on a microscopic scale.

Detailed CFD simulations of catalytic reactors, often including multistep reaction mechanisms, have been carried out for catalytic channel reactors with laminar [518] and turbulent [519] flow fields, monolithic reactors [520–524], fixed-bed reactors [525,526], wire-gauze reactors [527,528], reactors with multiphase flow [512], and others. CFD simulations are becoming a powerful tool for understanding the behavior of catalytic reactors and in supporting the design and optimization of reactors and processes.

7.3. Catalyst Deactivation and Regeneration

7.3.1. Different Types of Deactivation

As has been observed in the laboratory and in industrial application, heterogeneous catalysts are deactivated during time on stream. For example, in fluid-bed catalytic cracking and propene ammoxidation the catalyst life is limited to a few seconds or minutes, while in other reactions, such as NH_3 and CO oxidation the catalyst remains active for several years. Not only loss of activity but also a decrease in selectivity is usually caused by catalyst deactivation [529–531].

The activity loss can be compensated within certain limits by increasing the reaction temperature. However, if such compensation is not efficient enough, the catalyst must be regenerated or replaced.

The main reasons for catalyst deactivation are:

1. Poisoning
2. Fouling
3. Thermal degradation
4. Volatilization of active components

Some types of catalyst deactivation are reversible, e.g., catalyst fouling and some special types of poisoning. Other types of deactivation are mostly irreversible [529,530,532].

Catalyst Poisoning The blocking of active sites by certain elements or compounds accompanied by chemisorption or formation of surface complexes are the main causes of catalyst deactivation [529,530,532]. If the chemisorption is weak, reactivation may occur; if it is strong, deactivation results. Chemical species often considered as poisons can be divided in five classes:

1. Group 15 and 16 elements such as As, P, S, Se, and Te
2. Metals and ions, e.g., Pb, Hg, Sb, Cd
3. Molecules with free electron pairs that are strongly chemisorbed, e.g., CO, HCN, NO
4. NH_3, H_2O and organic bases, e.g., aliphatic or aromatic amines, pyridine, and quinoline
5. Various compounds which can react with different active sites, e.g., NO, SO_2, SO_3, CO_2.

Elements of class 1 and their compounds, for example, H_2S, mercaptans, PH_3, and AsH_3, are very strong poisons for metallic catalysts, especially for those containing Ni, Co, Cu, Fe, and noble metals [529,530,532].

Elements of the class 2 can form alloys with active metals and deactivate various systems in this way [529,533].

CO is chemisorbed strongly on Ni or Co and blocks active sites. Below 450 K and at elevated

pressure the formation of volatile metal carbonyls is possible [529,530], and catalyst activity is strongly reduced.

Ammonia, amines, alcohols, and water are well known poisons for acidic catalysts, especially for those based on zeolites [529,534].

Catalysts or carriers containing alkali metals are sensitive to CO_2, SO_2, and SO_3.

Catalyst Fouling Because most catalysts and supports are porous, blockage of pores, especially of micropores, by polymeric compounds is a frequent cause of catalyst deactivation. At elevated temperatures (> 770 K) such polymers are transformed to black carbonaceous materials generally called *coke* [529,535]. Catalysts possessing acidic or hydrogenating – dehydrogenating functions are especially sensitive to coking.

There are different types of coke, such as C_α, C_β, carbidic or graphitic coke, and whisker carbon [529]. C_α is atomic carbon formed as a result of hydrocarbon cracking on nickel surfaces above 870 K. C_α carbon can be transformed at higher temperatures to polymeric carbon (C_β) which has a strongly deactivating effect. C_α carbon can also dissolve in metals and forms metal carbides, and it may precipitate at grain boundaries. Metal-dissolved carbon may also initiate the growth of carbon whiskers, which can bear metal particles at their tops.

Coke formation can be minimized, for example, in methane steam reforming by sufficiently high steam/methane ratio or/and by the alkalization of the carrier.

Thermal Degradation One type of thermal degradation is the agglomeration of small metal crystallites below the melting point, called *sintering* [529]. The rate of sintering increases with increasing temperature. The presence of steam in the feed can accelerate the sintering of metal crystallites.

Another type of thermal degradation are solid-solid reactions occurring especially at higher temperatures (above 970 K). Examples are reactions between metals, such as Cu, Ni, Co, and alumina carriers which result in the formation of inactive metal aluminates [529,536].

Also, phase changes belong to the category of thermal degradations. A prominent example is the reduction of the surface area of alumina from 250 $m^2\ g^{-1}$ (γ phase) to 1 – 2 $m^2\ g^{-1}$ (α phase) by thermal treatment between 870 and 1270 K.

Alternating oxidation and reduction of the system, as well as temperature fluctuations, are often accompanied by activity losses and can cause mechanical strain in catalyst pellets. Therefore, mechanical strength of catalyst particles has major industrial importance.

Volatization of Active Components Some catalytic systems containing P_2O_5, MoO_3, Bi_2O_3, etc. lose their activity on heating close to the sublimation point. Cu, Ni, Fe and noble metals can escape from catalysts after conversion to volatile chlorides if traces of chlorine are present in the feed.

7.3.2. Catalyst Regeneration

The regeneration of metallic catalysts poisoned by Group 16 elements is generally rather difficult. For example, oxidation of sulfur-poisoned metallic catalysts converts metal sulfides to SO_3, which desorbs from metals. However, if the catalyst or carrier contains Al_2O_3, ZnO, MgO then SO_3 forms the corresponding sulfates. When the catalyst is subsequently brought on-line under reducing conditions, then H_2S is formed from sulfates and the catalyst will be repoisoned [529,537].

Therefore it is necessary to remove poisons from the feed as completely as possible. Further prevention is the installation of a guard-bed containing effective poison adsorbents in front of the reactor.

Ni catalysts poisoned with CO or HCN can be regenerated by H_2 treatment at temperatures that allow formation of methane and NH_3, respectively.

The original activity of acidic catalysts poisoned partially by H_2O, alcohols, NH_3, and amines can be restored by thermal treatment at sufficiently high temperatures.

From the industrial point of view, the regeneration of coked catalysts is very important. The removal of coke depends on its structure and on the catalyst composition. Alkali metals, especially potassium, accelerate coke gasification.

Oxidation is the fastest gasification reaction, but it is highly exothermic [529,538]. To maintain the temperature within allowed limits, mixtures of O_2, steam, and N_2 are mainly used to remove the coke.

Catalysts deactivated by thermal degradation are very difficult to regenerate. Certain Pt – Al_2O_3 catalysts, deactivated as a result of thermal Pt sintering, can be partly regenerated by chlorine treatment at elevated temperatures, which makes Pt redistribution possible.

7.3.3. Catalyst Reworking and Disposal

The leaching of precious metals from spent catalysts is widely practiced. Producers of noble metal catalysts, such as Engelhard Corp. BASF, Johnson Matthey, and Umicore have plants for this purpose. Yields of recovered precious metals are 90 – 98 % depending on the original metal content and on the nature of the support used.

Besides precious metals, Ni from spent Ni – kieselguhr catalysts used in fat and oil hydrogenations are reworked to a large extent. Before Ni leaching, fats must be removed.

Hydrotreating catalysts containing Mo, Ni or Co are also reworked. Before leaching of the metals, coke and sulfur are removed by roasting [529,530].

In various cases, however, problems arise when the price of recovered components does not cover the costs of catalyst reworking. The final alternative is the disposal of the spent catalyst. In general, catalysts containing Al, Si, Fe can be disposed of without any special precautions or can be used in construction materials. However, if such catalysts contain Ni or V accumulated during their use, then removal of these elements below legislative limits is necessary [529].

Spent Cu- and Cr-containing catalysts are sometimes accepted by metallurgical plants.

Before disposal, spent catalysts containing various contaminants need to be encapsulated to avoid their release into water. Materials used for encapsulation are, e.g., bitumen, cement, wax, and polyethylene [529]. Nevertheless, the disposal of encapsulated catalysts is not only expensive but is becoming increasingly difficult.

8. Industrial Application and Mechanisms of Selected Technically Relevant Reactions

8.1. Synthesis Gas and Hydrogen [539,540]

All fossil fuels, i.e., coal, petroleum, heavy oil, tar sands, shale oil, and natural gas, but also so-called renewable sources such as biomass, can be used for the production of synthesis gas (syngas), a mixture of hydrogen and carbon monoxide in various ratios. Syngas is an important raw material for many catalytic syntheses in the chemical industry as described in consecutive sections.

By conversion of CO to CO_2 in the water-gas shift reaction (WGS), and CO_2 separation, hydrogen can be produced.

$$H_2O + CO \rightarrow H_2 + CO_2$$

Direct hydrogen production can also be based on water electrolysis using electricity from nuclear power, solar, wind, hydro, geothermal, and oceanic sources as well as combustion (power plants) of any fuel. Due to current changes in energy resources, a variety of new routes are being discussed or are on the way to commercialization (see also → Gas Production and → Hydrogen), in many of which heterogeneous catalytic reactions play a significant role.

Syngas is manufactured from coal by coal gasification (see also → Hydrogen–Production from Coal and Hydrocarbons), and from gaseous or liquid hydrocarbons by endothermic steam reforming (SR),

$$C_nH_m + n\,H_2O \rightarrow n\,CO + (n + m/2)H_2$$

exothermic partial oxidation (POX)

$$C_nH_m + (n/2)\,O_2 \rightarrow n\,CO + (m/2)H_2$$

and a combination of both, called autothermal reforming (ATR) [541]. Today, natural gas is the dominant feedstock for syngas production.

The H_2/CO ratio can be adjusted by reforming and shift reactions according to the application, e.g., 1/1 for oxo synthesis, 2/1 for production of methanol and DME as well as Fischer – Tropsch (FT) synthesis, 3/1 for methanation. Syngas for ammonia synthesis ($H_2/N_2 = 3$) is manufactured by nitrogen addition in a second reforming step [542].

A survey on steam reforming is given in [542]. Nickel is the preferred catalyst but other group 8 – 10 metals are active as well, in particular Co and Fe [543]. The expensive metals Pt, Ru, and Rh show even higher activities [544]. A variety of industrial catalysts are available, most of which are based on Ni/alumina with alkali metal promoters, produced in the shape of pellets with large external diameter and high void fraction (rings, cylinders with holes, or ceramic foams), and used in tubular reformers [542]. Present developments focus on compact reformers, efficient coupling with heat exchangers, and heat recovery from the reformed gas.

An alternative technology for syngas generation is exothermic catalytic partial oxidation (CPOX) of hydrocarbons to syngas over metal catalysts, in particular Rh. The fuel (natural gas, vaporized liquid hydrocarbons, alcohols), premixed with oxygen at an atomic C/O ratio of 1 is fed into a catalytic bed or monolith, in which the fuel is almost completely converted to synthesis gas within few milliseconds at ca. 1000 °C (high-temperature catalysis) [545-547]. The largest hurdle for widespread application of CPOX seems to be safety issues; therefore, membrane [548] and microreactor [549] concepts are under development.

Autothermal reforming is a combination of SR and POX, in which the heat for the reforming reaction is supplied by internal combustion of the fuel with oxygen. Actually, CPOX can also be considered to be a two-stage process, in which the oxygen is first used to burn some of the fuel and consecutive steam reforming of the major part of the fuel produces the desired syngas [524]. ATR has already been widely used in chemical industry, and now is also considered for syngas production in new GTL (gas-to-liquid) plants [550]. ATR runs either on Ni- or Rh-based catalysts, usually with alumina or magnesium alumina supports to improve thermal stability and strength at the high operating temperatures. Current developments include air-blown ATR, in which eliminating the need for an oxygen plant is traded off by the compression costs, in particular in GTL with FT. ATR can also be operated without catalysts.

There are a variety of proposed methods for syngas production from alternative feeds [551] such as ethanol or any other biomass-derived fuel. In particular, CPOX and ATR techniques using noble metal catalysts have been shown to provide high syngas yields when operated at high temperatures and millisecond contact times [547,552–554].

WGS is the most important step in the industrial production of hydrogen, ammonia, and other bulk chemicals utilizing syngas in respect to the adjustment of the CO/H_2 ratio [540,555]. Depending on the required CO conversion the reaction is carried out in several stages. The first high-temperature shift (HTS) is carried out over FeCr catalysts at temperatures between 280 and 350 °C. Since the equilibrium at high temperature is unfavorable for complete conversion, a second stage, the low-temperature shift (LTS, 180 – 260 °C), is added, in which CuZn- or CuZnAl-based catalysts are used to give a CO content of 0.05 – 0.5 vol %. The produced CO_2 can be removed by scrubbing. Complete CO removal, e.g., as needed for ammonia synthesis, can be achieved by subsequent methanation over Ni catalysts. Since sulfur-containing compounds such as H_2S and carbonyl sulfide (COS) are not removed, separate catalytic treatment is usually necessary, e.g., hydrolysis of COS to H_2S or oxidation with SO_2 (Claus COS conversion) and sour gas shift over Mo catalysts [556].

The production of syngas and subsequent hydrogen is currently also of interest in the area of energy-related catalysis such as fuel cells. While for stationary applications natural gas is the major fuel option, logistic fuels are considered as potential feed in mobile applications, for instance, to provide electricity by an auxiliary power unit in a vehicle. Logistic fuels can, for instance, efficiently be converted to syngas in compact on-board CPOX reactors; the syngas is then fed to a SOFC or a PEMFC; in the latter case an additional fuel-processing system is needed for CO removal.

8.2. Ammonia Synthesis [48,557,534,558]

In the Haber – Bosch process, ammonia is synthesized over a promoted iron metal catalysts from its constituents, nitrogen and hydrogen, at approximately 400 °C and 15 MPa (for more details see also → Ammonia).

$$N_2 + 3\,H_2 \rightarrow 2\,NH_3$$

Reactors with capacities up to 1000 t/d are used. The reaction toward the target product NH_3 is therefore thermodynamically favored at low temperature and high pressure. This equilibrium limitation at practical conditions requires loop operation with recovery of the easily condensable product gas. The feed gases are prepared from air (nitrogen) and hydrogen via syngas (see also Section Synthesis Gas and Hydrogen).

Besides Fe, only Ru has been found to be a practically useful catalyst, although thousand of systems have been tested over the years [558].

The most important single application of ammonia is the production of artificial fertilizer. Ammonia is also required in the production of explosives, dyestuffs, plastics, and life-science products. In environmental catalysis, ammonia is applied as reducing agent for nitrogen oxides emitted in power plants and more recently also in automotive vehicles (see also Section Environmental Catalysis).

The mechanism of ammonia synthesis is one of the best known in heterogeneous catalysis, besides CO oxidation on Pt (see Chap. Theoretical Aspects), the reaction served as prototype for the understanding of heterogeneous catalysis by elucidation of the molecular behavior on the catalytic surface, and represents one of the few successful examples of bridging the materials and pressure gap between surface science and industrial heterogeneous catalysis. Three Nobel prizes in chemistry are closely related to ammonia synthesis (Haber 1921, Bosch 1931, Ertl 2007). Therefore, the mechanism of ammonia synthesis is discussed in more detail here.

The adsorption of N_2 on iron is slow and is characterized by a very low sticking coefficient (ca. 10^{-6}) and high activation energy [557]. Single-crystal surfaces of iron are reconstructed upon adsorption of nitrogen. Dinitrogen is dissociated above 630 K [559] and forms complex surface structures. These have been inferred to be surface nitrides with depths of several atomic layers [557]. Their composition is roughly Fe_4N. The corresponding bulk compound is thermodynamically unstable under conditions for which the surface structure is stable. The rate of dissociative adsorption of dinitrogen is structure-sensitive, the Fe(111) face being by far the most active, since the activation energy is the smallest and the rate of adsorption the highest [560]. The same crystal face is also the catalytically most active. These observations are consistent with the earlier suggestion [561] that dinitrogen adsorption is an activated process and that it is the rate-determining step in the catalytic cycle.

In contrast, the adsorption of dihydrogen on iron is fast and characterized by a high sticking coefficient (ca. 10^{-1}) and an extremely small activation barrier. This chemisorption is dissociative and yields covalently bonded H atoms which have high mobility on the iron surface.

Atomic nitrogen was shown to be the most stable and predominant chemisorbed species on Fe(111) after evacuation [87,88], and it was inferred to be an intermediate in the catalytic reaction. Adsorbed dinitrogen could be excluded as a reactive intermediate. The involvement of adsorbed N atoms in the rate-determining step was also demonstrated by kinetics experiments [562]. Other less stable and less abundant surface intermediates include NH and NH_2 species.

Based on these results the following sequence of elementary steps was formulated (* denotes a surface site):

$$N_2 + 2^* \rightarrow 2\,N_{ads} \quad (36)$$

$$H_2 + 2^* \rightarrow 2\,H_{ads} \quad (37)$$

$$N_{ads} + H_{ads} \rightarrow NH_{ads} + * \quad (38)$$

$$NH_{ads} + H_{ads} \rightarrow NH_{2ads} + * \quad (39)$$

$$NH_{2ads} + H_{ads} \rightarrow NH_3 + 2^* \quad (40)$$

A schematic potential-energy diagram for the catalytic cycle is shown in Figure 27. Decomposition of N_2 is exothermic, whereas the steps involved in successive hydrogenation yielding NH_x species are endothermic. The addition of the first H atom is the most difficult step.

The promotion of the iron catalyst with potassium lowers the activation energy for dissociative N_2 chemisorption [563].

8.3. Methanol and Fischer – Tropsch Synthesis

8.3.1. Methanol Synthesis [148]

Methanol is one of the most important organic chemicals (see also → Methanol). It is mainly

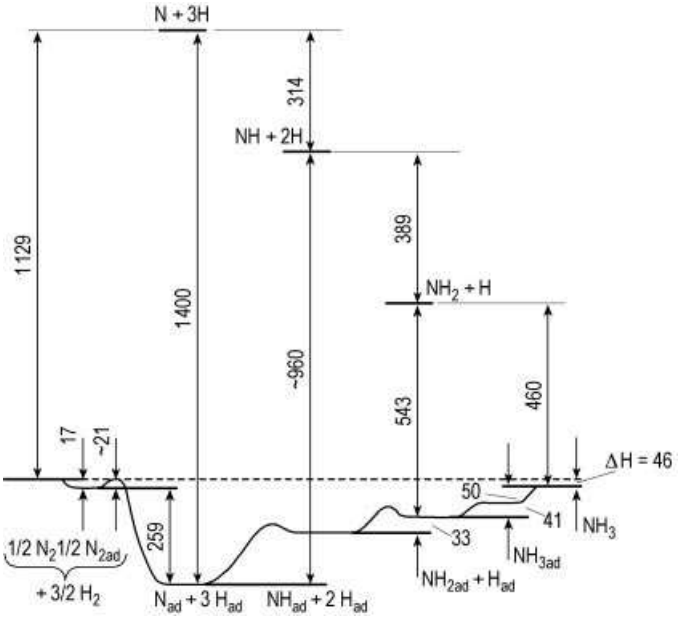

Figure 27. Potential-energy diagram for the sequence of elementary steps of the ammonia synthesis reaction (energies in kJ mol^{-1}) [234]

used as an intermediate for production of formaldehyde, methyl *tert*-butyl ether (MTBE), acetic acid, amines, and others. Methanol is produced from synthesis gas according to the following stoichiometry.

$$CO + 2\,H_2 \rightarrow CH_3OH$$

It is now generally accepted that this reaction proceeds by conversion of CO via the water-gas shift reaction followed by hydrogenation of carbon dioxide [564].

$$CO + H_2O \rightarrow H_2 + CO_2$$

$$CO_2 + 3\,H_2 \rightarrow CH_3OH$$

All these reactions are exothermic and equilibrium-limited. The achievable methanol yield is favored by high pressure and low temperature.

The first process for methanol synthesis, operating at about 30 MPa and 300 – 400 °C over a Zn/Cr_2O_3 catalyst, was developed by BASF in Germany in 1923. A substantial improvement was made by ICI in the 1960s through introduction of the more active $Cu/ZnO/Al_2O_3$ catalyst, which allowed for synthesis under much milder reaction conditions of 50 – 100 bar and 200 – 300 °C. Today, the vast majority of methanol plants use this more advanced low-pressure synthesis.

Although methanol synthesis on copper-base catalysts has been intensively studied for several decades, no general agreement about the nature of the active sites and the reaction mechanism could be achieved. Regarding the active site, it appears that metallic copper in close contact to ZnO is a requirement for an active and selective catalyst. This synergy has been explained by various mechanisms including hydrogen spillover from ZnO [565], stabilization of intermediates on ZnO or the interface between Cu and ZnO [566], and spreading of Cu on the ZnO surface [567]. The most important intermediates appear to be formate, methoxy, and formyl species. A possible reaction mechanism involves dissociative adsorption of hydrogen, hydrogenation of adsorbed CO to CO_2, conversion of atomic hydrogen to formate, further addition of hydrogen to give H_2COO, hydrogenation of this species to a methoxy species, and finally hydrogenation of this group to methanol. Simulations suggested that the rate-determining step in this sequence is hydrogenation of the H_2COO species to the methoxy group [568].

Several empirical and mechanistically based rate equations for methanol synthesis have been

proposed. An example using only statistically significant and physically meaningful parameters is given in [569]. The usual catalyst geometry comprises pellets of typically five millimeters in size. Under the commercial reaction conditions, pore diffusion resistances may occur [570].

In industrial practice, a variety of different reactor types for low-pressure methanol synthesis are used, but generally fixed beds of catalyst operated in the gas phase are employed. One possibility for temperature control during the exothermic reaction is a staged catalyst bed with interstage cooling through heat exchangers or injection of cold synthesis gas. The other frequently used possibility for exothermic reactions is a cooled multitubular reactor with fixed bed of catalyst in each tube. While the multitubular reactor allows the best temperature control and thus the longest catalyst life, the capital costs for adiabatic reactors are lower. Two-phase fluidized-bed reactors and three-phase reactors with an additional liquid product phase have also been extensively tested. However, the lack of mechanical stability and/or low catalyst effectiveness has until now prevented commercial implementation of these reactor designs.

Much effort has also been devoted to overcoming the equilibrium-limited methanol conversion in a single-pass reactor by removal of methanol from the reaction mixture. A particularly interesting system removes methanol by selective adsorption on a porous adsorbent trickling through a fixed-bed of catalyst [571]. However, this elegant multifunctional reactor suffers from severe practical mechanical problems. Another approach concentrates on operation close to the dew point of the product to allow removal of liquid methanol between beds of catalyst. In this case, highly active catalysts for operation at very low temperature and high pressure are required.

A possible future trend is the further processing of methanol to synthetic fuels via methanol-to-olefins as proposed by Lurgi.

8.3.2. Fischer – Tropsch Synthesis [148]

Fischer – Tropsch synthesis (FTS) is the direct production of hydrocarbon chains from synthesis gas. Details of the process can also be found in → Coal Liquefaction. The most important reaction, which is exothermic with a reaction enthalpy of about −150 kJ/mol, can be described by the following equation.

$$n\,CO+(2n+1)H_2 \rightarrow C_nH_{2n+2}+n\,H_2O$$

In side reactions, olefins and oxygenates are formed, and undesirable CO_2 and additional CH_4 may be produced via the water-gas shift reaction and CO methanation.

FTS has a long history starting with Fischer and Tropsch reporting the synthesis of liquid hydrocarbons from synthesis gas under moderate conditions in 1923 [572]. Within a short period, this new process was commercialized and provided, together with coal liquefaction, synthetic fuel on a large scale in Germany during World War II. After the era of cheap oil began in the 1950s it became evident that FTS was uneconomical at that time. Only South Africa continued production of fuels by FTS based on coal-derived synthesis gas for political reasons. The 1973 oil crisis stimulated new interest in FTS, and Shell started development of its middle distillate process. In 1993, the first plant based on natural gas came into operation in Malaysia. This gas-to-liquids (GTL) process is currently being realized on industrial scale at several sites. Commissioning of a plant with a capacity of 70 000 barrels per day built by Sasol and Qatar Petroleum took place in 2006 in Qatar. Further large-scale industrial plants in Escravos, Nigeria (Sasol Chevron) and Qatar (Shell, Qatar Petroleum) are under construction. It appears that FTS will play a major role for the future production of synfuels based on alternative feedstocks (natural gas, coal, biomass).

FTS has been considered as an ideal polymerization reaction [573]. According to this approach the distribution of mole fractions x_n of products can be described as a function of the number of carbon atoms n in the chain.

$$x_n = (1-\alpha)\alpha^{n-1}$$

The ideal product composition depends only on the chain-growth probability α, which is determined by the catalyst used. In reality significant deviations from ideal polymerization behavior are observed. Usually the methane mole fraction is higher, while the ethene/ethane mole fractions are lower than calculated. Many

mechanistic studies on FTS support the carbene mechanism, which starts with the decomposition of CO and involves the insertion of methylene (CH_2) species into the growing alkyl chain [574].

As FTS catalysts metals like iron, cobalt, and ruthenium can be used [575]. Due to the high price of ruthenium only iron and cobalt have industrial relevance. A disadvantage of iron catalysts is kinetic inhibition by the co-product water, whereas an advantage is the activity for the water-gas shift reaction that allows the use of carbon-dioxide-containing or hydrogen-depleted synthesis gas mixtures [576]. Compared to iron, cobalt catalysts are already active at lower reaction temperatures and have a durability of up to five years on stream compared to about six months in the case of iron [577]. On the other hand cobalt is more expensive than iron. In addition to the active component different promoters (Pt, Pd, Ru, Re, K) can be employed [578]. As carrier materials alumina, silica, and titania can be utilized. Typical chain-growth probabilities are 0.5 – 0.7 for iron and 0.7 – 0.8 for cobalt [579]. Currently the development of cobalt catalysts is aimed at maximizing the chain-growth probability to values of up to 0.95 [580]. Since the product mixtures obtained with these catalyst cannot directly used and must be further processed to achieve the desired fractions (diesel and gasoline fuels), it has been suggested to couple Fischer – Tropsch catalysts with hydrocracking catalysts in one reactor [581,582].

As liquid products often fill the pore system of working catalysts, resistances caused by pore diffusion may occur even with small catalyst particles. Catalyst efficiency is significantly reduced at characteristic catalyst dimensions above 100 μm [583]. Furthermore, the higher diffusion coefficient of hydrogen compared to carbon monoxide increases the H_2/CO ratio inside the porous catalyst. This leads to an increase of the chain-termination probability and thus to a decrease in chain length of the products [584].

The development of catalysts with very high chain-growth probabilities resulted in the development of the more advanced low-temperature FTS, in which synthesis gas and liquid products are present under reaction conditions. Industrial reactors are operated at typical conditions of 2 – 4 MPa and 220 – 240 °C. Two reactor types are presently applied in low-temperature FTS: a cooled fixed-bed reactor mainly used by Shell and a slurry bubble column developed by Sasol. Disadvantages of fixed-bed reactors are development of a hot spot, low catalyst utilization due to pore diffusion, and, especially in case of gas recycle for improved heat removal, high pressure drop. On the other hand, mechanical stress on catalyst particles, the need for separation of solid catalyst and liquid products and highly demanding scaleup are drawbacks of slurry bubble column reactors. New trends in FTS reactors are the use of monolith reactors for improved gas – liquid mass transfer [585] and isothermal microstructured reactors.

8.4. Hydrocarbon Transformations

8.4.1. Selective Hydrocarbon Oxidation Reactions

Selective hydrocarbon oxidation reactions include several important classes of heterogeneously catalyzed reactions, which find large-scale industrial application for the synthesis of bulk chemicals. Reviews on the mechanisms of selective hydrocarbon oxidation [200], oxidative dehydrogenation of alkanes [586], ammoxidation of alkenes, aromatics and alkanes [63], and epoxidation of alkenes [587] are available. Here, some mechanistic aspects of the epoxidation of alkenes and of the ammoxidation of hydrocarbons are discussed.

8.4.1.1. Epoxidation of Ethylene and Propene [587,588]

The epoxidation of ethylene by dioxygen is catalyzed by silver metal and yields ethylene oxide (→ Ethylene Oxide), an important intermediate for the synthesis of glycols and polyols.

Total oxidation of the reactant and the target product limit the selectivity of the

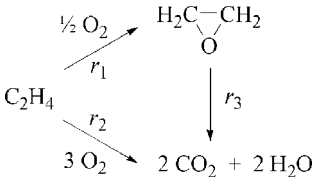

Scheme 1.

process. Scheme 1 shows the three competing reactions.

The catalyst therefore must be tuned such that the optimal selectivity for ethylene oxide is achieved. The active phase consists of large Ag particles supported on low surface area α-Al_2O_3 promoted by alkali metal salts. A beneficial effect is also obtained by adding chlorine-containing compounds such as vinyl chloride to the reaction feed. Under reaction conditions this additive is readily combusted on silver, and chlorine is adsorbed on the metal surface.

Oxygen can be adsorbed on transition metals in general and on silver in particular in three different states: (1) molecular dioxygen, (2) adsorbed atomic oxygen, and (3) subsurface atomic oxygen [588]. Molecular oxygen is stable on an Ag(111) surface at temperatures below ca. 220 K. It dissociates at higher temperatures. Oxygen dissociation occurs at high-coordination sites, since at least two neighboring metal atoms must be available. It has been shown that ensembles with a minimum of five silver atoms are required [589,590]. Oxygen atoms adsorbed originally on the external silver metal surface may move to subsurface lattice positions. Subsurface oxygen atoms have been proved to form on transition metals including Rh, Pd, and Ag [591]. The maximum oxygen coverage on silver surfaces is one oxygen atom per silver atom, corresponding to the composition of AgO [588].

The presence of subsurface oxygen atoms reduces the electron density on adjacent silver atoms. Hence, oxygen atoms adsorbed on the external surface which share bonds to silver surface atoms with subsurface oxygen atoms become highly polarizable. When exposed to ethylene, the interaction of the surface oxygen atoms with the π electrons of ethylene leads to a flow of electron density from the surface oxygen atom to the positively charged surface silver atom [592]. The surface oxygen atoms behave chemically as electrophilic oxygen atoms, which preferentially react with the part of the reactant molecule having the highest electron density. This situation is most likely at high oxygen coverages, consistent with the experimental observation that the epoxidation selectivity is dramatically enhanced by increasing oxygen coverage [593]. Scheme 2 illustrates this scenario [587]. At low oxygen coverages the density of subsurface oxygen atoms is also reduced so that the polarizability of oxygen atoms adsorbed on the external surface is reduced. Consequently, these oxygen atoms behave as nucleophilic oxygen atoms and tend to interact preferentially with hydrogen atoms of the ethylene molecule, thus leading to total oxidation. This situation is schematically shown in Scheme 3 [587]. Therefore, epoxidation selectivity must decrease with decreasing oxygen coverage. The fact that vacant silver sites exist in the vicinity of an adsorbed oxygen atom at low coverage (see Scheme 3), is also detrimental.

The influence of alkali metal and chlorine modifiers is complex. The effect of chlorine is twofold: (1) it suppresses vacant silver sites, and (2) it enhances the electron deficiency of silver. The latter effect is due to the ability of chlorine to also occupy subsurface positions [594] and thus to adopt the role of subsurface oxygen as illustrated in Scheme 4 [587]. These effects improve the initial selectivity r_1/r_2 (r_i denotes a reaction rate, see Scheme 1). The overall selectivity is also reduced by subsequent combustion of the epoxide (r_3 in Scheme 1), particularly at high conversions. The combustion of the epoxide is induced by the residual acidity of the α-Al_2O_3 support. The presence

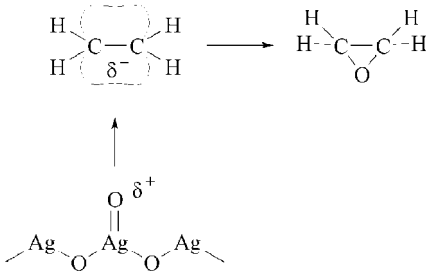

Scheme 2.

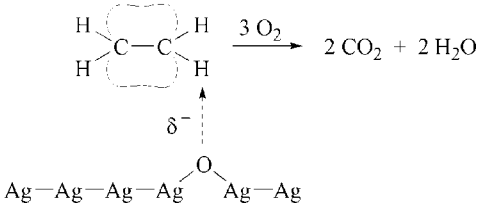

Scheme 3.

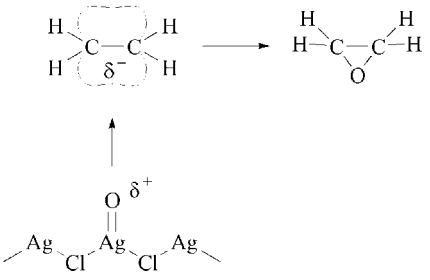

Scheme 4.

of alkali metal reduces the density of acid sites and thus has a beneficial effect on selectivity by blocking reaction step r_3.

The rate-limiting step of the epoxidation reaction is the dissociative chemisorption of dioxygen. Alkali metal compounds enhance the dissociation rate of dioxygen by reducing the activation barrier, and consequently the alkali metal modifier enhances the epoxidation rate as its coverage increases [587]. Interestingly, when a chlorine-modified catalyst is promoted by alkali metal compounds, the reaction rate decreases, and this is suggestive of an enhancement of the steady-state concentration of adsorbed chlorine, which leads to site blocking. Therefore, there is a very subtle interplay between the two additives which must be carefully controlled to optimize conversion and selectivity of the ethylene epoxidation reaction.

Details on the catalytic and engineering aspects of ethylene epoxidation can be found in [148,595]. The reaction is carried out in multitubular reactors in the gas phase, either with air or with pure oxygen, at residence times of about 1 s, temperatures between 230 and 290 °C and pressures between 1 and 3 MPa. In the earlier air-based process, a series of two or three reactors was employed. The ethylene conversion in the first reactor is kept relatively low (ca. 40%) to maintain high ethylene oxide selectivity, while the following reactors are used to increase the overall ethylene conversion. Modern ethylene oxide processes use pure oxygen in a single-stage reactor in recycling mode. In contrast to air-based processes, ethylene concentrations are relatively high (25 – 30 vol %) in order to stay above the upper flammability limit of the reaction mixture. The oxygen process gives rise to higher ethylene oxide yield, smaller equipment size, and smaller amount of vent gas and is therefore nowadays preferred over the air-based process.

The epoxidation of *propene* with dioxygen is unfavorable because of the enhanced reactivity of the methyl group for nucleophilic attack. Activation of the methyl group leads to the allyl or combustion of the propylene epoxide. Alternative oxidants are hydrogen peroxide or hydroperoxide (→ Propylene Oxide–Indirect Oxidation Routes). The reaction of propene with hydrogen peroxide yields the target product propylene epoxide and water (Eq. 41).

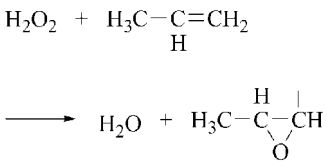

(41)

The preferred catalyst for this reaction is titanium silicalite-1 (TS-1) (see Section Metal Oxides), in which four coordinate Ti^{4+} plays the decisive role [596]. Although the exact nature of the reaction intermediate is not known yet, hydrogen peroxide may coordinate nondissociatively to a Lewis acidic tetrahedral Ti^{4+} site as shown in Scheme 5. This induces electron deficiency on the oxygen atoms of the peroxides, which is favorable for epoxidation. An analogous reaction path has been proposed for the homogeneous epoxidation of propene by peroxides [587].

The development of technical processes based on hydrogen peroxide and TS-1 catalysts has recently been reviewed [597]. These HPPO

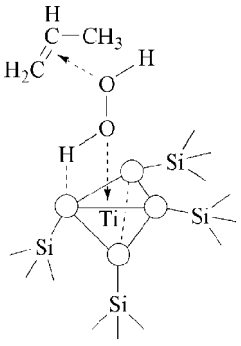

Scheme 5.

processes have been developed further by Degussa and Uhde, as well as by BASF and Dow, and startup of first production plants is scheduled for 2008 [598]. Degussa and Uhde have also investigated the gas-phase epoxidation of propene. Due to the safety risks associated with mixtures of gaseous propene and hydrogen peroxide as well as the danger of hydrogen peroxide decomposition during evaporation, new technical concepts based on microstructured devices had to be developed [495]. High productivities of more than 1 kg of propylene oxide per kilogram of catalyst and hour could be obtained at high propane-to-propene oxide selectivity of more than 90 %. If the decomposition of hydrogen peroxide can be significantly reduced, the gas-phase process could become interesting alternative to the commercial liquid-phase processes.

8.4.1.2. Ammoxidation of Hydrocarbons [63,599,600]

In ammoxidation, ammonia reacts with a reducible organic molecule, most frequently an alkene, alkane, or aromatic, in the presence of dioxygen to yield nitriles (e.g., Eq. 42).

$$2\,CH_2 = CRCH_3 + 2\,NH_3 + 3\,O_2 \rightarrow 2\,CH_2 = CRCN + 6\,H_2O \qquad (42)$$

The ammoxidation of an alkene is a six-electron oxidation that produces an unsaturated nitrile and water. The reaction is related to the four-electron oxidation of alkenes (Eq. 42) [75] producing unsaturated aldehydes and water, and to the two-electron oxydehydrogenation of alkenes to dienes and water (Eq. 43) [75].

$$CH_2 = CRCH_3 + O_2 \rightarrow CH_2 = CRCHO + H_2O$$

$$2\,CH_2 = CHCH_2CH_2R + O_2 \rightarrow 2\,CH_2 = CHCH = CHR + 2\,H_2O \qquad (43)$$

Catalysts for these reactions are complex mixed metal oxides containing variable-valence elements (see Section Metal Oxides), the ammoxidation catalysts typically being the most complex. These materials possess redox properties, i.e., they can readily be reduced by ammonia and reoxidized by dioxygen present in the gas phase. It is the lattice oxygen of the catalyst which reacts with ammonia and the hydrocarbon, and the reduced solid is reoxidized by gas-phase oxygen (Mars – van Krevelen mechanism [601], see also [200]).

The most important alkene ammoxidation is that of propene to acrylonitrile (Sohio Acrylonitrile Process, Eq. 44; see also → Acrylonitrile–Quality Specifications and Chemical Analysis) [586]

$$2\,CH_2 = CH{-}CH_3 + 2\,NH_3 + 3\,O_2 \rightarrow 2\,CH_2 = CHCN + 6\,H_2O \qquad (44)$$

Molybdates and antimonates can be used as catalysts for this reaction. The active sites are thought to have bifunctional nature [63,602,603]. A generalized catalytic cycle for alkene ammoxidation is shown in Figure 28 [63]. Ammonia is proposed to interact first with the bifunctional active site generating an ammoxidation site. The alkene coordinates to this site to form an allylic intermediate. After several rearrangements and oxidation steps, the surface intermediate is transformed into the nitrile, which subsequently desorbs. A reduced surface site is thus formed, which is restored to its original fully oxidized state by lattice oxygen O^{2-}, which is provided by adjacent reoxidation sites. These sites then dissociate dioxygen to lattice oxygen. The newly formed lattice oxygen then diffuses to the oxygen-deficient reduced surface site, from where vacancies simultaneously penetrate through the lattice of the solid to the reoxidation sites. Clearly, these sites must communicate with each other via a common solid-state lattice which is capable of facile transport of electron, anion vacancies, and lattice oxygen [63]. As an example, the proposed bifunctional active site of Bi_2MoO_6 (see Section Metal Oxides) is schematically illustrated in Figure 29 [213]. The various functionalities were assigned to specific elements and to specific lattice oxygen positions. Bridging oxygen atoms Bi–O–Mo are considered to be responsible for α-hydrogen abstraction from the alkene, while oxygen atoms associated with Mo are responsible for oxygen (Mo=O) and nitrogen (Mo=NH) insertion into an allylic intermediate. The oxygen dissociation and its reduction to lattice oxygen is assumed to occur in the region of high electron density generated by the two lone pair electron orbitals of Bi–O–Bi sites. More easily reducible elements than Bi are Fe, Ce, U, and Cu, which are components of

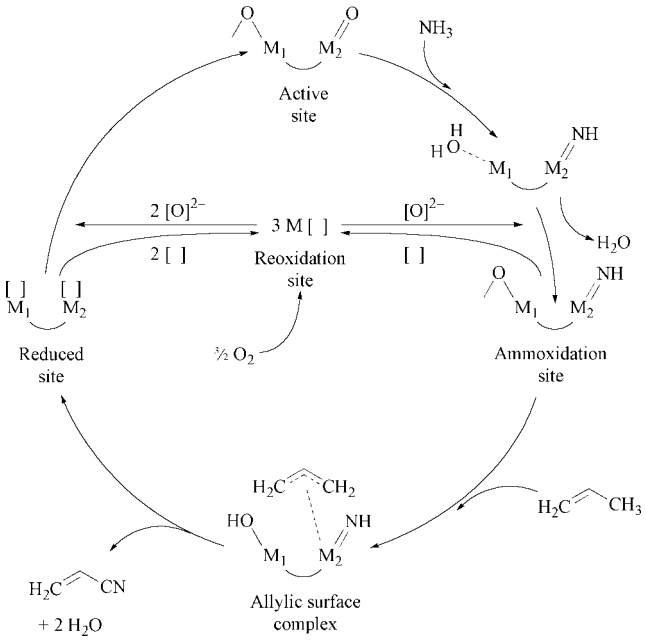

Figure 28. Generalized mechanistic cycle for alkene ammoxidation

more complex, multicomponent catalysts (see Section Metal Oxides) [63]. As an illustration of the mechanisms of ammoxidation and selective oxidation of propene, Figure 30 shows the proposed catalytic cycles for the two reactions [604].

More recently, selective catalytic oxidation and ammoxidation of alkanes as lower cost alternatives to alkenes has attracted considerable interest [600,605]. Multicomponent metal oxide catalysts have been intensively studied. Promising results have been obtained especially with the MoV – TeNbO system, both for oxidative dehydrogenation of ethane to ethylene and for ammoxidation of propane to acrylonitrile.

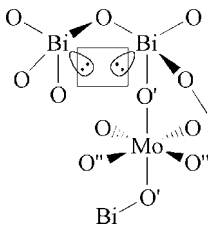

Figure 29. Schematic representation of the active site of Bi_2MoO_6 [446]
O′ = Oxygen responsible for α-H abstraction; O″ = Oxygen associated with Mo; responsible for oxygen insertion into the allylic intermediate; *f* = Proposed center for O_2 reduction and dissociative chemisorption.

8.4.2. Hydroprocessing Reactions [49,273, 274,606,607–148]

(see also → Oil Refining–Environmental Protection in Oil Refining)

Hydroprocessing treatment, including hydrodesulfurization (HDS), hydrodenitrogenation (HDN), hydrodeoxygenation (HDO), hydrometalation (HDM), hydrogenation, and hydrocracking, are among the largest industrial processes in terms of catalyst consumption. Crude petroleum contains particularly organosulfur and organonitrogen compounds, which are most abundant in heavy petroleum fractions. These contaminants must be removed for environmental reasons. The reactions take place in the presence of H_2 at high temperatures (ca. 600 – 700 K) and pressures of 500 kPa to 1 MPa. Because of the lower reactivity of organonitrogen compounds as compared to organosulfur compounds, the reaction conditions are more severe for HDN than for HDS.

Catalysts for hydroprocessing are highly dispersed metal sulfides (mainly MoS_2, but also

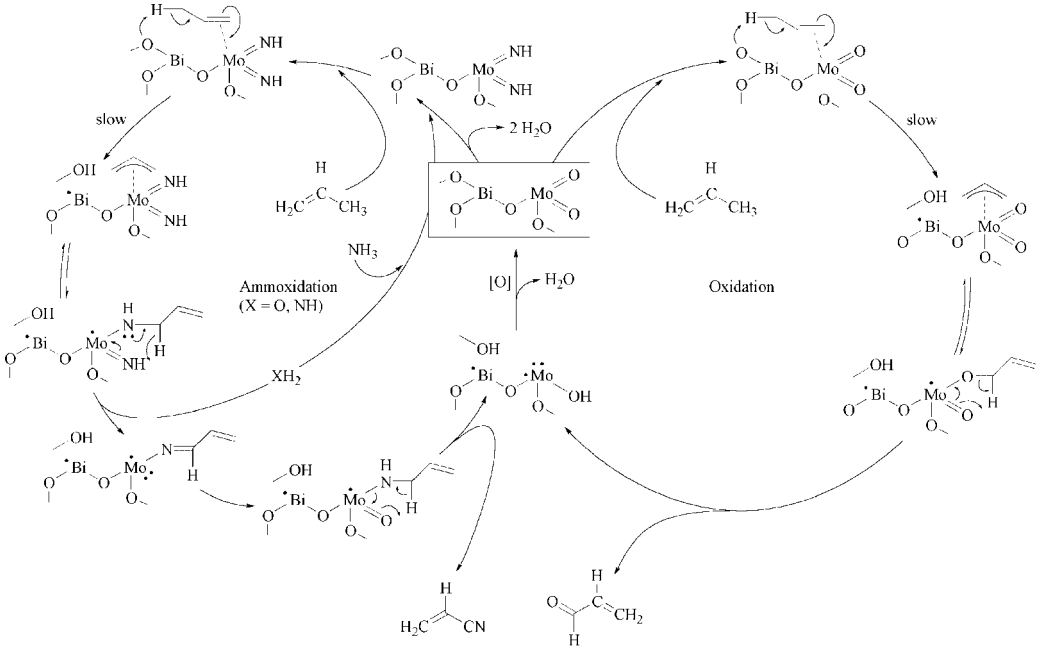

Figure 30. Mechanism of selective ammoxidation and oxidation of propene over bismuth molybdate catalysts [604]

WS_2) supported on γ-Al_2O_3. The materials are promoted by cobalt or nickel, depending on application.

Although the detailed mechanisms have not yet been elucidated, significant progress in understanding the chemistry of the various hydroprocessing reactions at a molecular level has been made [49,273,274,607,608]. In the following, however, the focus is on reaction networks of several hydroprocessing reactions with pseudo-first-order rate constants for individual reaction steps.

The organosulfur compounds in petroleum include sulfides, disulfides, and aromatics (including thiophene, benzothiophene, dibenzothiophene, and related compounds). Benzo- and dibenzothiophene are predominant in heavy fuels. The reaction network for hydrodesulfurization of dibenzothiophene, a representative member of organosulfur contaminants in fuel, is shown in Figure 31 [609]. Hydrogenation and hydrogenolysis take place in parallel. The latter reaction is essentially irreversible and leads to the formation of H_2S and biphenyl. At low H_2S concentrations in the feed, the sulfide catalysts are highly selective for hydrogenolysis. The selectivity, however, drops sharply as the H_2S concentration in the feed increases.

Hydroprocessing reactions accompanying hydrogenation and hydrodesulfurization include hydrodenitrogenation, whereby organonitrogen compounds in the feed react with H_2 to give NH_3 and hydrocarbons. As an example, a reaction network for the hydroprocessing of quinoline is shown in Figure 32 [606]. The supported metal sulfide catalysts are much less selective for nitrogen removal than for sulfur removal.

Hydroprocessing reactions are carried out in different reactor types [610]. The most commonly used is a fixed-bed reactor operated in the trickle-flow regime with cocurrent up- or downflow of gas and liquid. Alternative reactor designs are moving-bed and ebullated-bed reactors with greater flexibility, e.g., owing to easy replacement of spent catalyst during operation. Recently, structured packed columns of monolithic catalysts operated in countercurrent mode are gaining importance in hydroprocessing research, because higher conversions can be obtained. A future trend is the development of processes for the treatment of increasingly heavy oils and of various residues [611].

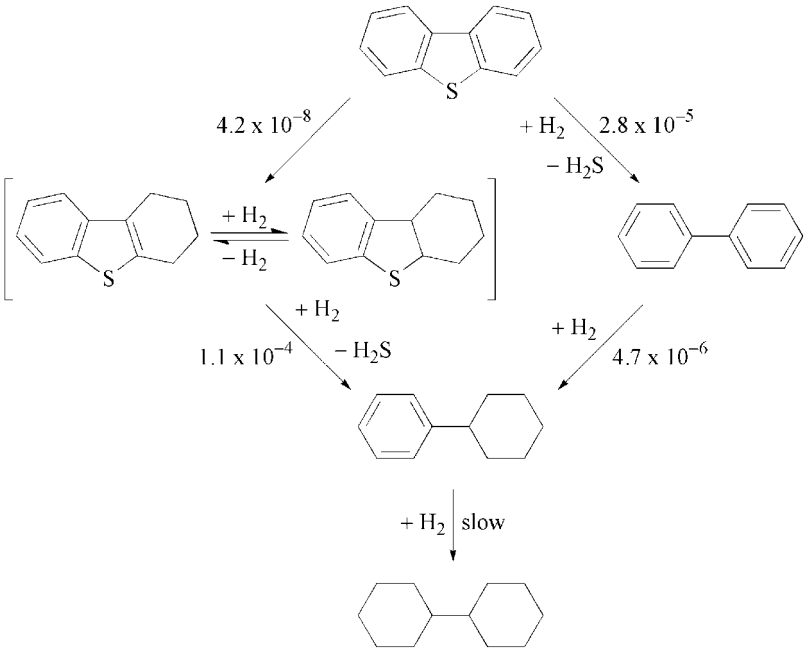

Figure 31. Reaction network for hydrodesulfurization and hydrogenation of dibenzothiophene catalyzed by sulfided Co – Mo/Al_2O_3 at 570 K and 10 MPa [609]
Numbers next to the arrows represent the pseudo-first-order rate constants in units of L/(g of catalyst · s) when the H_2S concentration is very small. Addition of H_2S markedly decreases the selectivity for hydrodesulfurization.

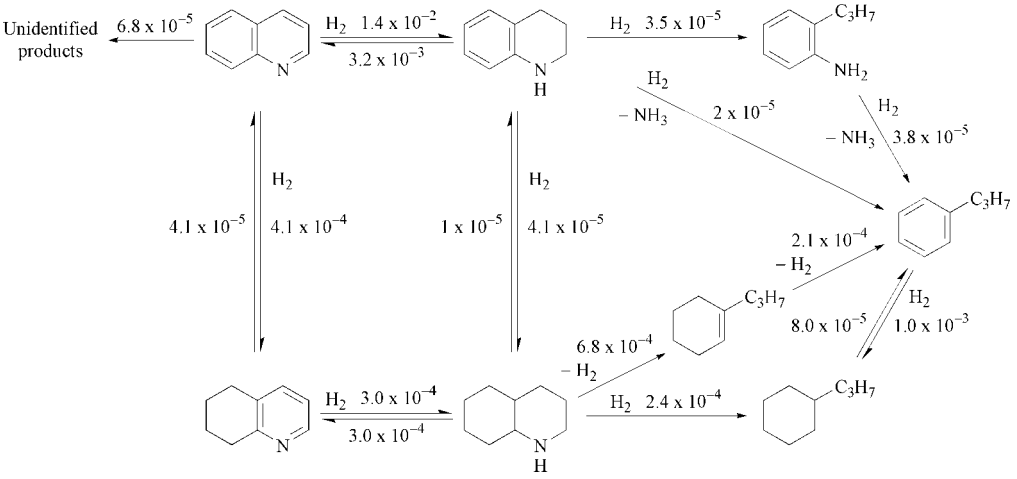

Figure 32. Reaction network for hydrogenation and the hydrogenolysis of quinoline catalyzed by sulfided Ni – Mo/**γ**-Al_2O_3 at 620 K and 3.5 MPa [606]
Numbers next to the arrows represent the pseudo-first-order rate constants in units of L/(g of catalyst · s) when the H_2S concentration is small but sufficient to maintain the catalysts in the sulfided forms.

8.5. Environmental Catalysis

8.5.1. Catalytic Reduction of Nitrogen Oxides from Stationary Sources [313]

Fossil fuels such as coal, oil, gas, and others are burnt or gasified for energy conversion. In Western European countries and Japan measures have been implemented since 1980 for reducing emissions, especially of NO_x from power plants. The preferred method to remove NO_x from exhaust gases of power plants, industrial boilers, and gas turbines is based on the so-called selective catalytic reduction (SCR) with ammonia in the presence of oxygen. The stoichiometry of the main desired reactions can be described as follows:

$$4\,NO + 4\,NH_3 + O_2 \rightarrow 4\,N_2 + 6\,H_2O \quad \text{(standard SCR)}$$

$$6\,NO_2 + 8\,NH_3 \rightarrow 7\,N_2 + 12\,H_2O \quad (NO_2\ SCR)$$

$$NO + NO_2 + 2\,NH_3 \rightarrow 2\,N_2 + 3\,H_2O \quad \text{(fast SCR)}$$

The standard SCR reaction is most important if NO_x originates from high-temperature combustion processes, where very little NO_2 is present. However, in exhaust streams containing higher amounts of nitrogen dioxide, the fast SCR reaction, which proceeds at least ten times faster than the standard SCR reaction, may become the predominant reaction [612].

At higher temperatures above ca. 450 °C, the reducing agent ammonia reacts with oxygen in undesirable parallel reaction to give the products N_2, N_2O, or NO. On the other hand, at temperatures below 200 °C, ammonia and NO_x may form solid deposits of ammonium nitrate and nitrite.

The SCR of nitrogen oxides was first carried out with Pt catalysts [613]. Due to the high nitrous oxide selectivity of this catalyst, base metal catalysts have been developed for NO_x reduction. Vanadia supported on titania (in the anatase form) and promoted with tungsten or molybdenum oxide exhibits the best catalytic properties. While BASF was the first to describe vanadia as active component for SCR [614], TiO_2-supported vanadia for treatment of exhaust gases was developed in Japan [615]. Anatase is the preferred support for SCR catalysts for two main reasons. Firstly, it is only moderately sulfated under real exhaust gas conditions, and catalytic activity even increases after sulfation [616]. Secondly, vanadia is able to spread in thin layers on the anatase support to give highly active structures with large surface area. However, the amount of vanadia in technical catalysts is limited to only a few weight percent, because it is also catalytically active for SO_2 oxidation.

The mechanism of the standard SCR reaction over vanadia-based catalysts is generally assumed to proceed via an Eley – Rideal mechanism involving adsorbed ammonia and gas-phase NO. Based on this mechanism, the following rate equation can be derived that has been successfully used to model the SCR reaction.

$$r_{NO} = k \cdot \frac{K_{NH_3} c_{NH_3} c_{NO}}{(1 + K_{NH_3} c_{NH_3})}$$

Water vapor has an additional inhibiting effect on the rate of NO removal. In recent studies, it was also possible to model and simulate the transient behavior of SCR catalysts exposed to changes in reactant concentration and temperature [313].

As the rate of the SCR reaction under industrially relevant conditions is quite high, external and intraparticle diffusion resistances play an important role, especially for the frequently used honeycomb monolith or plate-type catalysts operating in laminar flow regime. These geometries must be used to minimize the pressure drop over the catalyst bed. Monolithic elements usually have channel sized of 3 – 7 mm, cross sections of 15 × 15 cm, and lengths of 70 – 100 cm. Monoliths or packages of plate catalysts are assembled into standard modules, which are then placed in the SCR reactors as layers. These modules can be easily replaced to introduce fresh or regenerated catalysts.

SCR reactors can be used in different configurations, depending on fuel type, flue gas composition, NO_x threshold, and other factors. The first possibility is the location directly after the boiler (*high-dust arrangement*) where the flue gas usually has the optimal temperature for the catalytic reaction. On the other hand, dust deposition and erosion as well as catalyst deactivation are more pronounced than in other

configurations. A second possibility, which is common in Japan, uses the SCR reactor after a high-temperature electrostatic precipitator for dust removal (*low-dust arrangement*). In that case catalyst damage by dust can be prevented. On the other hand, ammonium sulfate deposition, which in the high-dust configuration mainly takes place on the particulate matter in the gas stream, may become more critical. For this reason, especially low limits for ammonia slip must be met. Finally, the SCR reactor may be located in the cold part after the flue gas desulfurization unit in the so-called *tail-end arrangement*. To achieve the required reaction temperature, the exhaust gases must be reheated by means of a regenerative heat exchanger and an additional burner. On the other hand, catalysts with very high activity can be used, since poisons are absent and SO_2 oxidation need not to be considered.

New promising catalysts for the removal of nitrogen oxides are iron-exchanged zeolites (e.g., MFI, BEA). Although field tests in flue gases of power plants have shown quite strong deactivation, notably by mercury [617], these catalysts appear to be especially suited for "clean" exhaust gases such as in nitric acid plants. Advantages of iron zeolite catalysts are a broader temperature window for operation and the ability to reduce N_2O emissions as well. Uhde has recently developed the EnviNO_x process for simultaneous reduction of NO_x and N_2O, which uses iron zeolite catalysts provided by Süd-Chemie [618].

8.5.2. Automotive Exhaust Catalysis [619–622]

This section focuses on the catalysis-related items of automobile emission control. A more detailed discussion considering all aspects can be found in → Automobile Exhaust Control.

Internal combustion engines in automobiles represent a major source for the emission of NO_x, CO, and unburnt hydrocarbons (HC), while diesel engines contribute to the emission of soot as well. The most appropriate way to minimize these air pollutants is the modification of the combustion process. Aside from these primary measures, current legislative emission standards can only be met by additional, secondary measures for exhaust purification by application of catalysts. The importance of environmental catalysis will further increase in future due to the tightening of emission limits and an increasing number of automobiles. Already today (ca. 2008), environmental applications exhibit a worldwide market share of 35 % among all catalytic processes, and more than 70×10^6 automotive catalyst devices are produced per year.

The catalytic system used for aftertreatment of the exhaust gas primarily depends on the fuel (gasoline, diesel, biofuels) and the operating conditions. In principle, a distinction is made between stoichiometrically operated gasoline engines, lean-operated gasoline engines, and diesel engines producing different major pollutants, namely, CO/NO_x/HC, NO_x, and NO_x/soot, respectively.

Three-Way Catalyst The most frequent type of catalytic converter in automobiles is the three-way catalyst (TWC) for stoichiometrically operated gasoline engines with an annual production of over 60×10^6 units. TWC systems have been applied in gasoline engines since the 1980s and contain Pt/Rh or Pd/Rh in the mass ratio of approximately 5/1 with a total loading of precious metals of ca. 1.7 g/L. The TWC simultaneously converts NO_x, CO, and HC to N_2, CO_2, and H_2O [619–623]. The catalytic components are supported by a cordierite honeycomb monolith coated with high surface area γ-Al_2O_3. This washcoat layer additionally contains thermal stabilizers, for instance, La_2O_3, as well as the oxygen-storage component CeO_2. Ceria is able to release oxygen under rich conditions and thus maintain HC and CO abatement and avoid the emission of H_2S. The TWC process exclusively occurs within a narrow range of O_2 content that is close to stoichiometric combustion conditions, i.e., when the air coefficient λ ranges from 0.99 to 1.01. To realize these conditions an oxygen sensor is used which measures the air coefficient of the exhaust stream and forces the engine management system to regulate the air/fuel ratio. The TWC process involves a complex network of numerous elementary reactions [624], whereby the effectiveness of the catalyst is closely related to the specific activity of the precious metals and their surface

coverage. The transfer of TWC technology to lean-burn gasoline and diesel motors is problematic because of the insufficient NO_x abatement. This is associated with the lower raw emissions of reducing agents as well as the high content of O_2, which enhances oxidation of HC and CO and thus suppresses NO_x reduction. Therefore, alternative concepts are required for the reduction of NO_x under lean-burn conditions. For this purpose selective catalytic reduction by NH_3 and NO_x storage and reduction catalysts are being considered in the automotive industry.

Selective Catalytic Reduction (SCR) of NO_x by Ammonia. The SCR procedure is the only technique that selectively converts NO_x to N_2, even under strongly oxidizing conditions. Thus, SCR has been considered as the technology of choice for NO_x removal in lean-burn engines. Indeed, the SCR process covers the relevant temperature range of diesel engines and provides effective NO_x abatement. Thus, SCR has advanced to a state-of-the-art technology for heavy-duty vehicles. However, in mobile applications the storage of NH_3 is a problem. Therefore, an aqueous solution of urea (32.5 wt %) called AdBlue is currently used. The urea solution is sprayed into the tailpipe, where ammonia is produced after thermolysis and hydrolysis of the vaporizing urea – water droplets. Current research focuses on optimization of the dosing system and the development of vanadia-free catalysts, for instance, by substitution with Fe-ZSM5 zeolites [622]. Alternative reducing agents such as hydrocarbons and hydrogen has been discussed as well.

NO_x Storage Reduction Catalysts NO_x storage reduction catalysts (NSC) were originally developed for lean spark-ignition engines and are currently being transferred to diesel passenger cars. The NSC procedure is based on periodic adsorption and reduction of NO_x [625]. The catalysts consist of Pt, Pd, and Rh in the mass ratio of approximately 10/5/1 with a total precious metal load of ca. 4 g L^{-1}. NSCs contain basic adsorbents like Al_2O_3 (160 g L^{-1}), CeO_2 (98 g L^{-1}) and $BaCO_3$ (29 g L^{-1}, as BaO equivalent) [626]. In the lean phase of the engine (general operation mode), NO_x of the exhaust is adsorbed on the basic components of the NSC, mainly on barium carbonate to form the nitrate. When the storage capacity is reached, the engine is operated under rich conditions for a few seconds to give an exhaust containing CO, HC, and H_2 as reducing agents for catalyst regeneration (back-transformation of the nitrate to the carbonate).The effect of the Ba component is to adsorb NO_x at temperatures above 250 °C, whereas substantial storage is also provided by Al_2O_3 and CeO_2 at lower temperatures [626].

Catalytic CO oxidation Catalytic CO oxidation is an essential reaction of TWC and NSC and has also applied in diesel engines since the 1990s in the so-called direct oxidation catalyst (DOC). Furthermore, the catalytic abatement of CO is also a state-of-the-art technology for gas turbine engines fed by natural gas. DOCs usually contain Pt as an active component showing outstanding performance. The expensive platinum can be substituted by the less active but cheaper palladium. The precious metal load of a DOC is ca. 3 g L^{-1}. DOCs also oxidize gaseous HC and HC adsorbed on soot particles.

Removal of Soot The diesel particulate filter (DPF) is used for the removal of soot from diesel exhaust. DPFs mechanically separate the particles by forcing the exhaust gas to diffuse through porous walls thus leading to high filtration efficiency [627]. The DPF application requires regeneration, i.e., oxidation of the stored soot particles. Soot deposits can produce a substantial backpressure leading to increased fuel consumption and decreased engine efficiency. The preferred method for DPF regeneration is the CRT (continuously regenerating trap) technology involving the initiation of soot oxidation by NO_2 produced by oxidation of NO on Pt catalysts, as in NSC and SCR. The Pt catalyst can be applied in form of a precatalyst, and coating on the DPF. Furthermore, so-called fuel-borne catalysts (FBC), which are organometallic compounds based on Ce or Fe, e.g., ferrocene, can be added to the fuel [628]. FBCs also decrease soot emissions from the engine by direct oxidation of soot in the engine. Additionally, they are embedded in the soot particles.

References

1 *Appl. Catal. A, General* **173** (1998) N3.
2 J. J. Berzelius, *Ann. Chim. Phys.* **61** (1836) 146.
3 B. H. Davis, "Development of the Science of Catalysis" in G. Ertl, H. Knözinger, J. Weitkamp (eds.): *Handbook of Heterogeneous Catalysis*, Vol. **1**, Wiley-VCH, Weinheim, 1997, p. 13.
4 W. Ostwald, *Nature* **65** (1902) 522.
5 P. Sabatier, J. B. Senderens, *C. R. Acad. Sci.* **134** (1902) 514.
6 H. Heinemann, "Development of Industrial Catalysis" in G. Ertl, H. Knözinger, J. Weitkamp (eds.): *Handbook of Heterogeneous Catalysis*, Vol. **1**, Wiley-VCH, Weinheim 1997, p. 35.
7 S. A. Topham in J. R. Anderson, M. Boudart (eds.): *Catalysis: Science and Technology*, Vol. **7**, Springer, Berlin 1987, p. 1.
8 F. Aftalion: *A History of the International Chemical Industry*, University of Pennsylvania Press, Philadelphia 1991.
9 A. Mittasch, *Adv. Catal.* **2** (1950) 81.
10 DE 301 231, 1919(F. Bergius, J. Billwiller).
11 F. Fischer, H. Tropsch, *Brennstoff-Chem.* **4** (1923) 276.
12 DE 103 362, 1943(O. Roelen).
13 J. K. A. Clarke, J. J. Rooney, *Adv. Catal.* **25** (1976) 125.
14 A. J. Gellman, *Curr. Opin. Solid State Mater. Sci.* **5** (2001) 85.
15 J. N. Armor, *Appl. Catal.* **78** (1991) 141.
16 A. Chauvel, B. Delmon, W. F. Hoelderich, *Appl. Catal. A* **115** (1994) 173.
17 M. Misono, N. Nojiri, *Appl. Catal.* **64** (1990) 1.
18 A. J. Gellman, *Acc. Chem. Res.* **33** (2000) 19.
19 M. Boudart in G. Ertl, H. Knözinger, J. Weitkamp (eds.): *Handbook of Heterogeneous Catalysis*, Wiley-VCH, Weinheim 1997, p. 1.
20 A. Balandin, *Adv. Catal. Rel. Subj.* **19** (1969) 1.
21 W. J. M. Rootsaert, W. M. H. Sachtler, *Z. Phys. Chem.* **26** (1960) 16.
22 I. Langmuir, *J. Am. Chem. Soc.* **37** (1915) 1139.
23 I. Langmuir, *Trans. Faraday Soc.* **17** (1922) 607.
24 H. S. Taylor, *Proc. Roy. Soc. (London)* **A 108** (1925) 105.
25 M. Che, C. O. Bennett, *Adv. Catal.* **36** (1989) 55.
26 G.-M. Schwab, E. Pietsch, *Z. Phys. Chem.* **131** (1929) 385.
27 S. M. Davis, G. A. Somorjai in D. A. King, D. P. Woodruff (eds.): *The Chemical Physics of Solid Surfaces and Heterogeneous Catalysis*, Vol. **4**, Elsevier, New York 1982, p. 217.
28 P. G. Menon, T. S. R. Prasada Rao, *Catal. Rev.-Sci. Eng.* **20** (1979) 97.
29 M. Boudart, A. Aldag, J. E. Benson, N. A. Dougharty, C. G. Harkins, *J. Catal.* **6** (1966) 92;M. Boudart, A. Aldag, L. D. Ptak, J. E. Benson, *J. Catal.* **11** (1968) 35.
30 G. A. Somorjai, *Ann. Rev. Phys. Chem.* **45** (1994) 721.
31 G. Ertl, *Adv. Catal.* **45** (2000) 1.
32 V. Ponec, W. M. H. Sachtler in G. C. Bond, P. B. Wells, F. C. Tompkins (eds.): *Proc. 5th Intern. Congr. Catal.*, Vol. **1**, The Chemical Society, London 1976, p. 645.
33 R. L. Burwell, G. L. Haller, K. C. Taylor, J. F. Read, *Adv. Catal.* **20** (1969) 1.
34 R. L. Burwell in J. R. Anderson, M. Boudart (eds.): *Catalysis: Science and Technology*, Vol. **9**, Springer, Heidelberg 1991, p. 1.
35 W. M. H. Sachtler in G. Ertl, H. Knözinger, J. Weitkamp (eds.): *Handbook of Heterogeneous Catalysis*, Vol. **3**, Wiley-VCH, Weinheim 1997, p. 1077.
36 B. Hammer, J. K. Nørskov, *Adv. Catal.* **45** (2000) 71.
37 R. A. van Santen: *Theoretical Heterogeneous Catalysis*, World Scientific, Singapore 1991.
38 R. A. van Santen, M. Neurock in G. Ertl, H. Knözinger, J. Weitkamp (eds.): *Handbook of Heterogeneous Catalysis*, Vol. **3**, Wiley-VCH, Weinheim 1997, p. 991.
39 J. M. Basset, J. P. Candy, A. Choplin, B. Didillon, F. Quignard, A. Theolier in J. M. Thomas, K. I. Zamaraev (eds.): *Perspectives in Catalysis*, Blackwell Scientific Publications, London 1992, p. 125.
40 J. M. Basset, B. C. Gates, J. P. Candy, A. Choplin, M. Leconte, F. Quignard, C. Santini (eds.): *Surface Organometallic Chemistry: Molecular Approaches to Surface Catalysis*, Kluwer Academic Publ., Dordrecht 1988.
41 K. Hauffe, H.-J. Engell, *Z. Elektrochem.* **56** (1952) 366.
42 K. Hauffe, *Adv. Catal. Rel. Subj.* **7** (1955) 213.
43 Th. Wolkenstein, *Adv. Catal. Rel. Subj.* **9** (1957) 807, 818.
44 F. S. Stone, *J. Solid State Chem.* **12** (1975) 271.
45 M. P. Kiskinova, Poisoning and Promotion in Catalysis, *Stud. Surf. Sci. Catal.* **70** (1992).
46 Z. Paal, G. A. Somorjai in G. Ertl, H. Knözinger, J. Weitkamp (eds.): *Handbook of Heterogeneous Catalysis*, Vol. **3**, Wiley-VCH, Weinheim 1997, p. 1084.
47 G. J. Hutchings, *Catal. Lett.* **75** (2001) 1.
48 R. Schlögl in G. Ertl, H. Knözinger, J. Weitkamp (eds.): *Handbook of Heterogeneous Catalysis*, Vol. **4**, Wiley-VCH, Weinheim 1997, p. 1697.

49 H. Topsøe, B. S. Clausen, F. E. Massoth in J. R. Anderson, M. Boudart (eds.): *Catalysis: Science and Technology*, Vol. **11**, Springer, Berlin 1996.
50 J. H. Sinfelt in G. Ertl, H. Knözinger, J. Weitkamp (eds.): *Handbook of Heterogeneous Catalysis*, Vol. **4**, Wiley-VCH, Weinheim 1997, p. 1939.
51 S. A. Stevenson, J. A. Dumesic, R. T. K. Baker, E. Ruckenstein: *Metal-Support Interactions in Catalysis*, Sintering and Redispersion, Van Nostrand Reinhold, New York 1987.
52 H. Knözinger, E. Taglauer in G. Ertl, H. Knözinger, J. Weitkamp (eds.): *Handbook of Heterogeneous Catalysis*, Vol. **1**, Wiley-VCH, Weinheim 1997, p. 216.
53 G. C. Bond in G. Ertl, H. Knözinger, J. Weitkamp (eds.): *Handbook of Heterogeneous Catalysis*, Vol. **2**, Wiley-VCH, Weinheim 1997, p. 752.
54 S. J. Tauster, *Acc. Chem. Res.* **20** (1987) 389.
55 G. M. Pajonk in G. Ertl, H. Knözinger, J. Weitkamp (eds.): *Handbook of Heterogeneous Catalysis*, Vol. **3**, Wiley-VCH, Weinheim 1997, p. 1064.
56 W. C. Conner, G. M. Pajonk, S. J. Teichner, *Adv. Catal.* **34** (1986) 1.
57 W. C. Conner, Jr., J. L. Falconer, *Chem. Rev.* **95** (1995) 759.
58 E. Keren, A. Soffer, *J. Catal.* **50** (1977) 43.
59 G. A. Somorjai, *J. Phys. Chem.* **94** (1990) 1013.
60 B. Delmon, *Stud. Surf. Sci. Catal.* **77** (1993) 1.
61 L. T. Weng, P. Ruiz, B. Delmon, *Stud. Surf. Sci. Catal.* **72** (1982) 399.
62 R. K. Grasselli, *Top. Catal.* **15** (2001) 93.
63 R. K. Grasselli in G. Ertl, H. Knözinger, J. Weitkamp (eds.): *Handbook of Heterogeneous Catalysis*, Vol. **5**, Wiley-VCH, Weinheim 1997, p. 2302.
64 J. L. Callahan, R. K. Grasselli, *AIChE J.* **9** (1963) 755.
65 P. B. Weisz, V. J. Frilette, R. W. Maatman, E. B. Mower, *J. Catal.* **1** (1962) 307.
66 S. M. Csicsery, *J. Catal.* **19** (1970) 394.
67 M. Boudart in J. M. Thomas, K. I. Zamaraev (eds.): *Perspectives in Catalysis*, Blackwell Scientific Publications, London 1992, p. 183.
68 M. Boudart in G. Ertl, H. Knözinger, J. Weitkamp (eds.): *Handbook of Heterogeneous Catalysis*, Vol. **2**, Wiley-VCH, Weinheim 1997, p. 958.
69 M. Boudart, *Catal. Rev.-Sci. Eng.* **23** (1981) 1.
70 G. F. Froment, L. Hosten in J. R. Anderson, M. Boudart (eds.): *Catalysis: Science and Technology*, Vol. **2**, Springer, Heidelberg 1980, p. 97.
71 M. Boudart, G. Djéga-Mariadassou: *Kinetics of Heterogeneous Catalytic Reactions*, Princeton University Press, Princeton 1984.
72 O. A. Hougen, K. M. Watson: *Chemical Process Principles. Part Three: Kinetics and Catalysis*, Wiley, New York, 1947.
73 J. A. Dumesic, D. F. Rudd, L. M. Aparicio, J. E. Rekoske, A. A. Trevino: *The Microkinetics of Heterogeneous Catalysis*, American Chemical Society, Washington 1993.
74 R. D. Cortright, J. A. Dumesic, *Adv. Catal.* **46** (2001) 161.
75 R. A. van Santen, J. W. Niemantsverdriet: *Chemical Kinetics and Catalysis*, Plenum Press, New York 1995.
76 *Catalysis Today*, 1999, Vol. 3, No. 2.
77 G. M. Schwab: *Katalyse vom Standpunkt der chemischen Kinetik*, Springer, Berlin, 1931.
78 M. I. Temkin, V. Pyzhev, *Acta Physicochim. URSS* **12** (1940) 217.
79 M. Boudart in *Catalysis*, Vol. **14**, The Royal Society of Chemistry, Cambdrigep. 93.
80 M. Boudart, *Topics Catal.* **14** (2001) 181.
81 M. Boudart, *I & EC Fundamentals* **25** (1986) 70.
82 R. D. Cortright, J. A. Dumesic, R. J. Madon, *Topics Catal.* **4** (1997) 15.
83 J. Horiuti, *J. Res. Inst. Catal. (Hokkaido Univ.)* **5** (1957) 1.
84 A. Varma, M. Morbidelli, H. Wu: *Parametric Sensitivity in Chemical Systems*, Cambridge Univ. Press, Cambridge 1999.
85 C. T. Campbell, *Topics Catal.* **1** (1994) 364.
86 G. Ertl in G. Ertl, H. Knözinger, F. Schüth, J. Weitkamp (eds.), *Handbook of Heterogeneous Catalysis*, 2nd ed., Vol. **3**, Wiley-VCH, Weinheim 2008, pp. 1492.
87 T. Engel, G. Ertl, *Adv. Catal.* **28** (1979) 1.
88 T. Engel, G. Ertl in D. P. Woodruff (ed.): *The Chemical Physics of Solid Surfaces and Heterogeneous Catalysis*, Vol. **4**, Elsevier, Amsterdam 1982, p. 73.
89 G. Emig, R. Dittmeyer in G. Ertl, H. Knözinger, J. Weitkamp (eds.): *Handbook of Heterogeneous Catalysis*, Vol. **3**, Wiley-VCH, Weinheim 1997, p. 1209.
90 W. J. Thomas in J. M. Thomas, K. I. Zamaraev (eds.): *Perspectives in Catalysis*, Blackwell Scientific Publications, London 1992, p. 251.
91 F. Kapteijn, J. A. Moulijn in G. Ertl, H. Knözinger, J. Weitkamp (eds.): *Handbook of Heterogeneous Catalysis*, Vol.Wiley-VCH, Weinheim 1997, p. 1189.
92 R. Mezaki, H. Inoue: *Rate Equations of Solid Catalyzed Reactions*, University of Tokyo Press, Tokyo 1991.
93 A. Wheeler, *Adv. Catal.* **2** (1951) 250.
94 http://www.gaussian.com/
95 http://www.turbomole.com/

96 http://www.tcm.phy.cam.ac.uk/castep/ and http://accelrys.com/
97 http://www.camd.dtu.dk/
98 http://cms.mpi.univie.ac.at/vasp/
99 M. Neurock, *Stud. Surf. Sci. Catal.* **109** (1997), 3.
100 L. D. Kieken, M. Neurock, D. H. Mei, *J. Phys. Chem. B* **109** (2005), 2234.
101 E. W. Hansen, M. Neurock, *Chem. Eng. Sci.* **54** (1999) 3411
102 A. A. Gokhale, S. Kandoi, J. P. Greely, M. Mavrikakis, J. A. Dumesic, *Chem. Eng. Sci.* **59** (2004) 4679.
103 R. A. van Santen, M. Neurock, *Chem. Rev. Sci. Eng.* **37** (1995) 557.
104 H. Toulhoat, P. Raybaud, *J. Catal.* **216** (2003) 63.
105 K. Reuter, D. Frenkel, M. Scheffler, *Phys. Rev. Lett.* **93** (2004) 116105.
106 S. Linic, M. A. Barteau, *J. Catal.* **214** (2003) 200.
107 J. Greeley, M. Mavrikakis, *J. Catal.* **208** (2002) 291.
108 A. Logadottir, J. K. Nørskov, *J. Catal.* **220** (2003) 273.
109 A. Heyden, A. T. Bell, F. J. Keil, *J. Catal.* **233** (2005) 26.
110 O. R. Inderwildi, D. Lebiedz, O. Deutschmann, J. Warnatz, *J. Chem. Phys.* **122** (2005) 034710.
111 A. Logadottir, T. H. Rod, J. K. Nørskov, B. Hammer, S. Dahl, C. J. H Jacobsen, *J. Catal.*, **197** (2001) 229.
112 P. Stoltze, *Prog. Surf. Sci.* , **65** (2000) 65.
113 H. C. Kang, W. H. Weinberg, *Surf. Sci.*, **299/300** (1994) 755.
114 V. P. Zhdanov, *Surf. Sci. Rep.*, **45** (2002) 231.
115 M. W. Deem, W. H. Weinberg, H. C. Kang, *Surf. Sci.* **276** (1992) 99.
116 V. P. Zhdanov, B. Kasemo, *Surf. Sci. Rep.* **20** (1994) 111.
117 D. J. Dooling, L. J. Broadbelt, *Ind. Eng. Chem. Res.* **40** (2001) 522.
118 S. Ovesson, B. I. Lundqvist, W. F. Schneider, A. Bogicevic, *Phys. Rev.* **B 71** (2005) 115406.
119 M. E. Coltrin, R. J. Kee, F. M. Rupley, SURFACE CHEMKIN (Version 4.0): A Fortran Package for Analyzing Heterogeneous Chemical Kinetics at a Solid-Surface – Gas-Phase Interface, SAND91-8003B, Sandia National Laboratories, 1991.
120 R. J. Kee, M. E. Coltrin, P. Glarborg, *Chemically Reacting Flow*, John Wiley & Sons, Hoboken, New Jersey, 2003, pp. 929
121 P. Stolze, J. K. Norskov in G. Ertl, H. Knözinger, F. Schüth, J. Weitkamp (eds.), *Handbook of Heterogeneous Catalysis*, 2nd ed., Vol. **3**, Wiley-VCH, Weinheim 2008, pp. 1479.
122 O. Deutschmann in G. Ertl, H. Knözinger, F. Schüth, J. Weitkamp (eds.), *Handbook of Heterogeneous Catalysis*, 2nd ed., Vol. **3**, Wiley-VCH, Weinheim 2008, p. 1815.
123 E. Shustorovich, *Surface Science* **176** (1986) L863 – L872
124 E. Shustorovich, H. Sellers, *Surf. Sci. Rep.* **31** (1998) 1 – 119.
125 W. R. Williams, C. M. Marks, L. D. Schmidt, *J. Phys. Chem.* **96** (1992) 5922.
126 B. Hellsing, B. Kasemo, V. P. Zhdanov, *J. Catal.* **132** (1991) 210.
127 M. Rinnemo, O. Deutschmann, F. Behrendt, B. Kasemo, *Combust. Flame* **111** (1997) 312.
128 G. Veser, *Chem. Eng. Sci.* **56** (2001) 1265.
129 P.-A. Bui, D. G. Vlachos, P. R. Westmoreland, *Industrial & Engineering Chemistry Research* **36** (1997) 2558.
130 J. Mai, W. von Niessen, A. Blumen, *J. Chem. Phys.* **93** (1990) 3685.
131 V. P. Zhdanov, B. Kasemo, *Appl. Surf. Sci.* **74** (1994) 147.
132 P. Aghalayam, Y. K. Park, D. G. Vlachos, *Proc. Combust. Inst.* **28** (2000) 1331.
133 O. Deutschmann, F. Behrendt, J. Warnatz, *Catal. Today* **21** (1994) 461 – 470.
134 G. Veser, J. Frauhammer, L. D. Schmidt, G. Eigenberger, in "Dynamics of Surfaces and Reaction Kinetics in Heterogeneous Catalysis", G. F. Froment, K. C. Waugh (eds.):Studies in Surface Science and Catalysis 109, Elsevier, Amsterdam 1997, p. 273.
135 P.-A. Bui, D. G. Vlachos, P. R. Westmoreland, *Surf. Sci.* **386** (1997) L1029.
136 P. Aghalayam, Y. K. Park, N. Fernandes, V. Papavassiliou, A. B. Mhadeshwar, D. G. Vlachos, *J. Catal.* **213** (2003) 23.
137 D. A. Hickman, L. D. Schmidt, *Am. Inst. Chem. Eng. J.* **39** (1993) 1164.
138 D. K. Zerkle, M. D. Allendorf, M. Wolf, O. Deutschmann, *J. Catal.* **196** (2000) 18.
139 F. Donsi, K. A. Williams, L. D. Schmidt, *Ind. Eng. Chem. Res.* **44** (2005) 3453.
140 M. C. Huff, I. P. Androulakis, J. H. Sinfelt, S. C. Reyes, *J. Catal.* **191** (2000) 46.
141 D. A. Hickman, L. D. Schmidt, *Am. Inst. Chem. Eng. J.* **39** (1993) 1164.
142 R. Schwiedernoch, S. Tischer, C. Correa, O. Deutschmann, *Chem. Eng. Sci.* **58** (2003) 633.
143 D. Chatterjee, O. Deutschmann, J. Warnatz, *Faraday Discuss.* **119** (2001) 371.
144 B. Ruf, F. Behrendt, O. Deutschmann, J. Warnatz, *Surf. Sci.* **352** (1996) 602.
145 S. J. Harris, D. G. Goodwin, *J. Phys. Chem.* **97** (1993) 23.

146 S. Romet, M. F. Couturier, T. K. Whidden, *J. Electrochem. Soc.* **148** (2001) G82.
147 C. D. Scott, A. Povitsky, C. Dateo, T. Gokcen, P. A. Willis, R. E. Smalley, *J. Nanosci. Nanotechnol.* **3** (2003) 63.
148 C. H. Bartholomew, R. J. Farrauto: *Fundamentals of Industrial Catalytic Processes*, 2nd ed., Wiley, Hobboken 2006.
149 S. Senkan, *Angew. Chem.* **113** (2001) 322;*Angew. Chem. Int. Ed.* **40** (2001) 312.
150 B. Jandeleit, D. J. Schaefer, T. S. Powers, H. W. Turner, H. W. Weinberg, *Angew. Chem.* **111** (1999) 2649;*Angew. Chem. Int. Ed.* **38** (1999) 2494.
151 J. N. Cawse, *Acc. Chem. Res.* **34** (2001) 313.
152 C. Hoffmann, H.-W. Schmidt, F. Schüth, *J. Catal.* **198** (2001) 348.
153 S. I. Woo, K. W. Kim, H. Y. Cho, K. S. Oh, M. K. Jeon, N. H. Tarte, T. S. Kim, A. Mahmood, *QSAR Comb. Sci.* **24** (2005) 138.
154 A. Hagemeyer, P. Strasser, A. F Volpe, Jr. (eds.): *High Throughput Screening in Chemical Catalysis*, Wiley-VCH, Weinheim 2004.
155 O. Trapp, *J. Chromatogr. A* **1184** (2008) 160.
156 U. Rodemerck, M. Baerns, M. Holena, D. Wolf, *Appl. Surf. Sci.* **223** (2004) 168.
157 O. Trapp, S. K. Weber, S. Bauch, W. Hofstadt, *Angew. Chem. Int. Ed.* **46** (2007) 7307.
158 M. Baerns, E. Körting in G. Ertl, H. Knözinger, J. Weitkamp (eds.): *Handbook of Heterogeneous Catalysis*, Vol. **1**, Wiley-VCH, Weinheim 1997, p. 419.
159 D. Wolf, O. V. Buyevskaya, M. Baerns, *Appl. Catal. A: General* **200** (2000) 63.
160 K. Kochloefl, *Chem. Eng. Technol.* **24** (2001) 3.
161 J. Greeley, J. K. Nørskov, M. Mavrikakis, *Annu. Rev. Phys. Chem.* **53** (2002) 319.
162 C. J. H. Jacobsen, S. Dahl, B. S. Clausen, S. Bahn, A. Logadottir, J. K. Nørskov, *J. Am. Chem. Soc.* **123** (2001) 8404.
163 B. C. Gates: *Catalytic Chemistry*, Wiley, New York 1992.
164 C. N. Satterfield: *Heterogeneous Catalysis in Industrial Practice*, McGraw-Hill, New York 1991.
165 R. J. Farrauto, C. H. Bartholomew: *Fundamentals of Industrial Catalytic Processes*, Blackie Academic and Professional, London 1997.
166 G. Ertl, H. Knözinger, J. Weitkamp (eds.): *Handbook of Heterogeneous Catalysis*, Vol**s. 1 – 5**, Wiley-VCH, Weinheim 1997.
167 J. Hagen: *Industrial Catalysis*, A Practical Approach, Wiley-VCH, Weinheim 1999.
168 K. Tanabe: *Solid Acids and Bases*, Kodansha, Tokyo, Academic Press, New York, London 1970.
169 M. Che, O. Clause, Ch. Marcilly in G. Ertl, H. Knözinger, J. Weitkamp (eds.): *Handbook of Heterogeneous Catalysis*, Vol. **1**, Wiley-VCH, Weinheim 1997, p. 191.
170 J. P. Brunelle, *Pure Appl. Chem.* **50** (1978) 1211.
171 B. G. Linsen (ed.): *Physical and Chemical Aspects of Adsorbents and Catalysts*, Academic Press, New York 1970.
172 H. Knözinger, P. Ratnasamy, *Catal. Rev.-Sci. Eng.* **17** (1978) 31.
173 H. Oechsner, *Scanning Microsc.* **2** (1988) 9.
174 H. P. Boehm, H. Knözinger in J. R. Anderson, M. Boudart (eds.): *Catalysis: Science and Technology*, Vol. **4**, Springer, Berlin 1983, p. 39.
175 C. S. John, M. S. Scurrell: *Catalysis, The Chemical Society, London*, **1** (1977) 136.
176 J. Wagner, W. Nehb in G. Ertl, H. Knözinger, J. Weitkamp (eds.): *Handbook of Heterogeneous Catalysis*, Vol. **4**, Wiley-VCH, Weinheim 1997, p. 1761.
177 E. F. Vansant, P. Van Der Voort, K. C. Vrancken (eds.): *Stud. Surf. Sci. Catal.* **93** (1995).
178 A. E. Legrand (ed.): *The Surface Properties of Silicas*, Wiley, Chichester, New York, Weinheim, Brisbane, Singapore, Toronto 1998.
179 H. Knözinger in P. Schuster, G. Zundel, C. Sandorfy (eds.): *The Hydrogen Bond*, Vol. **3**, North Holland, Amsterdam 1976, p. 1263.
180 J. M. Thomas, R. G. Bell, C. R. A. Catlow in G. Ertl, H. Knözinger, J. Weitkamp (eds.): *Handbook of Heterogeneous Catalysis*, Vol. **1**, Wiley-VCH, Weinheim 1997, p. 286.
181 C. T. Kresge, M. E. Leonowicz, W. J. Roth, J. C. Vartuli, J. S. Beck, *Nature* **359** (1992) 710.
182 J. S. Beck, J. C. Vartuli, W. J. Roth, M. E. Leonowicz, C. T. Kresge, K. D. Schmidt, C. T. W. Chu, D. H. Olson, E. W. Sheppard, S. B. McCullan, J. B. Higgins, J. L. Schlenker, *J. Am. Chem. Soc.* **114** (1992) 10834.
183 E. A. Colbourn, W. C. Mackrodt, *Surf. Sci.* **143** (1984) 391.
184 S. Coluccia, A. J. Tench: Proc. 7th Intern. Congr. Catal., Tokyo, 1980, Kodansha, Tokyo, Elsevier, Amsterdam 1981, p. 1154.
185 A. Zecchina, D. Scarano, S. Bordiga, G. Spoto, C. Lamberti, *Adv. Catal.* **46** (2001) 265.
186 R. N. Spitz, J. E. Barton, M. A. Barteau, R. H. Staley, A. W. Sleight, *J. Phys. Chem.* **90** (1986) 4067.
187 A. Zecchina, M. G. Lofthouse, F. S. Stone, *J. Chem. Soc. Faraday Trans. 1* **71** (1975) 1476.
188 S. Coluccia, A. M. Deane, A. J. Tench, *J. Chem. Soc. Faraday Trans. 1* **74** (1978) 2913.
189 H. Knözinger, *Science* **287** (2000) 1407.
190 A. Cimino, F. S. Stone in G. Ertl, H. Knözinger, J. Weitkamp (eds.): *Handbook of Heterogeneous*

Catalysis, Vol. **2**, Wiley-VCH, Weinheim 1997, p. 845.
191 C. N. R. Rao, B. Raveau: *Transition Metal Oxides*, VCH, Weinheim 1995.
192 P. A. Cox: *Transition Metal Oxides*, Clarendon Press, Oxford 1995.
193 H. H. Kung: *Transition Metal Oxides: Surface Chemistry and Catalysis*, Elsevier, Amsterdam 1995.
194 P. Pichat in G. Ertl, H. Knözinger, J. Weitkamp (eds.): *Handbook of Heterogeneous Catalysis*, Vol. **4**, Wiley-VCH, Weinheim 1997, p. 2111.
195 A. L. Linsebigler, G. Lu, J. T. Yates, Jr., *Chem. Rev.* **95** (1995) 735.
196 K. Arata, *Adv. Catal.* **37** (1990) 165.
197 W. Göpel, K. D. Schierbaum in G. Ertl, H. Knözinger, J. Weitkamp (eds.): *Handbook of Heterogeneous Catalysis*, Vol. **3**, Wiley-VCH, Weinheim 1997, p. 1284.
198 K. Kochloefl in G. Ertl, H. Knözinger, J. Weitkamp (eds.): *Handbook of Heterogeneous Catalysis*, Vol. **4**, Wiley-VCH, Weinheim 1997, p. 1831.
199 K. Kochloefl in G. Ertl, H. Knözinger, J. Weitkamp (eds.): *Handbook of Heterogeneous Catalysis*, Vol. **5**, Wiley-VCH, Weinheim 1997, p. 2151.
200 J. Haber in G. Ertl, H. Knözinger, J. Weitkamp (eds.): *Handbook of Heterogeneous Catalysis*, Vol. **5**, Wiley-VCH, Weinheim 1997, p. 2253.
201 M. Muhler in G. Ertl, H. Knözinger, J. Weitkamp (eds.): *Handbook of Heterogeneous Catalysis*, Vol. **5**, Wiley-VCH, Weinheim 1997, p. 2274.
202 R. M. Barrer: *Hydrothermal Chemistry of Zeolites*, Academic Press, London 1982.
203 W. M. Meier, D. H. Olson, Ch. Baerlocher: *Atlas of Zeolite Structure Types*, 4th Ed., Butterworth-Heinemann, London 1996.
204 J. Weitkamp, *Solid State Ionics* **131** (2000) 175.
205 G. Bellussi, V. Fattore in P. A. Jacobs, N. Jaeger, L. Kubelkova, B. Wichterlova (eds.): *Zeolite Chemistry and Catalysis*, Elsevier, Amsterdam 1991, p. 79.
206 D. Barthomeuf, *Catal. Rev.-Sci. Eng.* **38** (1996) 521.
207 J. M. Thomas, R. G. Bell, C. R. A. Catlow, G. Ertl, H. Knözinger, J. Weitkamp (eds.): *Handbook of Heterogeneous Catalysis*, Vol. **1**, Wiley-VCH, Weinheim 1997, p. 286.
208 T. Ishihara, H. Takita, *Catalysis* **12** (1996) 21.
209 J. J. Fripiat in G. Ertl, H. Knözinger, J. Weitkamp (eds.): *Handbook of Heterogeneous Catalysis*, Vol. **1**, Wiley-VCH, Weinheim 1997, p. 387.
210 P. G. Menon, B. Delmon in G. Ertl, H. Knözinger, J. Weitkamp (eds.): *Handbook of Heterogeneous Catalysis*, Vol. **1**, Wiley-VCH, Weinheim 1997, p. 100.
211 R. K. Grasselli, J. F. Brazdil: *Solid State Chemistry in Catalysis*, ACS Symposium Series, Amer. Chem. Soc., Washington, **279** (1985).
212 J. Haber, G. Ertl, H. Knözinger, J. Weitkamp (eds.): *Handbook of Heterogeneous Catalysis*, Vol. **5**, Wiley-VCH, Weinheim 1997, p. 2253.
213 R. K. Grasselli, *J. Chem. Ed.* **63** (1986) 216.
214 M. Egasihra, K. Matsuo, S. Kawaga, T. Seiyama, *J. Catal.* **58** (1979) 409.
215 US 4 370 279, 1983(Y. Sasaki, T. Nakamura, Y. Nakamura, K. Moriya, H. Utsumi, S. Saito).
216 A. W. Sleight in J. J. Burton, R. L. Garten (eds.): *Advanced Materials in Catalysis*, Academic Press, New York 1977, p. 181.
217 L. G. Tejuca, J. L. G. Fierro: *Properties and Applications of Perovskite-type Oxides*, M. Dekker, New York 1993.
218 P. Cavani, F. Trifiró, A. Vaccari, *Catal. Today* **11** (1991) 173.
219 F. Basile, M. Campanati, E. Serwicka, A. Vaccari, *Appl. Clay Sci.* **18** (2001) 1.
220 P. Gouzerh, A. Proust, *Chem. Rev.* **98** (1998) 77.
221 E. Coronado, C. J. Gómez-García, *Chem. Rev.* **98** (1998) 273.
222 K.-Y. Lee, M. Misono in G. Ertl, H. Knözinger, J. Weitkamp (eds.): *Handbook of Heterogeneous Catalysis*, Vol. **1**, Wiley-VCH, Weinheim 1997, p. 118.
223 M. Misono, *Catal. Rev.-Sci. Eng.* **30** (1988) 339.
224 J. B. Moffat: *Metal-Oxygen Clusters*, Kluwer Academic/Plenum Publishers, New York 2001.
225 J. A. Gamelas, F. A. S. Couto, M. C. N. Trovao, A. M. V. Cavaleiro, J. A. S. Cavaleiro, M. Guelton, *Thermochim. Acta* **326** (1999) 165.
226 T. Okuhara, M. Yamashita, K. Na, M. Misono, *Chem. Lett.*(1994) 1450.
227 Y. Izumi, M. Ogawa, W. Nohara, K. Krabe, *Chem. Lett.*(1992) 1987.
228 G. Centi, J. L. Nieto, C. Iapalucci, K. Brückman, E. M. Serwicka, *Appl. Catal.* **46** (1989) 197.
229 F. Cavani, M. Koutyrev, F. Trifiró, *Catal. Today* **28** (1996) 319.
230 E. Wagner, T. Fetzer in G. Ertl, H. Knözinger, J. Weitkamp (eds.): *Handbook of Heterogeneous Catalysis*, Vol. **4**, Wiley-VCH, Weinheim 1997, p. 1748.
231 M. S. Wainright in G. Ertl, H. Knözinger, J. Weitkamp (eds.): *Handbook of Heterogeneous Catalysis*, Vol. **1**, Wiley-VCH, Weinheim, Germany 1997, p. 64.
232 R. Schlögl in G. Ertl, H. Knözinger, J. Weitkamp (eds.): *Handbook of Heterogeneous Catalysis*, Vol. **1**, Wiley-VCH, Weinheim 1997, p. 54.

233 A. Baiker in G. Ertl, H. Knözinger, J. Weitkamp (eds.): *Handbook of Heterogeneous Catalysis*, Vol. **2**, Wiley-VCH, Weinheim 1997, p. 803.
234 J. R. Jennings (ed.): *Catalytic Ammonia Synthesis: Fundamentals and Practice*, Plenum Press, New York 1991.
235 S. T. Oyama in G. Ertl, H. Knözinger, J. Weitkamp (eds.): *Handbook of Heterogeneous Catalysis*, Vol. **1**, Wiley-VCH, Weinheim 1997, p. 132. in ref. [4], p. 132.
236 C. Bouchy, C. Pham-Huu, B. Heinrich, C. Chaumot, M. J. Ledoux, *J. Catal.* **190** (2000) 92.
237 R. Schlögl in G. Ertl, H. Knözinger, J. Weitkamp (eds.): *Handbook of Heterogeneous Catalysis*, Vol. **1**, Wiley-VCH, Weinheim 1997, p. 138.
238 H. Jüntgen, H. Kühl, *Chem. Phys. Carbon* **22** (1990) 145.
239 L. R. Radovic, F. Rodriguez-Reinoso, *Chem. Phys. Carbon* **35** (1997) 243.
240 P. Serp, M. Corria, P. Kalck, *Appl. Catal. A: General* **253** (2003) 337.
241 R. P. Raffaelle, B. J. Landi, J. D. Harris, S. G. Bailey, A. F. Hepp, *Mater. Sci. Eng. B* **116** (2005) 233.
242 F. de Dardel, T. V. Arden: *Ullmann's Encyclopedia of Industrial Chemistry*, 5th ed., Vol. **A 14**, VCH Verlagsgesellschaft, Weinheim 1987, p. 393.
243 A. Stüwe, C.-P. Hälsig, H. Tschorn in G. Ertl, H. Knözinger, J. Weitkamp (eds.): *Handbook of Heterogeneous Catalysis*, Vol. **4**, Wiley-VCH, Weinheim 1997, p. 1986.
244 G. A. Olah, A. Molnar: *Hydrocarbon Chemistry*, Wiley, New York 1995.
245 J.-P. Vigneron in G. Ertl, H. Knözinger, J. Weitkamp (eds.): *Handbook of Heterogeneous Catalysis*, Vol. **2**, Wiley-VCH, Weinheim 1997, p. 888.
246 K. Morihara, S. Doi, M. Takiguchi, T. Shimada, *Bull. Chem. Soc. Jpn.* **66** (1993) 2977.
247 G. Wulff in C. G. Gebelein (ed.): *Biomimetic Polymers*, Plenum Press, New York, 1990, p. 1.
248 K. Morihara, M. Takaguchi, T. Shimada, *Bull. Chem. Soc. Jpn.* **67** (1994) 1078.
249 M. Eddaoudi, D. B. Moler, H. L. Li, B. L. Chen, T. M. Reineke, M. O'Keefe, O. M. Yaghi, *Acc. Chem. Res.* **34** (2001) 319.
250 S. Kaskel in F. Schüth, K. S. W. Sing, J. Weitkamp (eds.): *Handbook of Porous Solids*, Vol. **2**, Wiley-VCH, Weinheim, 2002, p. 1190.
251 H. Li, M. Eddaoudi, M. O'Keefe, O. M. Yaghi, *Nature* **402** (1999) 276.
252 H. K. Chae, D. Y. Siberio-Perez, J. Kim, Y. Go, M. Eddaoudi, A. J. Matzger, M. O'Keefe, O. M. Yaghi, *Nature* **427** (2004) 523.
253 U. Mueller, M. Schubert, F. Teich, H. Pütter, K. Schierle-Arnd, J. Pastre, *J. Mater. Chem.* **16** (2006) 626.
254 F. X. L. I. Xamena, A. Abad, A. Corma, H. Garcia, *J. Catal.* **250** (2007) 294.
255 M. J. Ledoux, C. Pham-Huu, *CATTECH* **5** (2001) 226.
256 H. Sieber, C. Hoffmann, A. Kaindl, P. Greil, *Adv. Eng. Mater.* **2** (2000) 105.
257 J. L. Williams, *Catal. Today* **69** (2001) 3.
258 M. Valentini, G. Groppi, C. Cristiani, M. Levi, E. Tronconi, P. Forzatti, *Catal. Today* **69** (2001) 307.
259 E. S. J. Lox, B. H. Engler in G. Ertl, H. Knözinger, J. Weitkamp (eds.): *Handbook of Heterogeneous Catalysis*, Vol. **4**, Wiley-VCH, Weinheim 1997, p. 1569.
260 J. M. Thomas, *Angew. Chem.* **111** (1999) 380; *Angew. Chem. Int. Ed.* **38** (1999) 3588.
261 A. Stein, B. J. Melde, R. C. Schroden, *Adv. Mater.* **12** (2000) 1403.
262 D. E. De Vos, B. F. Sels, P. A. Jacobs, *Adv. Catal.* **46** (2001) 2.
263 D. C. Sherrington, A. P. Kybett (eds.): *Supported Catalysts and their Applications*, The Royal Society of Chemistry, Cambridge 2001.
264 B. K. Hodnett, A. Kybett, J. H. Clark, K. Smith: *Supported Reagents and Catalysts in Chemistry*, The Royal Society of Chemistry, Cambridge 1998.
265 B. Clapham, T. . Reger, K. D. Janda, *Tetrahedron* **57** (2001) 4637.
266 W. Keim, B. Driessen-Hölscher in G. Ertl, H. Knözinger, J. Weitkamp (eds.): *Handbook of Heterogeneous Catalysis*, Vol. **1**, Wiley-VCH, Weinheim 1997, p. 231.
267 I. E. Wachs: *Catalysis*, Vol. **13**, The Royal Society of Chemistry, Cambridge 1997, p. 37.
268 B. Delmon in G. Ertl, H. Knözinger, J. Weitkamp (eds.): *Handbook of Heterogeneous Catalysis*, Vol. **1**, Wiley-VCH, Weinheim 1997, p. 264.
269 G. C. Bond, J. C. Vedrine, *Catal. Today* **20** (1994) 1.
270 G. Centi, *Appl. Catal. A: General* **147** (1996) 267.
271 F. J. Janssen in G. Ertl, H. Knözinger, J. Weitkamp (eds.): *Handbook of Heterogeneous Catalysis*, Vol. **4**, Wiley-VCH, Weinheim 1997, p. 1633.
272 J. F. Armor, *Chem. Mat.* **6** (1994) 730.
273 R. Prins in G. Ertl, H. Knözinger, J. Weitkamp (eds.): *Handbook of Heterogeneous Catalysis*, Vol. **4**, Wiley-VCH, Weinheim 1997, p. 1908.
274 R. Prins, *Adv. Catal.* **46** (2001) 399.
275 M. Hino, K. Arata: *Chem. Commun.* 1988, 1259.
276 S. Kuba, P. Concepcion, R. K. Grasselli, B. C. Gates, M. Che, H. Knözinger, *Phys. Chem. Chem. Phys.* **3** (2001) 146.

277 S. Kuba, B. C. Gates, P. Vijayanand, R. K. Grasselli, H. Knözinger: *Chem. Commun.* 2001, 57.
278 J. C. Mol in G. Ertl, H. Knözinger, J. Weitkamp (eds.): *Handbook of Heterogeneous Catalysis*, Vol. **5**, Wiley-VCH, Weinheim 1997, p. 2387.
279 F. Buonomo, D. Sanfilippo, F. Trifiro in G. Ertl, H. Knözinger, J. Weitkamp (eds.): *Handbook of Heterogeneous Catalysis*, Vol. **5**, Wiley-VCH, Weinheim 1997, p. 2140.
280 S. H. Overbury, P. A. Bertrand, G. A. Somorja, *Chem. Rev.* **75** (1975) 547.
281 Y. Ono, T. Baba: *Catalysis*, Vol. **15**, The Royal Society of Chemistry, Cambridge 2000, p. 1.
282 K. Tanabe, H. Hattori in G. Ertl, H. Knözinger, J. Weitkamp (eds.): *Handbook of Heterogeneous Catalysis*, Vol. **1**, Wiley-VCH, Weinheim 1997, p. 404.
283 X. Song, A. Sayari, *Catal. Rev.-Sci. Eng.* **38** (1996) 329.
284 *Topics in Catalysis* **6** (1998).
285 K. Foger in J. R. Anderson, M. Boudart (eds.): *Catalysis: Science and Technology*, Vol. **6**, Springer, Berlin 1984, p. 228.
286 B. C. Gates in G. Ertl, H. Knözinger, J. Weitkamp (eds.): *Handbook of Heterogeneous Catalysis*, Vol. **2**, Wiley-VCH, Weinheim 1997, p. 793.
287 B. C. Gates, *Chem. Rev.* **95** (1995) 511.
288 J. H. Sinfelt: *Bimetallic Catalysts*, Wiley, New York 1983.
289 C. T. Campbell in G. Ertl, H. Knözinger, J. Weitkamp (eds.): *Handbook of Heterogeneous Catalysis*, Vol. **2**, Wiley-VCH, Weinheim 1997, p. 814.
290 A. Baiker, *Curr. Opin. Sol. State Mater. Sci.* **3** (1998) 86.
291 J. Wei in G. Ertl, H. Knözinger, J. Weitkamp (eds.): *Handbook of Heterogeneous Catalysis*, Vol. **4**, Wiley-VCH, Weinheim 1997, p. 1928.
292 S. Helveg, J. V. Lauritsen, E. Lægsgaard, I. Stensgaard, J. K. Nørskov, B. S. Clausen, H. Topsøe, F. Besenbacher, *Phys. Rev. Lett.* **84** (2000) 951.
293 D. E. De Vos, I. F. J. Vankelecom, P. A. Jacobs: *Chiral Catalyst Immobilization and Recycling*, Wiley-VCH, Weinheim 2000.
294 D. E. De Vos, S. de Wildman, B. F. Sels, P. J. Grobet, P. A. Jacobs, *Angew. Chem.* **111** (1999) 1033;*Angew. Chem. Int. Ed.* **38** (1999) 980.
295 K. Dranz, H. Waldmann: *Enzyme Catalysis in Organic Synthesis*, VCH Verlagsgesellschaft, Weinheim 1994.
296 A. W. Bosman, H. M. Janssen, E. W. Meijer, *Chem. Rev.* **99** (1999) 1665.
297 H. Brunner, *J. Organomet. Chem.* **500** (1995) 39.
298 A. Kirschning, H. Monenschein, R. Wittenberg, *Angew. Chem. Int. Ed.* **40** (2001) 650.
299 B. Cornils, W. A. Herrmann: *Applied Homogeneous Catalysis with Organometallic Compounds*, Wiley-VCH, Weinheim 1996, p. 619.
300 J. P. Arhancet, M. E. Davis, J. S. Merola, B. E. Hanson, *Nature* **339** (1989) 454;K. T. Wan, M. E. Davis, *Nature* **370** (1994) 449.
301 J. Adlkofer in G. Ertl, H. Knözinger, J. Weitkamp (eds.): *Handbook of Heterogeneous Catalysis*, Vol. **4**, Wiley-VCH, Weinheim 1997, p. 1774.
302 A. Riisager, P. Wasserscheid, R. van Hal, R. Fehrmann, *J. Catal.* **219** (2003) 452.
303 A. Riisager, R. Fehrmann, M. Haumann, P. Wasserscheid, *Top. Catal.* **40** (2006) 91.
304 U. Kernchen, B. Etzold, W. Korth, A. Jess, *Chem. Eng. Technol.* **30** (2007) 985.
305 G. Schulz-Ekloff, S. Ernst in G. Ertl, H. Knözinger, J. Weitkamp (eds.): *Handbook of Heterogeneous Catalysis*, Vol. **1**, Wiley-VCH, Weinheim 1997, p. 374.
306 D. E. De Vos, P. P. Knops-Gerrits, R. F. Parton, B. M. Weckhuysen, P. A. Jacobs, R. A. Schoonheydt, *J. Incl. Phnom.* **21** (1995) 185.
307 R. Parton, D. E. De Vos, P. A. Jacobs in E. G. Derouane, F. Lemos, C. Naccache, F. Ramoa Ribeiro (eds.): *Zeolite Microporous Solids: Synthesis*, Structure and Reactivity, Kluwer Academic Publ., Dordrecht 1995, p. 555.
308 J.-M. Lehn: *Supramolecular Chemistry*, VCH Verlagsgesellschaft, Weinheim 1995.
309 M. P. McDaniel in G. Ertl, H. Knözinger, J. Weitkamp (eds.): *Handbook of Heterogeneous Catalysis*, Vol. **5**, Wiley-VCH, Weinheim 1997, p. 2400.
310 W. Kaminsky, *Adv. Catal.* **46** (2001) 89.
311 W. Kaminsky, *Macromol. Chem. Phys.* **197** (1996) 3907.
312 S. Roy, T. Bauer, M. Al-Dahhan, P. Lehner, T. Turek, *AIChE J.* **50** (2004) 2918.
313 I. Nova, A. Beretta, G. Groppi, L. Lietti, E. Tronconi, P. Forzatti in A. Cybulski, J. A. Moulijn (eds.)*Structured Catalysts and Reactors*, 2nd ed., Taylor & Francis, Boca Raton 2006.
314 K. Pangarkar, T. J. Schildhauer, J. R. van Ommen, J. Nihenhuis, F. Kapteijn, J. A. Moulijn, *Ind. Eng. Chem. Res.* **47** (2008) 3720.
315 M. V. Twigg, J. T. Richardson, *Ind. Eng. Chem. Res.* **46** (2007) 4166.
316 Y. Melatov-Meytal, M. Sheintuch, *Appl. Catal. A: General* **231** (2002) 1.
317 B. A. A. L. van Setten, M. Makee, J. A. Moulijn, *Catal. Rev. Sci. Eng.* **43** (2001) 489.
318 V. Mehta, J. S. Cooper, *J. Power Sources* **114** (2003) 32.
319 E. Klemm, H. Döring, A. Geisselmann, S. Schirrmeister, *Chem. Eng. Technol.* **30** (2007) 1615.

320 K. Kochloefl, *Quo vadis heterogene Katalyse*, Dechema Tagung, XXVI Jahrestreffen deutscher Katalytiker, Schloß Reinhardsbrunn, Germany, 1993.
321 H. Heinemann: "Development of Industrial Catalysis" in G. Ertl, H. Knözinger, J. Weitkamp (eds.): *Handbook of Heterogeneous Catalysis*, Vol. **1**, Wiley-VCH, Weinheim 1997, p. 35.
322 J. T. Richardson in M. V. Twigg, M. S. Spencer (eds.): *Principle of Catalyst Development*, Plenum Press, New York 1989, p. 95.
323 J. A. Cusumano in J. M. Thomas, K. I. Zamaraev (eds.): *Perspectives in Catalysis*, Blackwell Scient. Publ., Oxford 1991, p. 1.
324 K. Fouhy, G. Samdani, S. Moore, *Chem. Eng.*, October (1992) 47.
325 J. M. Fulton, *Chem. Eng.* **7** (1986) 59.
326 P. Courty, C. Marcilly in G. Poncelet, P. Grange, P. Jacobs (eds.): *Preparation of Catalysts III*, Elsevier, Amsterdam 1983, p. 485.
327 M. Sitting: *Handbook of Catalyst Manufacture*, Noyes Data Corp., Park Ridge 1971.
328 B. Stiles, T. A Koch, *Catalyst Manufacture*, 2nd. ed., M. Dekker, NewYork 1995.
329 F. Schüth, K. Unger in G. Ertl, H. Knözinger, J. Weitkamp (eds.): *Handbook of Heterogeneous Catalysis*, Vol. **1**, Wiley-VCH, Weinheim 1997, p. 72.
330 E. I. Ko in G. Ertl, H. Knözinger, J. Weitkamp (eds.): *Handbook of Heterogeneous Catalysis*, Vol. **1**, Wiley-VCH, Weinheim 1997, p. 86.
331 H. Jacobsen, P. Kleinschmit in G. Ertl, H. Knözinger, J. Weitkamp (eds.): *Handbook of Heterogeneous Catalysis*, Vol. **1**, Wiley-VCH, Weinheim 1997, p. 94.
332 J. W. Geus, J. van Dillen: "Preparation of Supported Catalysts by Deposition – Precipitation" in G. Ertl, H. Knözinger, J. Weitkamp (eds.): *Handbook of Heterogeneous Catalysis*, Vol. **1**, Wiley-VCH, Weinheim 1997, p. 240.
333 E. J. P. Feijen, J. A. Martens, P. A. Jacobs in G. Ertl, H. Knözinger, J. Weitkamp (eds.): *Handbook of Heterogeneous Catalysis*, Vol. **1**, Wiley-VCH, Weinheim 1997, p. 311.
334 J. Barbier in G. Ertl, H. Knözinger, J. Weitkamp (eds.): *Handbook of Heterogeneous Catalysis*, Vol. **1**, Wiley-VCH, Weinheim 1997, p. 257.
335 J. F. Le Page in G. Ertl, H. Knözinger, J. Weitkamp (eds.): *Handbook of Heterogeneous Catalysis*, Vol. **1**, Wiley-VCH, Weinheim 1997, p. 412.
336 J. W. Fulton, *Chem Eng.*,May 12 (1986) 97.
337 *General Catalogue*, Süd-Chemie AG, Catalyst Division, Munich Germany.
338 V. Meille, *Appl. Catal. A: General* **315** (2006) 1.
339 D. Hönicke, E. Dietzsch in F. Schüth, K. S. W. Sing, J. Weitkamp (eds.): *Handbook of Porous Solids*, Vol. **3**, Wiley-VCH, Weinheim 2002, p. 1395.
340 T. A. Nijhuis, A. E. W. Beers, T. Vergunst, I. Hoek, F. Kapteijn, J. A. Moulijn, *Catal. Rev. Sci. Eng.* **43** (2001) 345.
341 G. Ertl, H. Knözinger, J. Weitkamp (eds.): *Handbook of Heterogeneous Catalysis*, Vol. **2**, Wiley-VCH, Weinheim 1997.
342 K. S. W. Sing, D. H. Everett, R. A. W. Haul, L. Moscou, R. A. Pierotti, J. Rouquerol, T. Siemieniewska, *Pure Appl. Chem.* **57** (1985) 603.
343 K. S. W. Sing, J. Rouquerol in G. Ertl, H. Knözinger, J. Weitkamp (eds.): *Handbook of Heterogeneous Catalysis*, Vol. **1**, Wiley-VCH, Weinheim 1997, p. 427.
344 J. Rouquerol, D. Avnir, C. W. Fairbridge, D. H. Everett, J. M. Haynes, N. Pernicone, J. D. F. Ramsay, K. S. W. Sing, K. K. Unger, *Pure Appl. Chem.* **66** (1994) 1739.
345 B. C. Lippens, J. H. de Boer, *J. Catal.* **4** (1965) 319.
346 K. S. W. Sing, D. H. Everett, R. H. Ottewill (eds.): *Surface Area Determination*, Butterworths, London 1970, p. 25.
347 K. Datye in G. Ertl, H. Knözinger, J. Weitkamp (eds.): *Handbook of Heterogeneous Catalysis*, Vol. **2**, Wiley-VCH, Weinheim 1997, p. 493.
348 G. Bergeret, P. Gallezot in G. Ertl, H. Knözinger, J. Weitkamp (eds.): *Handbook of Heterogeneous Catalysis*, Vol. **2**, Wiley-VCH, Weinheim 1997, p. 439.
349 P. Gallezot in J. R. Anderson, M. Boudart (eds.): *Catalysis: Science and Technology*, Vol. **5**, Springer, Berlin 1984, p. 221.
350 R. J. Matyi, L. R. Schwartz, J. B. Butt, *Catal. Rev.-Sci. Eng.* **29** (1987) 41.
351 A. K. Datye, D. J. Smith, *Catal. Rev.-Sci. Eng.* **34** (1992) 129.
352 H. Poppa, *Catal. Rev.-Sci. Eng.* **35** (1993) 359.
353 M. J. Yacaman, G. Diaz, A. Gomez, *Catal. Today* **23** (1995) 161.
354 G. Bergeret in G. Ertl, H. Knözinger, J. Weitkamp (eds.): *Handbook of Heterogeneous Catalysis*, Vol. **2**, Wiley-VCH, Weinheim 1997, p. 464.
355 B. S. Clausen, G. Steffensen, B. Fabius, J. Villadsen, L. R. Feidenhaus, H. Topsøe, *J. Catal.* **132** (1991) 524.
356 M. Vaarkamp, D. C. Konigsberger in G. Ertl, H. Knözinger, J. Weitkamp (eds.): *Handbook of Heterogeneous Catalysis*, Vol. **2**, Wiley-VCH, Weinheim 1997, p. 475.
357 J. H. Sinfelt, G. D. Meitzner, *Acc. Chem. Res.* **26** (1993) 1.

358 J. C. Conesa, P. Esteban, H. Dexpert, D. Bazin, *Stud. Surf. Sci. Catal.* **57** (1990) 225.
359 J. M. Thomas, *Chem. Eur. J.* **3** (1997) 1557.
360 D. J. Smith, M. R. McCartney, J. K. Weiss, *Ultramicroscopy* **52** (1993) 591.
361 R. T. K. Baker, *Catal. Rev.-Sci. Eng.* **19** (1979) 161;R. T. K. Baker, N. M. Rodriguez, *Energy and Fuels* **8** (1994) 330.
362 G. Mestl, H. Knözinger in G. Ertl, H. Knözinger, J. Weitkamp (eds.): *Handbook of Heterogeneous Catalysis*, Vol. **2**, Wiley-VCH, Weinheim 1997, p. 539.
363 C. Li, P. C. Stair, *Catal. Lett.* **36** (1995) 119.
364 H. Knözinger, *Catal. Today* **32** (1996) 71.
365 Y. R. Shen, *Surface Sci.* **299/300** (1994) 551.
366 K. B. Eisenthal, *Chem. Rev.* **96** (1996) 1343.
367 H. Jobic in G. Ertl, H. Knözinger, J. Weitkamp (eds.): *Handbook of Heterogeneous Catalysis*, Vol. **2**, Wiley-VCH, Weinheim 1997, p. 574.
368 J. W. Niemantsverdriet, T. Butz in G. Ertl, H. Knözinger, J. Weitkamp (eds.): *Handbook of Heterogeneous Catalysis*, Vol. **2**, Wiley-VCH, Weinheim 1997, p. 512.
369 A. M. van der Kraan, J. W. Niemantsverdriet in G. J. Lang, J. G. Stevens (eds.): *Industrial Applications of the Mössbauer Effect*, Plenum Press, New York 1985, p. 609.
370 A. Lerf, T. Butz, *Angew. Chem.* **99** (1987) 113.
371 P. Mottner, T. Butz, A. Lerf, G. Ledezma, H. Knözinger, *J. Phys. Chem.* **99** (1995) 8260.
372 G. Engelhardt in G. Ertl, H. Knözinger, J. Weitkamp (eds.): *Handbook of Heterogeneous Catalysis*, Vol. **2**, Wiley-VCH, Weinheim 1997, p. 525.
373 G. Engelhardt, D. Michel: *High-Resolution Solid-State NMR of Silicates and Zeolites*, Wiley, Chichester 1987.
374 A. T. Bell, A. Pines (eds.): *NMR Techniques in Catalysis*, M. Dekker, New York 1994.
375 E. Taglauer in G. Ertl, H. Knözinger, J. Weitkamp (eds.): *Handbook of Heterogeneous Catalysis*, Vol. **2**, Wiley-VCH, Weinheim 1997, p. 614.
376 J. W. Niemandsverdriet: *Spectroscopy in Catalysis*, VCH Verlagsgesellschaft, Weinheim 1995.
377 D. Briggs, M. P. Seah: *Practical Surface Analysis by Auger and X-ray Photoelectron Spectroscopy*, Wiley, New York 1985.
378 E. Taglauer in A. W. Czanderna, D. M. Hercules (eds.): *Ion Spectroscopies for Surface Analysis*, Plenum Press, New York 1991, p. 363.
379 H. Niehus, W. Heiland, E. Taglauer, *Surf. Sci. Rep.* **17** (1993) 217.
380 W. K. Chu, J. W. Mayes, M. A. Nicolet: *Backscattering Spectrometry*, Academic Press, New York 1978.
381 L. C. Feldman in A. W. Czanderna, D. M. Hercules (eds.): *Ion Spectroscopies for Surface Analysis*, Plenum Press, New York 1991, p. 311.
382 A. Benninghoven, F. G. Rüdenauer, H. W. Werner: *Secondary Ion Mass Spectrometry*, Wiley, New York 1987.
383 H. J. Borg, J. W. Niemandsverdriet in J. J. Spivey, S. Agarwal (eds.): *Catalysis*, Vol. **11**, The Royal Society of Chemistry, Cambridge 1994, p. 1.
384 J. C. Vickerman, A. Swift in J. C. Vickerman (ed.): *Surface Analysis — The Principal Techniques*, Wiley, Chichester 1997,
385 J. C. Vickerman (ed.): *Surface Analysis — The Principal Techniques*, Wiley, Chichester 1997, p. 135.
386 G. Moretti in G. Ertl, H. Knözinger, J. Weitkamp (eds.): *Handbook of Heterogeneous Catalysis*, Vol. **2**, Wiley-VCH, Weinheim 1997, p. 632.
387 C. D. Wagner, A. Joshi, *J. Electron Spectrosc.* **47** (1988) 283.
388 M. Che, F. Bozon-Verduraz in G. Ertl, H. Knözinger, J. Weitkamp (eds.): *Handbook of Heterogeneous Catalysis*, Vol. **2**, Wiley-VCH, Weinheim 1997, p. 641.
389 W. N. Delgass, G. L. Haller, R. Kellerman, J. H. Lunsford: *Spectroscopy in Heterogeneous Catalysis*, Academic Press, New York 1979.
390 R. A. Schonheydt in F. Delannay (ed.): *Characterization of Heterogeneous Catalysts*, Dekker, New York 1984, p. 125.
391 F. Stone in J. P. Bonella, B. Delmon, E. G. Deronane (eds.): *Surface Properties and Catalysis by Non-Metals*, Reidel, Boston 1983, p. 237.
392 M. Gerlach, E. C. Constable: *Transition Metal Chemistry*, VCH Verlagsgesellschaft, Weinheim, Germany 1994.
393 G. Kortüm: *Reflexionsspektroskopie*, Springer, Berlin 1969.
394 M. Anpo in G. Ertl, H. Knözinger, J. Weitkamp (eds.): *Handbook of Heterogeneous Catalysis*, Vol. **2**, Wiley-VCH, Weinheim 1997, p. 664.
395 M. Anpo, M. Che, *Adc. Catal.* **44** (1999) 119.
396 J. H. Lunsford in J. R. Anderson, M. Bondart (eds.): *Catalysis — Science and Technology*, Vol. **8**, 1997, p. 227.
397 K. Dyrek, M. Che, *Chem. Rev.* **97** (1997) 305.
398 P. D. Garn: *Thermoanalytical Methods of Investigation*, Academic Press, New York 1965.
399 R. C. Mackenzie: *Differential Thermal Analysis*, Academic Press, London, New York 1972.
400 S. D. Robertson, B. D. McNicol, J. H. de Bass, S. C. Kloet, J. W. Jenkins, *J. Catal.* **37** (1975) 424.
401 H. Knözinger in G. Ertl, H. Knözinger, J. Weitkamp (eds.): *Handbook of Heterogeneous Catalysis*, Vol. **2**, Wiley-VCH, Weinheim 1997, p. 676.

402 D. A. M. Monti, A. Baiker, *J. Catal.* **83** (1983) 323.
403 P. Malet, A. Caballero, *J. Chem. Soc. Faraday Trans. I* **84** (1988) 2369.
404 V. B. Kazansky in G. Ertl, H. Knözinger, J. Weitkamp (eds.): *Handbook of Heterogeneous Catalysis*, Vol. **2**, Wiley-VCH, Weinheim 1997, p. 740.
405 W. K. Hall in G. Ertl, H. Knözinger, J. Weitkamp (eds.): *Handbook of Heterogeneous Catalysis*, Vol. **2**, Wiley-VCH, Weinheim 1997, p. 692.
406 H. A. Benesi, *J. Phys. Chem.* **61** (1957) 970.
407 M. Deeba, W. K. Hall, *J. Catal.* **60** (1979) 417.
408 B. E. Spiewak, R. D. Cartright, J. A. Dumesic in G. Ertl, H. Knözinger, J. Weitkamp (eds.): *Handbook of Heterogeneous Catalysis*, Vol. **2**, Wiley-VCH, Weinheim 1997, p. 698.
409 J. L. Falconer, J. A. Schwarz, *Catal. Rev.-Sci. Eng.* **25** (1983) 414.
410 H. Karge, V. Dondur, *J. Phys. Chem.* **94** (1990) 765.
411 S. Chatterjee, H. L. Greene, Y. J. Park, *J. Catal.* **138** (1992) 179.
412 A. Auroux, A. Gervasini, *J. Phys. Chem.* **94** (1990) 6371.
413 D. T. Chen, L. Zhang, C. Yi, J. A. Dumesic, *J. Catal.* **146** (1994) 257.
414 W. E. Farneth, R. J. Gorte, *Chem. Rev.* **95** (1995) 615.
415 H. Knözinger in G. Ertl, H. Knözinger, J. Weitkamp (eds.): *Handbook of Heterogeneous Catalysis*, Vol. **2**, Wiley-VCH, Weinheim 1997, p. 707.
416 E. A. Paukshtis, E. N. Yurchenko, *Russ. Chem. Rev.* **52** (1983) 42.
417 J. C. Lavalley, *Trends Phys. Chem.* **2** (1991) 305.
418 J. A. Lercher, C. Gründling, G. Eder-Mirth, *Catal. Today* **27** (1996) 353.
419 J. C. Lavalley, *Catal. Today* **27** (1996) 377.
420 H. Knözinger, S. Huber, *J. Chem. Soc. Faraday Trans.* **94** (1998) 2047.
421 G. C. Pimentel, A. L. McClellan: *The Hydrogen Bond*, Freeman, San Francisco, London 1960.
422 S. Huber, H. Knözinger, *J. Mol. Catal.* **141** (1999) 117.
423 A. M. Ferrari, S. Huber, H. Knözinger, K. M. Neyman, N. Rösch, *J. Phys. Chem. B* **102** (1998) 4548.
424 H. Knözinger, H. Krietenbrink, H. D. Müller, W. Schulz: *Proceedings of the 6th International Congress on Catalysis*, London, 1976, The Chemical Society, London 1977, p. 183.
425 H. Pfeifer in G. Ertl, H. Knözinger, J. Weitkamp (eds.): *Handbook of Heterogeneous Catalysis*, Vol. **2**, Wiley-VCH, Weinheim 1997, p. 732.
426 V. M. Mastikhin, I. L. Mundrakovsky, A. V. Nosov, *Progress NMR Spectrosc.* **23** (1991) 259.
427 M. Hunger, *Solid State Nucl. Magn. Res.* **6** (1996) 1.
428 V. Bosácek, *J. Phys. Chem.* **97** (1993) 10732; and*Z. Phys. Chem.* **189** (1995) 241.
429 J. F. Le Page: *Applied Heterogeneous Catalysis™ Design*, Manufacture, Use of Solid Catalysts, Editions Technip, Paris 1987.
430 J. C. Dart, *Chem. Eng. Prog.* **71** (1975) 46; and E. R. Beaver, *Chem. Eng. Prog.* **71** (1975) 44.
431 W. L. Forsythe, W. R. Hertwig, *Ind. Eng. Chem.* **41** (1949) 1200.
432 C. O. Bennett, *Adv. Catal.* **44** (1999) 329.
433 K. Tamaru in J. R. Anderson, M. Boudart (eds.): *Catalysis: Science and Technology*, Vol. **9**, Springer, Berlin, 1991, p. 87.
434 J. T. Gleaves, J. R. Ebner, T. C. Kuechler, *Catal. Rev.-Sci. Eng.* **30** (1988) 49.
435 O. V. Buyevskaya, M. Rothaemel, H. W. Zanthoff, M. Baerns, *J. Catal.* **150** (1994) 71.
436 G. Creten, D. S. Lafyatis, G. F. Froment, *J. Catal.* **154** (1995) 151.
437 S. L. Shannon, J. G. Goodwin, Jr., *Chem. Rev.* **95** (1995) 677.
438 A. Ozaki: *Isotopic Studies of Heterogeneous Catalysis*, Kodansha, Tokyo and Academic Press, New York, 1977.
439 G. F. Berndt in *Catalysis*, Vol. **6**, The Royal Society of Chemistry, London, 1983, p. 144.
440 G. Liu, D. Willcox, M. Garland, H. H. Kung, *J. Catal.* **96** (1985) 251.
441 R. P. Bell, *Chem. Soc. Rev.* **3** (1974) 513.
442 L. Melander, W. H. Sauder, Jr., *Reaction Rates of Isotopic Molecules*, Wiley, New York 1980.
443 S. Siegel, *Adv. Catal.* **16** (1966) 124.
444 M. Kraus, *Adv. Catal.* **29** (1980) 151.
445 M. Kraus in G. Ertl, H. Knözinger, J. Weitkamp (eds.): *Handbook of Heterogeneous Catalysis*, Vol. **3**, Wiley-VCH, Weinheim 1997, p. 1051.
446 H. Knözinger, *Adv. Catal.* **25** (1976) 184.
447 C. Appel, J. Mantzaras, R. Schaeren, R. Bombach, A. Inauen, *Combust. Flame*, **140** (2005) 70.
448 T. Horstmann, H. Leuckel, B. Maurer, U. Maas, *Proc. Safety Progr.* **20** (2001) 215.
449 H. P. A. Calis, J. Nijenhuis, B. C. Paikert, F. M. Dautzenberg, C. M. van den Bleek, *Chem. Eng. Sci.* **56** (2001) 1713.
450 C. Appel, J. Mantzaras, R. Schaeren, R. Bombach, B. Kaeppeli, A. Inauen, *Proc. Combust. Inst.* **29** (2003) 1031.
451 M. Reinke, J. Mantzaras, R. Schaeren, R. Bombach, W. Kreutner, A. Inauen, *Proc. Combust. Inst.* **29** (2002) 1021.
452 U. Dogwiler, P. Benz, J. Mantzaras, *Combust. Flame* **116** (1999) 243.

453 M. Reinke, J. Mantzaras, R. Schaeren, R. Bombach, A. Inauen, S. Schenker, *Combust. Flame* **136** (2004) 217.
454 U. Kunz, U. Peuker, T. Turek, M. Estenfelder in U. Bröckel, W. Meier, G. Wagner (eds.): *Product Design and Engineering*, Wiley-VCH, Weinheim 2007.
455 C. N. Satterfield, T. K. Sherwood: *Role of Diffusion in Catalysis*, Addison-Wesley, Reading, Mass. 1963, p. 56.
456 C. N. Satterfield: *Mass Transfer in Heterogeneous Catalysis*, MIT Press, Cambridge, Mass., 1970, p. 129.
457 E. W. Thiele, *Ind. Eng. Chem.* **31** (1939) 916.
458 G. Damköhler, *Chem. Ing.* **3** (1939) 430.
459 Y. B. Zeldowitch, *Acta Physicochim. USSR* **10** (1939) 582.
460 P. B. Weisz, *Adv. Catal.* **13** (1962) 137.
461 C. D. Prater, *Chem. Eng. Sci.* **8** (1958) 284.
462 P. B. Weisz, C. D. Prater, *Adv. Catal.* **6** (1954) 143.
463 E. Wicke, *Angew. Chem.* **19** (1947) 57.
464 E. Wicke, *Z. Elektrochem.* **60** (1956) 774.
465 R. Aris: *The Mathematical Theory of Diffusion and Reaction in Permeable Catalysts*, Vols. **1 and 2**, Clarendon Press, Oxford 1975.
466 J. J. Carberry in J. R. Anderson, M. Boudart (eds.): *Catalysis — Science and Technology*, Vol. **8**, Springer, Berlin 1987, p. 131.
467 P. B. Weisz, J. S. Hicks, *Chem. Eng. Sci.* **17** (1962) 265.
468 A. Wheeler, *Adv. Catal.* **2** (1951) 250.
469 F. Kapteijn, J. A. Moulijn in G. Ertl, H. Knözinger, J. Weitkamp (eds.): *Handbook of Heterogeneous Catalysis*, Vol. **3**, Wiley-VCH, Weinheim 1997, p. 1359.
470 K. C. Pratt in J. R. Anderson, M. Boudart (eds.): *Catalysis — Science and Technology*, Vol. **8**, Springer, Berlin 1987, p. 173.
471 R. J. Farrauto, C. H. Bartholomew: *Fundamentals of Industrial Catalytic Processes*, Blackie Academic & Professional, London 1997, p. 199.
472 J. M. Berty, *Plant Oper. Progr.* **3** (1984) 163.
473 L. K. Doraiswamy, D. G. Tjabl, *Cat. Rev.-Sci. Eng.* **10** (1974) 177.
474 J. Weitkamp in G. Ertl, H. Knözinger, J. Weitkamp (eds.): *Handbook of Heterogeneous Catalysis*, Vol. **3**, Wiley-VCH, Weinheim 1997, p. 1376.
475 G. Eigenberger in G. Ertl, H. Knözinger, J. Weitkamp (eds.): *Handbook of Heterogeneous Catalysis*, Vol. **3**, Wiley-VCH, Weinheim 1997, p. 1399.
476 G. F. Froment, K. B. Bischoff: *Chemical Reactor Analysis and Design*, Wiley, New York 1990.
477 K. R. Westerterp, W. P. M. van Swaaj, A. A. C. M. Beenackers: *Chemical Reactor Design and Operation*, Wiley, New York 1984.
478 K. R. Westerterp, *Chem. Eng. Sci.* **47** (1992) 2195.
479 J. Werther, H. Schoenfelder in G. Ertl, H. Knözinger, J. Weitkamp (eds.): *Handbook of Heterogeneous Catalysis*, Vol. **3**, Wiley-VCH, Weinheim 1997, p. 1426.
480 D. Geldart (ed.): *Gas Fluidization Technology*, Wiley, Chichester 1986.
481 J. F. Davidson, R. Clift, D. Harrison: *Fluidization*, Academic Press, London 1985.
482 M. Pell: *Gas Fluidization*, Elsevier, Amsterdam 1990.
483 A. A. C. M. Beenackers in G. Ertl, H. Knözinger, J. Weitkamp (eds.): *Handbook of Heterogeneous Catalysis*, Vol. **3**, Wiley-VCH, Weinheim 1997, p. 1444.
484 L. K. Doraiswamy, M. M. Sharma: *Heterogeneous Reactions*, Vol. **2**, Wiley, New York 1984, p. 9.
485 B. Jager, R. Espinoza, *Catal. Today* **23** (1995) 17.
486 W. Ehrfeld, V. Hessel, H. Löwe: *Microreactors*, Wiley-VCH, Weinheim 2000.
487 K.-F. Jensen, *Chem. Eng. Sci.* **56** (2001) 293.
488 S. J. Haswell, R. J. Middleton, B. O'Sullivan, V. Skelton, P. Watts, P. Styring, *J. Chem. Soc. Chem. Commun.* 2001, 391.
489 T. Wirth (ed.): *Microreactors in Organic Synthesis and Catalysis*, Wiley-VCH, Weinheim 2008.
490 K. Jähnisch, V. Hessel, H. Löwe, M. Baerns, *Angew. Chem. Int. Ed.* **43** (2004) 406.
491 L. Kiwi-Minsker, A. Renken, *Catal. Today* **110** (2005) 2.
492 G. Veser, *Chem. Eng. Sci.* **56** (2001) 1265.
493 T. Inoue, M. A. Schmidt, K. F. Jensen, *Ind. Eng. Chem. Res.* **46** (2007) 1153.
494 P. D. I. Fletcher, S. J. Haswell, *Chem. Br.* **35** (1999) 38.
495 E. Klemm, E. Dietzsch, T. Schwarz, T. Kruppa, A. L. de Oliveira, F. Becker, G. Markowz, S. Schirrmeister, R. Schütte, K. J. Caspary, F. Schüth, D. Hönicke, *Ind. Eng. Chem. Res.* **47** (2008) 2086.
496 Y. Sh. Matros, G. A. Bunimovich in G. Ertl, H. Knözinger, J. Weitkamp (eds.): *Handbook of Heterogeneous Catalysis*, Vol. **3**, Wiley-VCH, Weinheim 1997, p. 1464.
497 A. Renken, *Int. Chem. Eng.* **33** (1993) 61.
498 J.-A. Dalmon in G. Ertl, H. Knözinger, J. Weitkamp (eds.): *Handbook of Heterogeneous Catalysis*, Vol. **3**, Wiley-VCH, Weinheim 1997, p. 1387.
499 H. P. Hsieh, *Catal. Rev.-Sci. Eng.* **33** (1991) 1.
500 G. Sarraco, V. Specchia, *Catal. Rev.-Sci. Eng.* **36** (1994) 305.
501 R. Soria, *Catal. Today* **25** (1995) 285.
502 G. Donati, N. Habashi, I. Miracca, D. Sanfilippo in G. Ertl, H. Knözinger, J. Weitkamp (eds.):

Handbook of Heterogeneous Catalysis, Vol. **3**, Wiley-VCH, Weinheim 1997, p. 1479.
503 D. B. Keyes, *Ind. Eng. Chem.* **24** (1932) 1096.
504 D. F. Othmer, *Ind. Eng. Chem.* **33** (1941) 1106.
505 P. E. Sauvage in G. Ertl, H. Knözinger, J. Weitkamp (eds.): *Handbook of Heterogeneous Catalysis*, Vol. **3**, Wiley-VCH, Weinheim 1997, p. 1339.
506 A. Baiker, *Chem. Rev.* **99** (1999) 453.
507 P. G. Jessop, W. Leitner (eds.): *Chemical Synthesis Using Supercritical Fluids*, Wiley-VCH, Weinheim 1999.
508 R. Wandeler, A. Baiker, *Cattech* **4** (2000) 128.
509 R. J. Kee, F. M. Rupley, J. A. Miller, M. E. Coltrin, J. F. Grcar, E. Meeks, H. K. Moffat, A. E. Lutz, G. Dixon-Lewis, M. D. Smooke, J. Warnatz, G. H. Evans, R. S. Larson, R. E. Mitchell, L. R. Petzold, W. C. Reynolds, M. Caracotsios, W. E. Stewart, P. Glarborg, C. Wang, O. Adigun, CHEMKIN, 3.6 ed., Reaction Design, Inc., www.chemkin.com, San Diego, 2000.
510 D. G. Goodwin,CANTERA. An open-source, extensible software suite for CVD process simulation, www.cantera.org, 2003.
511 O. Deutschmann, S. Tischer, C. Correa, D. Chatterjee, S. Kleditzsch, V. M. Janardhanan, DETCHEM software package, 2.0 ed., www.detchem.com, Karlsruhe, 2004.
512 Fluent, Fluent Incorporated, www.fluent.com, Lebanon, NH, 2005.
513 CD-adapco, London Office, 200 Shepherds Bush Road, London, W6 7NY, United Kingdom, www.cd-adapco.com.
514 FIRE, AVL LIST GmbH, www.avl.com, Graz, Austria, 2005.
515 CFD-AC+, CFD Research Corporation, www.cfdrc.com, Huntsville, AL, 2005.
516 CFX, www-waterloo.ansys.com, 2005.
517 J. Shadid, S. Hutchinson, G. Hennigan, H. Moffat, K. Devine, A. G. Salinger, *Parallel Comput.* **23** (1997) 1307.
518 L. L. Raja, R. J. Kee, O. Deutschmann, J. Warnatz, L. D. Schmidt, *Catal. Today* **59** (2000) 47.
519 J. Mantzaras, C. Appel, P. Benz, U. Dogwiler, *Catal. Today* **59** (2000) 3.
520 R. Jahn, D. Snita, M. Kubicek, M. Marek, *Catal. Today* **38** (1997) 39.
521 G. C. Koltsakis, P. A. Konstantinidis, A. M. Stamatelos, *Appl. Catal. B* **12** (1997) 161.
522 S. Tischer, C. Correa, O. Deutschmann, *Catal. Today* **69** (2001) 57.
523 S. Tischer, O. Deutschmann, *Catal. Today* **105** (2005) 407.
524 R. Schwiedernoch, S. Tischer, C. Correa, O. Deutschmann, *Chem. Eng. Sci.* **58** (2003) 633.
525 M. Nijemeisland, A. G. Dixon, *Am. Inst. Chem. Eng. J.* 2004, **50** () 906.
526 T. Zeiser, P. Lammers, E. Klemm, Y. W. Li, J. Bernsdorf, G. Brenner, *Chem. Eng. Sci.* **56** (2001) 1697.
527 J. Neumann, H. Golitzer, A. Heywood, I. Ticu, *Revista Chim.* **53** (2002) 721.
528 R. Quiceno, J. Pérez-Ramírez, J. Warnatz, O. Deutschmann, *Appl. Catal. A* **303** (2006) 166.
529 D. L. Trimm in G. Ertl, H. Knözinger, J. Weitkamp (eds.): *Handbook of Heterogeneous Catalysis*, Vol. **3**, Wiley-VCH, Weinheim 1997, p. 1263.
530 J. R. Rostrup-Nielsen in C. H. Bartholomew, J. B. Butt (eds.): *Catalyst Deactivation*, Elsevier Science, Amsterdam 1991.
531 J. Barbier in J. Oudar, H. Wise (eds.): *Deactivation and Poisoning of Catalysts*, M. Dekker, New York 1985.
532 C. H. Bartholomew, P. K. Agrawal, J. R. Katzer, *Adv. Catal.* **31** (1982) 135.
533 P. Dufresne, A. Quesada, S. Miguarel in D. L. Trimm, S. Akasheh, M. Absi-Halabi, A. Bishara (eds.): *Catalysis in Petroleum Refining*, Elsevier Science, Amsterdam 1990.
534 K. Tanabe, M. Misono, Y. Ono, H. Hattori: *New Solid Acids and Bases*, Elsevier, Amsterdam 1989.
535 D. L. Trimm, *Chem. Eng. Process* **18** (1984) 137.
536 D. C. McCulloch in B. Leach (ed.): *Applied Industrial Catalysis*, Vol. **1**, Academic Press, New York 1983, p. 103.
537 Y. Huang, N. W. Cant, J. Guerbios, D. L. Trimm, A. Walpole: *Proc. Third Intern. Congress on Catal. and Automotive Pollution Control*, Brussels, Elsevier, Amsterdam 1995, p. 56.
538 C. A. Bernardo, D. L. Trimm, *Carbon* **17** (1979) 115.
539 H. Hiller *et al.*: "Gas Production", in *Ullmann's Encyclopedia of Industrial Chemistry*, Vol. **A12**, Wiley-VCH, Weinheim 2006.
540 P. Häussinger, R. Lohmüller, A. M. Watson: "Hydrogen", in *Ullmann's Encyclopedia of Industrial Chemistry*, Vol. **A13**, Wiley-VCH, Weinheim 2002, p. 189.
541 S. Ernst, W. Petzny in R. Dittmeyer, W. Keim, G. Kreysa, A. Oberholz (eds.): *Winnacker-Küchler*, 5. ed, Vol. **4**, Wiley-VCH, Weinheim 2005, p. 523.
542 J. R. Rostrup-Nielsen in G. Ertl, H. Knözinger, F. Schüth, J. Weitkamp (eds.): *Handbook of Heterogeneous Catalysis*, 2nd ed., Vol. **6**, Wiley-VCH, Weinheim 2008, p. 2882.
543 J. R. Rostrup-Nielsen, J. Sehested, J. K. Norskov.*Adv. Catal.* **47** (2002) 65.

544 J. Wei, E. Iglesia, *J. Phys. Chem. B* **108** (2004) 4094.
545 D. A. Hickman, L. D. Schmidt, *J. Catal.* **138** (1992) 267.
546 J. J. Krummenacher, K. N. West, L. D. Schmidt, *J. Catal.* **215** (2003) 332.
547 J. R. Salge, G. A. Deluga, L. D. Schmidt, *J. Catal.* **235** (2005) 69.
548 J. N. Armor, *J. Membrane Sci.* **147** (1998) 217.
549 I. Aartun, B. Silberova, H. Venvik, P. Pfeifer, O. Gorke, K. Schubert, A. Holmen, *Catal. Today* **105** (2005) 469.
550 T. J. Remans, G. Jenzer, A. Hoek in G. Ertl, H. Knözinger, F. Schüth, J. Weitkamp (eds.): *Handbook of Heterogeneous Catalysis*, 2nd ed., Vol. **6**, Wiley-VCH, Weinheim 2008, p. 2994.
551 G. A Olah, A. Goeppert, G. K. S. Prakash: *Beyond Oil and Gas: The Methanol Economy*, Wiley-VCH, Weinheim 2006.
552 D. C. Rennard, P. J. Dauenhauer, S. A. Tupy, L. D. Schmidt, *Energy Fuels* **22** (2008) 1318.
553 P. J. Dauenhauer, B. J. Dreyer, N. J. Degenstein, L. D. Schmidt, *Angew. Chem. Int. Ed.* **46** (2007) 5864.
554 E. C. Wanat, B. Suman, L. D. Schmidt, *J. Catal.* **235** (2005) 18.
555 K.-O. Hinrichsen, K. Kochloefl, M. Muhler in G. Ertl, H. Knözinger, F. Schüth, J. Weitkamp (eds.): *Handbook of Heterogeneous Catalysis*, 2nd ed., Vol. **6**, Wiley-VCH, Weinheim 2008, p. 2905.
556 D. S. Newsome, *Catal. Rev. Sci. Eng.* **21** (1980) 275.
557 G. Ertl in J. R. Jennings (ed.): *Catalytic Ammonia Synthesis: Fundamentals and Practice*, Fundamental and Applied Catalysis, Plenum Press, New York 1991, p. 109.
558 R. Schlögel in G. Ertl, H. Knözinger, F. Schüth, J. Weitkamp (eds.): *Handbook of Heterogeneous Catalysis*, 2nd ed., Vol. **5**, Wiley-VCH, Weinheim 2008, p. 2501.
559 K. Aika, A. Ozaki, *J. Catal.* **16** (1970) 97.
560 F. Bozso, G. Ertl, M. Weiss, *J. Catal.* **50** (1977) 519.
561 P. H. Emmett, S. Brunauer, *J. Am. Chem. Soc.* **59** (1937) 310.
562 M. Boudart, *Catal. Rev.-Sci. Eng.* **23** (1981) 1.
563 G. Ertl, M. Weiss, S. B. Lee, *Chem. Phys. Lett.* **60** (1979) 391.
564 M. Muhler, E. Törnqvist, L. P. Nielsen, B. S. Clausen, H. Topsøe, *Catal. Lett.* **25** (1994) 1.
565 R. Burch, R. J. Chappell, S. E. Golunski, *J. Chem. Soc. Faraday Trans. 1* **85** (1989) 3569.
566 J. Nakamura, I. Nakamura, T. Uchima, T. Watanabe, T. Fujitani, *Stud. Surf. Sci. Catal.* **101** (1996) 1389.
567 H. Topsøe, N. Topsøe, *Top. Catal.* **8** (1999) 267.
568 T. S. Askgaard, J. K. Norskov, C. V. Ovesen, P. Stoltze, *J. Catal.* **156** (1995) 229.
569 K. M. Vanden Bussche, G. F. Froment, *J. Catal.* **161** (1996) 1.
570 B. Lommerts, G. Graff, A. Beenackers, *Chem. Eng. Sci.* **55** (2000) 5589.
571 R. G. Herman in L. Guczi (ed.): *New Trends in CO Activation*, Elsevier, New York 1991.
572 F. Fischer, H. Tropsch, *Brennst. Chem.* **4** (1923) 276.
573 R. B. Anderson in P. H. Emmett (ed.): *Catalysis*, Vol. **4**, Van Nostrand-Rheinhold, New York 1956.
574 A. T. Bell, *Catal. Rev. Sci. Eng.* **23** (1981) 203.
575 G. P. van der Laan, A. A. C. M. Beenackers, *Catal. Rev. Sci. Eng.* **41** (1999) 255.
576 T. Riedel,PhD thesis, Universität Karlsruhe (TH), Karlsruhe2002.
577 B. H. Davis, *Top. Catal.* **32** (2005) 143.
578 R. Oukaci, A. H. Singleton, J. G. Goodwin, Jr., *Appl. Catal. A* **186** (1999) 129.
579 M. E. Dry, *J. Mol. Catal.* **17** (1982) 133.
580 S. T. Sie, *Rev. Chem. Eng.* **14** (1988) 109.
581 F. G. Botes, W. Böhringer, *Appl. Catal A: General* **267** (2004) 217.
582 A. M. Subiranas, G. Schaub, *Int. J. Chem. React. Eng.* **5** (2007) A78.
583 M. F. M. Post, A. C. van't Hoog, J. K. Minderhoug, S. T. Sie, *AIChE J.* **35** (1989) 1107.
584 Y.-N. Wang, Y.-Y. Xu, H.-W. Xiang, Y.-W. Li, B. J. Zhang, *Ind. Eng. Chem. Res.* **40** (2001) 4324.
585 A.-M. Hilmen, E. Bergene, O. A. Lindvag, D. Schanke, S. Eri, A. Holmen, *Catal. Today* **69** (2001) 227.
586 R. K. Grasselli in G. Ertl, H. Knözinger, J. Weitkamp (eds.): *Handbook of Heterogeneous Catalysis*, Vol. **5**, Wiley-VCH, Weinheim 1997, p. 2302.
587 R. A. van Santen G. Ertl, H. Knözinger, J. Weitkamp (eds.): *Handbook of Heterogeneous Catalysis*, Vol. **5**, Wiley-VCH, Weinheim 1997, p. 2244.
588 R. A. van Santen, H. C. P. E. Kuipers, *Adv. Catal.* **35** (1988) 265.
589 M. C. Zonnevylle, J. J. C. Geerlings, R. A. van Santen, *J. Catal.* **148** (1994) 417.
590 M. Neurock, R. A. van Santen, W. Biemolt, A. P. J. Jansen*J. Am. Chem. Soc.* **116** (1994) 6860.
591 J. W. He, U. Memmert, K. Griffiths, P. R. Norton, *J. Chem. Phys.* **90** (1989) 5082.
592 P. J. van den Hoek, E. J. Baerends, R. A. van Santen, *J. Phys. Chem.* **93** (1989) 6469.
593 L. M. Akella, H. N. Lee, *J. Catal.* **86** (1984) 465.
594 M. Bowker, R. C. Waugh, *Surf. Sci.* **155** (1984) 1.

595 P. Arpentinier, F. Cavani, F. Trifiro: *The Technology of Catalytic Oxidations*, Vol. **1**, Editions Technip, Paris 2001, p. 245.
596 G. Bellussi, M. S. Rigutto, *Stud. Surf. Sci. Catal.* **85** (1991) 177.
597 M. G. Clerici, *Oil Gas Eur. Mag.* **32** (2006) 77.
598 B. Ford, *Chem. Market. Rep.* **269** (2006) 24.
599 P. N. Rylander in J. R. Anderson, M. Boudart (eds.): *Catalysis: Science and Technology*, Vol. **4**, Springer, Berlin 1983, p. 1.
600 J. F. Brazdil, *Top. Catal.* **38** (2006) 289.
601 P. Mars, D. W. van Krevelen, *Chem. Eng. Sci. Special Suppl.* **3** (1954) 41.
602 R. K. Grasselli, J. D. Burrington, *I & EC Res. & Dev.* **23** (1984) 393.
603 T. P. Snyder, C. G. Hill, *Catal. Rev.-Sci. Eng.* **31** (1989) 43.
604 J. D. Burrington, C. T. Kartisek, R. K. Grasselli, *J. Catal.* **87** (1984) 363.
605 J. M. Lopez Nieto, *Top. Catal.* **41** (2006) 3.
606 B. C. Gates: *Catalytic Chemistry*, Wiley, New York 1992, p. 406.
607 R. Prius in G. Ertl, H. Knözinger, J. Weitkamp (eds.): *Handbook of Heterogeneous Catalysis*, Vol. **4**, Wiley-VCH, Weinheim 1997, p. 1908.
608 D. D. Whitehurst, T. Isoda, I. Mochida, *Adv. Catal.* **42** (1998) 345.
609 M. Houalla, N. K. Nag, A. V. Sapre, D. H. Broderick, B. C. Gates, *AIChE J.* **24** (1978) 1015.
610 A. Kundu, K. D. P. Nigam, A. M. Duquenne, H. Delmas, *Rev. Chem. Eng.* **6** (2003) 531.
611 M. S. Rana, V. Sámano, J. Ancheyta, J. A. I. Diaz, *Fuel* **86** (2007) 1216.
612 M. Koebel, M. Elsener, G. Madia, *Ind. Eng. Chem. Res.* **40** (2001) 52.
613 US 2 975 025, 1961(G. Cohn, D. Steele, H. Andersen).
614 US 3 279 884, 1966(K. Kartte, H. Nonnenmaker).
615 US 4 085 193, 1978(F. Nakajima, M. Takeuchi, S. Matsuda, S. Uno, T. Mori, Y. Watanabe, M. Inamuri).
616 C. Orsenigo, L. Lietti, E. Tronconi, P. Forzatti, F. Bregani, *Ind. Eng. Chem. Res.* **37** (1998) 2350.
617 G. S. Qi, R. T. Yang, R. Chang, S. Cardoso, R. A. Smith, *Appl. Catal. A: General* **275** (2005) 207.
618 M. Groves, M. Schwefer, R. Siefert, *TCE* **778** (2006) 30.
619 M. Votsmeier, T. Kreuzer, G. Lepperhoff: "Automobile Exhaust Control" in *Ullmann's Encyclopedia of Industrial Chemistry*, Vol. **A3**, Wiley-VCH, Weinheim 2005, p. 189
620 S. J. Lox in G. Ertl, H. Knözinger, F. Schüth, J. Weitkamp (eds.): *Handbook of Heterogeneous Catalysis*, 2nd ed., Vol. **5** Wiley-VCH, Weinheim 2008, p. 2274.
621 R. M. Heck, R. J. Farrauto, S. T. Gulati, *Catalytic Air Pollution Control*, Wiley-InterSci., New York 2002.
622 S. Kureti,Habilitation thesis, Fakultät für Chemie und Biowissenschaften, Universität Karlsruhe (TH), 2008.
623 M. V. Twigg, *Appl. Catal. B* **70** (2007) 2.
624 D. Chatterjee, O. Deutschmann, J. Warnatz, *Faraday Discuss.* **119** (2001) 371.
625 N. Fekete, R. Kemmler, D. Voigtländer, B. Krutzsch, E. Room, G. Wenninger, W. Strehlau, J. A. A. van den Tillaart, J. Leyrer, E. S. Lox, W. Müller, *SAE Technical Paper* **960133** (1996)
626 F. Rohr, S. D. Peter, E. Lox, M. Kögel, A. Sassi, L. Juste, C. Rigaudeau, G. Belot, P. Gelin, M. Primet, *Appl. Catal. B* **56** (2005) 201.
627 P. Zelenka, W. Cartellieri, P. Duke, *Appl. Catal. B* **7** (1996) 3.
628 O. Salvat, P. Marez, G. Belot, *SAE Technical Paper* 2000-01-0473(2000).